REPORT UAG - 36

WORLD DATA CENTER A
for
Solar-Terrestrial Physics

AN ATLAS OF EXTREME ULTRAVIOLET FLASHES OF SOLAR FLARES OBSERVED VIA SUDDEN FREQUENCY DEVIATIONS DURING THE ATM-SKYLAB MISSIONS

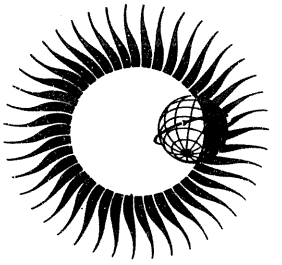

OCTOBER 1974

WORLD DATA CENTER A

National Academy of Sciences

2101 Constitution Avenue, N. W. Washington, D. C., U.S.A., 20418

World Data Center A consists of the Coordination Office and eight subcenters:

World Data Center A
Coordination Office
National Academy of Sciences
2101 Constitution Avenue, N.W.
Washington, D. C., U.S.A. 20418
Telephone (202) 389-6478

Solar and Interplanetary Phenomena, Ionospheric Phenomena, Flare-Associated Events, Geomagnetic Variations, Magnetospheric and Interplanetary Magnetic Phenomena, Aurora, Cosmic Rays, Airglow:
World Data Center A
for Solar-Terrestrial Physics
National Oceanic and Atmospheric Administration
Boulder, Colorado, U.S.A. 80302
Telephone (303) 499-1000 Ext. 6467

Geomagnetism, Seismology, Gravity (and Upper Mantle Project Archives):
World Data Center A:
Geomagnetism, Seismology and Gravity
Environmental Data Service, NOAA
Boulder, Colorado, U.S.A. 80302
Telephone (303) 499-1000 Ext. 6311

Glaciology:
World Data Center A:
Glaciology
U.S. Geological Survey
1305 Tacoma Avenue South
Tacoma, Washington, U.S.A. 98402
Telephone (206) 593-6502

Longitude and Latitude:
World Data Center A:
Longitude and Latitude
U. S. Naval Observatory
Washington, D. C., U.S.A. 20390
Telephone (202) 254-4547

Meteorology (and Nuclear Radiation):
World Data Center A:
Meteorology
National Climatic Center
Federal Building
Asheville, North Carolina, U.S.A. 28801
Telephone (704) 254-0683

Oceanography:
World Data Center A:
Oceanography
National Oceanic and Atmospheric Administration
Rockville, Maryland, U.S.A. 20852
Telephone (202) 426-9052

Rockets and Satellites:
World Data Center A:
Rockets and Satellites
Goddard Space Flight Center
Code 601
Greenbelt, Maryland, U.S.A. 20771
Telephone (301) 982-6695

Tsunami:
World Data Center A:
Tsunami
National Oceanic and Atmospheric Administration
2525 Korrea Road
Honolulu, Hawaii, U.S.A. 96822
Telephone (808) 948-8083

Notes:

(1) World Data Centers conduct international exchange of geophysical observations in accordance with the principles set forth by the International Council of Scientific Unions. WDC-A is established in the United States under the auspices of the National Academy of Sciences.
(2) Communications regarding data interchange matters in general and World Data Center A as a whole should be addressed to: World Data Center A, Coordination Office (see address above).
(3) Inquiries and communications concerning data in specific disciplines should be addressed to the appropriate subcenter listed above.

WORLD DATA CENTER A
for
Solar-Terrestrial Physics

REPORT UAG - 36

AN ATLAS OF EXTREME ULTRAVIOLET FLASHES OF SOLAR FLARES OBSERVED VIA SUDDEN FREQUENCY DEVIATIONS DURING THE ATM-SKYLAB MISSIONS

by

R.F. Donnelly[1], E.L. Berger[1], Lt. J.D. Busman[2], B. Henson[3], T.B. Jones[4], G.M. Lerfald[5], K. Najita[6], W.M. Retallack[1], and W.J. Wagner[7]

Author Affiliation:

1. NOAA Space Environment Laboratory, Boulder, Colorado 80302 USA
2. NOAA Commissioned Corps, Boulder, Colorado 80302 USA
3. NASA Marshall Space Flight Center, Alabama 35812 USA
4. Department of Physics, University of Leicester, Leicester, England, UK
5. NOAA Wave Propagation Laboratory, Boulder, Colorado 80302 USA
6. Radio Science Laboratory, Department of Electrical Engineering, University of Hawaii, Honolulu, Hawaii 96822 USA
7. Sacramento Peak Observatory, AFCRL, Sunspot, New Mexico 88349 USA

OCTOBER 1974

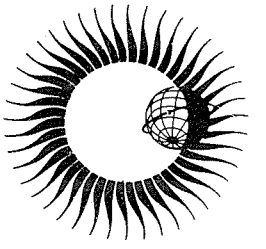

Prepared by World Data Center A for
Solar-Terrestrial Physics, NOAA, Boulder, Colorado
and published by

U.S. DEPARTMENT OF COMMERCE
NATIONAL OCEANIC AND ATMOSPHERIC ADMINISTRATION

ENVIRONMENTAL DATA SERVICE
Asheville, North Carolina, USA 28801

SUBSCRIPTION PRICE: $9.00 a year; $2.50 additional for foreign mailing; single copy price varies.* Checks and money orders should be made payable to the Department of Commerce, NOAA. Remittance and correspondence regarding subscriptions should be sent to the National Climatic Center, Federal Building, Asheville, NC 28801, Attn: Publications.

*PRICE THIS ISSUE .55

TABLE OF CONTENTS

		Page
ABSTRACT		1
1.	INTRODUCTION	1
2.	HF DOPPLER OBSERVATIONS	2
	2.1 At Sacramento Peak Observatory	3
	2.2 Near Boulder, Colorado	5
	2.3 In England	7
	2.4 At NASA Marshall Space Flight Center	8
	2.5 In Hawaii	8
3.	SFD ANALYSIS PROCEDURES	9
4.	OBSERVATIONS DURING TWO SOLAR ROTATIONS BEFORE THE ATM-SKYLAB	11
5.	OBSERVATIONS DURING THE FIRST MANNED MISSION OF ATM-SKYLAB	42
6.	OBSERVATIONS DURING THE FIRST UNMANNED MISSION OF ATM-SKYLAB	51
7.	OBSERVATIONS DURING THE SECOND MANNED MISSION OF ATM-SKYLAB	60
8.	OBSERVATIONS DURING THE SECOND UNMANNED MISSION OF ATM-SKYLAB	85
9.	OBSERVATIONS DURING THE THIRD MANNED MISSION OF ATM-SKYLAB	89
10.	DISCUSSION	94
11.	ACKNOWLEDGEMENTS	94
	REFERENCES	95

AN ATLAS OF EXTREME ULTRAVIOLET FLASHES OF SOLAR FLARES OBSERVED VIA SUDDEN FREQUENCY DEVIATIONS DURING THE ATM-SKYLAB MISSIONS

by

R. F. Donnelly[1], E. L. Berger[1], Lt. J. D. Busman[2],

B. Henson[3], T. B. Jones[4], G. M. Lerfald[5], K. Najita[6],

W. M. Retallack[1], and W. J. Wagner[7]

ABSTRACT

The 10-1030A impulsive solar flux enhancements of solar flares during the ATM-SKYLAB missions are presented. The extreme-ultraviolet (EUV) enhancements were observed via sudden frequency deviations (SFD), an ionospheric effect caused by the enhancement of ionospheric photoionization produced by EUV bursts. The SFD measurements were made at Sacramento Peak Observatory; Boulder, Colorado; Leicester, England; Huntsville, Alabama; and Hawaii. EUV bursts are reported for the period April 1, 1973 to February 8, 1974, which includes several solar rotations before the first manned mission of ATM-SKYLAB. Compared to SFD observations from September, 1960 to July, 1970, the ATM-SKYLAB missions were periods of low solar activity when no large SFDs occurred. However, several medium sized events did occur with quasi-periodic or extensive fine time structure.

1. INTRODUCTION

A sudden frequency deviation (SFD) is a rapid change in the received frequency of a high-frequency radio wave propagated from an ultrastable transmitter and reflected at altitudes in the range 120 to 300 km in the ionosphere. This particular type of frequency deviation results from the time-varying ionospheric electron density produced by the time-varying ionizing radiation from a solar flare. In effect, SFD observations are like those from a broadband satellite detector, except SFDs are particularly sensitive to impulsive 10-1030A bursts and relatively insensitive to gradual rise and fall events [Donnelly, 1970]. SFDs have fairly good time resolution, namely several seconds for some of the measurements discussed later. SFDs supplement the excellent ATM-SKYLAB observations, which have high spatial and spectral resolution, by providing high time resolution measurements of the impulsive flare emissions originating from source regions that are like the chromosphere and chromosphere-corona transition region, and by providing background information on the occurrence of EUV bursts at times or spatial locations unobserved by the ATM experiments.

ATM-SKYLAB observations [Reeves, 1972] are the best soft x-ray and EUV observations of the sun made to date, because of their high spatial resolution and long duration and because measurements were simultaneously recorded at many wavelengths. The ATM (Apollo Telescope Mount) measurements of the quiet sun, solar prominences and active regions are excellent, and should lead to major advances in understanding their physical properties and processes. The ATM solar observations covered the period May 29 through June 18, 1973, during the first manned mission of SKYLAB; the period August 7 through September 21, 1973, during the second manned mission; and the period November 26, 1973 through February 3, 1974, during the final manned mission. The Harvard EUV experiment operated also during the interim unmanned periods. This atlas of SFD observations presents the events in chronological order in six time periods as shown in Figure 1.1, namely: (1) before the ATM observations, (2) during the first manned ATM observing period, (3) the first unmanned ATM observing period, (4) the second mannned ATM observing period, (5) the second unmanned ATM observing period, and (6) the third manned ATM observing period.

Author Affiliation:

1. NOAA Space Environment Laboratory, Boulder, Colorado 80302 USA
2. NOAA Commissioned Corps, Boulder, Colorado 80302 USA
3. NASA Marshall Space Flight Center, Alabama 35812 USA
4. Department of Physics, University of Leicester, Leicester, England, UK
5. NOAA Wave Propagation Laboratory, Boulder, Colorado 80302 USA
6. Radio Science Laboratory, Department of Electrical Engineering, University of Hawaii, Honolulu, Hawaii 96822 USA
7. Sacramento Peak Observatory, AFCRL, Sunspot, New Mexico 88349 USA

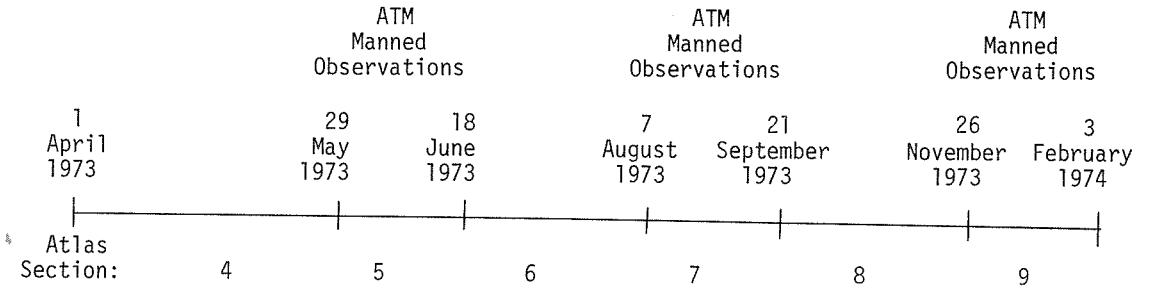

Figure 1.1 Observation periods.

2. HF DOPPLER OBSERVATIONS

Measurements of frequency deviations on HF radio waves reflected from the ionosphere are called HF Doppler measurements. The 0.1 to 100 Hz range of frequency deviations are recorded on magnetic tape along with time codes. The instrumentation used is like that described by Baker *et al.* [1968]. A variety of events other than SFDs are observed in HF Doppler measurements. Somewhat different HF Doppler experiments are conducted according to the type of event to be studied. The ideal experiment for observing SFDs consists of a ground-range separation between transmitter and receiver of about 600 to 1200 km so that the horizontal length of the radio wave propagation path is long enough relative to local time-varying ionospheric irregularities to average out their contribution to the observed frequency deviation. Longer paths are undesirable because multiple-hop paths occur and it is difficult to accurately determine their ray paths. Transmitter and receiver antennas should be quite directional along the great circle path between the transmitter and receiver stations to suppress propagation paths that deviate significantly from the great circle plane of the transmitter and receiver stations. The receiver and transmitter antennas should also be directional in the vertical plane with the main beam at elevation angles in the 15^{0} to 27^{0} range in order to enhance one-hop propagation paths reflected in the F-region of the ionosphere because such paths are sensitive to the ionospheric effects of flare radiation in the full 1-1030A wavelength range. Both antennas should have low gain at elevation angles below 15^{0} in order to suppress one-hop paths reflected from the bottom of the E-layer, or from sporadic E-layers. Such paths are sensitive mainly to the ionospheric effects of 1-10A soft x-rays that are routinely well observed by satellites. Similarly, the antennas should have low gain at elevation angles above about 30^{0} in order to suppress multiple-hop paths because it is more difficult to determine accurately their ray paths. Ideally, an ionosonde station should be located at the midpoint of the path in order to provide measurements of the electron density as a function of height just before flares. The stations should be at equatorial or low midlatitudes since the magnitude of SFDs decreases with increasing solar zenith angle. About five different transmission frequencies, e.g., 8, 9, 10, 11 and 12 MHz, should be used to insure that, at any particular time, at least one of the propagation paths is one-hop with a true reflection height near 200 km.

An oblique-path experiment has several advantages relative to near-vertical path experiments. First, the effects of time-varying local ionospheric irregularities, which are unrelated to the flare effects and which may produce frequency deviations as large in magnitude as small SFDs, are smoothed out in oblique-path observations of frequency deviations. Secondly, higher frequencies are used on oblique paths which suffer less absorption in the ionosphere. Thirdly, the ground wave is not received on long paths while on short paths it must be nulled out as much as possible by the antenna patterns. The flare-induced ionospheric absorption of radio waves is less of a problem for the oblique path than for a vertical path. For an SFD accompanied by a large SWF (short wave fade-out, or flare-induced enhancement of D-region absorption of HF radio waves), the vertical-path observations show the SFD until the strength of the ionosphere-reflected radio wave is so weak relative to the residual signal from the ground wave that the latter dominates and consequently the receivers stop automatically increasing their gain to track the SFD signal. A fourth advantage is that the propagation paths are less influenced by the earth's magnetic field because of the higher frequencies.

Most of the HF Doppler observations discussed below were intended to observe frequency-deviation events other than SFDs, e.g., traveling ionospheric disturbances (TIDs) due to aurora sources, severe storms, or static rocket test firings, etc. Consequently, most of the observations were made with nearly vertical paths and the SFD observations were a fortunate by-product. Table 2.1 quantitatively presents the geographic locations, path lengths and frequencies of the HF Doppler observations studied. All of the observations were processed by sub-audio frequency spectral analysis, which permits detection of SFDs as small as 0.1 Hz peak frequency deviation and separation of two different signals with frequency deviations that differ by more than about 0.1 Hz when processed with time resolution of several seconds.

TABLE 2.1

SFD Observatories

Receiving Station Name and Geographic Coordinates	Transmitter Station Name	Transmitter Station Geographic Coordinates	Received Frequencies MHz	Great-Circle Ground Range km	Comments
Sacramento Peak Observatory 32°47'12"N 105°49'12"W	WWV	40°40'49.0"N 105°02'27.0"W	5, 10, 15	881	Operated to observe SFDs during ATM-SKYLAB.
	WWVH	21°59'26.0"N 159°46'00.0"W	10, 15	5,404	Observations from April 1, 1973 to February 4, 1974 were thoroughly searched for SFDs. Preliminary reports or observed SFDs were published in *Solar-Geophysical Data*.
Table Mountain, Boulder, Colorado 40°7'42"N 105°14'18"W	Sunset	40°2'25"N 105°27'5"W	2.4, 4.8, 6.0	20.5	Observations from April 1, 1973 to February 4, 1974 were thoroughly searched for SFDs.
	Keenesburg	40°4'30"N 104°30'30"W		62.7	
	Fort Collins	40°35'0"N 105°9'30"W		51.1	
Leicester, England 52°23'N 1°3'W	Four Stations Near Gainsborough, Upwood, Bicester and Stafford, England	52.4°N 1°W	4.793	66 to 90	SFDs for certain flares observed by ATM-SKYLAB were studied in detail.
Marshall Space Flight Center Huntsville, Alabama 34°43'N 86°35'W	Nickajack Dam	35°1'N 85°37'W	4.0125	94	SFDs for certain flares observed by ATM-SKYLAB were studied.
	Muscle Shoals, Alabama	34°47'N 87°37'W	4.759	95	
	Fort McClellan, Alabama	33°44'N 85°44'W	5.374	134	
Honolulu, Oahu, Hawaii 21.3°N 157.5°W	WWVH	21°59'26.0"N 159°46'00.0"W	5, 10	216	SFDs are routinely scaled and reported in *Solar-Geophysical Data*.
Hana, Maui, Hawaii 20.8°N 156.0°W	WWVH	21°59'26.0"N 159°46'00.0"W	5, 10	410	SFDs for certain flares observed by ATM-SKYLAB were studied in detail.
Kona, Hawaii, Hawaii 19.6°N 156.0°W	WWVH	21°59'26.0"N 159°46'00.0"W	5, 10	470	

2.1 HF Doppler Observations at Sacramento Peak Observatory

HF Doppler receivers were installed at Sacramento Peak Observatory to receive the frequency standard transmissions of station WWV at 5, 10, and 15 MHz in order to measure SFDs during the ATM-SKYLAB missions. Figure 2.1 shows the locations of the transmitters and receivers. The ground range of 881 km is ideal. The WWV transmissions were used because funds were not available to operate separate transmitters. WWV transmits 10 kW of power at each of the three frequencies received at Sacramento Peak Observatory.

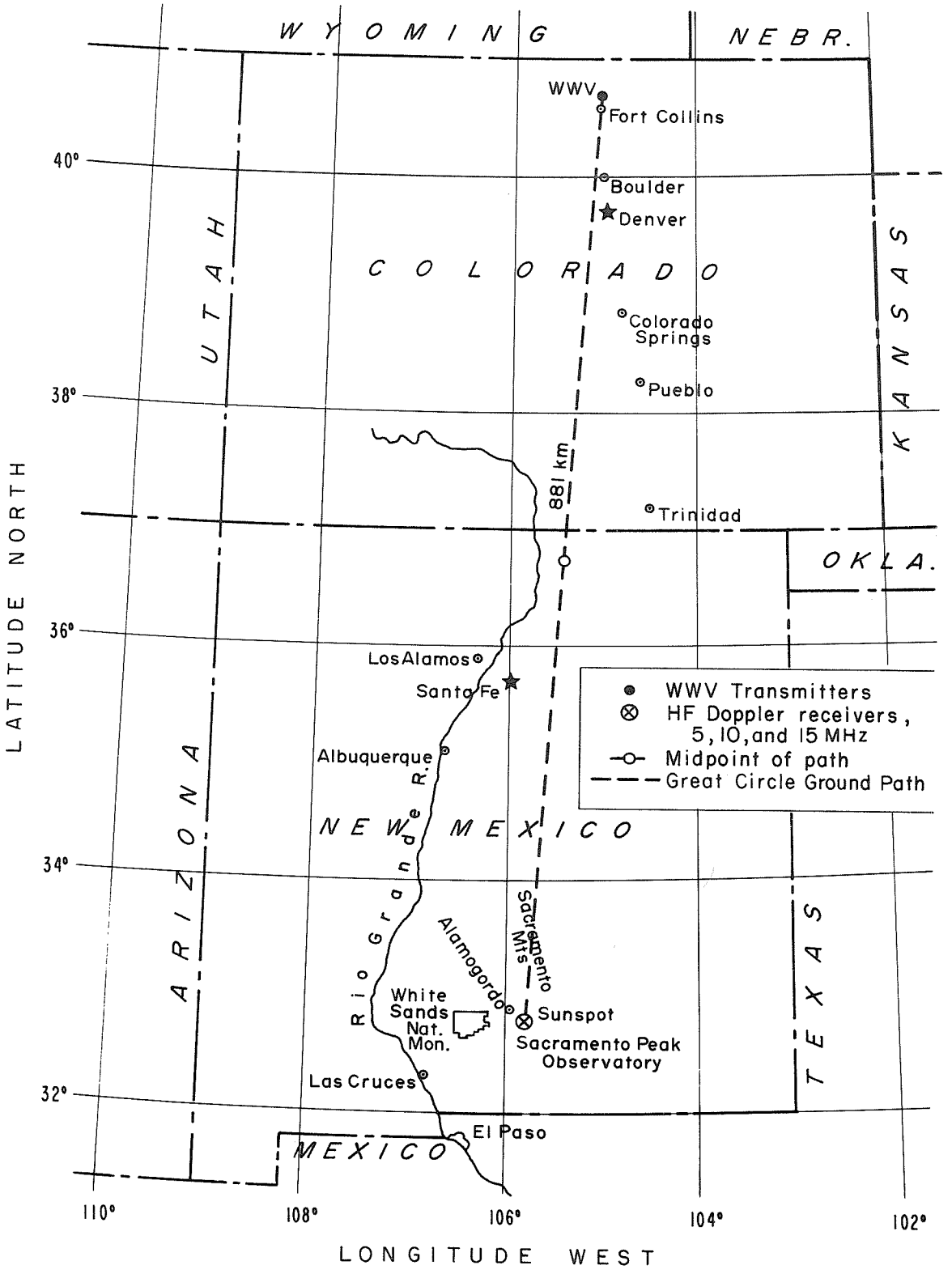

Figure 2.1 Locations of transmitters, receivers and great-circle ground path for SFD observations at Sacramento Peak Observatory from WWV Transmissions.

In order to provide worldwide time and frequency standard information, the WWV antennas are half-wave vertical dipoles that radiate omnidirectionally in the horizontal plane with strong radiation at low elevation angles. The results for the SFD measurements are that radio waves reflected from the bottom of the E-layer or paths outside the great circle plane of the transmitter and receiver locations are stronger than ideal. The receiving antennas were half-wave horizontal dipoles strung about one-quarter wavelength above the ground. The axis of each antenna was oriented approximately perpendicularly to the great circle plane of the transmitter and receiver locations which provides a mild directivity in support of great circle propagation paths reflected in the F-region.

Usually 5 MHz was too low for propagation paths to be reflected from the F-region to Sacramento Peak, i.e., 5 MHz was normally reflected from the bottom of the E-layer. Usually 15 MHz was too high a frequency to be reflected in the ionosphere to as short a range as 881 km, i.e., the skip-distance usually exceeded 881 km. So 10 MHz provided the main measurements of SFDs, but frequently the only 10 MHz daytime path was reflected from the bottom of the E-layer or sporadic E-layers.

The time and frequency standard station WWVH in Hawaii also transmits at 5, 10 and 15 MHz. The WWVH antenna patterns are cardioid shaped in a horizontal plane with the minimum radiation in the easterly direction. Also, the orientation of the receiving antennas at Sacramento Peak Observatory results in a minimum sensitivity to radio waves from the west. Consequently, reception at Sacramento Peak Observatory of WWVH was not expected. However, frequently 15 MHz WWVH and occasionally 10 MHz WWVH were received, as was evident from the voice announcements. The great circle ground range from WWVH, Kauai, Hawaii to Sacramento Peak Observatory is about 5,404 km. The WWVH propagation paths were multiple-hop and may have deviated significantly from the great circle plane. For several SFDs reported later, 15 MHz WWVH to Sacramento Peak Observatory provided the sole observation of the event.

No ionograms were available from near the midpoint of the path from WWV to Sacramento Peak. Ionograms were obtained from near the end points of the propagation path, namely Boulder, Colorado, and from White Sands Missile Range, near White Sands National Monument (see Figure 2.1). For many of the SFDs observed, preflare ionograms of sufficient quality for computing the ionospheric electron density as a function of height were not available from White Sands.

The Sacramento Peak HF Doppler observations commenced March 30, 1973 and terminated February 4, 1974. These observations were examined to detect SFDs, first by looking directly at the records and secondly by checking the data at the times of flares listed in *Solar-Geophysical Data*. Loss of data due to equipment malfunction, power failures or the time required to change magnetic tapes totaled less than ½% of the total observing period, where most of the lost data occurred on November 30, 1973, because of a power failure. Preliminary reports of SFDs observed at Sacramento Peak were published in *Solar-Geophysical Data*.

2.2 HF Doppler Observations Near Boulder, Colorado

Figure 2.2 illustrates the geographic layout of an HF Doppler observatory near Boulder, Colorado, that was operated under ARPA Order No. 1361 to observe moving ionospheric irregularities. Three paths are used for triangulation of the motions. The observation of SFDs was a fortunate by-product. The frequencies transmitted from the three stations were offset from each other by about a 1 kHz interval at 2.4 MHz, 2 kHz at 4.8 MHz and 2.5 kHz at 6 MHz, so the received signals could be recorded on separate channels, e.g., 4.8 MHz from Fort Collins is recorded on a different magnetic tape than 4.8 MHz from Sunset or 4.8 MHz from Keenesburg. The three transmission frequencies of about 2.4, 4.8 and 6.0 MHz and the three different propagation paths result in nine channels of HF Doppler data. The main disadvantage for observing SFDs on nearly vertical propagation paths like these is that time-varying local ionospheric irregularities cause sizeable frequency deviations that constitute noise relative to the flare-induced frequency deviation. Because the frequency deviations from local irregularities are not simultaneous while the SFD is simultaneous for the three different propagation paths, the three sets of data can be used to average out or reduce the noise from local irregularities.

Usually during the daytime, 2.4 MHz was reflected from the bottom of the E-layer and was therefore insensitive to the 10-1030A flare radiation. During June (first ATM manned mission), 6 MHz was usually too high a frequency for reflection from the ionosphere for such short path lengths. For many of the SFDs, 4.8 MHz was reflected only as an extraordinary wave because the ionosphere peak electron density was too low for reflection of the ordinary wave. The nine channels of Boulder HF Doppler data for the period April 1, 1973 through February 3, 1974, were searched for SFDs. Ionograms recorded at Boulder were used to determine the preflare electron density as a function of height.

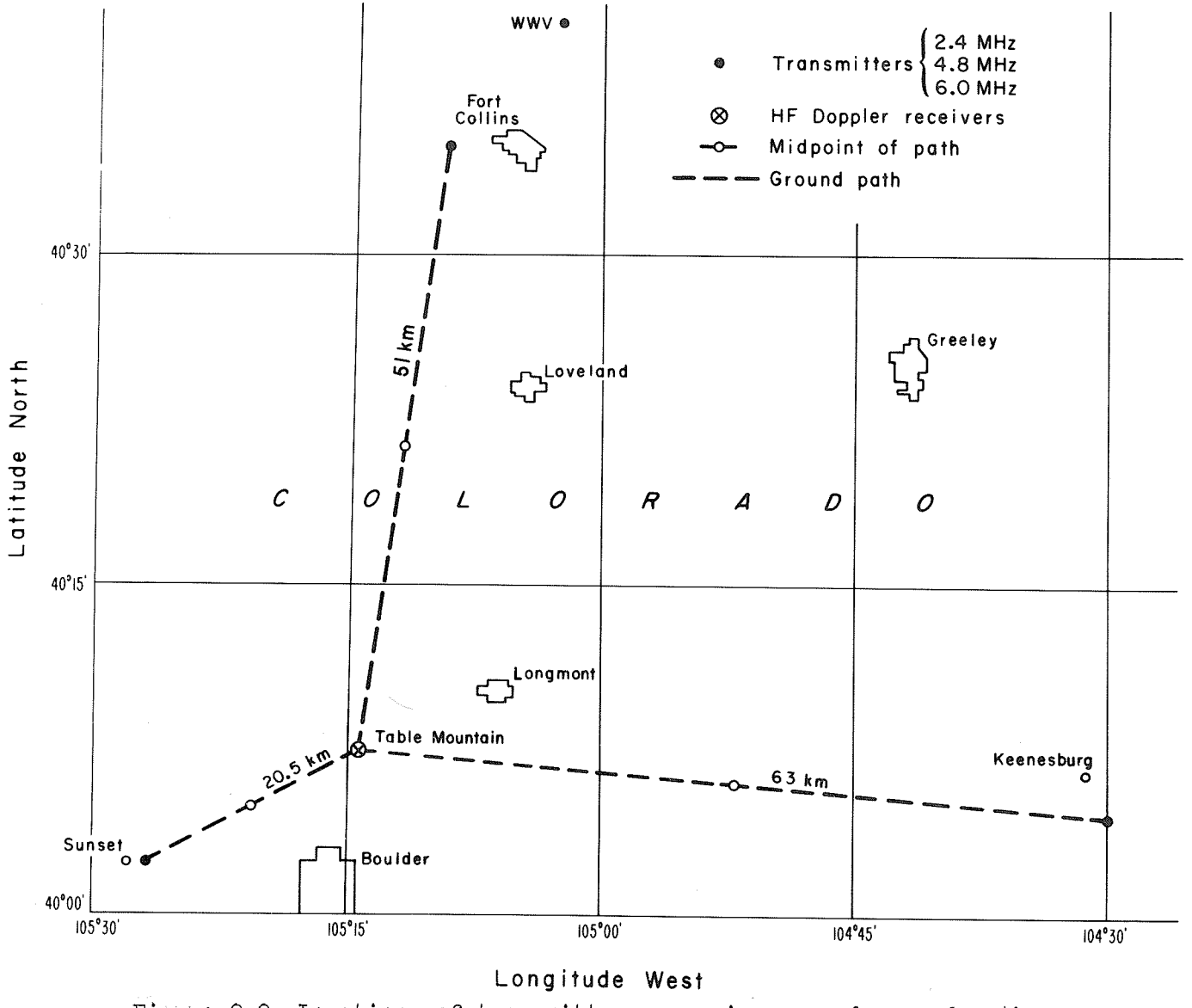

Figure 2.2 Locations of transmitters, receivers, and ground paths for HF Doppler observations near Boulder, Colorado.

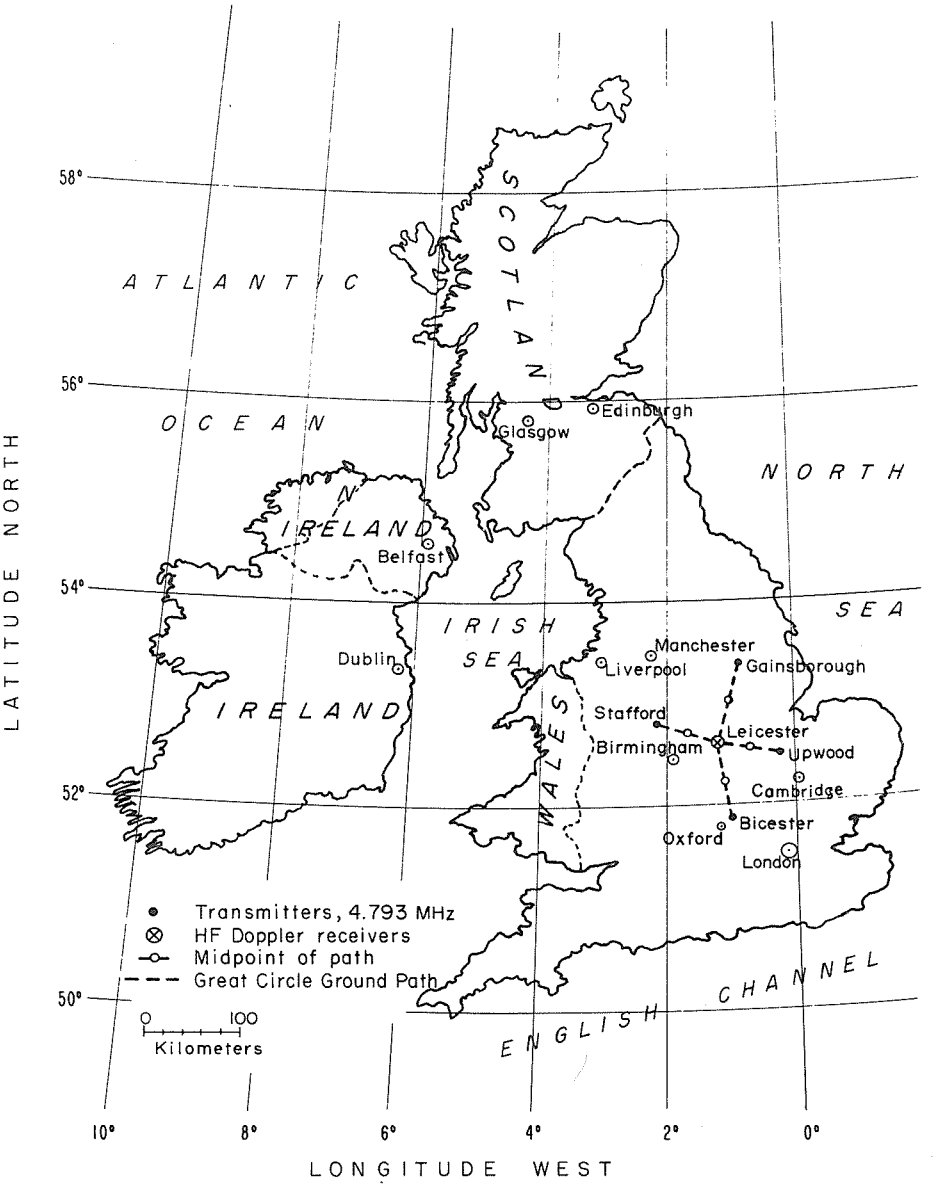

Figure 2.3 Locations of transmitters, receivers and ground paths for HF Doppler observations at Leicester, England.

2.3 HF Doppler Observations in England

HF Doppler observations are made at the University of Leicester in England in order to study traveling ionospheric disturbances that are excited in the auroral region and travel toward the southeast over England. Four nearly vertical propagation paths are used. The ground paths are shown in Figure 2.3. The four transmissions are separated by 3 Hz intervals and are therefore observed by one receiver. The individual frequency deviations are separated through frequency spectral analysis. These observations were studied for several of the solar flares observed by ATM-SKYLAB at times too early for SFD observations in Boulder or Sacramento Peak Observatory. Ionograms from Slough, just west of London, were used to estimate the preflare ionosphere over Leicester.

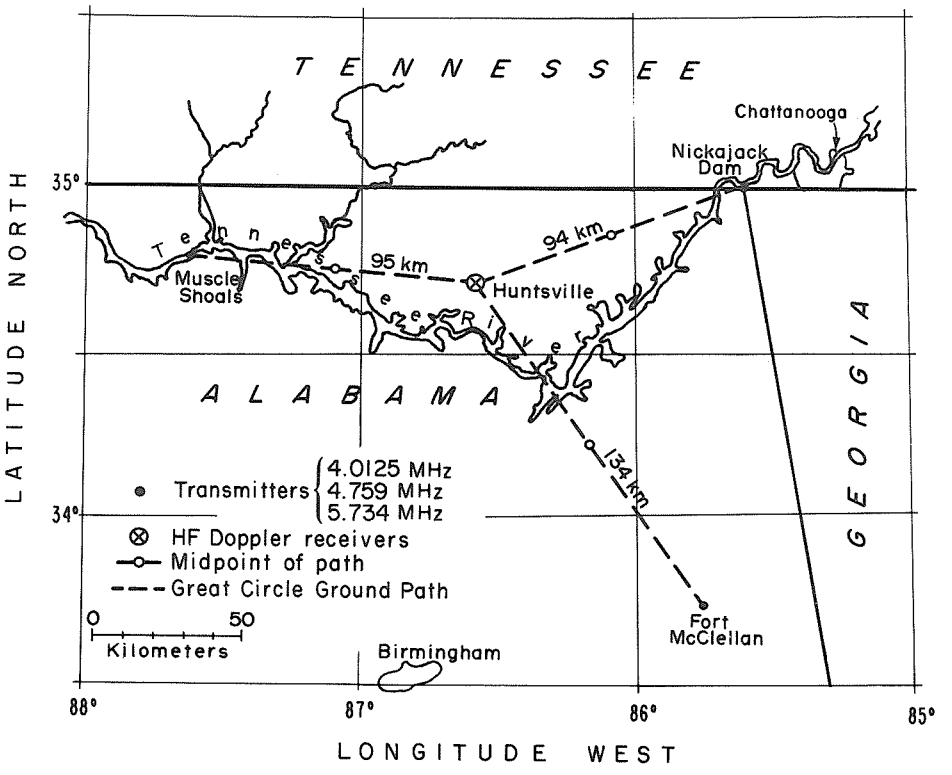

Figure 2.4 Locations of transmitters, receivers, and ground paths for HF Doppler observations at the NASA Marshall Space Flight Center, near Huntsville, Alabama.

2.4 HF Doppler Observations at NASA Marshall Space Flight Center

Figure 2.4 illustrates the HF Doppler experiment at NASA Marshall Space Flight Center near Huntsville, Alabama, which was designed to study moving ionospheric irregularities including traveling waves excited by static ground tests of large rocket engines. The experiment is similar to that at the University of Leicester, but includes more frequencies to obtain information on the variations with height. Observations for several flares observed by the ATM-SKYLAB experiments during the second and third manned missions were studied. Ionograms were not available for this locality for these events, so the preflare ionosphere was estimated from ionospheric conditions at similar latitudes and local times.

2.5 HF Doppler Observations in Hawaii

HF Doppler measurements are made by the Radio Science Laboratory of the University of Hawaii at the field stations shown in Figure 2.5, under Grant Number GA-23964 of the National Science Foundation, to observe SFDs, various types of traveling ionospheric disturbances, and other time variations of the ionosphere. SFDs are routinely detected, scaled, and then reported in *Solar-Geophysical Data*. Ionograms recorded at Maui, Hawaii, were used to determine the preflare ionosphere electron density as a function of height. SFDs observed in Hawaii were used to confirm the detailed time structure of many of the SFDs observed near Boulder, and were the sole source of data for many flares observed by ATM-SKYLAB, especially during the 0000 to 0400 UT period.

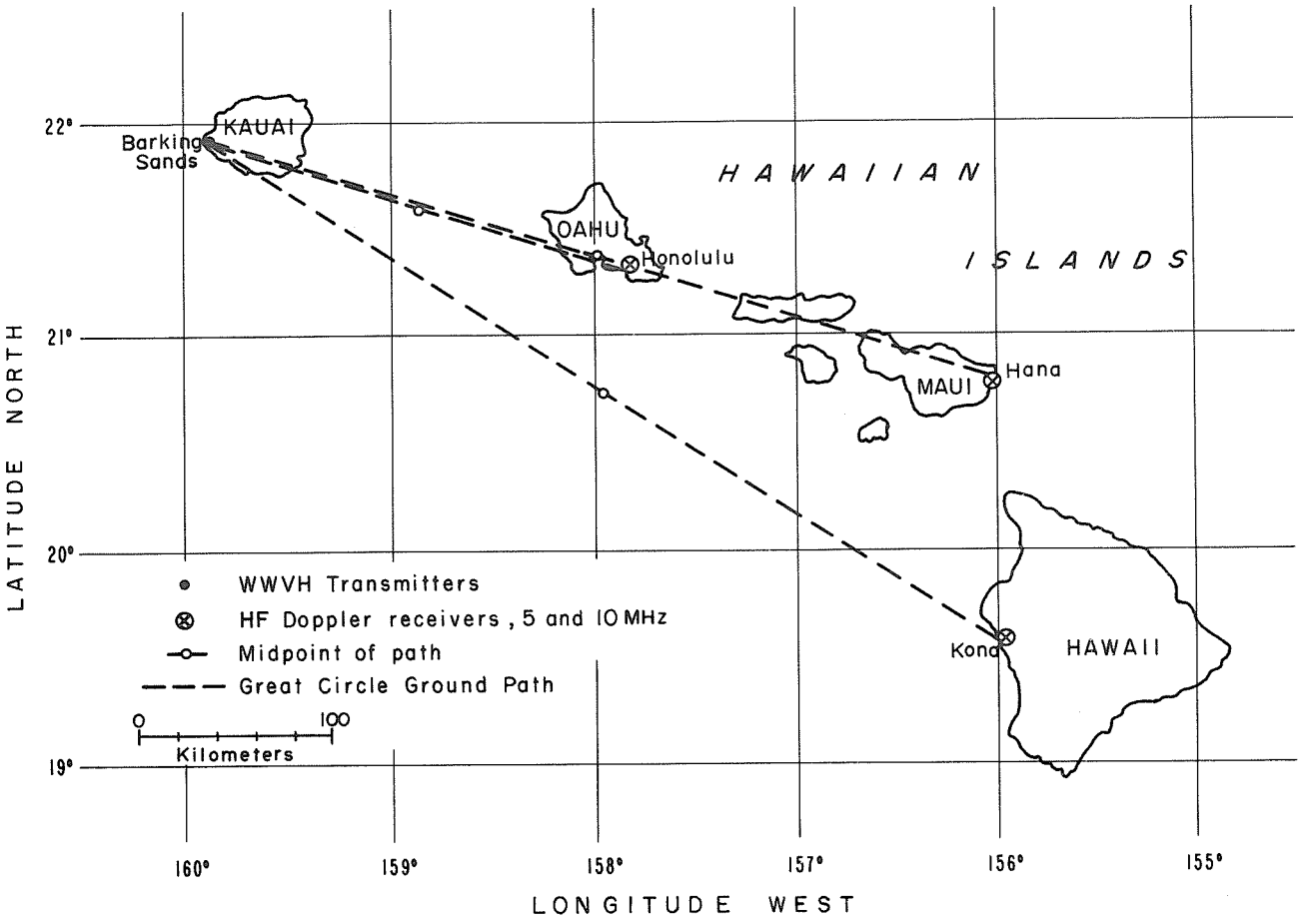

Figure 2.5 Locations of transmitters, receivers, and ground paths for HF Doppler observations in Hawaii.

3. SFD ANALYSIS PROCEDURES

The magnetic tape recordings of frequency deviations in the 0.1 to 100 Hz range are replayed at speeds from about 25 times up to about 2,000 times the speed at which the data were recorded, where the lower speeds are used for large SFDs when high time resolution is desired and the higher speeds are used when searching for the occurrence of events. The speed-up in replaying the data shifts the frequency range into the audio range. The data are then processed by standard audio spectral analyzers. Two types of spectra analyzers are usually used. First a Rayspan is employed to make records of an entire data tape, which usually contains two weeks of data. These records are used in searching for the occurrence of special events, e.g. SFDs, and to study daily variations. The latter information is used in the analysis of SFDs by determining the extent of changes in the ionosphere between the latest available preflare ionogram and the start of the SFD. One can also tell whether the HF Doppler propagation path is reflected from the bottom of the E-layer or from the F-layer because the amplitude of the background frequency deviations are much larger in the latter case than in the former.

Once the times of SFDs are determined, sonagrams like that shown in Figure 3.1 are made for a small time interval including the SFD for each channel of data. The preflare frequency deviation is offset from zero by the HF Doppler recording instrumentation so one can distinguish a decrease from an increase with respect to the average value. Several sonagrams are usually made for each HF Doppler channel for each SFD for the following reasons. When significant absorption of the HF radio wave occurs during the solar flare, one playback gain is used to show the preflare and postflare frequency deviations clearly. A second higher gain is used to show the main part of the SFD, where now the preflare and postflare period will usually be complicated by minor noise. Higher gains may then be used for the late portion of the SFD when the soft x-ray and flare-induced absorption are at a maximum. Slower playback speeds are used to attain higher time resolution, but unfortunately, while the time scale is increased, the frequency scale is decreased. Nonlinear amplification is used to generate harmonics of the primary frequency deviation in order to effectively increase the frequency deviation scale for the harmonics. Some of the SFDs discussed later were scaled from third or fifth harmonics. The frequency as a function of time f(t) is then digitized for each HF Doppler channel that observed the SFD clearly, using a Hewlett-Packard scaler and calculator Model 9820A. The frequency deviation $\Delta f(t)$ during an SFD is simply $\Delta f(t) = f(t) - f_0$, where f_0 is the preflare value of f(t).

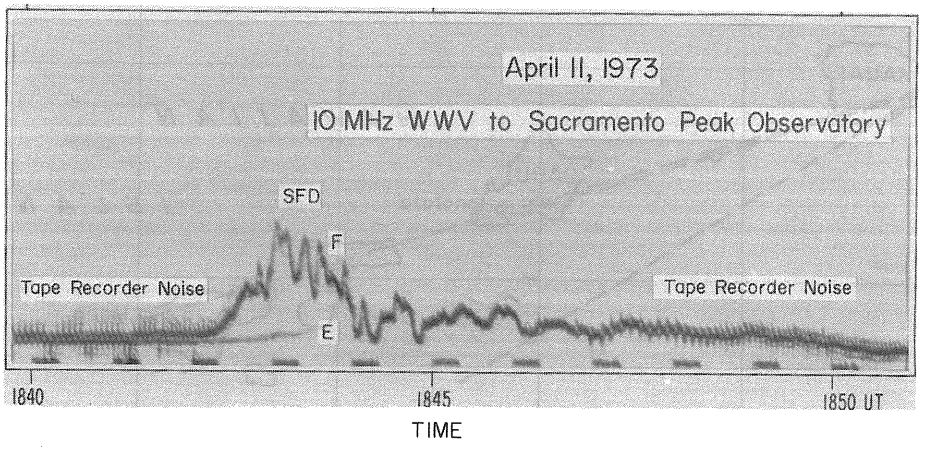

Figure 3.1 The sonagraph record of the SFD of 1843UT April 11, 1973.

The procedure used to calculate the 10-1030A flux enhancement ($\Delta\Phi$) for all the results in this atlas was method 3 of Donnelly [1970, p. 75]. It is the most suitable method for application to a large number of events. This method involves two main related simplifying assumptions, namely (1) that the time rate of change of electron density (dN_e/dt) in the ionosphere during the solar flare is approximately constant with height from just above the bottom of the E-layer (h_o) to the height of reflection (h_r) and (2) the electron loss time constant $\tau(h)$ is approximately constant with height over the range from h_o to h_r. The first assumption is approximately satisfied at heights below about 200 km if the second assumption is true and because the EUV flare spectrum is spread over the 10-1030A range in continuum emission and in a large number of emission lines. This spread spectrum leads to the rate of production of ionization being roughly constant in the 110 to 200 km altitude range. The second assumption is not strictly valid for some of the events, so those cases are identified later in the atlas. For those events of particular relevance to the ATM-SKYLAB observations, the sensitivity of the results to the assumed effective electron-loss time constant is illustrated.

The first assumption simplifies the relation between Δf and dN_e/dt [Agy *et al.*, 1965], namely

$$\frac{dN_e}{dt} \approx \Delta f \frac{f_v c}{k(h'_r - h_o)} \qquad (1)$$

in the altitude range from h_o to h_r, where $k = 80.6\ Hz^2m^3$, f_v is the equivalent vertical incidence frequency, c is the speed of light and h'_r is the virtual height of reflection. Transmission curves [Smith, 1939] and ionograms taken just before the flare at a location near the HF Doppler propagation path were used to determine h'_r, h_o and f_v for each event and channel analyzed.

Equation (1) was evaluated numerically and also integrated from the start of the event to time t to determine $\Delta N_e(t)$ in the upper E- and F1-region of the ionosphere. The rate of flare-enchanced production of ionization $\Delta q(t)$ was then computed for an effective electron loss time constant τ_{eff} from the electron continuity equation,

$$\Delta q(t) = \frac{dN_e}{dt} + \frac{\Delta N_e}{\tau_{eff}} + B_{eff}(\Delta N_e)^2 \qquad (2)$$

The nonlinear term in (2) was small relative to the $\frac{\Delta N_e}{\tau}$ term for all the flares discussed in this atlas.

The energy flux enhancement was then computed from

$$\Delta\Phi(10\text{-}1030A,t) = a \sec(\chi)\, \Delta q(t) \qquad (3)$$

where χ is the solar zenith angle at the midpoint of the propagation path at the time of the peak of the event and a = 6.56×10^{-13} Watt-m-sec. [Donnelly, 1970].

The values of τ_{eff} and B_{eff} were determined from models of $\alpha_{eff}(h)$ $\beta_{eff}(h)$. The electron density as a function of height was calculated for each flare and HF Doppler observatory using the corresponding preflare ionograms and the methods of Wright [1967]. The true height of reflection h_r was then determined from $N_e(h)$, where $N_e(h_r) = f_v^2/k$. Using several models of $\alpha_{eff}(h)$ and $\beta_{eff}(h)$, including those of Mitra and Banerjee [1971], τ and B were computed as a function of altitude from $\tau(h) = [2\alpha_{eff}(h)N_e(h)]^{-1}$, or $\tau(h) = \beta^{-1}$ at the higher altitudes, and $B(h) = \alpha_{eff}(h)$, or $B(h) = 0$ at altitudes where β applies. Averages of $\tau(h)$ and B(h) were computed over the height range from h_o to h_r to determine τ_{eff} and B_{eff}.

The $\Delta\Phi_{max}$(10-1030A) values computed using method 3 are estimated to be accurate to within a factor of four [Donnelly, 1970]. The impulsive structure in $\Delta\Phi$(10-1030A, t) with time constants less than τ_{eff} (see (2)) are insensitive to the height variations of τ or to the $\alpha(h)$ and $\beta(h)$ models, while the flux variations with time variations larger than τ_{eff} are quite sensitive. Ionospheric variations unrelated to the solar flare effects produce noise in the SFD observations that mainly affect the $\Delta\Phi$(10-1030A) estimates during the slow flare emissions. SFD data provide good information on the impulsive emissions of flares, poor information on the slow flare emission, and no information on the nonflare solar radiation.

4. OBSERVATIONS DURING TWO SOLAR ROTATIONS BEFORE THE ATM-SKYLAB

In order to provide background information on the EUV flaring of the active regions whose remnants were observed during the first manned mission of ATM, and to place the EUV bursts during the ATM observations in perspective, the SFD observations from April 1 to May 28, 1973 will be discussed. The Zurich relative sunspot numbers in April and May were lower on the average than in 1967 through 1972, but were generally higher than during the first and third manned ATM observations. The sunspot numbers during the first week in September during the second period of manned ATM observations exceeded the sunspot numbers in April and May; however, this pre-ATM period was richer in large EUV bursts, at least during the daylight observing period of the SFD observations studied.

Figures 4.1 and 4.2 demarcate the periods when SFDs ($\Delta f_{max} \geq 0.2$Hz) could have been observed on at least one of the HF Doppler data channels at Sacramento Peak Observatory and near Boulder, respectively. Sunrise in the ionosphere preceeds sunrise at the ground. The dotted lines indicate the times when all the channels of received transmissions were dominated by paths reflected off the bottom of the E-layer or sporadic E-layers. Such propagation paths are much less sensitive to EUV bursts than propagation paths reflected in the F-region because they involve only the ionospheric effects at heights below about 110 km produced mainly by the 1-10A flare radiation. Hence, the dotted lines mark periods of low sensitivity for detecting SFDs. Once an SFD is detected, further spectral analysis of oblique path data with high gain may bring out a larger SFD on a weaker F-region path in spite of the strong E-region path. In Figure 3.1, the E-region path is weaker than the F-region path and is lost due to the large flare-induced absorption enhancement (SWF).

The frequency deviations caused by the rising sun and the transient build-up of the ionosphere are of the order of 1 Hz and complicate the detection of SFDs. Large solar zenith angles (χ) reduce the magnitude of the SFD for a given strength of EUV burst. For $\chi \leq 85°$, $\Delta f \propto \cos \chi$. Usually, SFDs are not analyzed for $\chi \geq 80°$ because the frequency deviations are small, because the ionosphere cannot be adequately approximated as a horizontally or spherically stratified medium, and because χ and the background frequency deviaitons and nonflare ionization are time varying. Sunset at the ionospheric heights of the HF Doppler paths does not produce a distinct signature in the frequency deviations, so $\chi = 90°$ was used as a practical end to SFD observations.

Table 4.1 lists the main features of SFDs observed. Note that some events have results listed for more than one transmission frequency or receiving station. These were cases that were analyzed in detail. Secondary peaks are listed when their peak frequency deviation was greater than one-third the maximum value and the adjacent valleys were less than two-thirds that particular peak. The time of a peak in the frequency deviation marks the time of impulsive structure in the 10-1030A radiation, i.e., either a peak in the radiation or the end of rapid rise, which may then be followed by a slow rise in the radiation and a slow decrease in the frequency deviation. The time of the main zero crossing is important in that $\Delta\Phi_{max}$(10-1030A) will occur at or before the main zero crossing and at or later than the maximum frequency deviation. The start time in the case of initial gradual rises may vary from one SFD channel to another by about one minute, depending on the background of frequency deviations unrelated to flares. The end time of an SFD is usually very uncertain, since the SFD frequency deviation approaches asymptotically the background non-flare variations. The SFD end time probably preceeds the end of the 10-1030A flare radiation. Although the magnitude of $\Delta\Phi_{max}$(10-1030A) is usually proportional to Δf_{max}, their relation also depends on the solar zenith angle, transmission frequency, and the path of the HF Doppler radio wave in the ionosphere. SFDs observed on paths reflected from the bottom of the E-layer (see comment 15 in Table 4.1) have small Δf_{max} values relative to $\Delta\Phi_{max}$(10-1030A). Note that several of the SFDs are classified as large ($\Delta f_{max} \geq 4.5$ Hz). None of the SFDs during ATM-SKYLAB was that large.

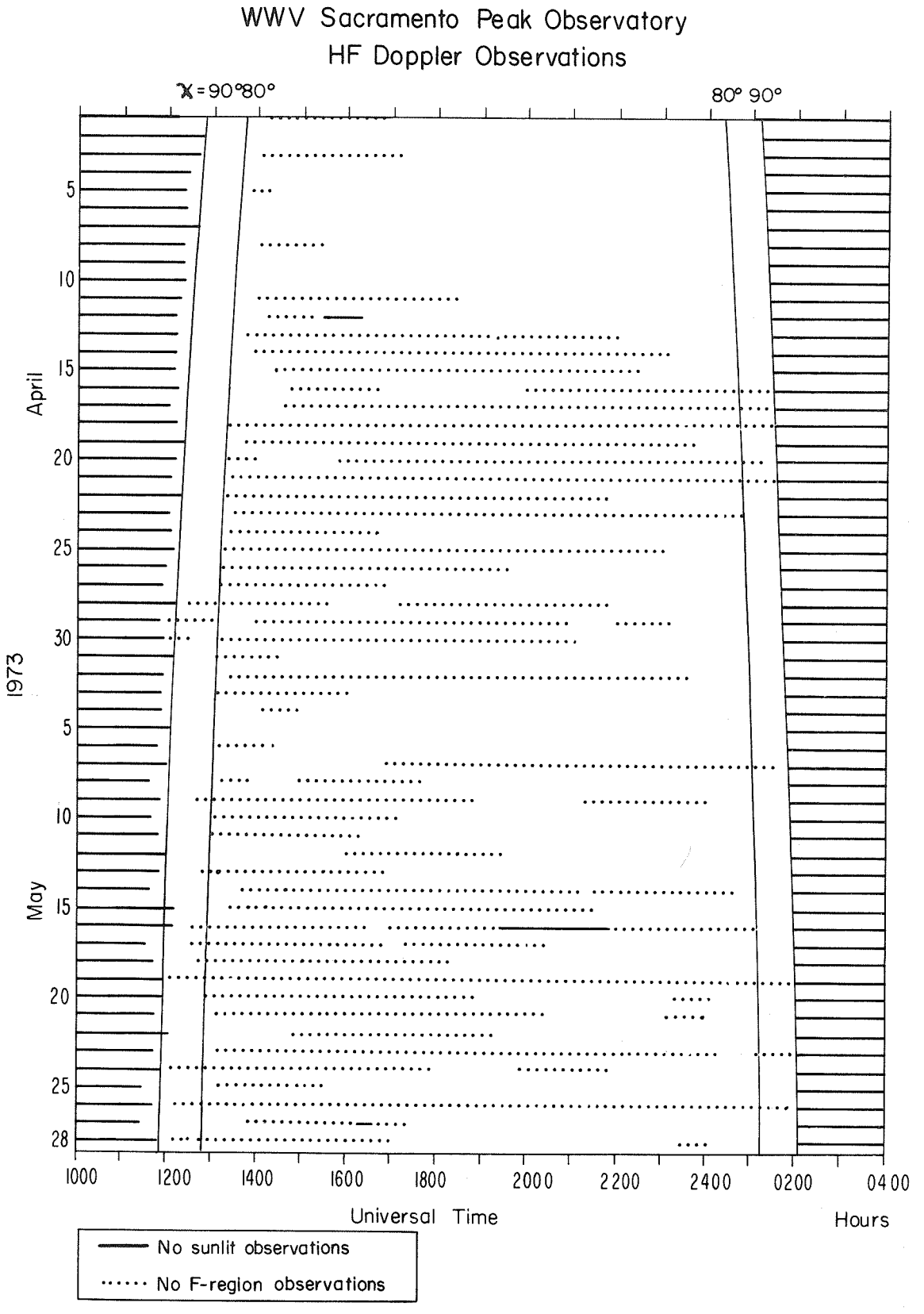

Figure 4.1 SFD observing time at Sacramento Peak Observatory during two solar rotations prior to the ATM observations.

Clear areas indicate good observations, dotted indicate reduced sensitivity, solid line indicates no observations.

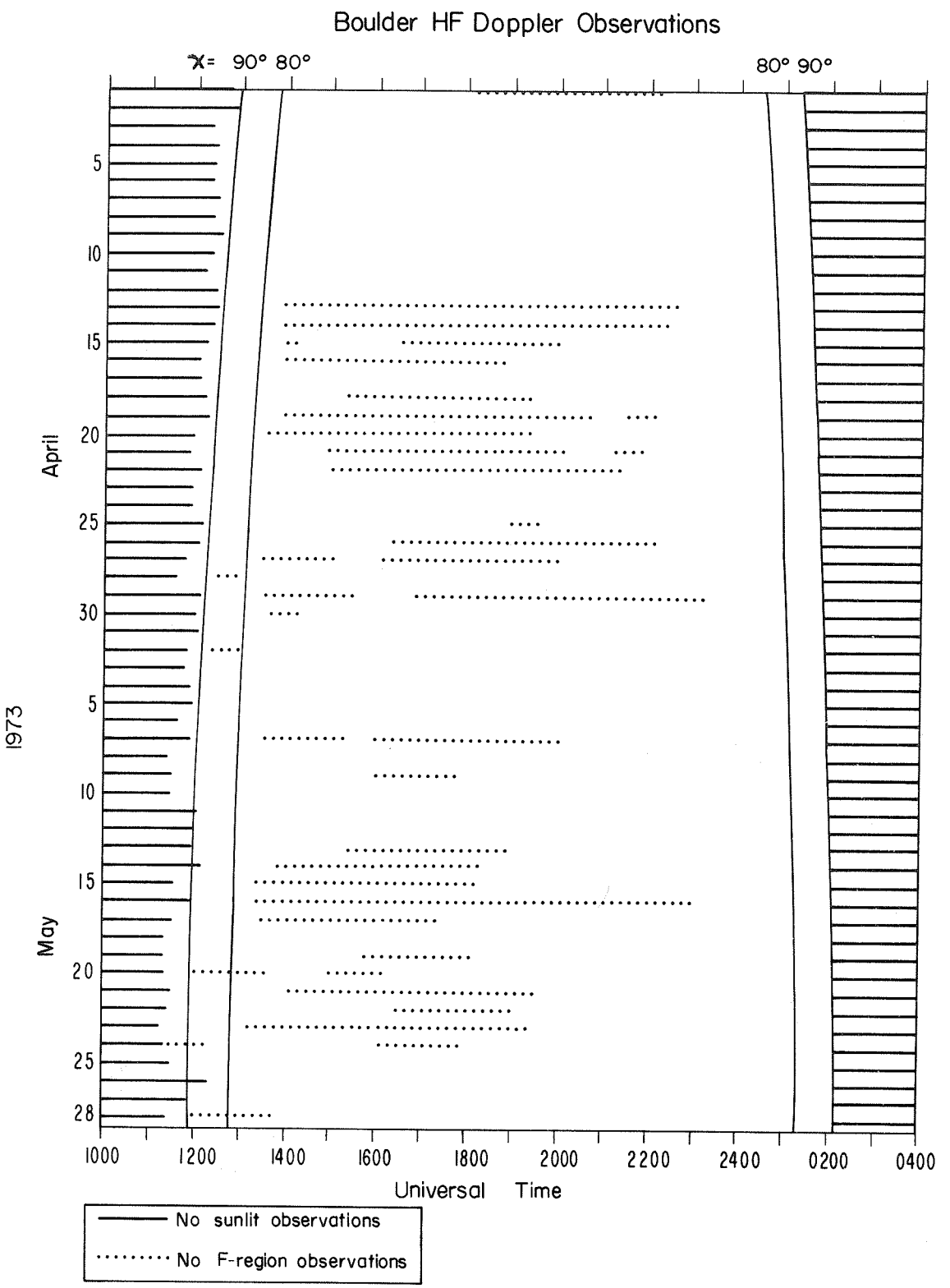

Figure 4.2 SFD observing time near Boulder, Colorado during two solar rotations prior to the ATM observations.

Clear areas indicate good observations, dotted indicate reduced sensitivity, solid line indicates no observations.

Table 4.1 SFDs During Two Solar Rotations Before the ATM-SKYLAB Observations

SFD OBSERVATIONS

DATE			UNIVERSAL TIME				PEAK FREQUENCY DEVIATION		TRANSMITTER CALL LETTERS	FREQUENCY		
MONTH	DAY	YEAR	START	MAXIMUM	ZERO CROSSING	END	HZ	HF DOPPLER STATION		MHZ		COMMENTS
4	1	1973	1529. U	1534.6	1540. U	1548. U	1.2	SUNSET, COLCRADO		6.0	10	4 8 18
				1536.1			1.0					
4	1	1973	1529. U	1534.6	1540. U	1550. U	1.3	FORT COLLINS, COLORADO		6.0	10	4 8 17 18
				1536.0			1.0					
4	1	1973	1524. U	1534.6	1538. U	1555. U	1.6	FT. COLLINS TO SAC PEAK	WWV	5.000	10	4 15
4	1	1973	1702. U	1703.2	1706.6	1714. U	0.6	FT. COLLINS TO SAC PEAK	WWV	15.000	4	10 19
				1705.1			1.2					
4	1	1973	2202.	2202.9	2216.7	2235.	0.8	FT. COLLINS TO SAC PEAK	WWV	5.000	4	5 7
				2205.1			0.9					
				2207.0			1.1					
4	2	1973	1937.	1939.8	1943.7	1950. U	0.4	FT. COLLINS TO SAC PEAK	WWV	10.000		
4	3	1973	1523. U	1534.	1531.	1535. U	0.1	FT. COLLINS TO SAC PEAK	WWV	10.000	9	15
4	3	1973	1850. U	1852.7	U	1913. U	0.5	FT. COLLINS TO SAC PEAK	WWV	10.000	9	
4	3	1973	1921. U	1921.2	1921.4	1923. U	0.2	FT. COLLINS TO SAC PEAK	WWV	10.000	9	
4	3	1973	1920.	1921.	U	1922.	0.2	KAUAI TO U. OF HAWAII	WWVH	5.000	9	
4	4	1973	2200.	2202.8	2205.2	2215	0.4	FT. COLLINS TO SAC PEAK	WWV	10.000		
				2204.9			0.2					
4	7	1973	2252. U	2256.0	2256.6U	2305. U	0.2	FT. COLLINS TO SAC PEAK	WWV	10.000	11	
4	8	1973	2238. U	2242.3	2243.3U	2256. U	0.4	FT. COLLINS TO SAC PEAK	WWV	10.000	11	
4	8	1973	2241.	2242.	2243.	2245.	0.3	KAUAI TO U. OF HAWAII	WWVH	5.000		
4	9	1973	1542.	1543.3	1543.5	1548. U	0.5	FT. COLLINS TO SAC PEAK	WWV	10.000	2	
4	9	1973	1617.3	1623.8	1924.1	1629. U	1.7	FT. COLLINS TO SAC PEAK	WWV	10.000	2	
4	9	1973	1731.3	1732.7	1747.7	1800. U	0.7	FT. COLLINS TO SAC PEAK	WWV	15.000	6	8 19 20
				1734.6			0.8					
				1745.8			3.8					

Table 4.1 - (continued)

DATE			UNIVERSAL TIME				PEAK FREQUENCY DEVIATION		TRANSMITTER CALL LETTERS	FREQUENCY			
MONTH	DAY	YEAR	START	MAXIMUM	ZERO CROSSING	END	HZ	HF DOPPLER STATION		MHZ			COMMENTS
4	9	1973	1742.7	1745.8	1747.3	1800. U	1.3	FT. COLLINS TO SAC PEAK	WWV	10.000	6		
4	9	1973	1840. U	1845.0	U	1902. U	0.2	FT. COLLINS TO SAC PEAK	WWV	15.000	11	6	
				1847.4			0.4						
4	9	1973	1904. U	1906.2	1903. U	1910. U	0.2	FT. COLLINS TO SAC PEAK	WWV	10.000	11		
4	9	1973	1928. U	1932. U	1934. U	1940. U	0.4	FT. COLLINS TO SAC PEAK	WWV	15.000	11		
4	9	1973	2026.	2028.2	2029.0	2043. U	0.6	FT. COLLINS TO SAC PEAK	WWV	15.000	2	10	
4	10	1973	1907.5	1909.8	1910.8	1918. U	0.8	FT. COLLINS TO SAC PEAK	WWV	10.000			
				1910.1			1.4						
				1910.5			2.0						
4	10	1973	1908.1	1910.1	1910.8	1918. U	1.2	SUNSET, COLORADO		4.8			
				1910.5			1.8						
4	10	1973	1908.3	1910.0	1910.8	1917. U	1.0	SUNSET, COLORADO		6.0			
				1910.4			1.5						
4	10	1973	1908.	1910.		1911.	1.2	KAUAI TO U. OF HAWAII	WWVH	5.000			
4	10	1973	2135.0	2135.9	2136.6	2144. U	1.7	SUNSET, COLORADO		4.8			
				2136.3			1.0						
4	10	1973	2135.1	2136.0	2136.7	2142. U	1.3	SUNSET, COLORADO					
				2136.3			0.6						
4	10	1973	2134.3	2135.6	2136.5	2143. U	1.3	FT. COLLINS TO SAC PEAK	WWV	10.000			
				2136.2			0.7						
4	10	1973	2135.	2136.		2137. U	1.8	KAUAI TO U. OF HAWAII	WWVH	5.000			
				2136.5			0.8						
4	11	1973	1400.2	1405.3	1406.0	1415.	3.9	SUNSET, COLORADO		4.8	2	4	18
4	11	1973	1400.6	1405.3	1406.0	1415.	4.1	KEENESBURG, COLORADO		4.8	2	4	18
4	11	1973	1400.3	1405.3	1405.9	1415.	2.8	FT. COLLINS TO SAC PEAK	WWV	10.000	2	4	10
4	11	1973	1842.2	1842.8	1849.7	1857.	2.8	FT. COLLINS TO SAC PEAK	WWV	10.000	1	7	19 22
				1843.1			4.5						
				1843.4			3.8						
				1843.6			3.6						
				1843.9			2.8						
				1844.6			1.6						

Table 4.1 - (continued)

DATE			UNIVERSAL TIME				PEAK FREQUENCY DEVIATION		TRANSMITTER CALL LETTERS	FREQUENCY	
MONTH	DAY	YEAR	START	MAXIMUM	ZERO CROSSING	END	HZ	HF DOPPLER STATION		MHZ	COMMENTS
4	11	1973	1841.	1843.			1.2	KAUAI TO U. OF HAWAII	WWVH	5.000	13
4	11	1973	1841.	1843.			1.2	KAUAI TO U. OF HAWAII	WWVH	10.000	6
				1844.			0.5				
4	11	1973	2020.	2026.5		2036.	0.3	FT. COLLINS TO SAC PEAK	WWV	10.000	6 9 10
4	11	1973	2251.	2251.4	2257.0	2255.	0.22	FT. COLLINS TO SAC PEAK	WWV	10.000	9 10
4	13	1973	0030.	0031.		0032.	0.4	KAUAI TO U. OF HAWAII	WWVH	5.000	
4	13	1973	0437.	0439.		0441.	0.5	KAUAI TO U. OF HAWAII	WWVH	10.000	
4	13	1973	2051.	2052.0		2055.	0.1	FT. COLLINS TO SAC PEAK	WWV	10.000	9 15
4	14	1973	2139.	2140.2	2140.8	2146.	0.7	FT. COLLINS TO SAC PEAK	WWV	5.000	2
4	14	1973	2136.8	2140.3	2140.6	2145. U	2.3	SUNSET, COLORADO		4.8	2 4 18
4	15	1973	1716.	1716.3		1719.	0.7	FT. COLLINS TO SAC PEAK	WWV	5.000	11
4	15	1973	2236.	2237.9	2238.8	2241.	0.2	FT. COLLINS TO SAC PEAK	WWV	10.000	15
4	15	1973	2236.	2237.	2238.	2239.	0.9	KAUAI TO U. OF HAWAII	WWVH	5.000	
4	15	1973	2313.	2315.1	2315.3	2316.	0.3	KAUAI TO U. OF HAWAII	WWVH	5.000	
4	16	1973	1724.	1731.8	1733.	1740.	0.5	FT. COLLINS TO SAC PEAK	WWV	5.000	
4	22	1973	1407.	1409.2		1415.	0.1	FT. COLLINS TO SAC PEAK	WWV	5.000	11
4	24	1973	1411.5	1412.6	1414.3		0.3	FT. COLLINS TO SAC PEAK	WWV	10.000	
4	24	1973	1925.	1930.	1933	1945.	0.1	FT. COLLINS TO SAC PEAK	WWV	10.000	3 12 15
4	24	1973	1925.	1927.	1928.	1930.	0.7	KAUAI TO U. OF HAWAII	WWVH	5.000	
				1928.			0.5				
4	26	1973	1958.			2025.		FT. COLLINS TO SAC PEAK	WWV	10.000	13 15
4	29	1973	1841.3	1843.3	1845.0	1850.	0.2	FT. COLLINS TO SAC PEAK	WWV	10.000	15
4	29	1973	1841.	1842.	1844	1845.	0.7	KAUAI TO U. OF HAWAII	WWVH	5.000	
				1843.			0.6				
4	29	1973	2056.5	2059. +				FT. COLLINS TO SAC PEAK	WWV	10.000	13
4	30	1973	1727.5	1729.4	1731.	1740.	0.3	FT. COLLINS TO SAC PEAK	WWV	10.000	
4	30	1973	1727.	1729.	1730.	1730.	1.1	KAUAI TO U. OF HAWAII	WWVH	5.000	
				1729.5			0.7				

Table 4.1 - (continued)

DATE			UNIVERSAL TIME			PEAK FREQUENCY DEVIATION		TRANSMITTER CALL LETTERS	FREQUENCY	
MONTH	DAY	YEAR	START	MAXIMUM	ZERO CROSSING	END	HZ	HF DOPPLER STATION		MHZ	COMMENTS
4	30	1973	2252.3	2256. +		2308.	0.6	FT. COLLINS TO SAC PEAK	WWV	10.000	13 15
4	30	1973	2249. U	2253.3	2259.2	2306.	1.2	SUNSET, COLORADO		4.8	4 6 8
				2254.4			0.6				
				2255.9			0.5				
4	30	1973	2252.	2253.5		2300.	0.5	KAUAI TO U. OF HAWAII	WWVH	10.000	
				2254.			0.5				
				2255.			0.3				
				2256.			0.3				
5	1	1973	1914.0	1915.2	1915.6	1921.	1.1	FT. COLLINS TO SAC PEAK	WWV	10.000	2
5	1	1973	1914.1	1915.1	1915.6	1919.	3.9	SUNSET, COLORADO		4.8	
5	1	1973	1914.	1915.	1916.	1921.	1.2	KAUAI TO U. OF HAWAII	WWVH	5.000	
5	1	1973	2032.	2034.6+		2115.	0.3+	FT. COLLINS TO SAC PEAK	WWV	10.000	13
5	2	1973	0032.6	0033.2	0034.0	0037.	0.3	FT. COLLINS TO SAC PEAK	WWV	10.000	2 22
5	2	1973	2040.	2044.0		2102.-	0.2	FT. COLLINS TO SAC PEAK	WWV	10.000	3 13 15
5	2	1973	2039.	2040.	U	2100	0.3	KAUAI TO U. OF HAWAII	WWVH	5.000	13
				2041.			0.6				
5	3	1973	0146.	0148. -	0148.	0150.	0.5	KAUAI TO U. OF HAWAII	WWVH	5.000	
5	3	1973	0151.	0153.	0155.	0156.	0.4	KAUAI TO U. OF HAWAII	WWVH	5.000	
				0154.			0.3				
5	4	1973	2038.5	2039.5		2050.	0.3	FT. COLLINS TO SAC PEAK	WWV	10.000	10
5	5	1973	1711.2	1716.0	1722.3	1735.	8.8	FT. COLLINS TO SAC PEAK	WWV	10.000	1 6
				1717.4			3.0				
				1717.8			4.5				
				1718.7			3.7				
5	5	1973	1714.1	1716.0	U		12.3	SUNSET, COLORADO		4.8	1 6 13
5	5	1973	1713.4	1716.0	U		7.0	KEENESBURG, COLORADO		6.0	1 6 13
5	5	1973	1713.7	1716.0	U		6.6	FORT COLLINS, COLORADO		6.0	1 6 13
5	5	1973	1714.	1716.	1722.	1740. U	3.3	KAUAI TO U. OF HAWAII	WWVH	5.000	6
				1717.			1.8				
				1718.			1.5				
				1720.			1.0				

Table 4.1 - (continued)

DATE			UNIVERSAL TIME				PEAK FREQUENCY DEVIATION HZ	HF DOPPLER STATION	TRANSMITTER CALL LETTERS	FREQUENCY MHZ	COMMENTS
MONTH	DAY	YEAR	START	MAXIMUM	ZERO CROSSING	END					
5	6	1973	1456.5	1505.	1503.	1457.4	0.4	FT. COLLINS TO SAC PEAK	WWV	10.000	10
5	17	1973	1908.	1908.9	1912.8	1929.	0.5	FT. COLLINS TO SAC PEAK	WWV	10.000	14 15
5	18	1973	1527.4	1528.2	1534.0	1547.	0.2	FT. COLLINS TO SAC PEAK	WWV	10.000	3 15 22
				1531.3			0.2				
5	18	1973	2153.5	2155.8	2156.8	2219.	5.7	FT. COLLINS TO SAC PEAK	WWV	10.000	1 6
				2156.0			3.6				
				2156.4			2.8				
5	18	1973	2154.6	2155.8	2156.9	2215.	6.8	SUNSET, COLORADO		4.8	1 6
				2155.9			4.3				
				2156.4			3.3				
5	18	1973	2154.4	2155.8	2156.9	2215.	7.5	FORT COLLINS, COLORADO		4.8	1 6
				2156.0			4.7				
				2156.5			3.7				
5	18	1973	2154.4	2155.8	2157.0	2215.	8.7	FORT COLLINS, COLORADO		6.0	1 6
				2156.0			5.4				
				2156.5			4.0				
5	19	1973	2243.	2244.2	2247.8	2255.	10.	KAUAI TO U. OF HAWAII	WWVH	10.000	1
				2244.5			10.5				
5	20	1973	0444.	0445.		0447. +	0.3	KAUAI TO U. OF HAWAII	WWVH	5.000	
5	20	1973	2020.	2022.3	2022.8	2025.	0.4	FT. COLLINS TO SAC PEAK	WWV	10.000	10 22
5	20	1973	2146.5	2147.2		2155.	0.2	FT. COLLINS TO SAC PEAK	WWV	10.000	9 10 22
5	28	1973	1734.2	1735.9		1757. U	1.2	FT. COLLINS TO SAC PEAK	WWV	15.000	6 8 20
				1736.9			1.7				
				1737.8			1.3				
				1739.1			1.1				
				1740.8			1.2				
5	28	1973	1734.9	1735.8	U	1754. U	0.5	KEENESBURG, COLORADO		4.8	4 6 8 21
				1736.8			0.8				
				1739.1			1.0				
				1741.0			1.4				

Table 4.1 - (continued)

DATE			UNIVERSAL TIME				PEAK FREQUENCY DEVIATION		TRANSMITTER CALL LETTERS	FREQUENCY		
MONTH	DAY	YEAR	START	MAXIMUM	ZERO CROSSING	END	HZ	HF DOPPLER STATION		MHZ		COMMENTS
5	28	1973	1734.1	1735.9	1749. U	1755. U	0.7	KEENESBURG, COLORADO		6.0	6	8 18 22
				1736.8			0.9					
				1737.3			0.4					
				1737.7			0.8					
				1738.3			0.6					
				1738.6			0.8					
				1739.0			0.8					
				1740.9			1.0					
5	28	1973	1734. U	1735.9	1746. U	1753. U	0.9	FORT COLLINS, COLORADO		6.0	6	8 18 21 22
				1736.9			1.3					
				1737.7			1.1					
				1739.0			1.2					
				1740.9			1.3					
5	28	1973	1735.0	1736.0	1742.5	1755. U	0.3	KAUAI TO U. OF HAWAII	WWVH	5.000	6	8
				1736.8			0.4					
				1737.9			0.3					
				1738.6			0.5					
				1741.0			0.5					

U uncertain

COMMENT NUMBERS

1. Large SFD, $\Delta f_{max} \geq 4.5$ Hz.
2. Simple spike.
3. Gradual rise and fall, no impulsive structure.
4. Combination of impulsive spikes and gradual fall and rise.
5. Impulsive structure is weak relative to the gradual rise and fall.
6. Much fine-time structure.
7. Marked quasi-periodic fine time structure.
8. SFD very long lasting, $\Delta f > 0$ for >5 minutes.
9. SFD too small for quantitative analysis.
10. Poor SFD data.
11. SFD data too poor for quantitative analysis.
12. SWF
13. Large SWF, SFD trace lost.
14. Time code is inaccurate.
15. Propagation path reflected off the bottom of the E layer, causing the SFD observation to be insensitive to the impulsive EUV burst.
16. Peak frequency deviation not measurable.
17. Δf data inverted.
18. Extraordinary wave.
19. No solution for propagation path.
20. Possibly WWVH rather than WWV.
21. Vertical-incidence data affected by local ionospheric time variations.
22. Data complicated by tape recorder noise.

Table 4.2 lists the times and flux values of up to three peaks in $\Delta\Phi$(10-1030A, t). When more than one channel of data were used to compute $\Delta\Phi$(10-1030A, t) (see column 2 in the table), the times and flux values were averaged to obtain the results in Table 4.2. The peak flux values and peak times from different channels agreed quite well, usually to within 10% of the average value or to within two seconds respectively, although the flux results for the May 5 event range 70% from the average value. For each event in Table 4.2, all available SFD observations were compared to help determine noise and non-flare variations in $\Delta f(t)$, even for the cases where only one channel was carried through to computing $\Delta\Phi$(10-1030A, t). The underlined flux value is the maximum value for that flare event. Some flares had slow peaks, which were larger and later than the impulsive values given in Table 4.2, that are not listed in Table 4.2 because SFDs do not provide accurate estimates for such slow emissions. Two of the events listed in Table 4.2 vary slowly near their maxima and therefore their peak time is less accurately known. Many of the events in Table 4.1 do not appear in Table 4.2 and were not analyzed to compute $\Delta\Phi$(10-1030A) because the SFD was either not large enough, not of sufficient quality, not from an F-region path, the solar zenith angle was too large, or a large SWF caused the SFD data to be lost. None of the events is a large EUV enhancement, i.e., ($\Delta\Phi_{max}$(10-1030A) $\geq$ 2×10^{-3} Watts m^{-2}) [Donnelly, 1970]. The largest (1716 UT May 5, 1973) is more than an order of magnitude smaller than the largest events observed from 1960 to 1970, e.g., 1328 UT November 12, 1960; 1527 UT August 28, 1966; and 1841 UT May 23, 1967 [Donnelly, 1970]. Five of the EUV bursts are in the medium class ($5\times10^{-4} \leq \Delta\Phi_{max}$(10-1030A) $< 2\times10^{-3}$ Watts m^{-2}).

Figure 4.3 shows the SFD of 1535 UT April 1, 1973; and Figure 4.4 shows the $\Delta\Phi$(10-1030A, t) estimate that was computed from the SFD using a model for $\alpha_{eff}(h)$ used previously in analyzing SFD data [Donnelly, 1968], herein called Model 3. These $\Delta\Phi$(10-1030A) results are our best estimate relative to results based on Models 4-7. Models 4, 5, 6 and 7 refer to models of α_{eff} that are equal to $\frac{1}{2}$, $\frac{1}{\sqrt{2}}$, $\sqrt{2}$, and 2 times the α_{eff} of Model 3 respectively. Models 4-7 are intended only to demonstrate the sensitivity of $\Delta\Phi$(10-1030A, t) to the assumed ionospheric electron loss rates. Results using Model 2 based on $\alpha_{eff}(h)$ and $\beta_{eff}(h)$ models of Mitra and Banerjee [1971] are shown for several events later in the atlas. The value of τ_{eff} in Figure 4.4 is unusually high and results from the height of reflection being very high.

The remainder of the chapter presents figures of the SFD observations and derived $\Delta\Phi$(10-1030A, t) estimates. Information on the associated Hα flares and microwave bursts are presented below the figure of the SFD, along with comments on any complications involved in the calculation of $\Delta\Phi$(10-1030A,t). When no comments to the contrary are made, the radio wave was an ordinary wave, the HF Doppler propagation path was adequately determined, and $\tau(h)$ was approximately constant over the range from h_o to h_r. The $\Delta\Phi$(10-1030A, t)/$\Delta\Phi_{max}$ curves are dotted below 0.05 to signify less accuracy for such small values. These curves are sometimes also dashed late in the flare to signify lower accuracy of the flux estimate than for the solid line. Calculations were made using Models 2-7 but best-estimate $\Delta\Phi$(10-1030A, t) results based on Model 3 are the only ones presented here, in order to conserve space. Similarly, results for only one channel of SFD are presented. More extensive results are given later for flares during the ATM observing periods. The exception to these two limitations are the results for the flare of May 18, 1973, shown in Figures 4.27 - 4.38. That SFD was selected for detailed illustration because it includes a long duration slow component which is small in $\Delta f(t)$ yet large in $\Delta\Phi$(10-1030A, t). It is therefore an excellent event for demonstrating how well SFDs determine the impulsive EUV emission and how poorly the slow 10-1030A enhancement, as a function of transmission frequency, path length of the HF Doppler radio wave, and the assumed ionospheric electron loss rates. Discussion of these features is included below the captions of Figures 4.27, 4.29, 4.31, and 4.33.

No estimates of $\Delta\Phi_{max}$(10-1030A) were made for the 2B flare of 2100 UT April 29, 1973, because all the available HF Doppler data were lost due to the large SWF from the soft x-ray enhancement. The HF Doppler traces were lost before any impulsive SFD structure was detected. The 2-35 GHz microwave burst was the largest observed during the periods covered in this atlas. Another type of ionospheric observation that is sensitive to the 1-1030A flare radiation is the measurement of total columnar ionospheric electron content using geostationary radio beacons, where the observed flare effect is called a SITEC. The observed SITEC for this flare was quite large. The time rate of change of the total columnar ionospheric electron density was comparable to that for the flares of 1844 UT April 11, 1973 and 1716 UT, May 5, 1973 (R. Fritz, NOAA, Boulder, Colorado, private communication).

TABLE 4.2

The Impulsive 10-1030A Flux Enhancements Deduced
from SFDs During Two Solar Rotations Before the ATM-SKYLAB Observations

Date 1973	Number of Channels of SFD Data Analyzed To $\Delta\Phi$(10-1030A)	Start Time UT	Peak Time UT	$\Delta\Phi$ (10-1030A)* Peak	Peak Time UT	$\Delta\Phi$ (10-1030A)* Peak	Peak Time UT	$\Delta\Phi$ (10-1030A)* Peak
April 1	2	1529.3	1531.2	2.5×10^{-5}	1534.6	$\underline{6.7\times10^{-5}}$	1536.1	5.8×10^{-5}
April 1	1	1702.4	1703.2	2.5×10^{-5}	1705.5	$\underline{6.1\times10^{-5}}$		
April 1	1	2201.8	2203.8	1.0×10^{-5}	2210.7†	$\underline{4.2\times10^{-5}}$		
April 9	1	1617.3	1623.8	$\underline{2.7\times10^{-4}}$				
April 9	1	1728.7	1732.7	8.4×10^{-5}	1734.7	$\underline{1.4\times10^{-4}}$		
April 9	2	1743.	1745.8	$\underline{1.9\times10^{-4}}$				
April 10	3	1908.1	1910.5	$\underline{4.0\times10^{-4}}$				
April 10	3	2134.4	2135.9	2.6×10^{-4}	2136.3	$\underline{2.7\times10^{-4}}$		
April 11	2	1400.2	1405.3	$\underline{6.1\times10^{-4}}$				
April 11	1	1842.2	1843.1	3.6×10^{-4}	1843.4	3.7×10^{-4}	1843.6	$\underline{4.0\times10^{-4}}$
April 14	1	2137.1	2140.3	$\underline{2.4\times10^{-4}}$				
April 30	1	2249.1	2254.0	2.9×10^{-4}	2254.6	2.9×10^{-4}	2258.9†	$\underline{5.1\times10^{-4}}$
May 1	1	1914.1	1915.2	$\underline{3.2\times10^{-4}}$				
May 5	4	1713.	1716.0	$\underline{9.6\times10^{-4}}$	1717.8	6.8×10^{-4}	1718.7	7.0×10^{-4}
May 18	4	2153.8	2155.8	6.6×10^{-4}	2156.0	5.7×10^{-4}	2156.4	6.0×10^{-4}
May 19	1	2242.2	2244.5	$\underline{6.7\times10^{-4}}$				
May 28	5	1734.	1741.0	$\underline{3.9\times10^{-4}}$				

Underlined peak flux values are the maximum values for the event.

* $\Delta\Phi$(10-1030A) values have the units watts m^{-2}

† Gradual peak

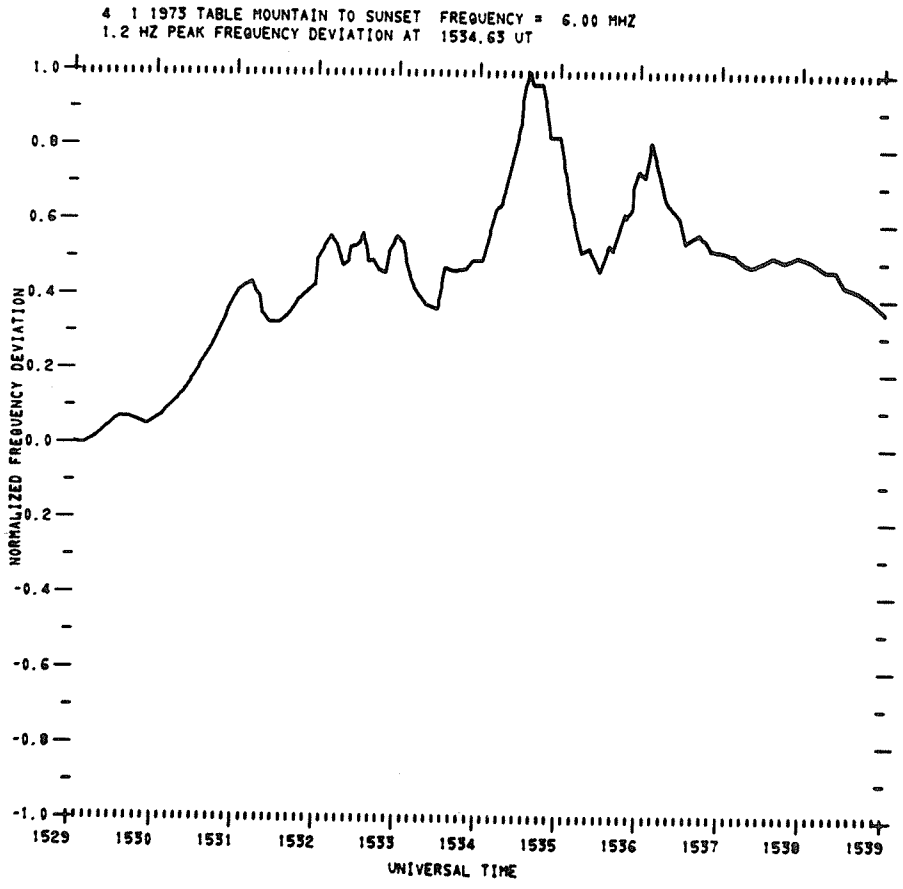

Figure 4.3 SFD of 1535 UT April 1, 1973.

This SFD and impulsive EUV burst accompanied an H_α flare of importance 1N located at S04 E10 (McMath Plage Region 12293), which started at about 1530 UT with maximum phase at 1536 UT. Microwave bursts were reported in Solar-Geophysical Data (SGD) at frequencies up to 15.4 GHz with peak times at frequencies above 2GHz in the range 1536.1 to 1536.5 UT. The HF Doppler radio propagation at 6 MHz was an extraordinary wave; the ordinary wave penetrated the ionosphere. Because of the unusually high altitude of reflection (289 km) of the HF Doppler radio wave for this event, τ_{eff} was very large (~ 22 minutes) and $\tau(h)$ varied significantly near the height of reflection so that the assumption of τ constant with height in the range h_o to h_r is a poor one. However, the secondary peaks (see Tables 4.1 and 4.2) are quite real. Only $\Delta\Phi_{max}$ and which peak produces the maximum (1534.6 or 1536.2 UT would be influenced by the inadequacy of the $\tau(h)$ assumption.

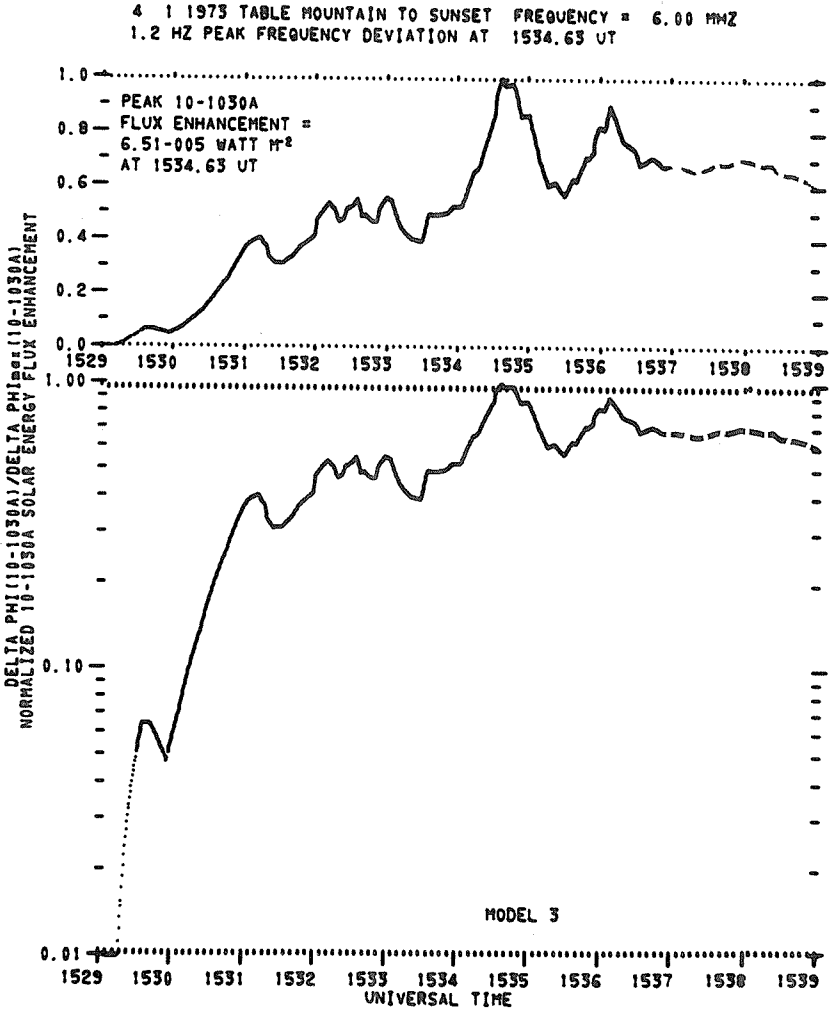

Figure 4.4 Best-estimate 10-1030A flux enhancement of 1535 UT April 1, 1973.

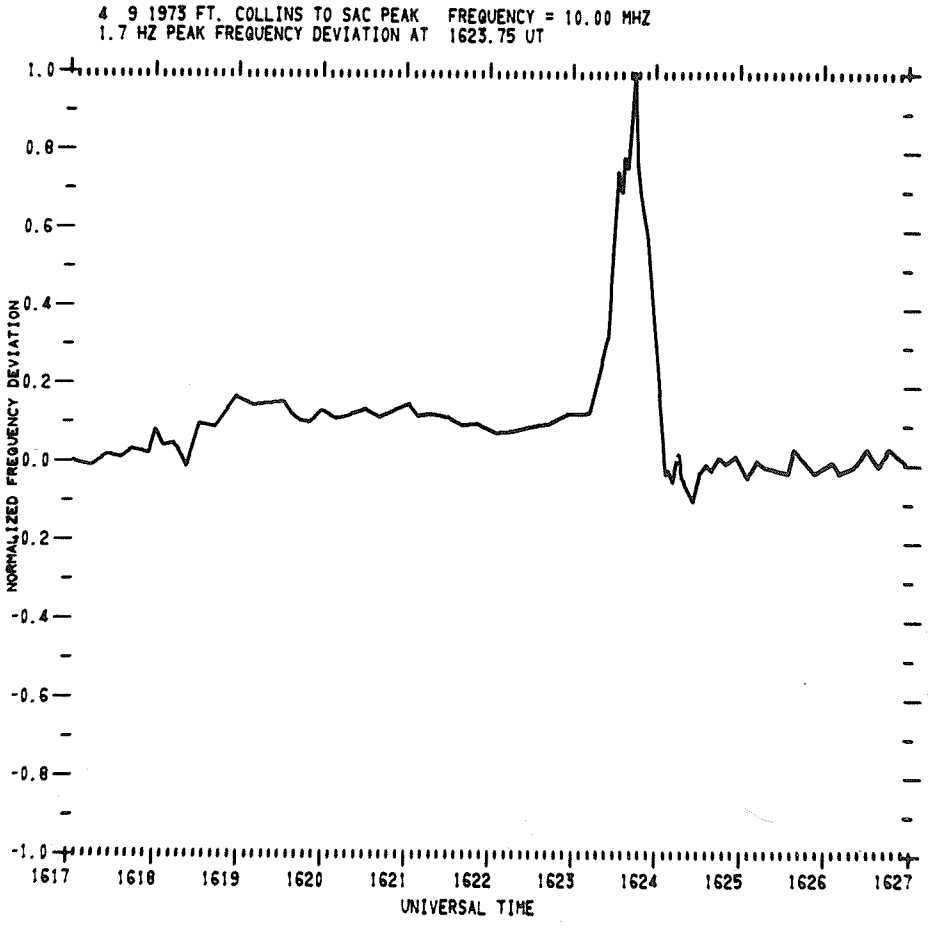

Figure 4.5 SFD of 1624 UT April 9, 1973.

This SFD and impulsive EUV burst accompanied an H_α subflare of normal intensity at S09 E16 (McMath Plage Region 12306, a prolific flare producer), which started at 1621 UT with its maximum phase at 1624 UT. Suprisingly, at 7.0, 8.8 and 10.7 GHz, the main microwave peak is near 1620 UT (SGD); while at 4.995 and 2.8 GHz, the main peak is near 1624 UT, in better agreement with the SFD. The gradual rise in the SFD and EUV enhancement starting near 1618 UT is quite real and was well observed in the channels of SFD data studied. The main complication with the analysis of this SFD is that the propagation path was not accurately determined; it is possible the received signal was WWVH rather than WWV. This does not affect much the relative time dependence of the computed EUV burst. It mainly affects $\Delta\Phi_{max}$.

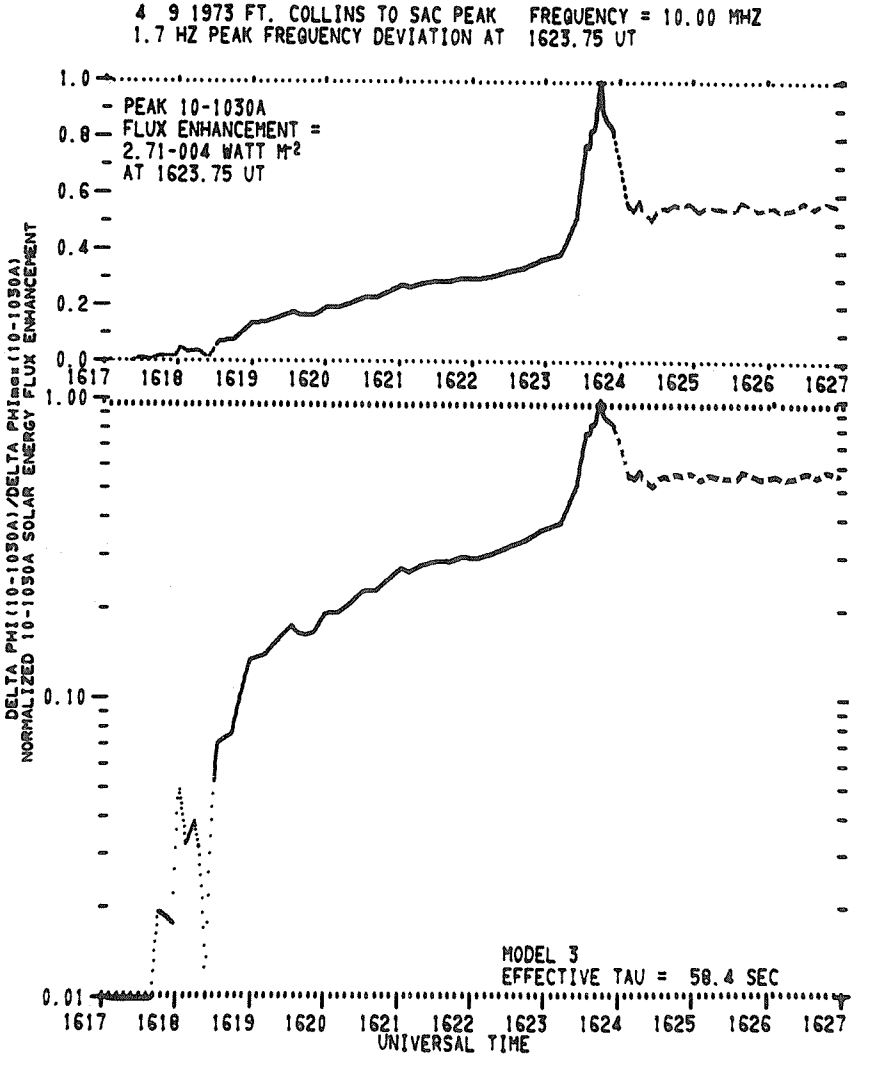

Figure 4.6 Best-estimate 10-1030A flux enhancement of 1624 UT April 9, 1973.

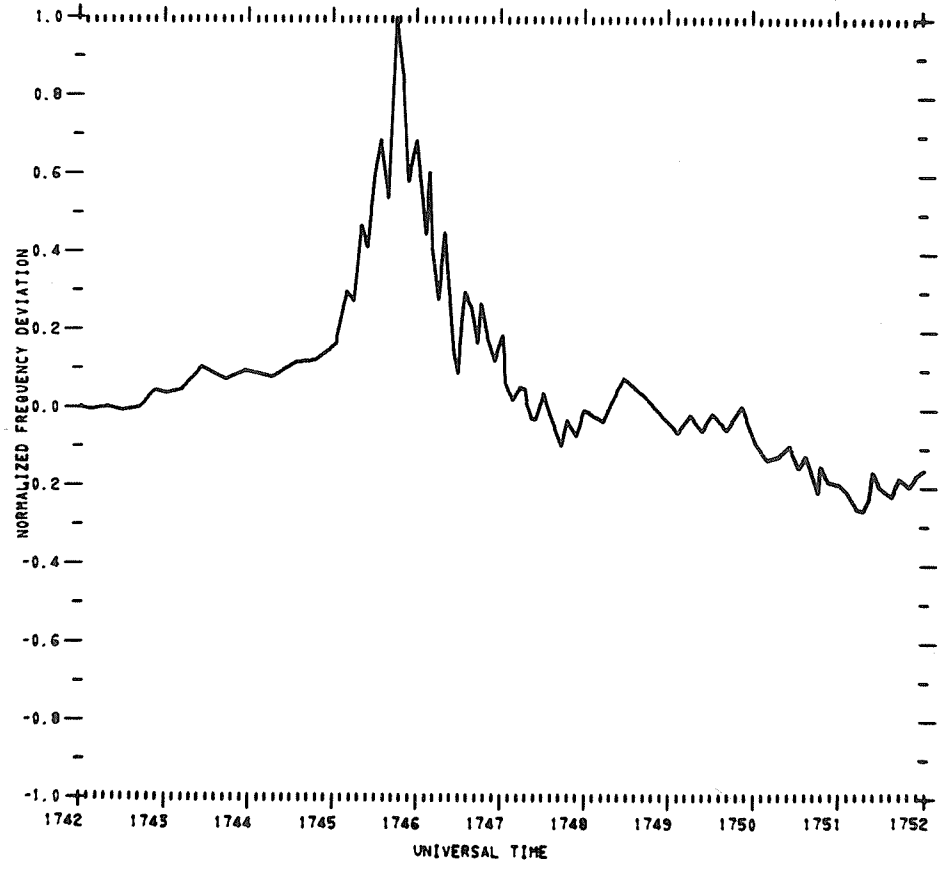

Figure 4.7 SFD of 1746 UT April 9, 1973.

This SFD and EUV burst accompanied an H_α subflare of normal intensity at S08 E20 (McMath Plage 12306, the same region as the flare of figure 4.5), which started at about 1743 UT with maximum phase at 1746 UT. The microwave burst at frequencies from 5 to 15 GHz peaked at times in the range 1745.6 to 1746.6 UT (SGD). Note that the series of peaks in figure 4.8 ranges from 1745.7 to 1747 UT.

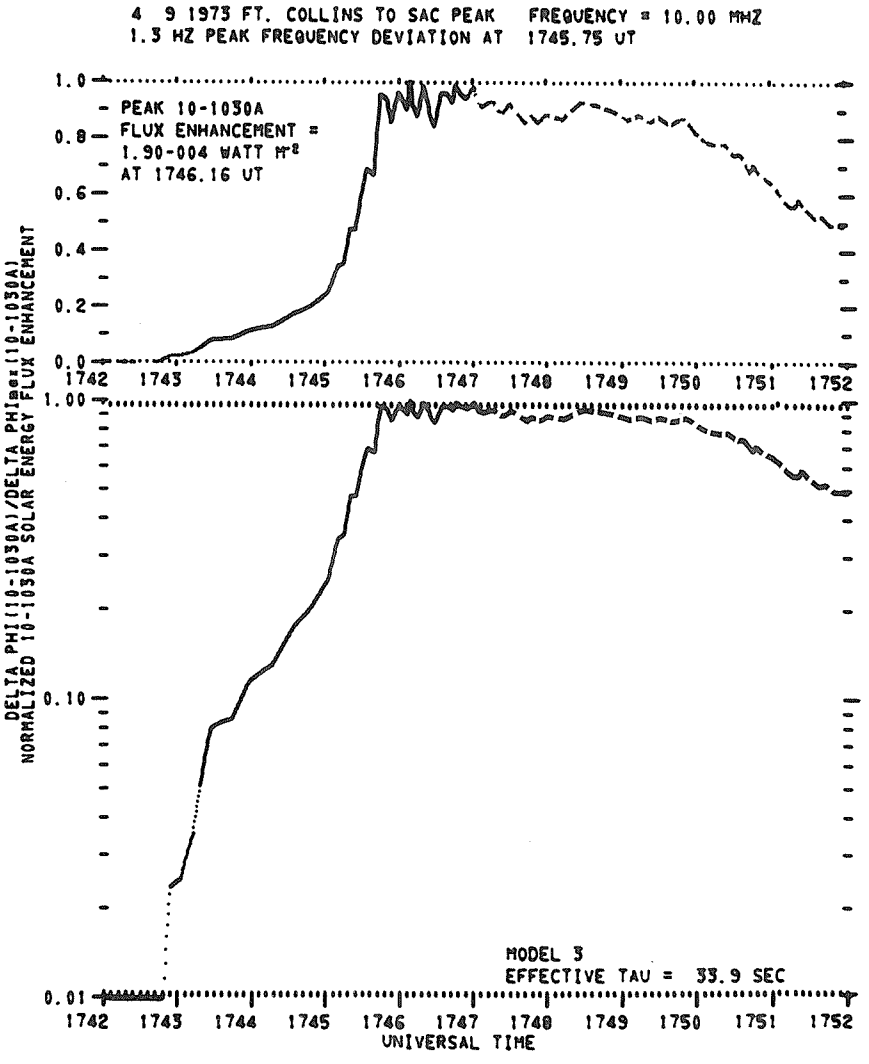

Figure 4.8 Best-estimate 10-1030A flux enhancement of 1746 UT April 9, 1973.

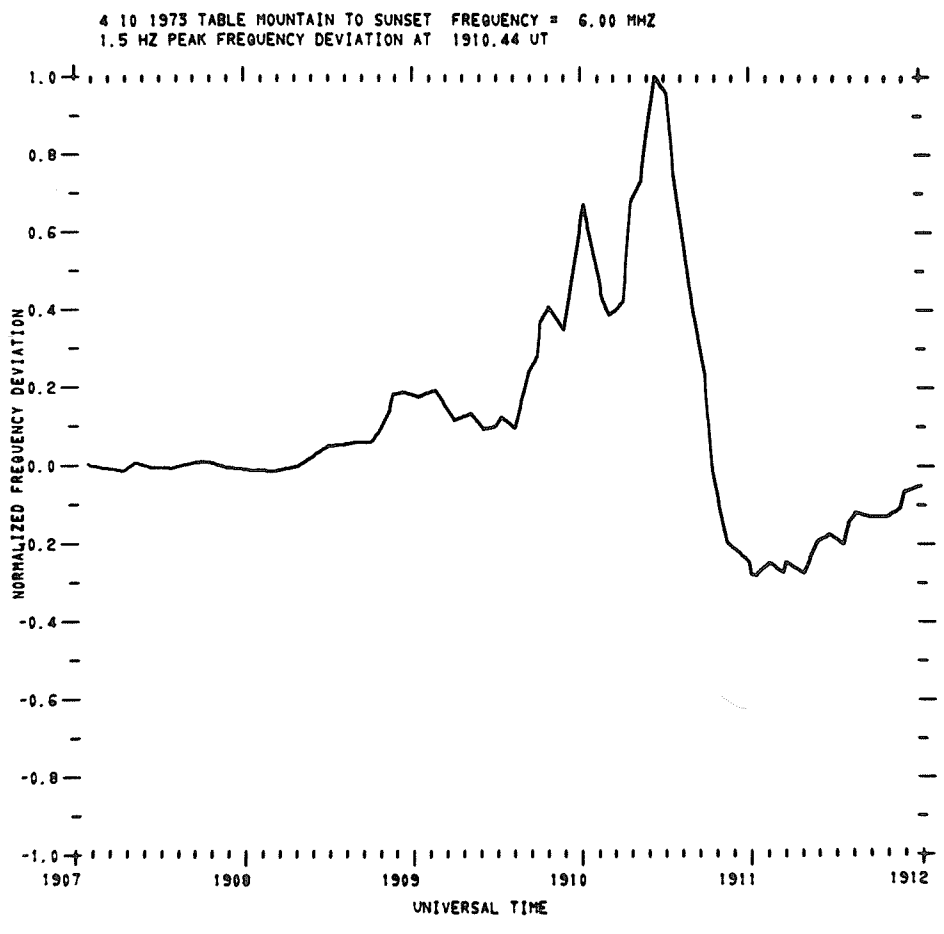

Figure 4.9 SFD of 1910 UT April 10, 1973.

The EUV burst and resultant SFD was a bright $H\alpha$ subflare at S06 E06 (McMath Plage Region 12306, that flare prolific region). The $H\alpha$ flare started at 1905 UT and reached maximum phase at 1910 UT. The microwave burst in the 2 to 15 GHz range peaked at about 1909.2 UT (SGD), more than one minute before the EUV impulsive peak.

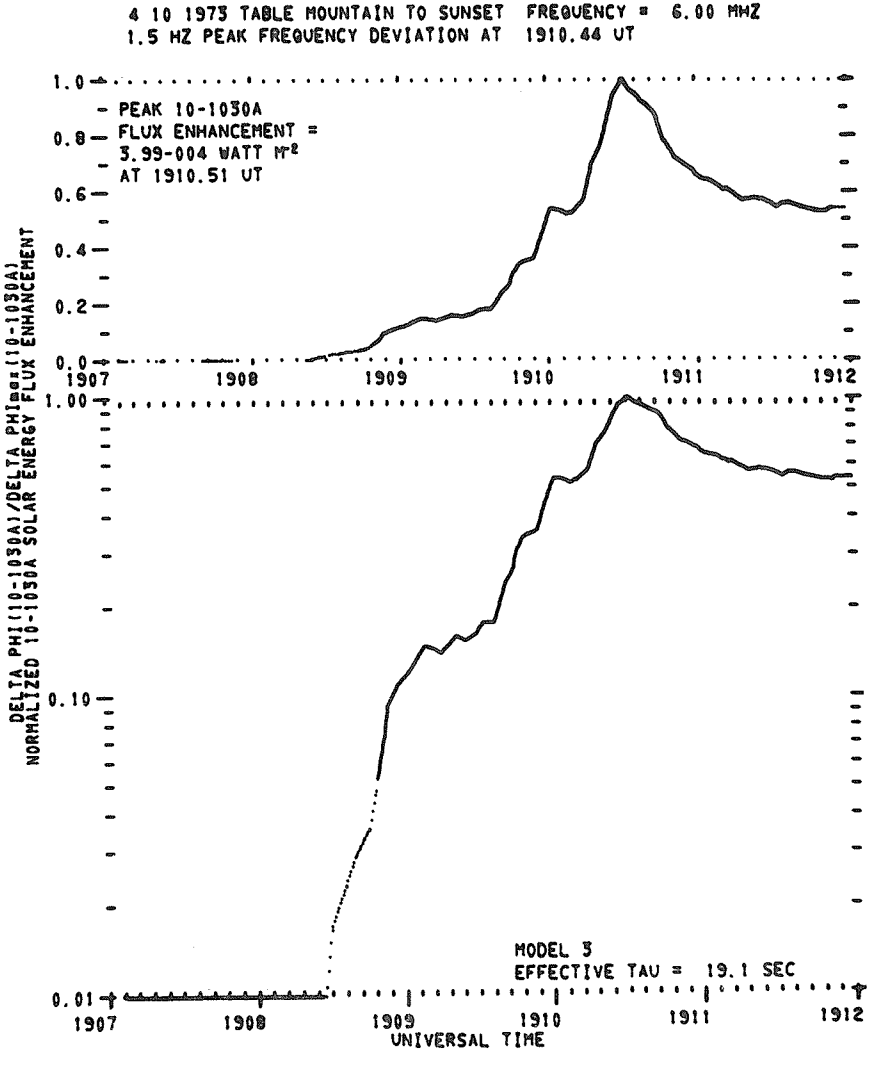

Figure 4.10 Best-estimate 10-1030A flux enhancement of 1910 UT April 10, 1973.

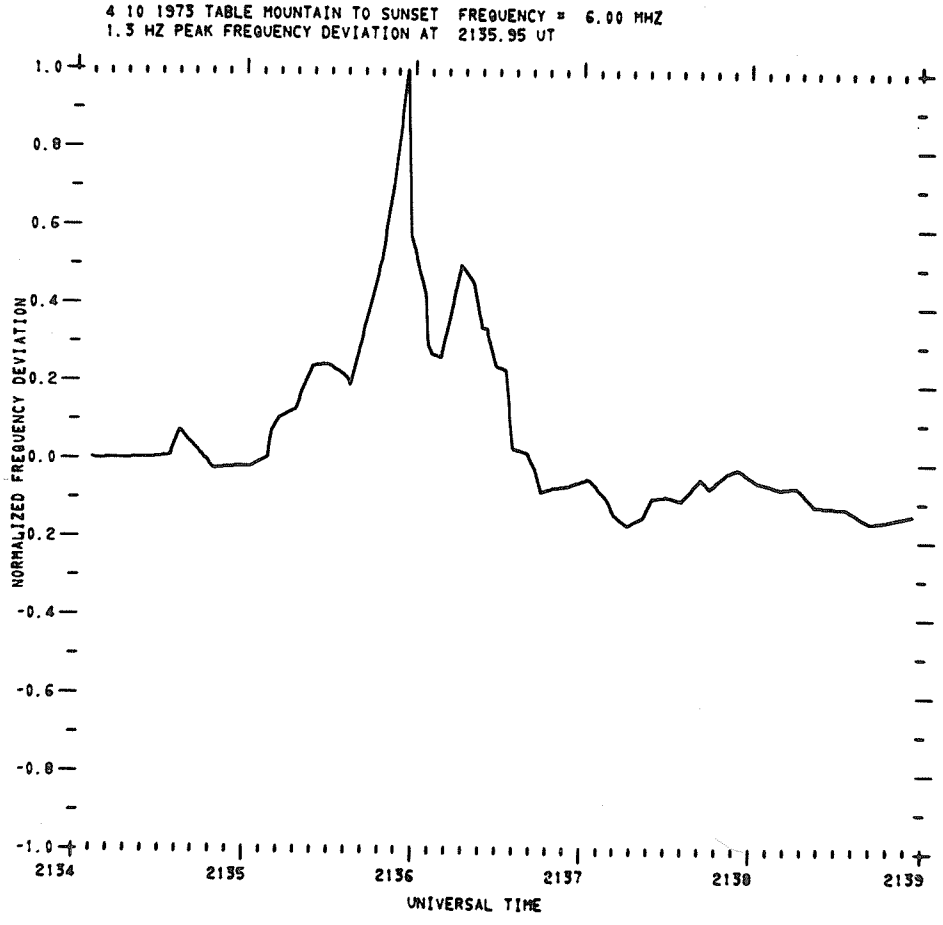

Figure 4.11 SFD of 2136 UT April 10, 1973.

The associated Hα subflare was of normal intensity at S06 E02 in McMath Plage Region 12306. It started at 2134 UT with maximum phase at 2135 UT, which is almost one minute prior to the EUV peak. However, this Hα flare was reported by only one observatory, so the Hα peak time may be less accurate than usual. The microwave burst in the 2 to 11 GHz frequency range peaked from 2135.5 to 2136.5 UT (SGD).

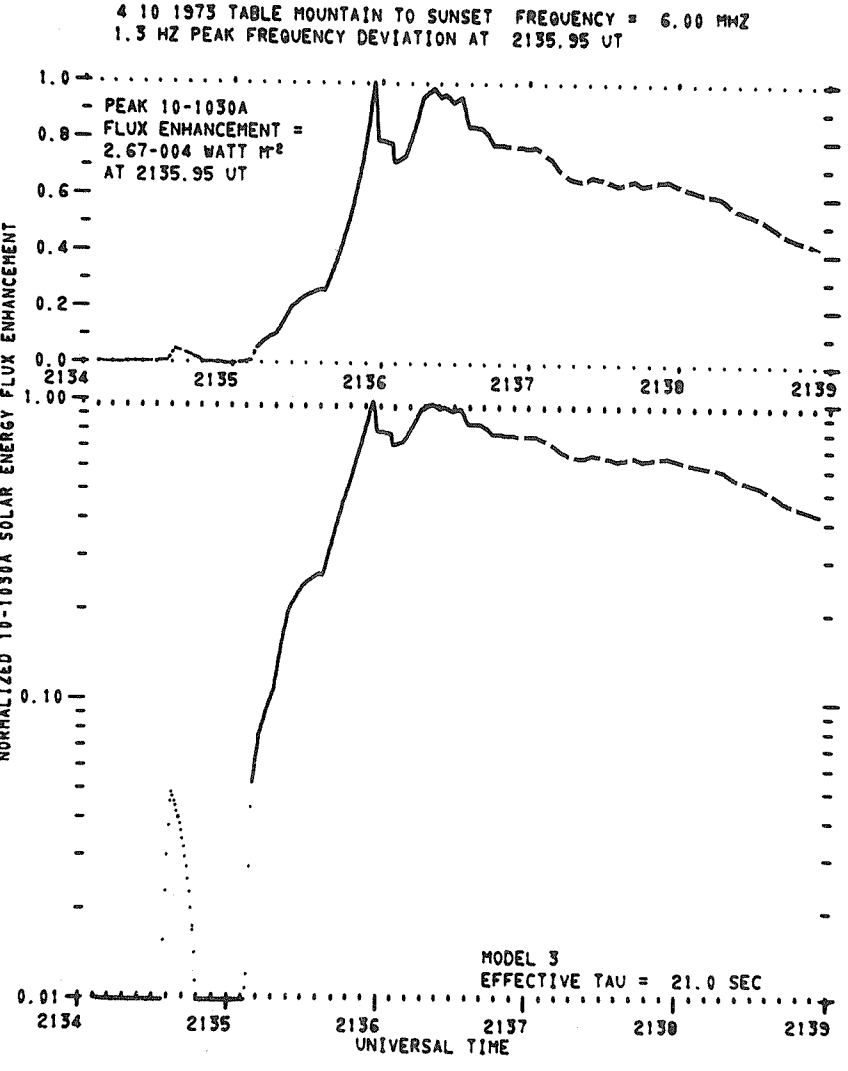

Figure 4.12 Best-estimate 10-1030A flux enhancement of 2136 UT April 10, 1973.

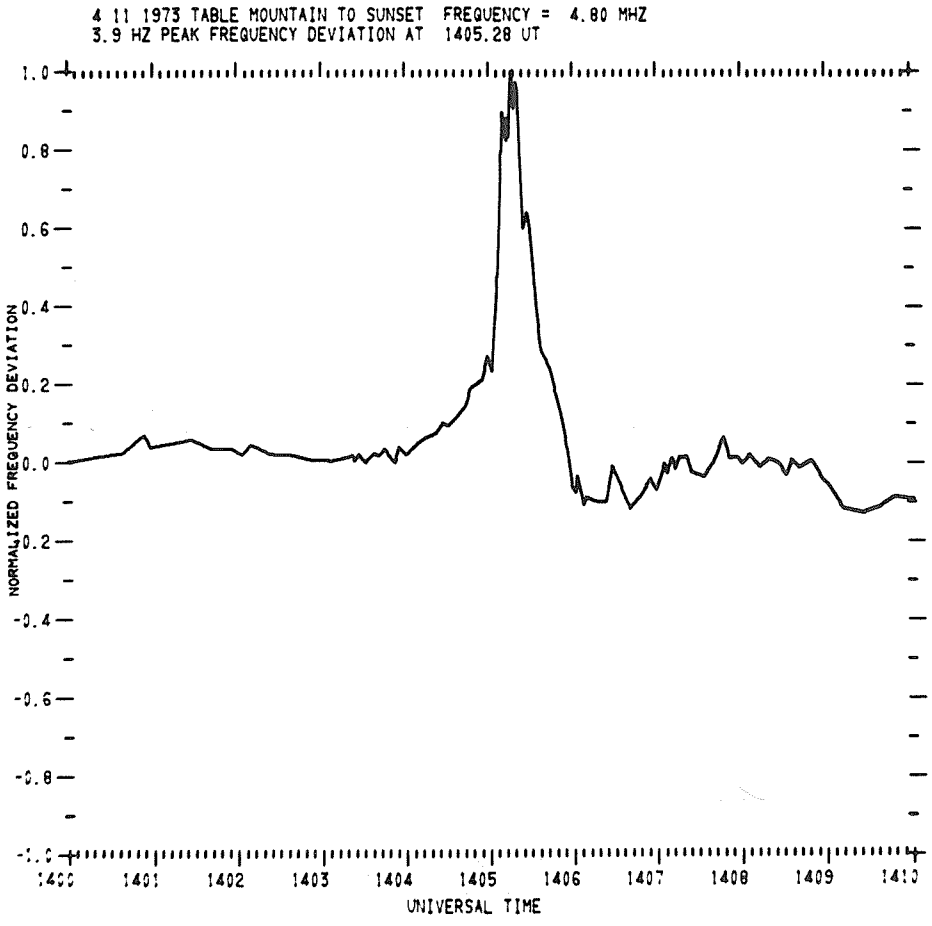

Figure 4.13 SFD of 1405 UT April 11, 1973.

This SFD is larger than those in the preceeding figures, and the 10-1030A burst is a medium class event rather than small. The H_α flare was of importance 1B at S12 W07 (McMath Plage Region 12306 again), which started at 1400 UT and peaked at 1405 UT, according to McMath Observatory (SGD). The microwave burst peaked from 1405.2 to 1405.7 UT at frequencies in the range 2 to 11 GHz. The rise in the SFD from 1401 to 1404 UT and also the post burst feature from 1406 to 1409 UT were well observed in several channels. The HF Doppler radio propagation was via the extraordinary mode.

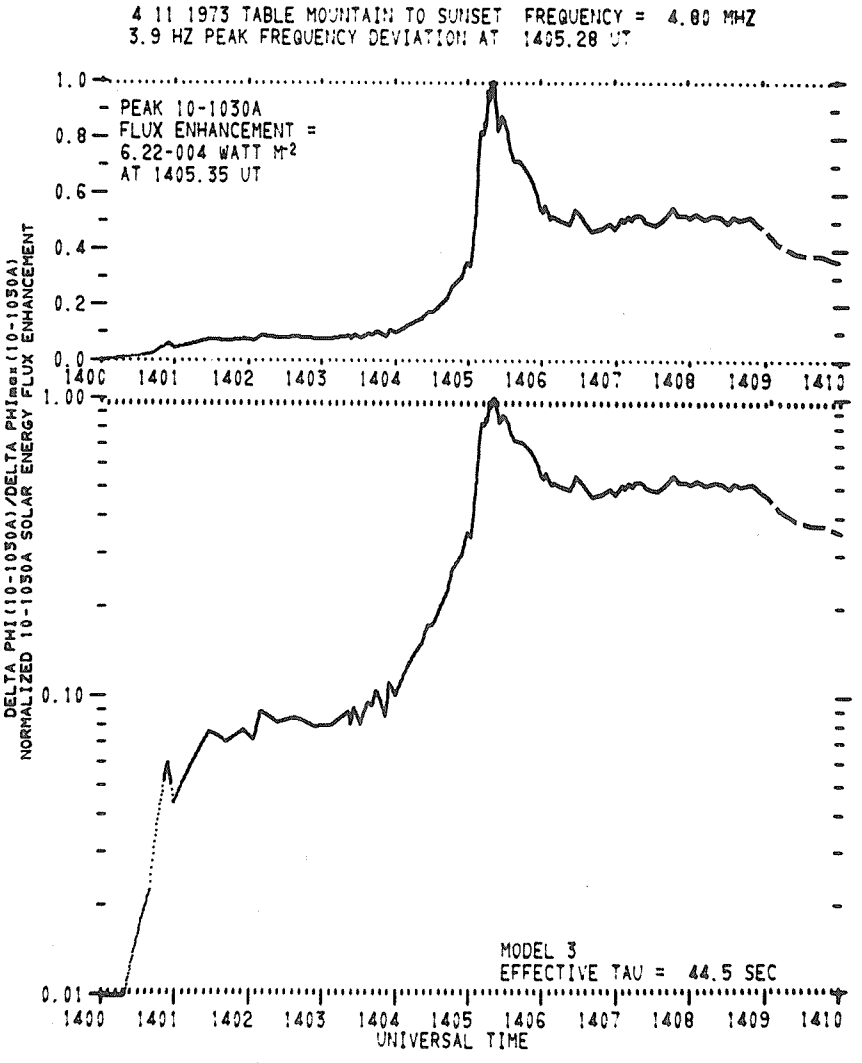

Figure 4.14 Best-estimate 10-1030A flux enhancement of 1405 UT April 11, 1973.

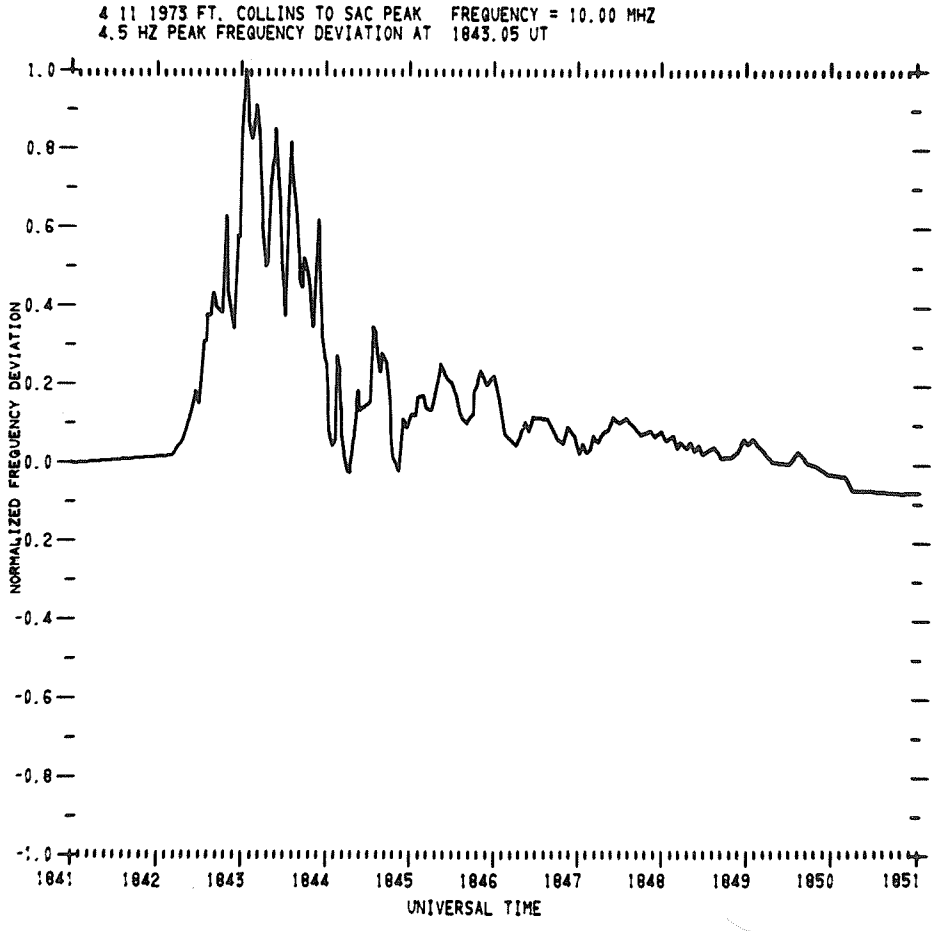

Figure 4.15 SFD of 1843 UT April 11, 1973.

The raw SFD data for this event is shown in Figure 3.1. The tape recorder gear noise in figure 3.1 was abnormally high. Several other channels of HF Doppler data were used to help distinguish the SFD fine structure from the gear noise. The 1B $H\alpha$ flare was at S09 W10 (McMath Plage Region No. 12306 again), starting near 1838 UT, with maximum phase at about 1846 UT. The microwave burst in the 2-35 GHz range peaked from about 1843 to 1845 UT (SGD). Because of the lack of a solution for the 10 MHz propagation path, the SFD was analyzed by renormalizing the 10 MHz $\Delta f(t)$ to the 4.8 MHz Sunset data and then using the 4.8 MHz propagation path. These two sets of $\Delta f(t)/\Delta f_{max}$ were nearly identical up to 1844 UT, after which the 4.8 MHz data were lost because of the large SWF. The assumption that $\tau(h)$ is approximately constant was good over the lower 82% of the h_o to h_r range, where τ was increasing with height at h_r.

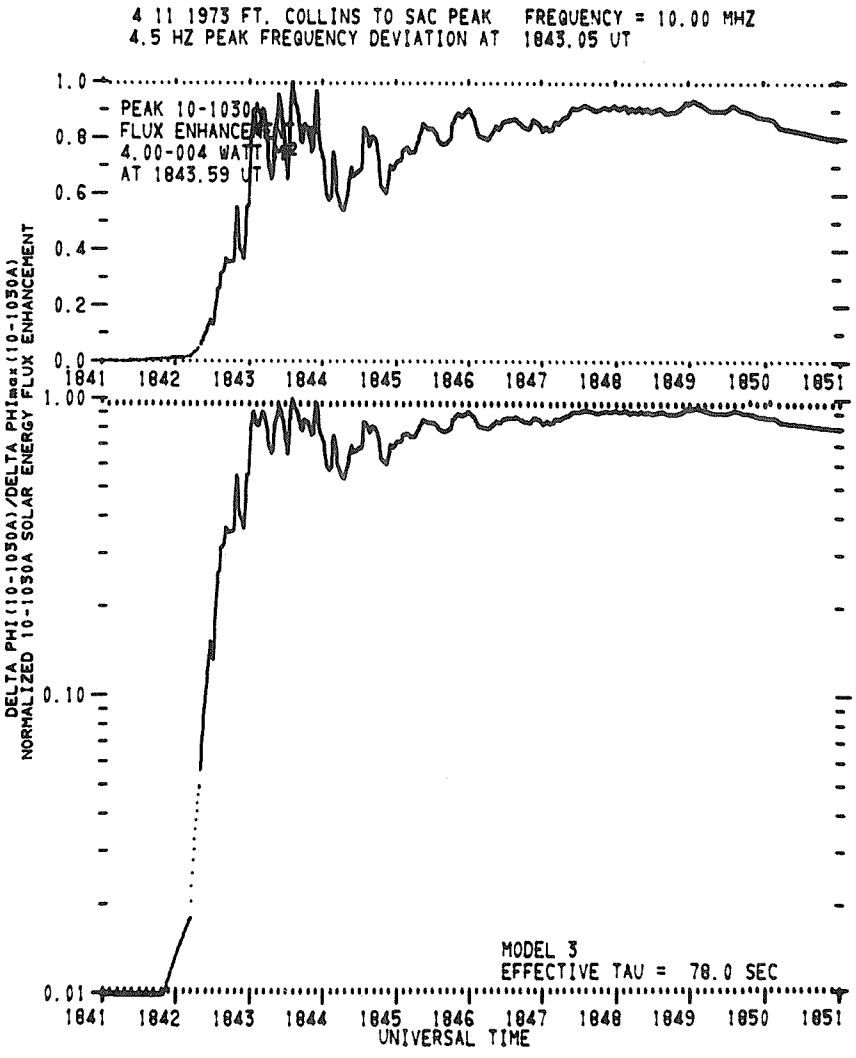

Figure 4.16 Best-estimate 10-1030A flux enhancement of 1843 UT April 11, 1973.

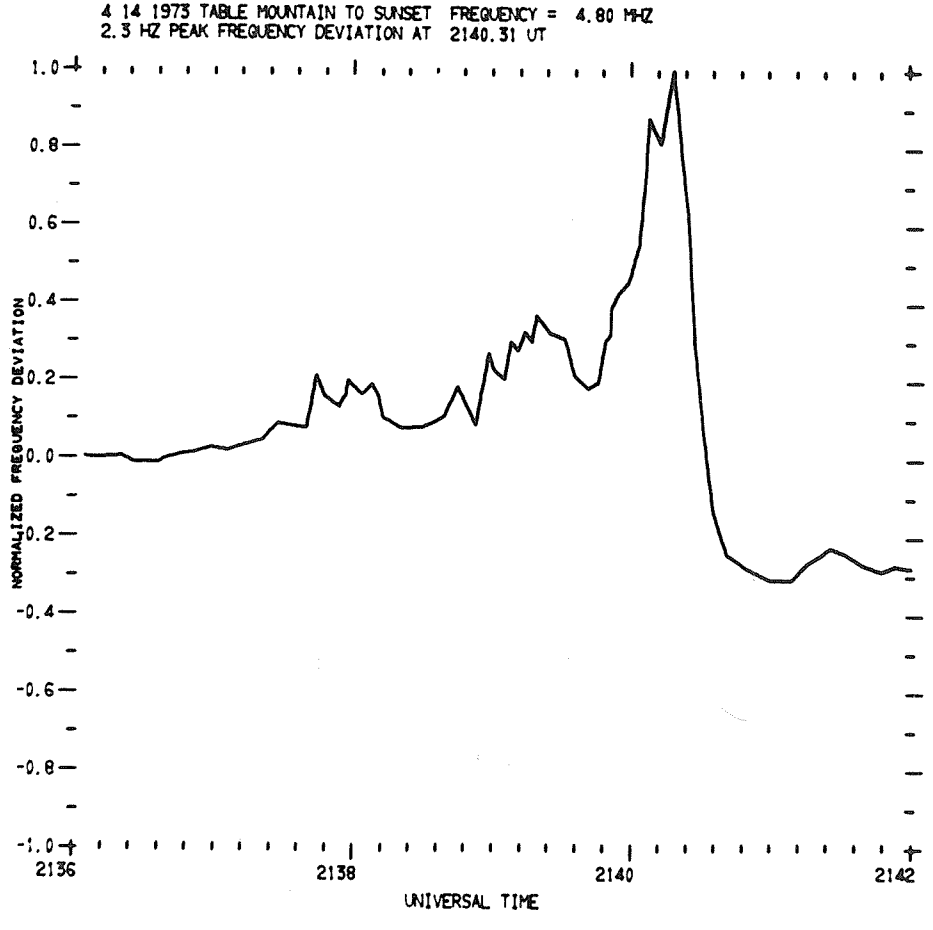

Figure 4.17 SFD of 2140 UT April 14, 1973.

The associated faint H_α subflare was again from McMath Plage Region 12306 (S08 W53), starting at 2137 UT, with its maximum phase at 2142 UT. The microwave burst peaked from 2139.5 to 2140.5 UT in the 2-11 GHz range (SGD). The HF Doppler radio propagation was via the extraordinary mode.

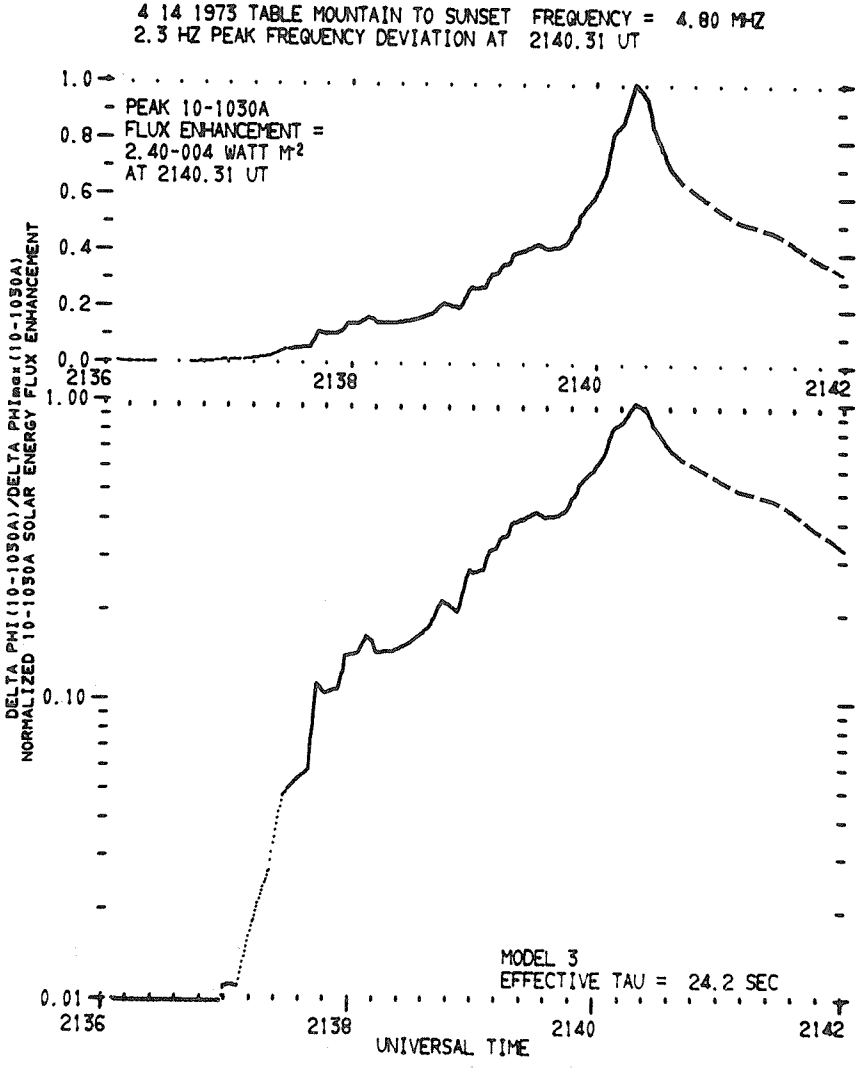

Figure 4.18 Best-estimate 10-1030A flux enhancement of 2140 UT April 14, 1973.

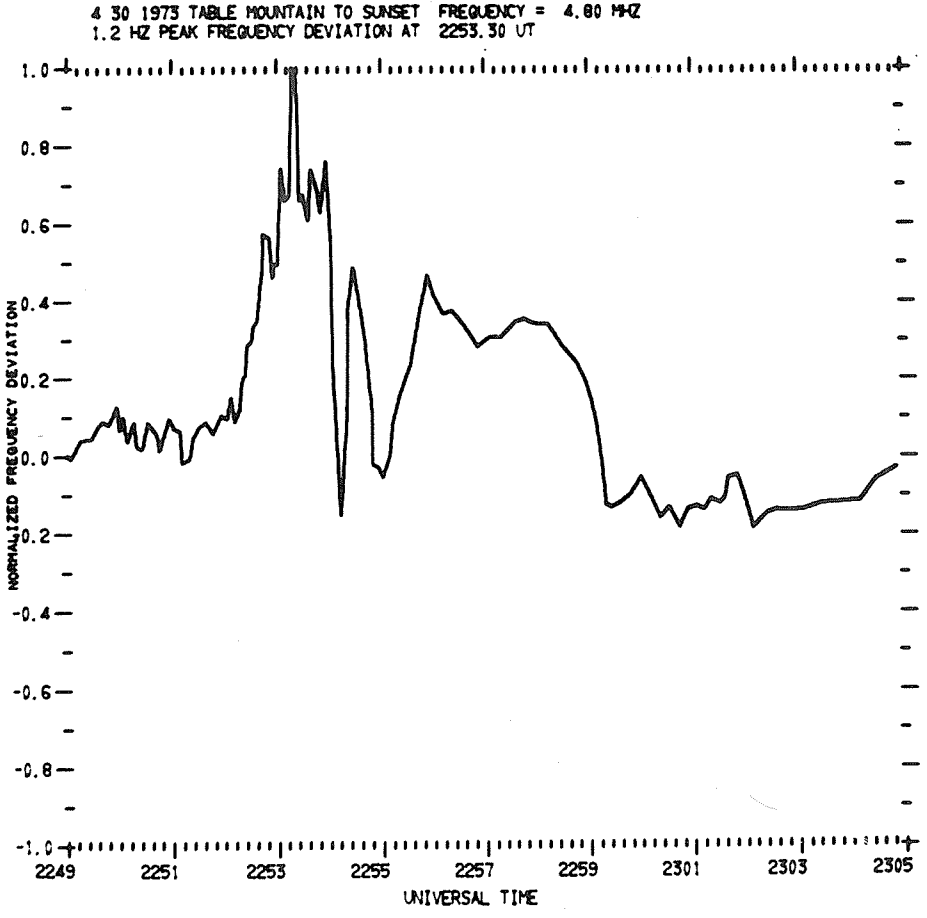

Figure 4.19 SFD of 2253 UT April 30, 1973.

The corresponding H_α bright subflare started at 2247 UT, with its maximum phase at 2259 UT, in McMath Plage Region 12322 at N13 W89 . The microwave burst peaked from 2255 to 2256.5 UT in the 2 to 15 GHz range, (SGD). The slow feature in the SFD is devoid of the usual fine structure from 2256 to 2259 UT. This event qualifies as a long-duration SFD, like those studied by Donnelly [1970, pp 38-48]. Such events have a marked preference for large solar central meridian distances, which is consistent with the W89 location of this flare.

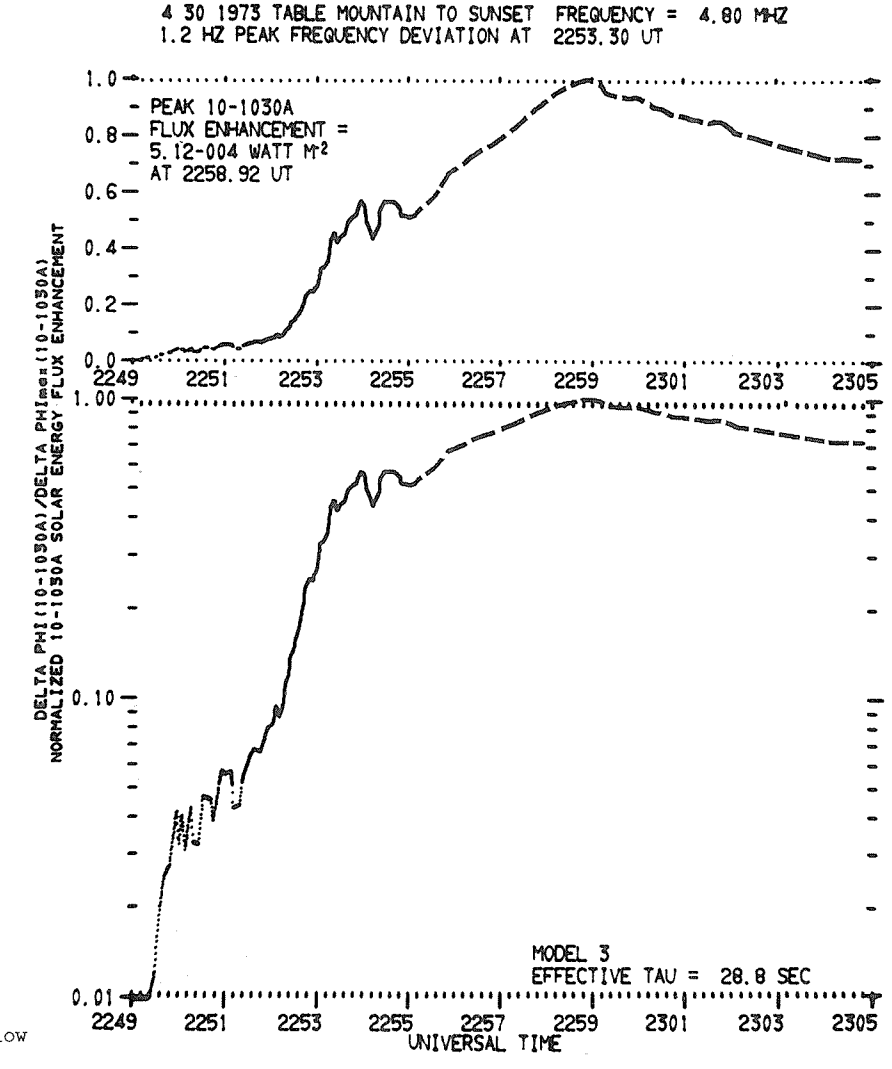

Figure 4.20 Best-estimate 10-1030A flux enhancement of 2253 UT April 30, 1973.

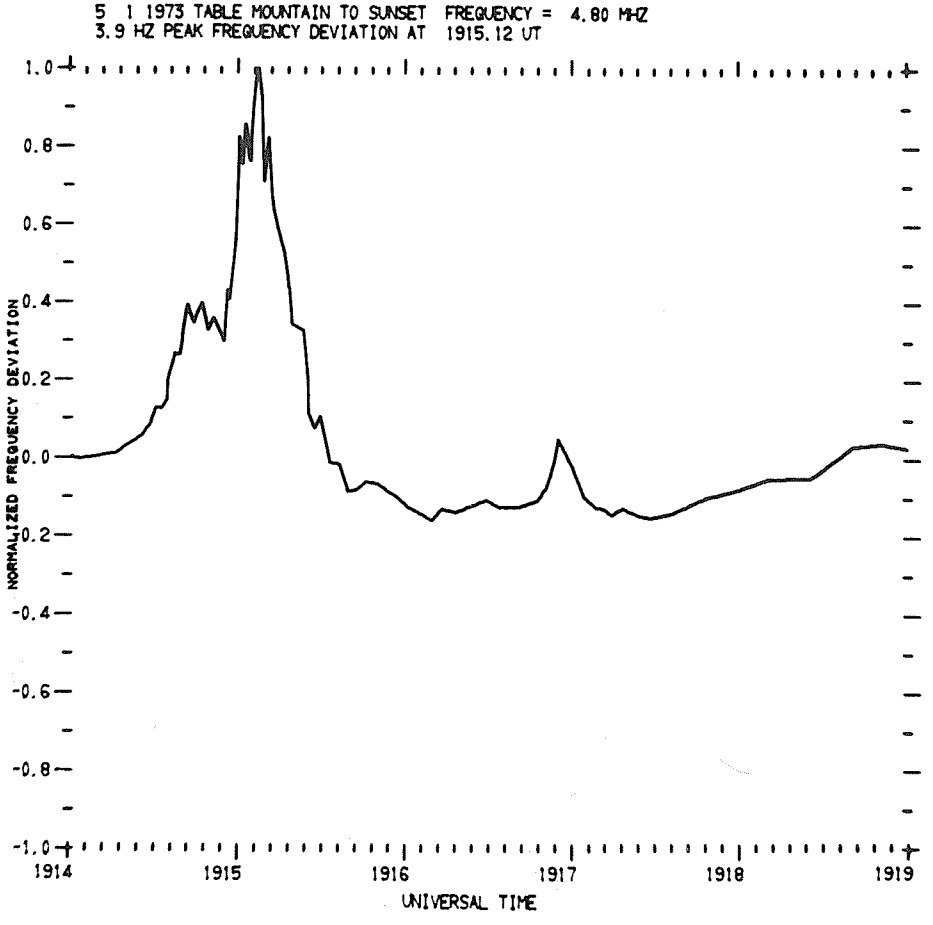

Figure 4.21 SFD of 1915 UT May 1, 1973.

The accompanying faint Hα subflare at S11 E75 (McMath Plage Region 12336) had its maximum phase at 1915 UT. Faint subflares are rarely accompanied by detectable SFDs, and this SFD is medium size, i.e., much larger than the detectable threshold of about 0.1 Hz. The microwave burst in the 1 to 11 GHz range peaked at about 1915.2 UT (SGD), which is concurrent with the EUV burst.

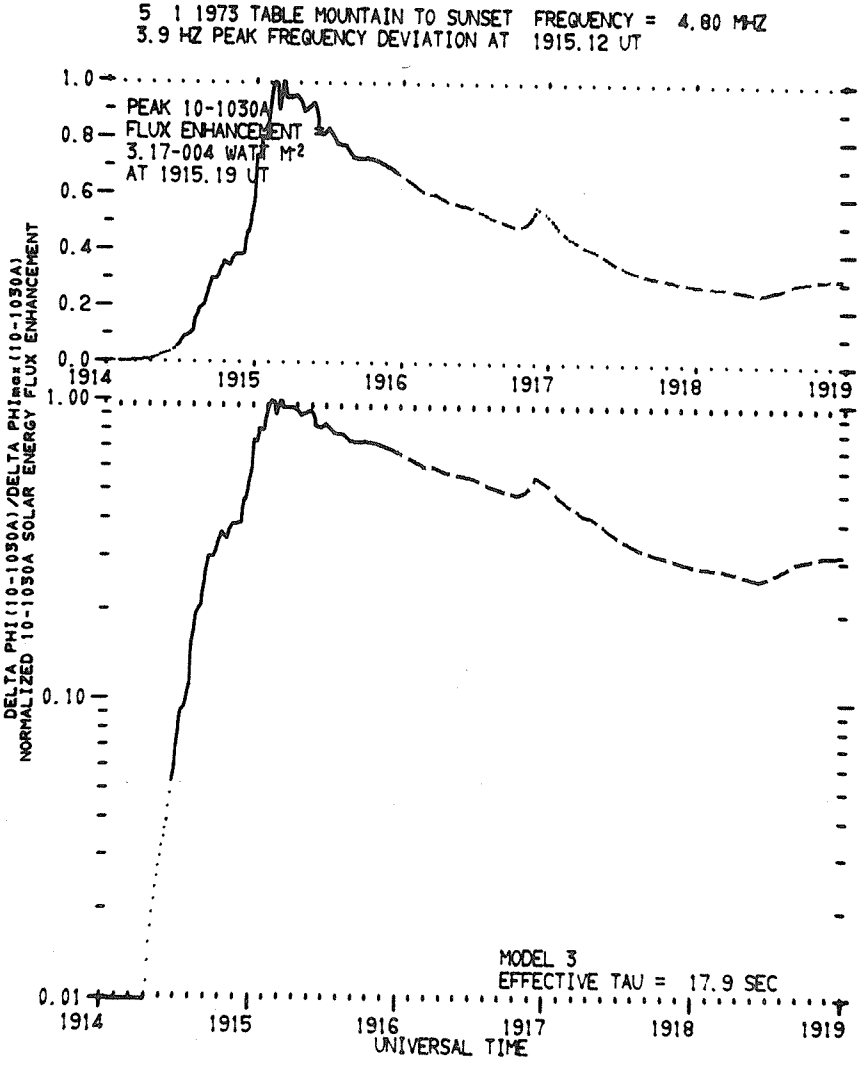

Figure 4.22 Best-estimate 10-1030A flux enhancement of 1915 UT May 1, 1973.

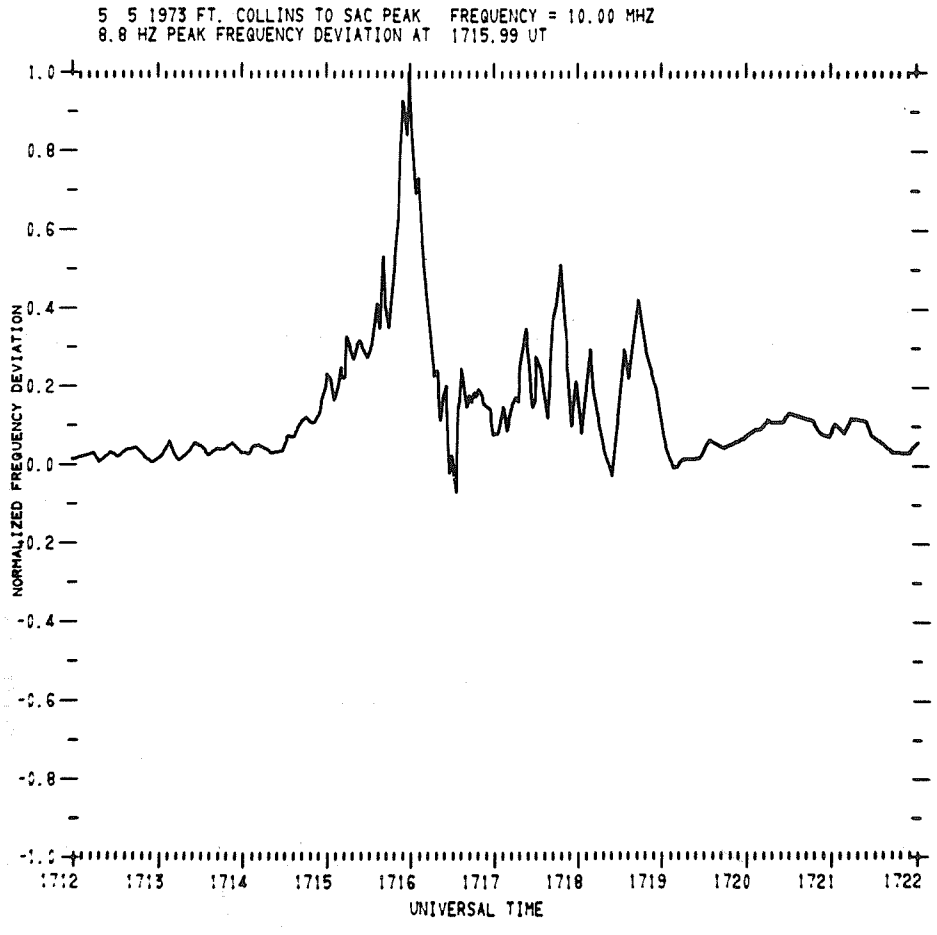

Figure 4.23 SFD of 1716 UT May 5, 1973.

This large SFD and medium sized EUV burst accompanied an Hα flare of importance 2B at S16 E18 (McMath Plage Region 12336), starting at 1703 UT, with its maximum phase at 1719 UT, according to McMath Observatory (SGD). The microwave burst peaked near 1716 and 1718 UT in the 2 to 35 GHz range. The height of reflection for the 10 MHz radio wave was quite high (254 km), which resulted in τ_{eff} being higher than usual and $\tau(h)$ was increasing with altitude at h_r.

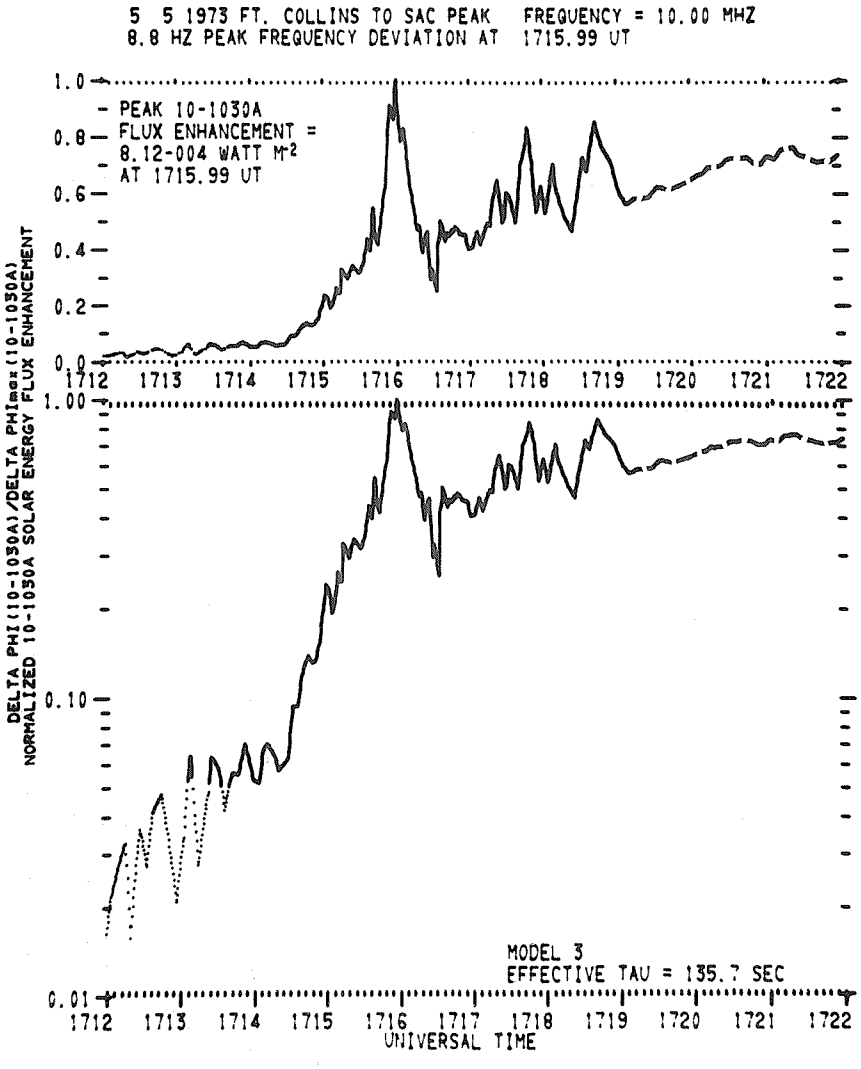

Figure 4.24 Best-estimate 10-1030A flux enhancement of 1716 UT May 5, 1973.

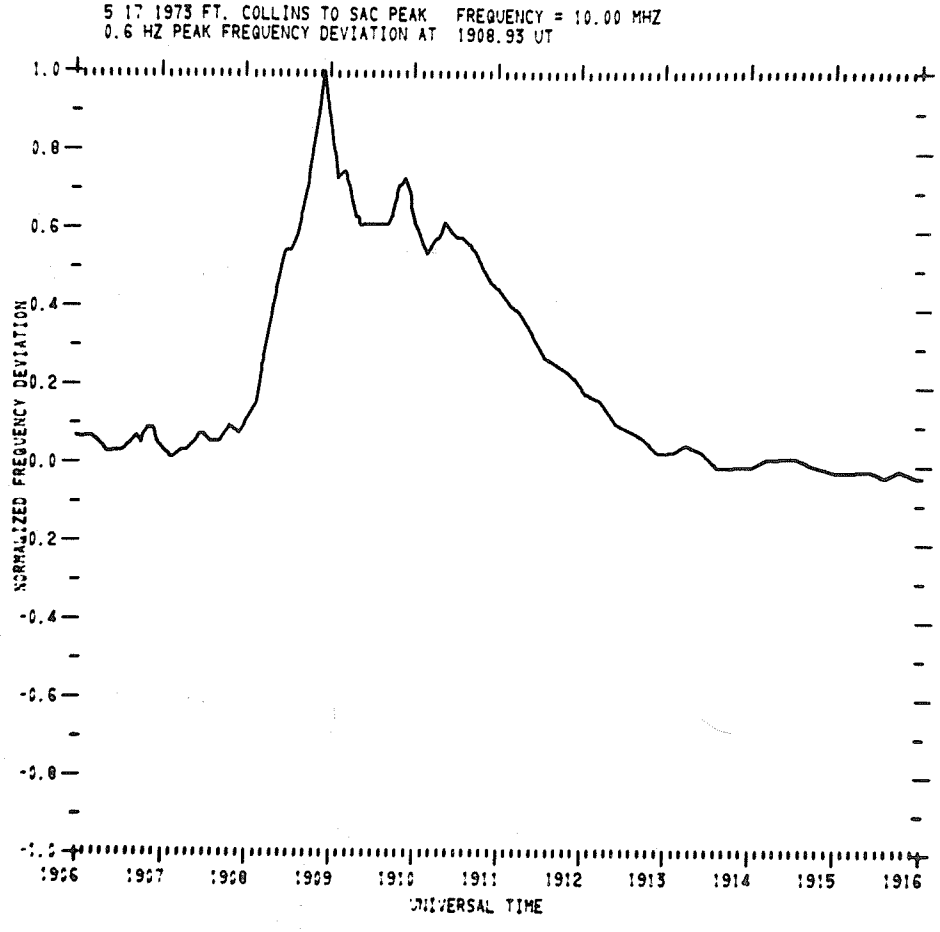

Figure 4.25 SFD of 1909 UT May 17, 1973.

The associated $H\alpha$ subflare was of normal intensity and located at N06 E52° in McMath Plage No. 12352. The $H\alpha$ flare started earlier than 1908 UT and reached maximum phase near 1911 UT. The microwave burst at frequencies of 2.8 and 8.8 GHz peaked near 1909 UT (SGD). The propagation path for this SFD observation was not well determined. The height of reflection was abnormally low (131 km), which makes the SFD relatively more sensitive to the slow soft x-ray emission than to the impulsive EUV emission than for most SFDs.

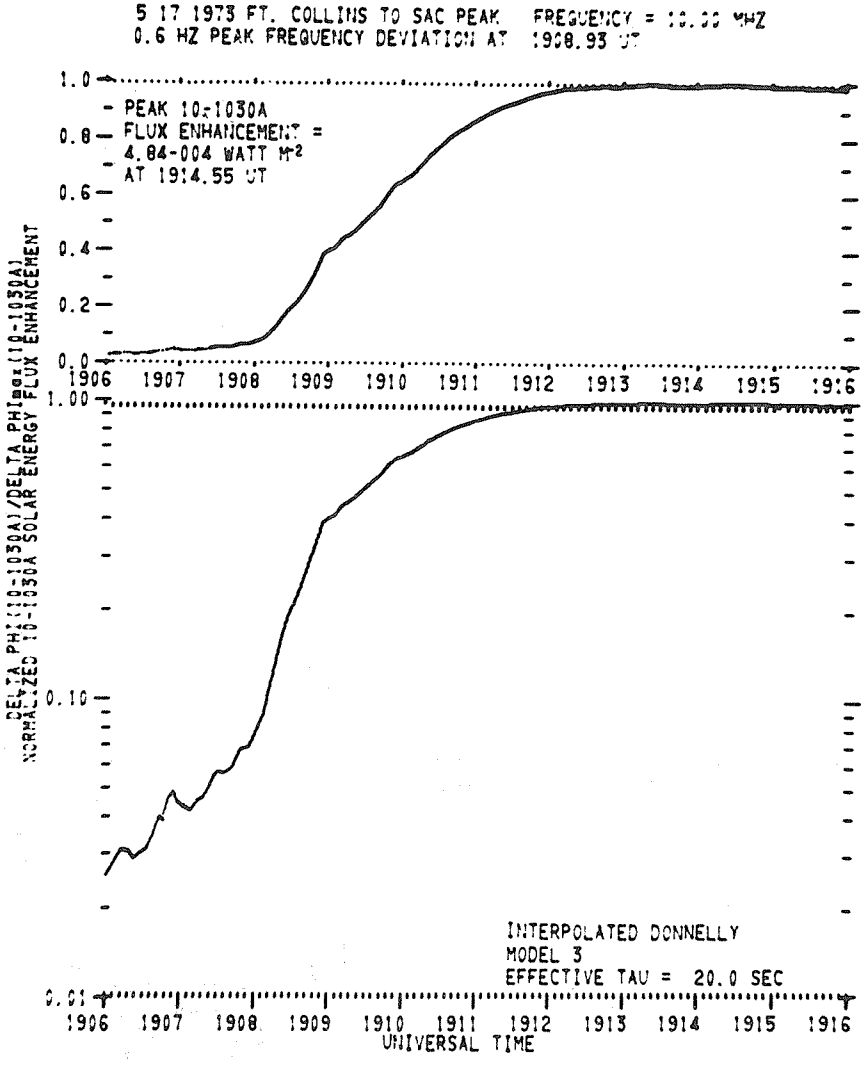

Figure 4.26 Best-estimate 10-1030A flux enhancement of 1909 UT May 17, 1973.

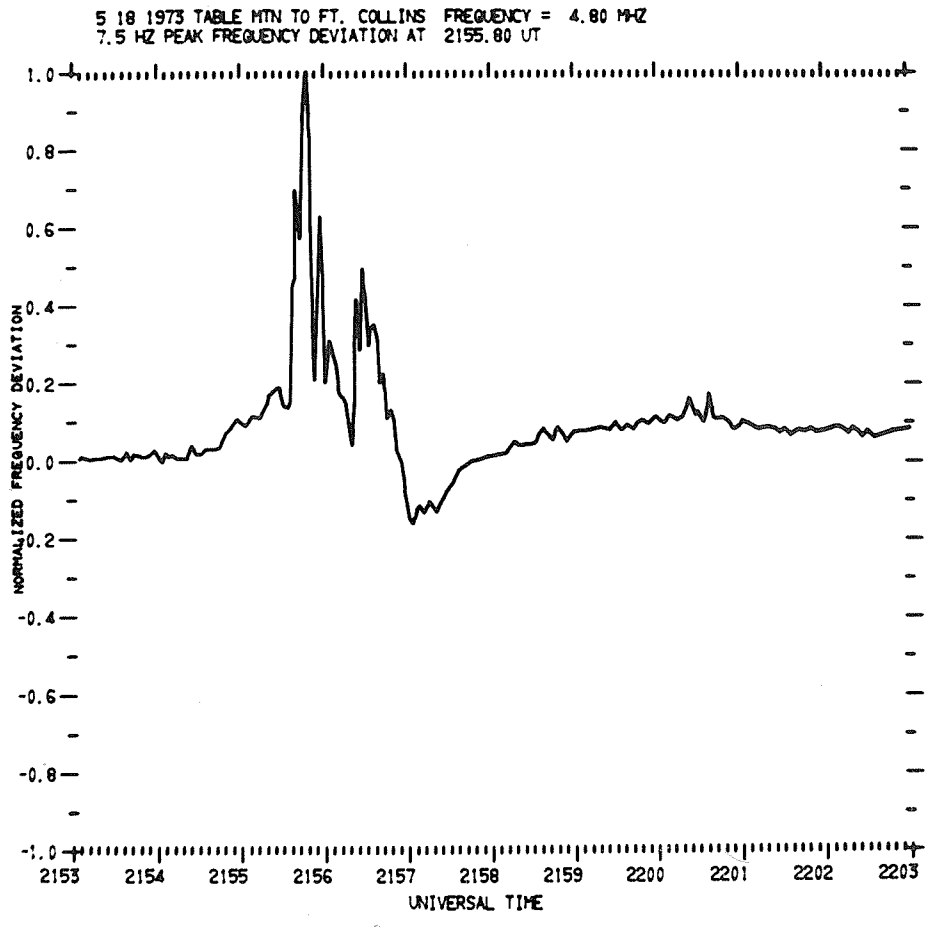

Figure 4.27 SFD of 2156 UT May 18, 1973 on 4.8 MHz at Fort Collins, Colorado.

This large SFD accompanied a bright H_α subflare in McMath Plage Region 12352 at N09 E33 , that started at 2154 UT, peaked at 2157 UT and again at 2200 UT. The microwave burst peaked near 2156.5 UT with a secondary peak at 2201 UT in the 2 to 35 GHz range (SGD). Note that the SFD has a gradual rise from 2158 to 2201 UT which corresponds to a large slow rise in $\Delta\Phi$(10-1030A, t). This flare is also presented in figures 4.29 to 4.38 to illustrate how well SFD data observe the impulsive EUV burst and how poorly the gradual rise and fall emission.

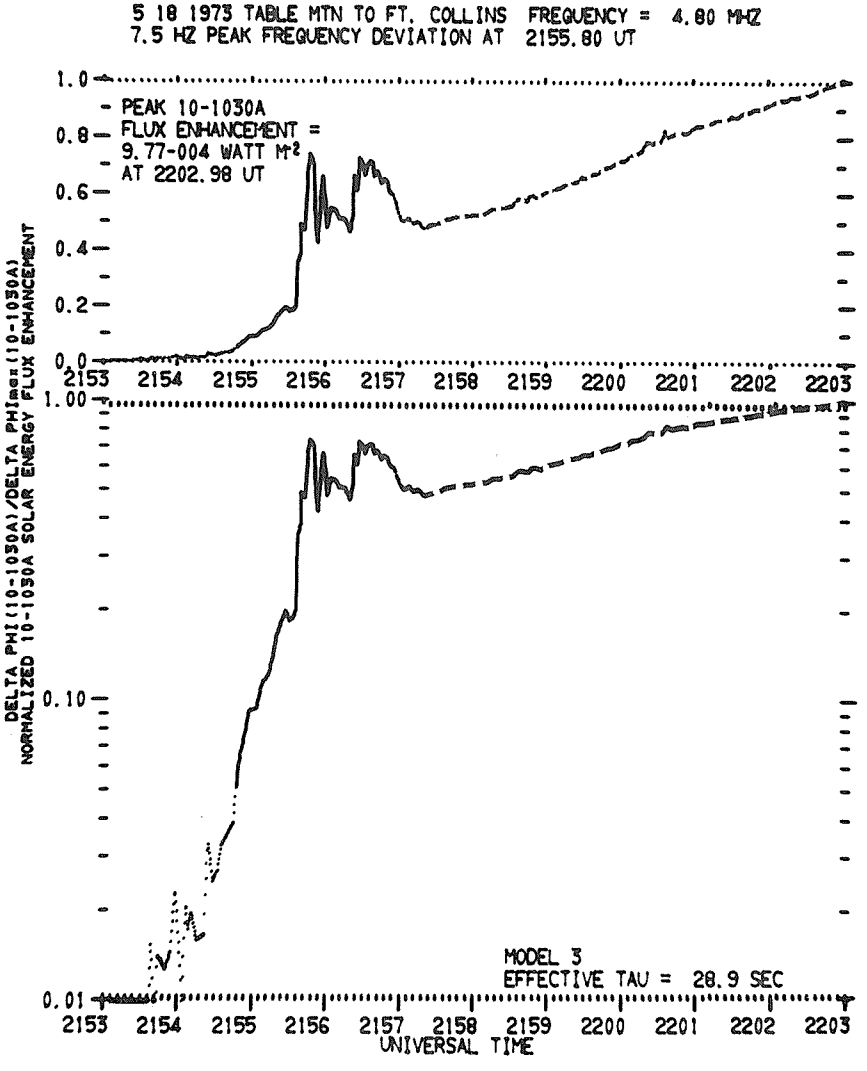

Figure 4.28 Best-estimate 10-1030A flux enhancement of 2156 UT May 18, 1973, based on 4.8 MHz at Fort Collins, Colorado.

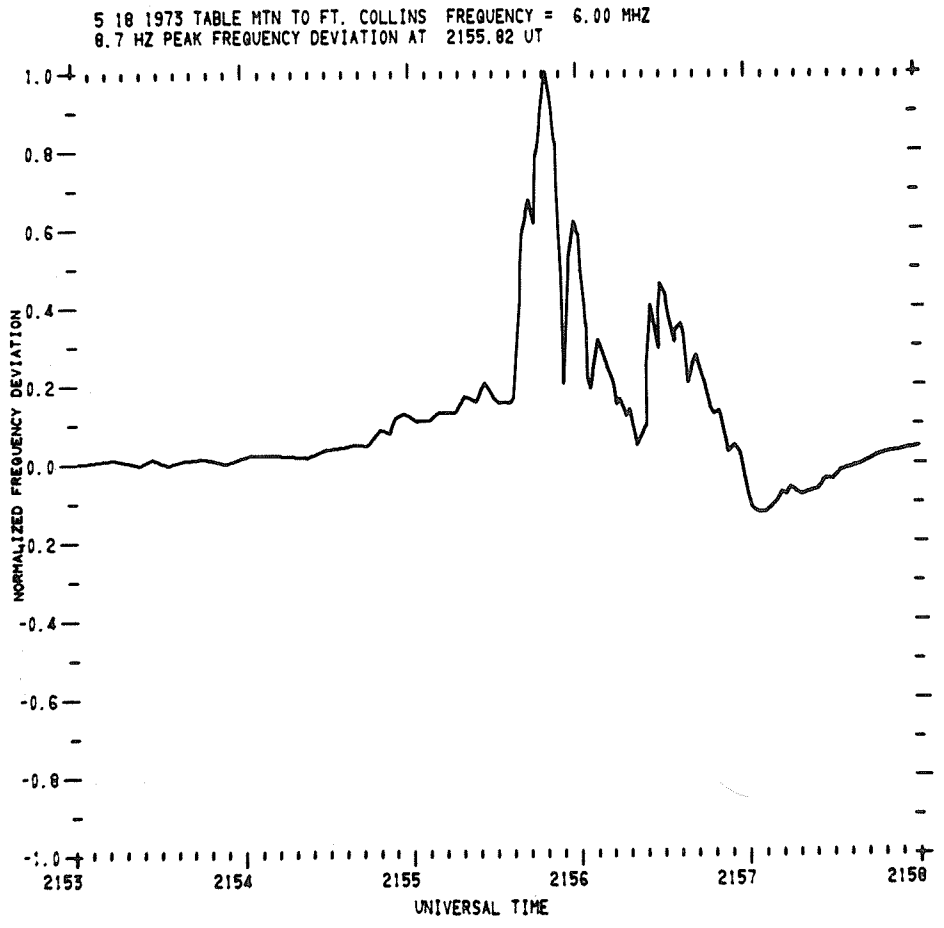

Figure 4.29 SFD of 2156 UT May 18, 1973, on 6.0 MHz at Fort Collins, Colorado. This is the same SFD as in Figure 4.27, except this data was measured at a higher transmission frequency. The time scale was spread by a factor of two to show more clearly the fine structure. The main spike at 2155.8 UT rose in about 10 sec and fell in about 6 sec, where both these times are smaller than τ_{eff}. Similarly the rise and fall of the spike at 2156.0 UT and the rise at 2156.4 UT are also small relative to τ_{eff}. Consequently the corresponding features in the computed 10-1030A flux enhancement are nearly independent of the assumed models for the ionospheric electron loss rates. The 6.0 MHz HF Doppler radio propagation was an extraordinary wave.

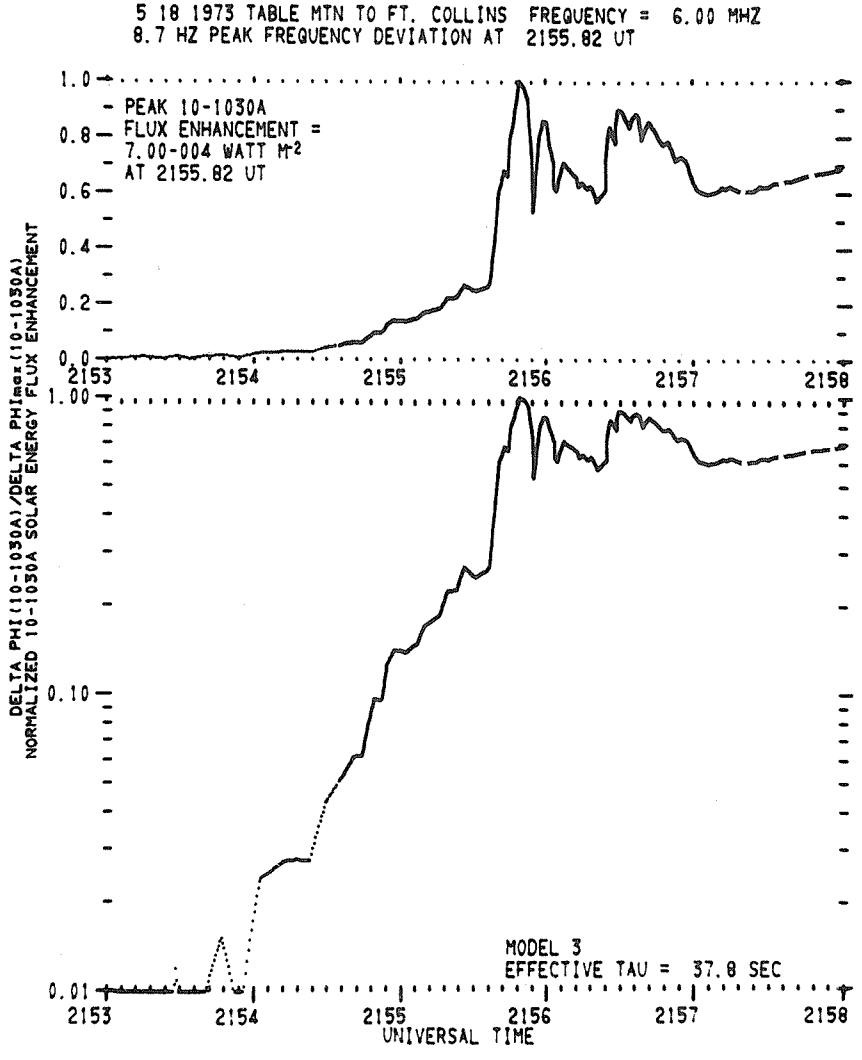

Figure 4.30 Best-estimate 10-1030A flux enhancement of 2156 UT May 18, 1973, based on 6.0 MHz at Fort Collins, Colorado.

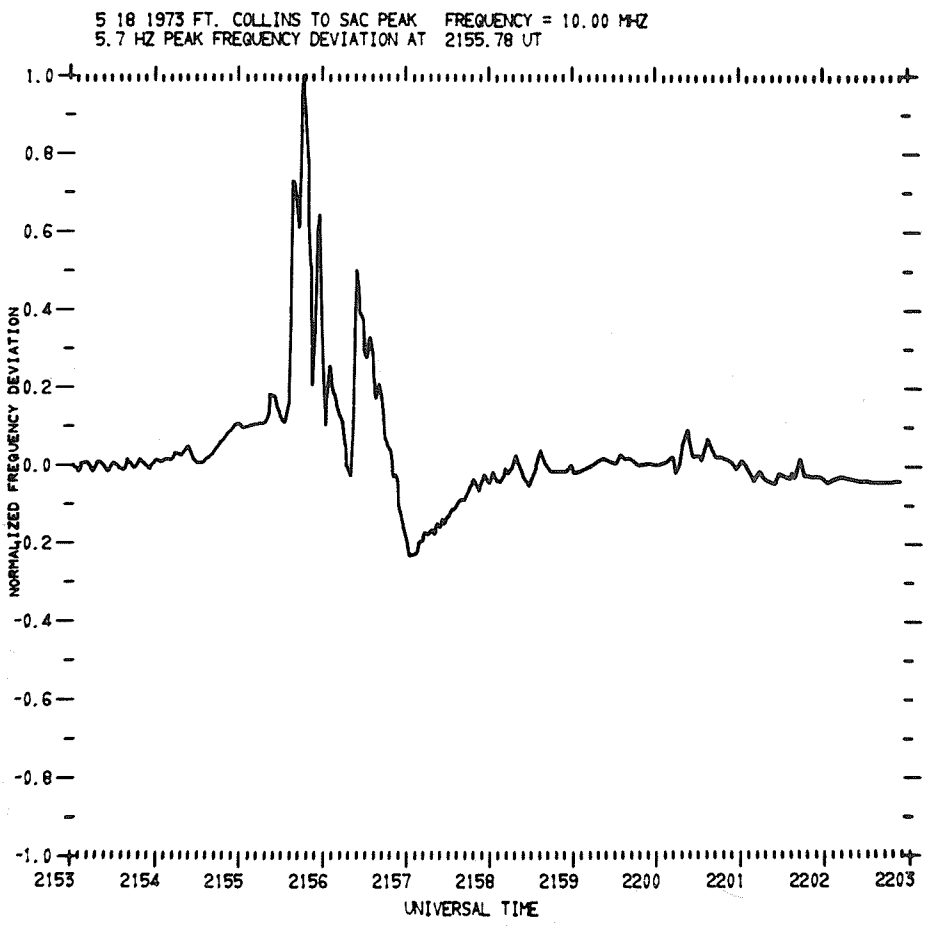

Figure 4.31 SFD of 2156 UT May 18, 1973, on 10 MHz at Sacramento Peak Observatory.

Figures 4.27, 4.31, and 4.33 show the same SFD observed on three different propagation paths with the same time scales. The major impulsive fine structure is essentially the same in the various channels. Some of the minor fine structure is not identical, which thereby illustrates the noise in the SFD observations. The 10-1030A flux changes during the impulsive bursts agree quite well, much better than indicated by the $\Delta\Phi_{max}$(10-1030A) values. In Figures 4.28, 4.30, 4.32, and 4.34, $\Delta\Phi$(10-1030A, t) = 7.2×10^{-4}, 7.0×10^{-4}, 5.6×10^{-4} and 6.6×10^{-4} watts m^{-2} respectively at 2155.8 UT at the main impulsive peak, which amounts to a variation of 16% from the average value. The enhancement during the impulsive rise alone from 2155.6 to 2155.8 UT is 5.5×10^{-4}, 5.3×10^{-4}, 4.6×10^{-4} and 5.1×10^{-4} watts m^{-2} respectively in these same four cases, which gives a variation of 10% from their average.

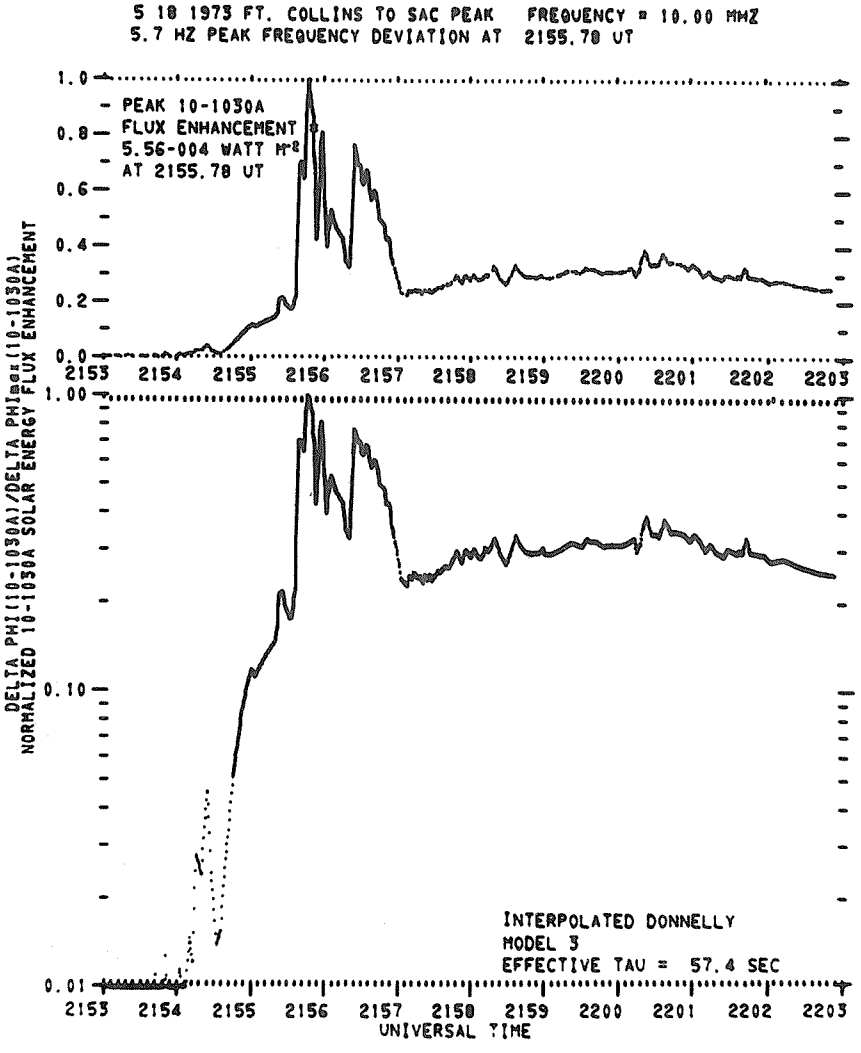

Figure 4.32 Best-estimate 10-1030A flux enhancement of 2156 UT May 18, 1973, based on 10 MHz at Sacramento Peak Observatory.

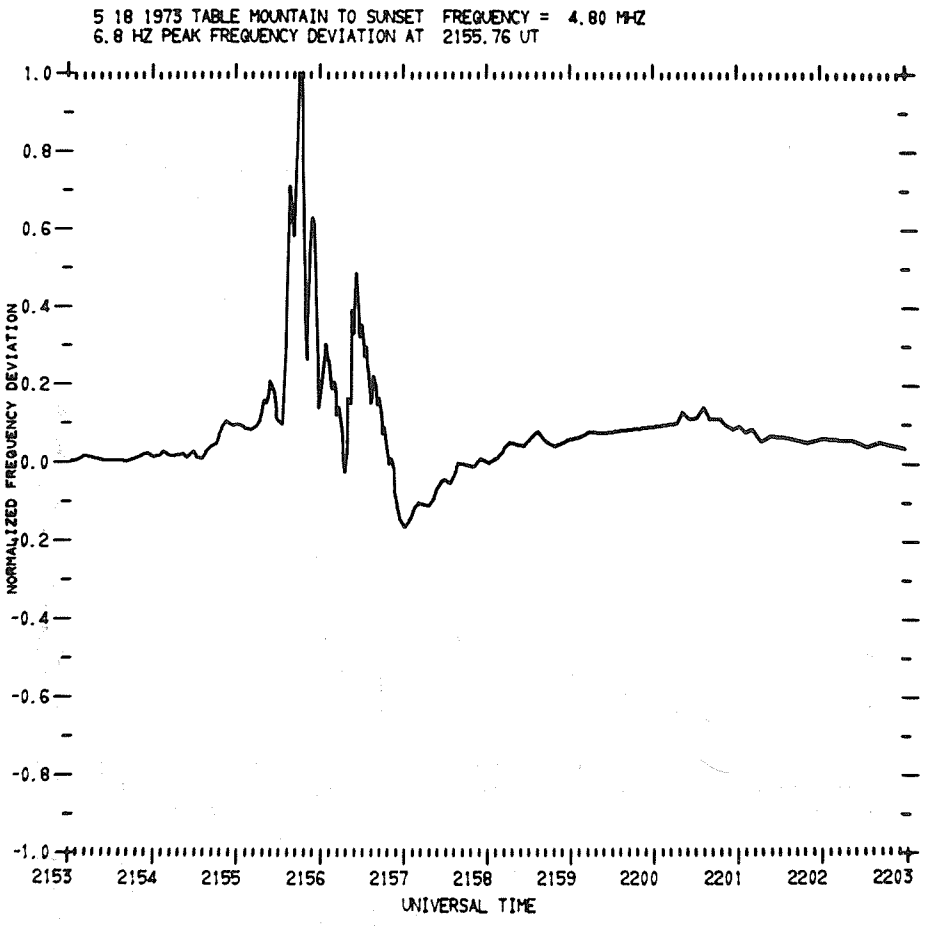

Figure 4.33 SFD of 2156 UT May 18, 1973, on 4.8 MHz at Sunset, Colorado.

The slow enhancement is less consistent in Figures 4.28, 4.30, 4.32 and 4.34 than the flux enhancements during the impulsive structure of the flare. Figures 4.35 to 4.38 correspond to ionospheric electron loss rates equal to $\frac{1}{2}$ x's, $\frac{1}{\sqrt{2}}$ x's, $\sqrt{2}$ x's, and 2 x's the electron loss rate model used for Figure 4.34. This series of figures illustrates that the slow enhancement is quite sensitive to the ionospheric-electron loss rates, with $\Delta\Phi$(10-1030A) at 2203 being inversely proportional to τ_{eff}. Note that this large slow flux enhancement estimate was derived from a small frequency deviation from 2158 to 2203 UT. Frequency deviations caused by ionospheric variations unrelated to solar flares can therefore easily distort the $\Delta\Phi$(10-1030A, t) estimates for slow enhancements with time constants large relative to τ.

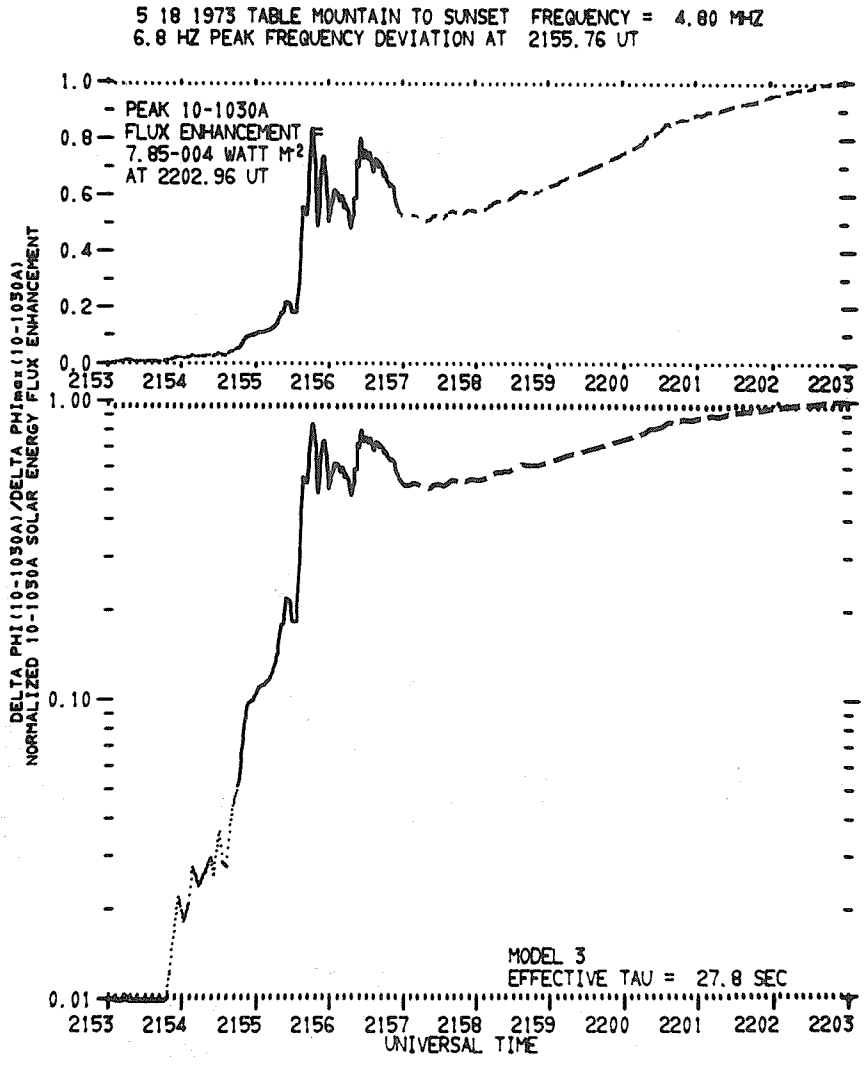

Figure 4.34 Best-estimate 10-1030A flux enhancement of 2156 UT May 18, 1973, based on 4.8 MHz at Sunset, Colorado.

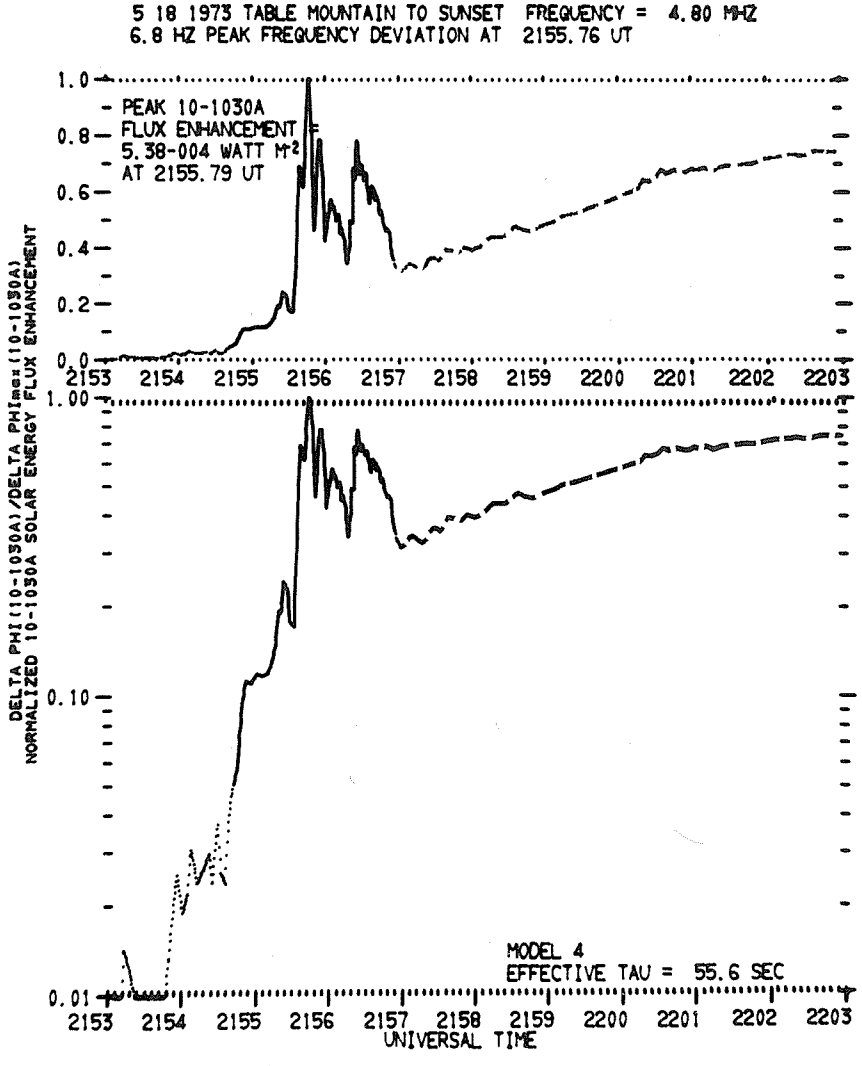

Figure 4.35 The 10-1030A flux enhancement of 2156 UT May 18, 1973, based on very low ionospheric electron-loss rates.

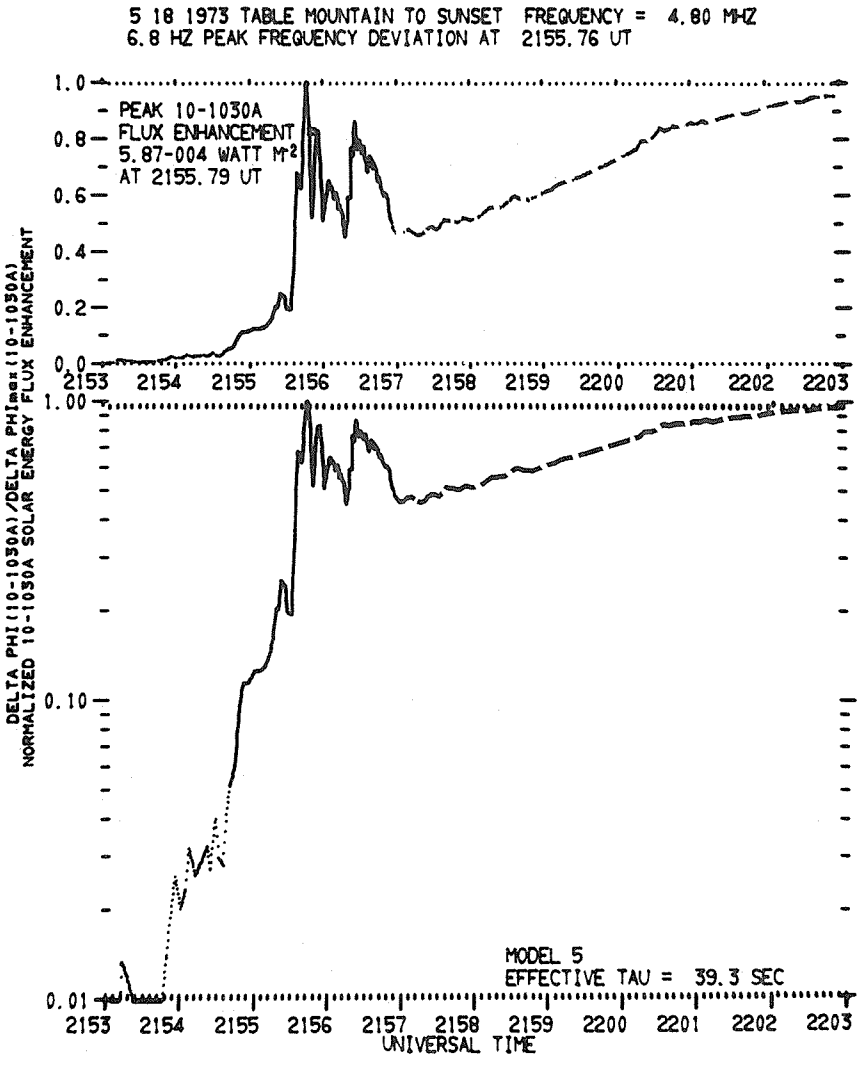

Figure 4.36 The 10-1030A flux enhancement of 2156 UT May 18, 1973, based on low ionospheric electron-loss rates.

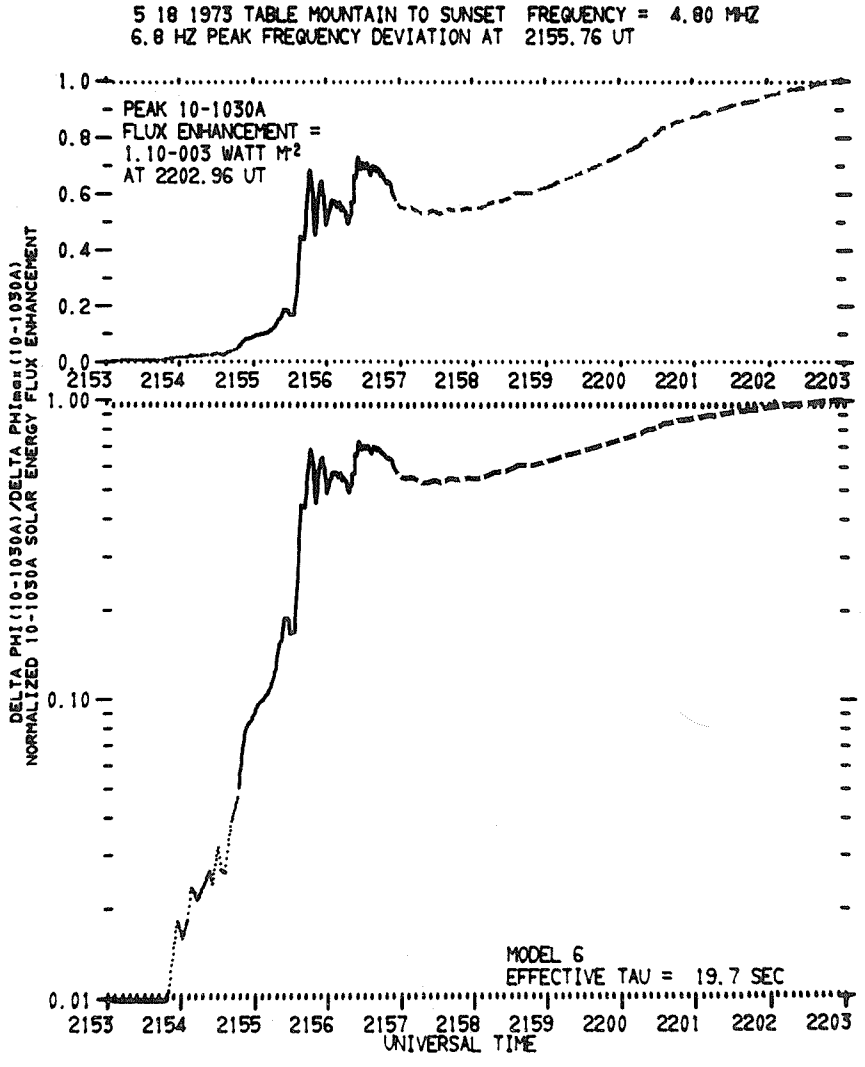

Figure 4.37 The 10-1030A flux enhancement of 2156 UT May 18, 1973, based on high ionospheric electron-loss rates.

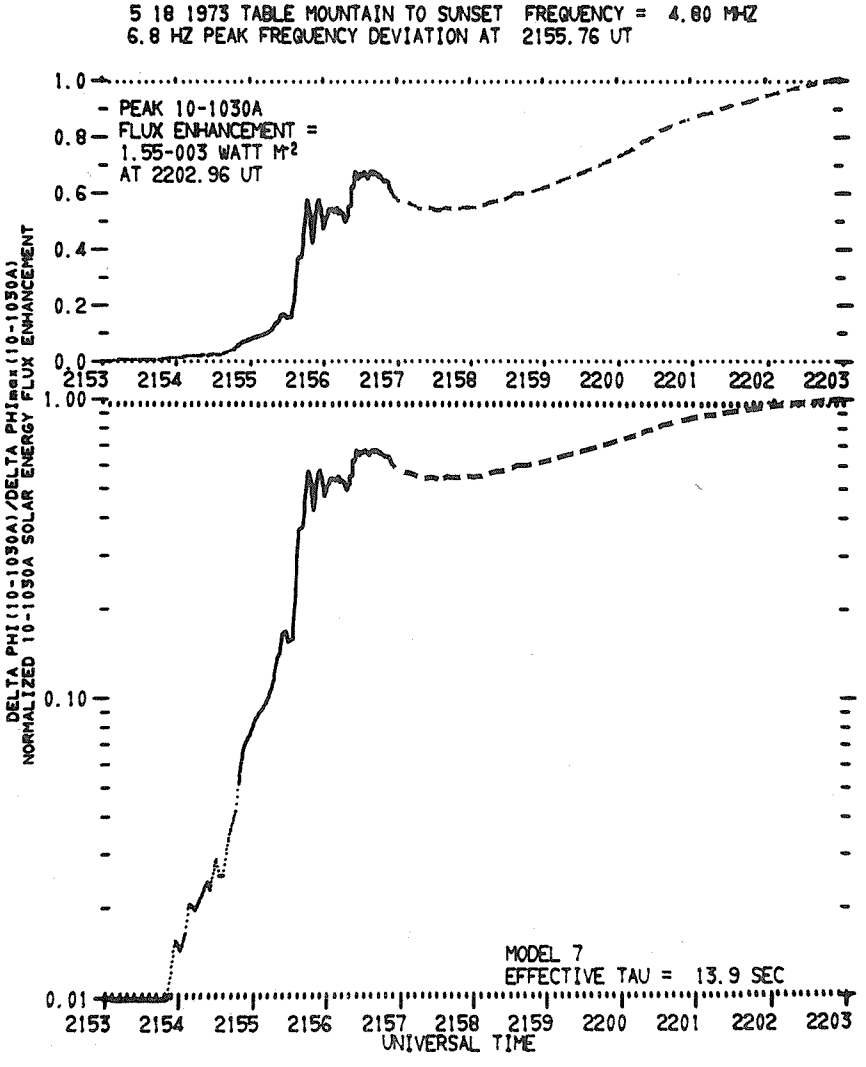

Figure 4.38 The 10-1030A flux enhancement of 2156 UT May 18, 1973, based on very high ionospheric electron-loss rates.

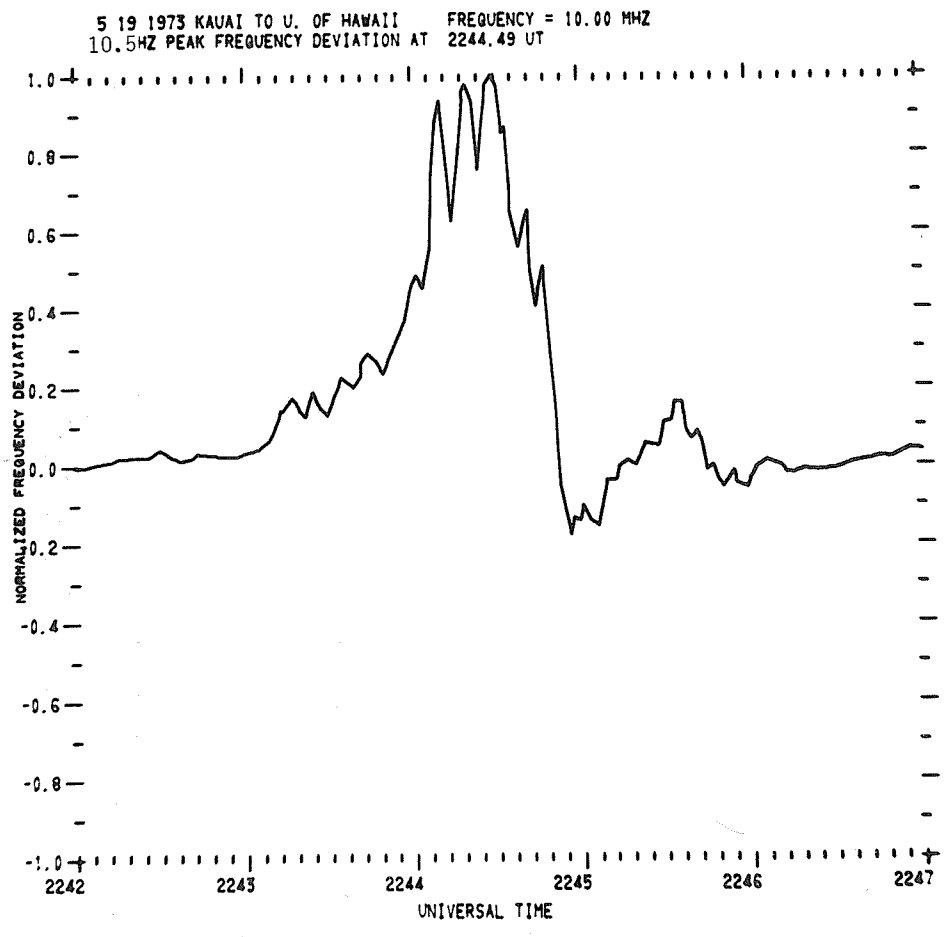

Figure 4.39 SFD of 2244 UT May 19, 1973.

This large SFD accompanied a 1B $H\alpha$ flare in McMath Plage Region 12352 at N09 E20 , starting at 2233 and peaking at 2245 UT. The microwave burst peaked at 2244.5 UT in the 2 to 11 GHz range (SGD) in close agreement with the EUV burst.

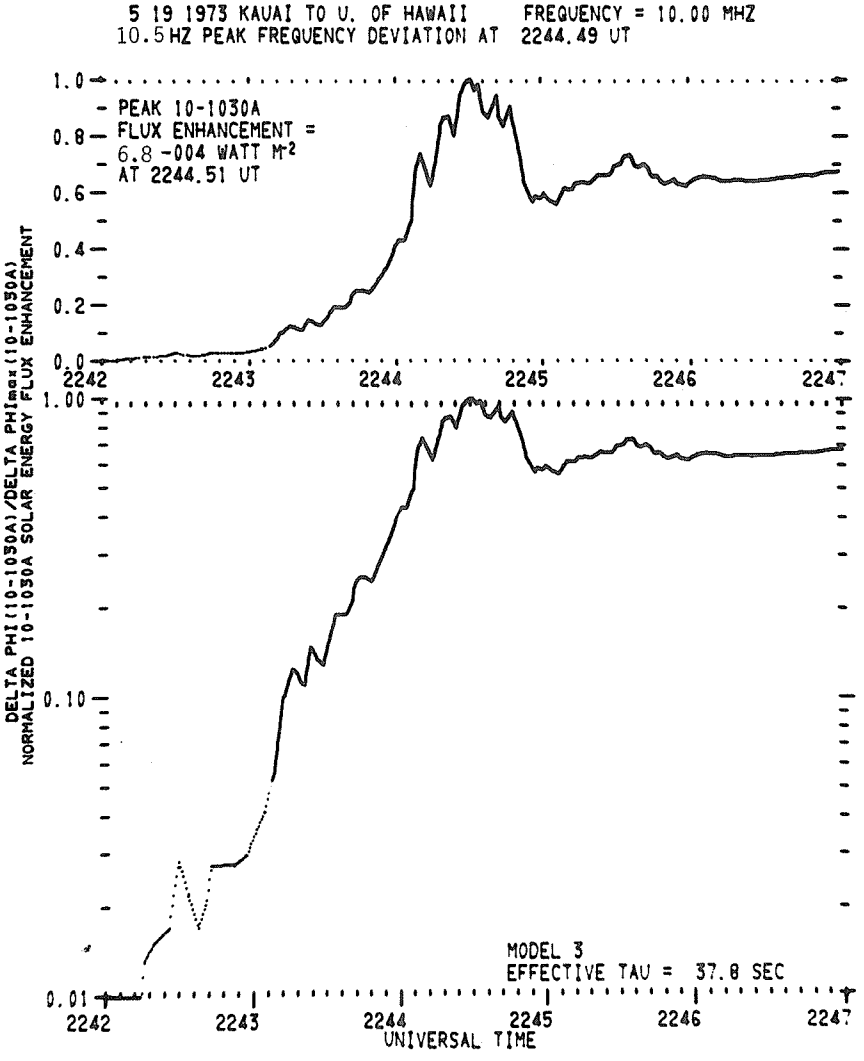

Figure 4.40 Best-estimate of 10-1030A flux enhancement of 2244 UT May 19, 1973.

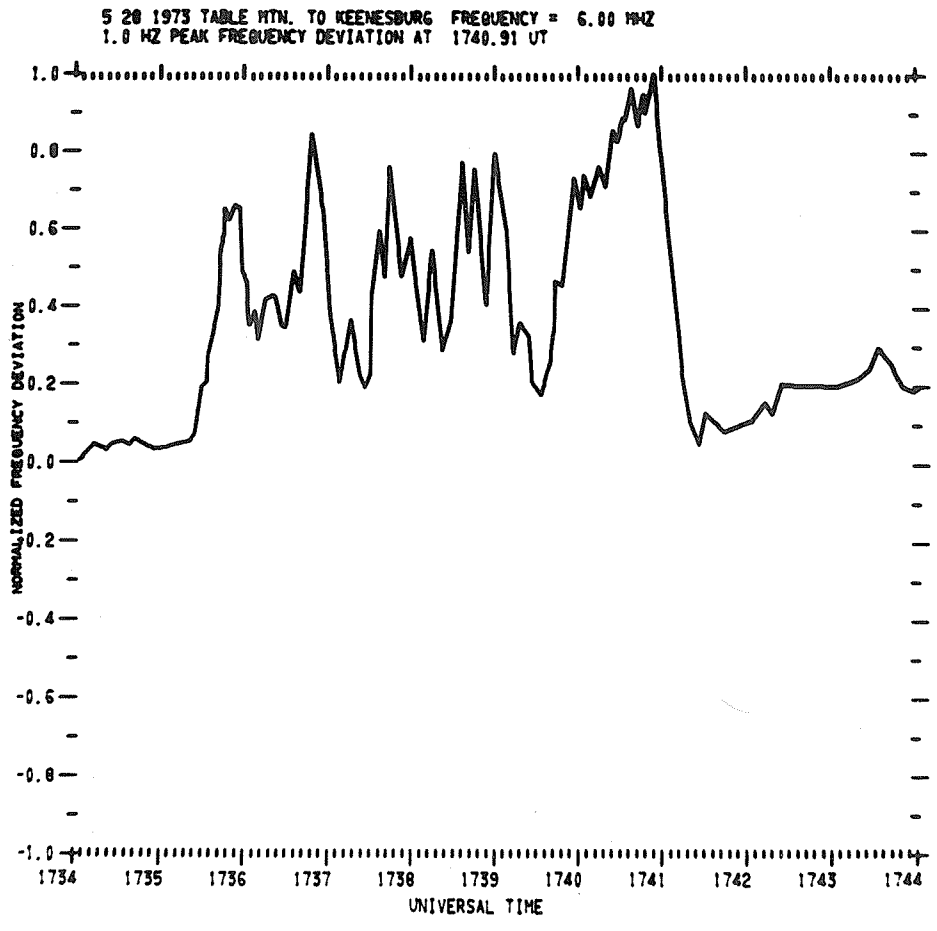

Figure 4.41 SFD of 1741 UT May 28, 1973.

The bright subflare associated with this SFD was at S00 W49 (McMath Plage Region 12357), starting at 1735 UT and peaking at 1741 UT. The 2-5 GHz burst peaked from 1741 to 1742 UT and was quite small, only 3×10^{-22} W m^{-2} Hz^{-1} at 2.8 GHz. The 6 MHz radio propagation was an extraordinary wave.

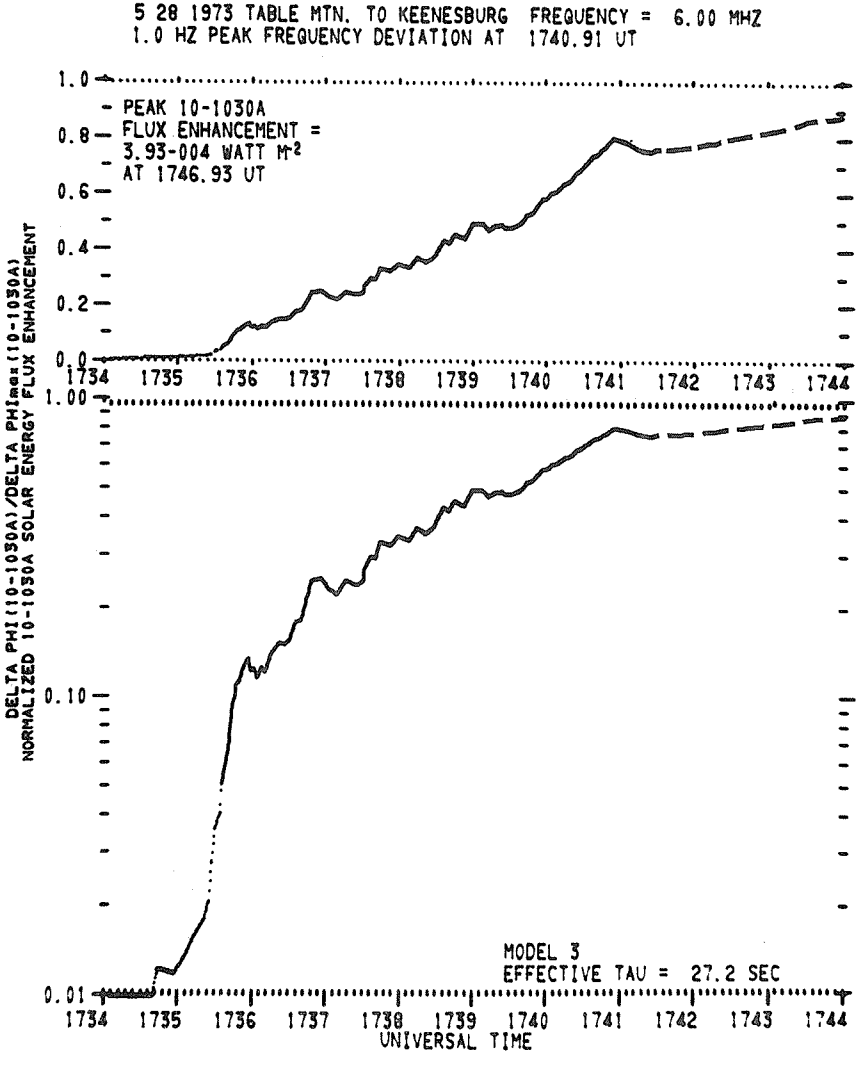

Figure 4.42 Best-estimate 10-1030A flux enhancement of 1741 UT May 28, 1973.

5. OBSERVATIONS DURING THE FIRST MANNED MISSION OF ATM-SKYLAB

The first manned ATM observations during SKYLAB II covered the period May 29 to June 18, 1973. The SFD observing times during the first manned ATM mission are illustrated in Figures 5.1 and 5.2 for the Sacramento Peak and Boulder HF Doppler observations respectively. The Boulder observations included at least one high sensitivity path reflected from the F-region 96% of the time. The level of solar activity was quite low during this three-week period; the daily average 10 cm flux measured at ARO, Ottawa, was below 100 the entire period. Few SFDs were observed. Their main features are listed in Table 5.1. The two events where the SFD was large enough and the data of sufficient quality were analyzed to estimate $\Delta\Phi(10\text{-}1030A, t)$; the main results are presented in Table 5.2.

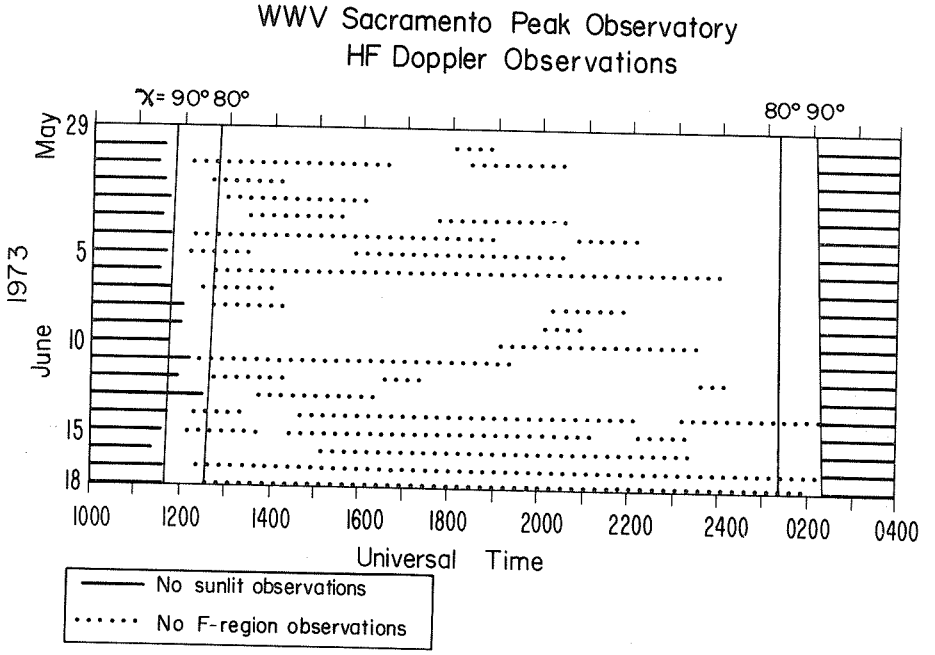

Figure 5.1 SFD observing time at Sacramento Peak Observatory during the first manned observations with ATM.

Clear areas indicate good observations, dotted indicate reduced sensitivity, solid line indicates no observations.

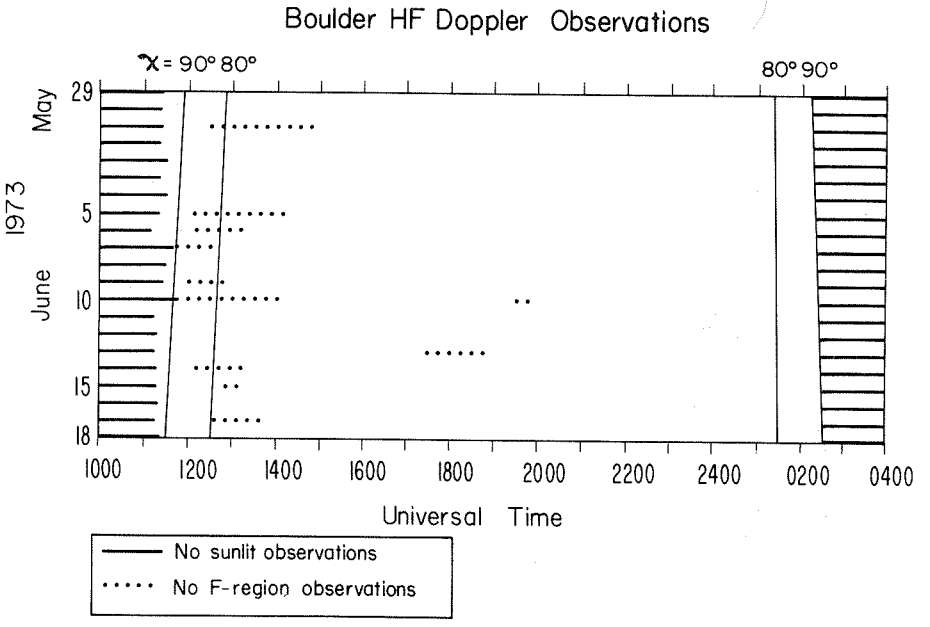

Figure 5.2 SFD observing time near Boulder, Colorado during the first manned observations with ATM.

Clear areas indicate good observations, dotted indicate reduced sensitivity, solid line indicates no observations.

Table 5.1 SFDs During the First Manned Mission of ATM-SKYLAB

SFD OBSERVATIONS

DATE			UNIVERSAL TIME				PEAK FREQUENCY DEVIATION		TRANSMITTER		
MONTH	DAY	YEAR	START	MAXIMUM	ZERO CROSSING	END	HZ	HF DOPPLER STATION	CALL LETTERS	FREQUENCY MHZ	COMMENTS
5	29	1973	1920.8	1921.4	1922.3	1925.	0.2	FT. COLLINS TO SAC PEAK	WWV	10.000	9 10
6	6	1973	2114.	2114.8	2117.	2119.	0.2	KAUAI TO U. OF HAWAII	WWVH	5.000	
				2116.2			0.4				
6	6	1973	2114.	2116.1	2117.3	2121. U	0.2	FORT COLLINS, COLORADO		4.8	11
6	6	1973	2115.	2116.1	2116.8	2120.	0.1	FT. COLLINS TO SAC PEAK	WWV	10.000	11 15
6	12	1973	2314.	2316.	2318.	2320. U	0.3	KAUAI TO U. OF HAWAII	WWVH	10.000	
6	15	1973	0026.	0027.	0028.	0030. U	0.3	KAUAI TO U. OF HAWAII	WWVH	5.000	
6	15	1973	1406. U	1409.5	1411.1	1420. U	3.0	SUNSET, COLORADO		4.8	7 10 18
				1409.8			2.8				
				1410.2			1.7				
				1410.4			2.2				
				1410.6			2.2				
				1410.9			2.3				
6	15	1973	1407. U	1409.3	1411.1	1422. U	3.0	FORT COLLINS, COLORADO		4.8	7 10 18
				1409.8			2.6				
				1410.5			2.1				
				1410.9			2.4				
6	15	1973	1407.	1409.7	1411.1	1422. U	4.7	KEENESBURG, COLORADO		4.8	7 10 18 1 21
				1410.3			4.3				
				1410.8			3.0				
6	15	1973	1407.	1409.7	1411.3	1420. U	1.8	U. OF LEICESTER, ENGLAND		4.793	7 21
				1410.1			2.1				
				1410.9			2.2				
				1411.1			2.7				
6	16	1973	1421.4	1423.1	1424.8	1430. U	2.2	KEENESBURG, COLORADO		4.8	10 18
6	16	1973	1421.	1423.3	1428.	1435. U	0.2	FT. COLLINS TO SAC PEAK	WWV	10.000	10 15
6	16	1973	1945.	1946.	1947.	1948. U	0.3	KAUAI TO U. OF HAWAII	WWVH	5.000	

U uncertain

See Table 4.1 for the numbered comments.

Table 5.2 The Impulsive 10-1030A Flux Enhancements Deduced From SFDs During the First Manned Mission of ATM-SKYLAB May 29 - June 18, 1973

Date 1973	Number of Channels of SFD Data Analyzed to $\Delta\Phi$(10-1030A)	Start Time UT	Peak Time UT	$\Delta\Phi$(10-1030A)* Peak	Peak Time UT	$\Delta\Phi$(10-1030A)* Peak
June 15	4	1407	1410.9	7.1×10^{-4}		
June 16	1	1421.4	1423.2	2.0×10^{-4}	1424.5	$\underline{3.1 \times 10^{-4}}$

Underlined peak flux values are the maximum values for the event.

*$\Delta\Phi$(10-1030A) flux units are Watts m^{-2}.

The quality of the SFD data for the SFDs illustrated in Figures 5.3, 5.10 and 5.12 is generally lower than for the events selected for illustration in Section 4. The June 15th event was quasi-periodic (10.4 sec) and had the largest peak 10-1030A flux enhancement of all the SFDs observed during the ATM missions. It was a medium sized 10-1030A burst, comparable to the larger events in Table 4.2, but more than an order of magnitude smaller than the largest events observed during 1960 to 1970. The ATM observations of this flare commenced their flare mode just after 1411 UT, so the impulsive phase of the flare was missed but the rising slow component was well observed.

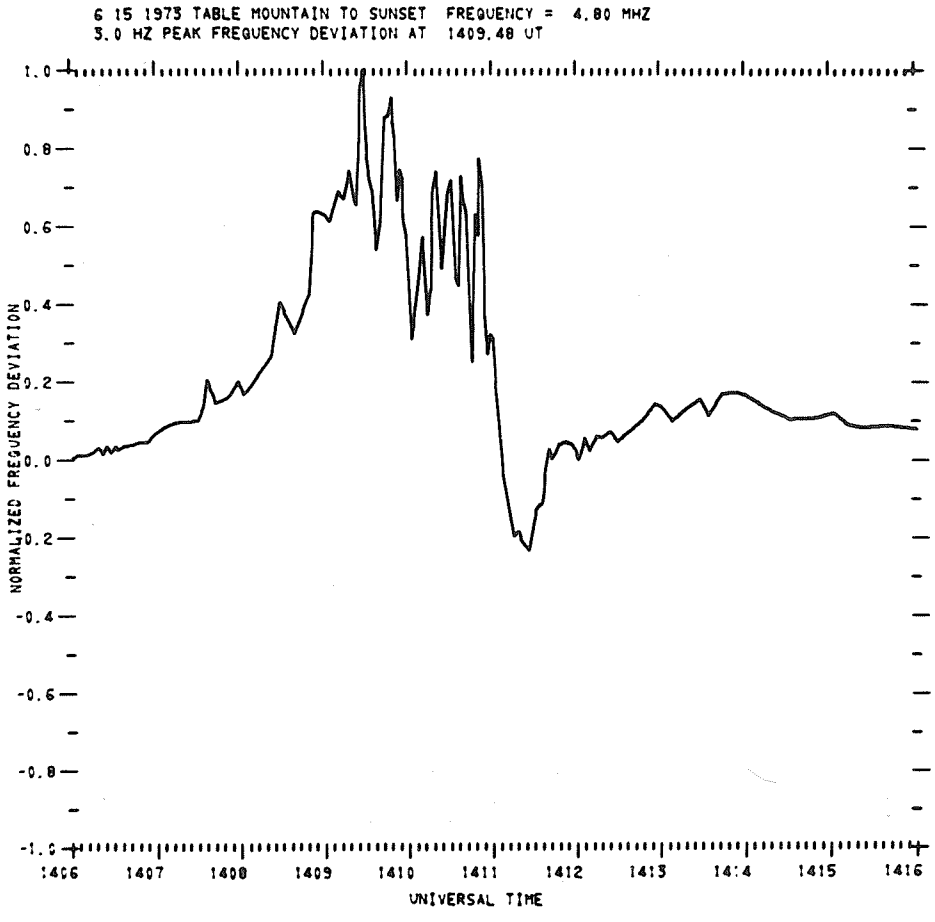

Figure 5.3 SFD of 1409 UT June 15, 1973, on 4.8 MHz at Sunset, Colorado.

This medium sized SFD accompanied a 1B flare at N17 W32 (McMath Plage Region 12379), which started at about 1405 UT and reached maximum phase at 1413 UT. The microwave bursts observed at fixed frequencies in the range 2 to 15 GHz peaked at various times ranging from 1410 to 1420 UT (SGD). The fine structure in the SFD is quasi-periodic with the strongest period being 10.4 sec which was accompanied by weaker harmonics and subharmonics. However, the amplitude of the quasi-periodic structure is quite weak relative to $\Delta\Phi_{max}$ (10-1030A) (see figure 5.4), which is typical of most quasi-periodic EUV bursts. Figures 5.5 and 5.9 illustrate that the slow 10-1030A enhancement peaking at 1416 UT is sensitive to the model used for ionospheric electron loss rates. For most SFDs discussed in this atlas, the results for Model 3 agree well with those based on the Mitra-Banerjee model; however, for this event there is a significant difference as shown in Figure 5.9.

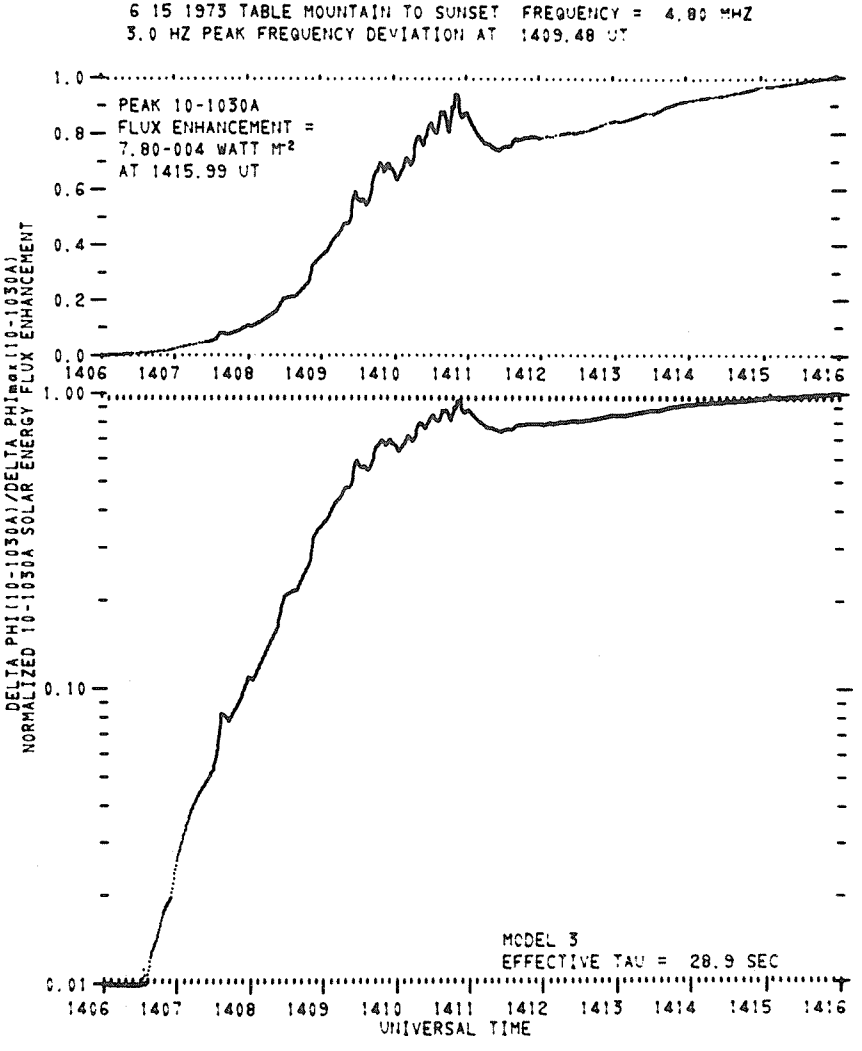

Figure 5.4 Best-estimate 10-1030A flux enhancement of 1411 UT June 15, 1973, based on 4.8 MHz at Sunset, Colorado.

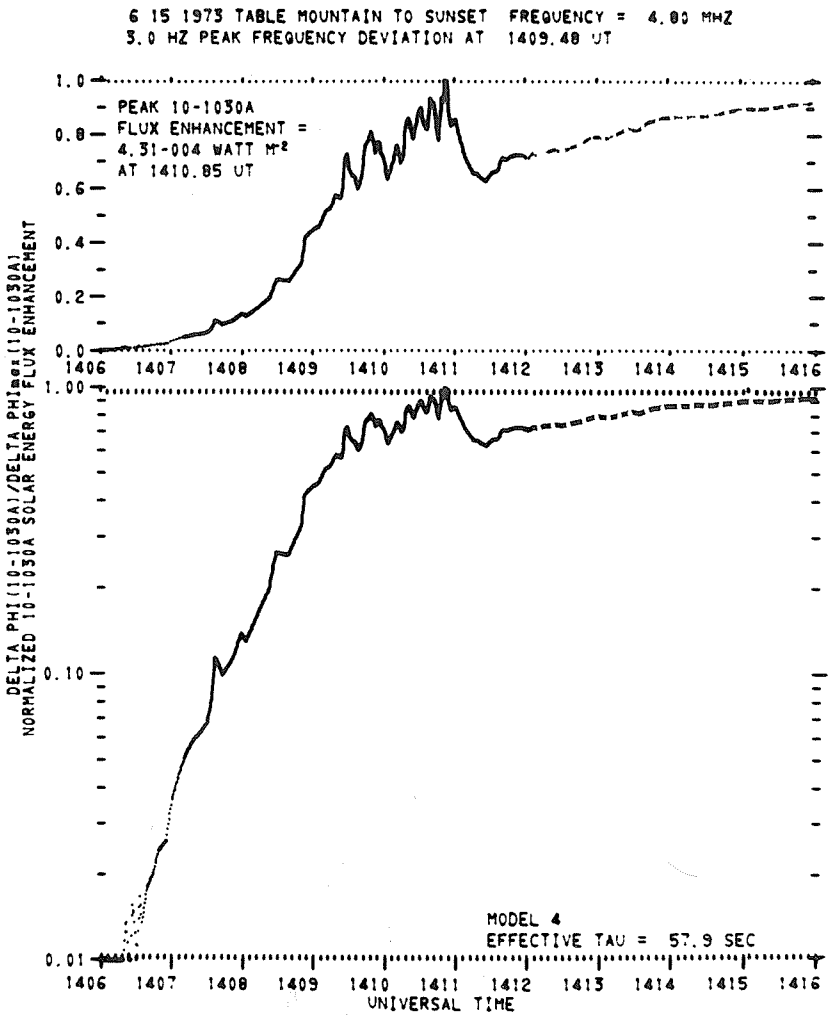

Figure 5.5 The 10-1030A flux enhancement of 1411 UT June 15, 1973, based on very low ionospheric electron loss rates.

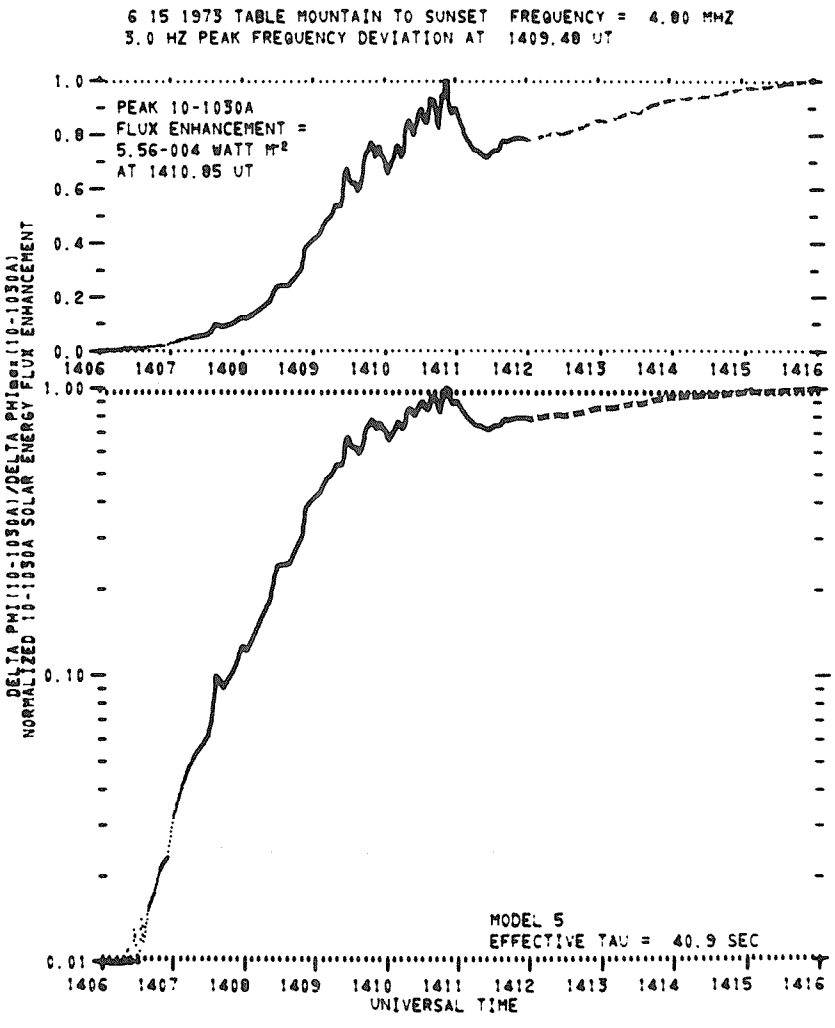

Figure 5.6 The 10-1030A flux enhancement of 1411 UT June 15, 1973, based on low ionospheric electron loss rates.

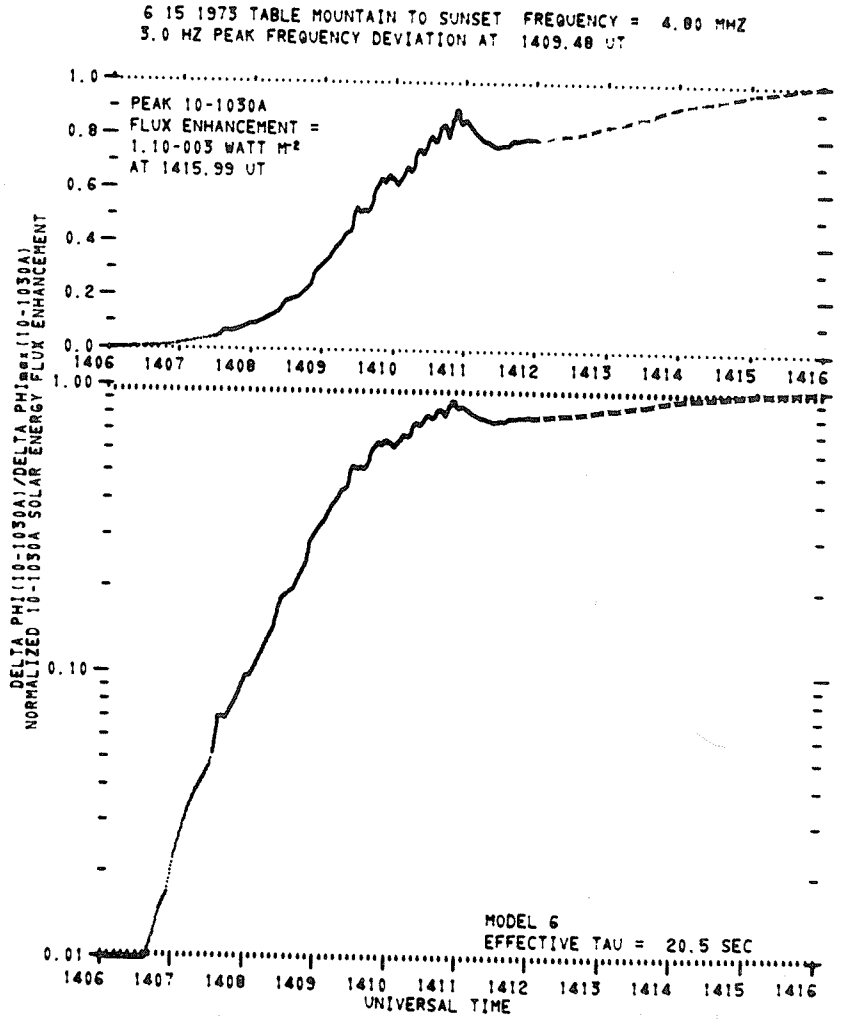

Figure 5.7 The 10-1030A flux enhancement of 1411 UT June 15, 1973, based on high ionospheric electron loss rates.

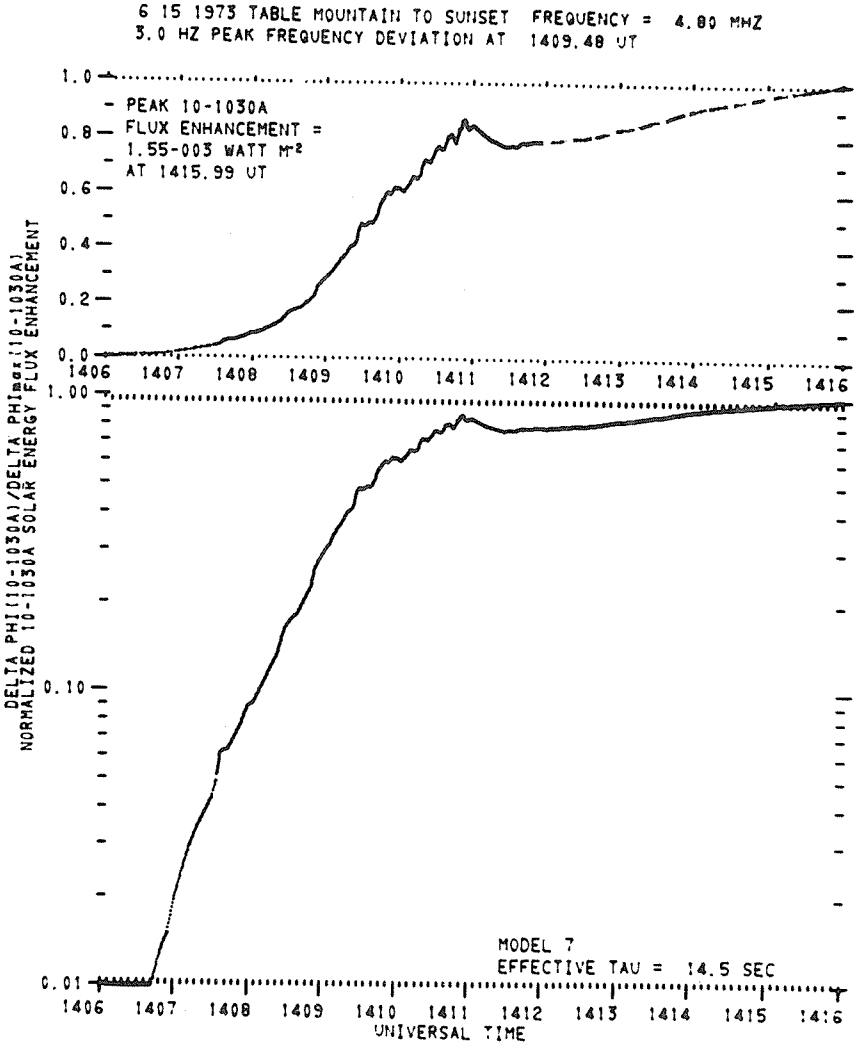

Figure 5.8 The 10-1030A flux enhancement of 1411 UT June 15, 1973, based on very high ionospheric electron loss rates.

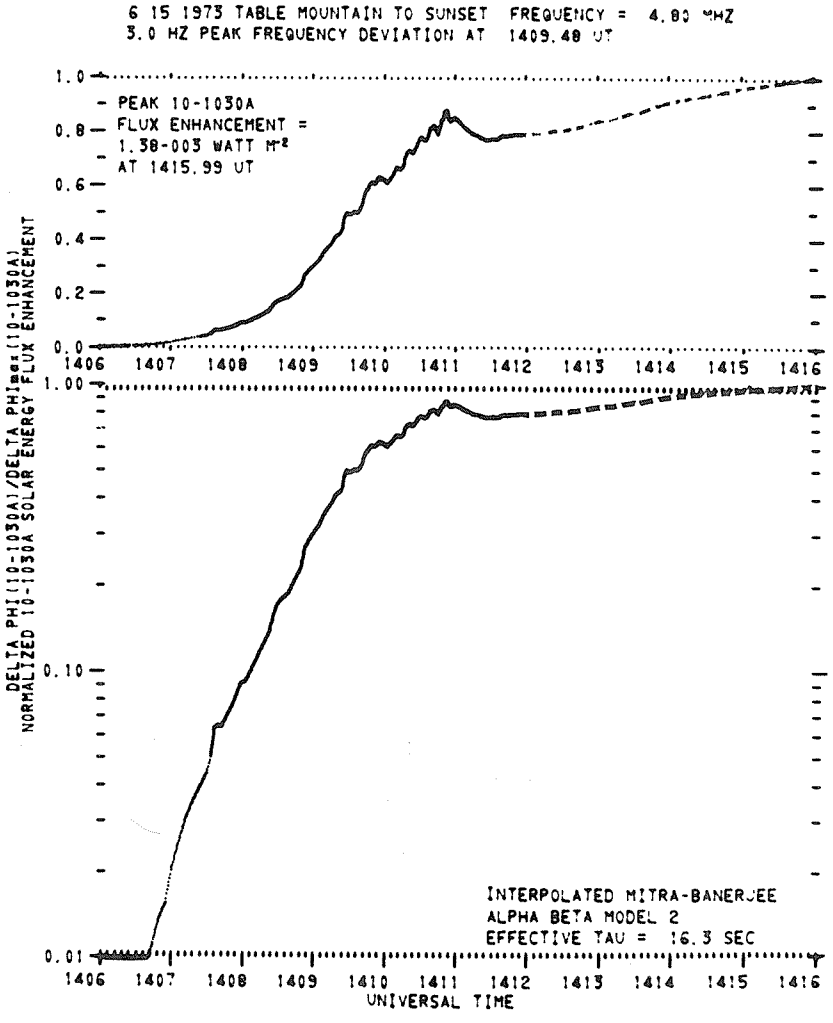

Figure 5.9 The 10-1030A flux enhancement of 1411 UT June 15, 1973, based on Mitra-Banerjee models of the ionospheric electron loss rates.

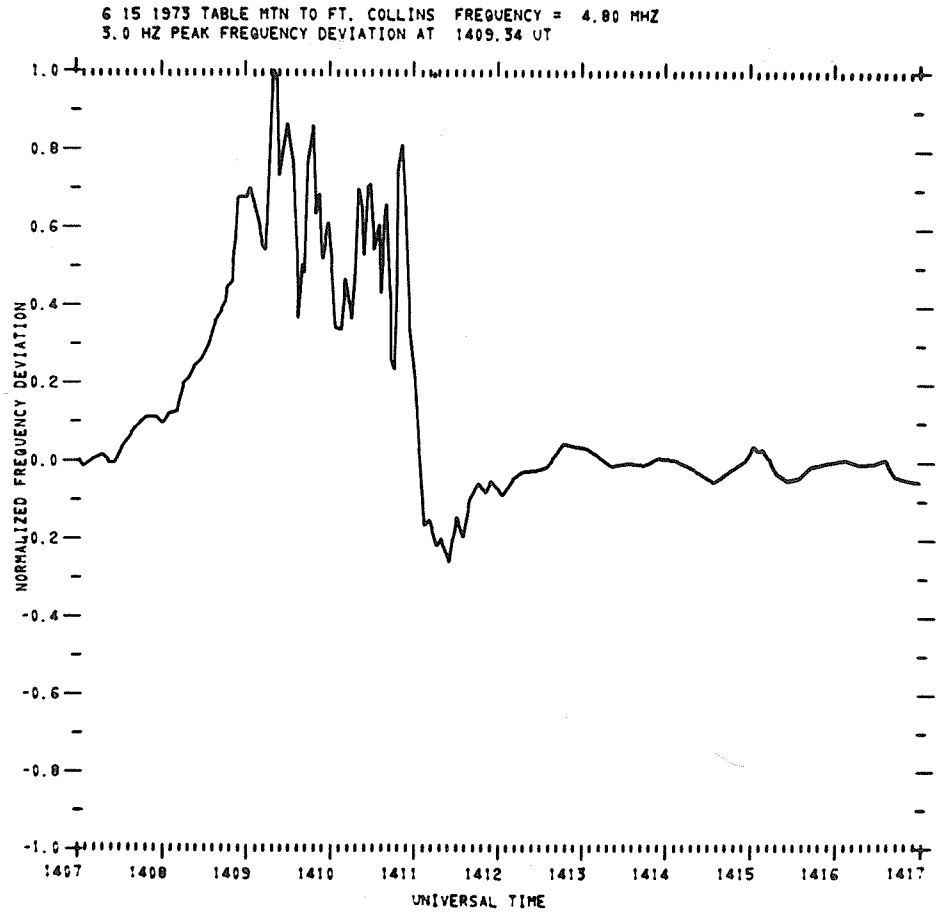

Figure 5.10 SFD of 1409 UT June 15, 1973, on 4.8 MHz at Fort Collins, Colorado.

Figure 5.10 shows another channel of SFD data for the same flare as in Figure 5.3. All the Boulder SFD data were noisy before 1409 UT, and the small fine structure before 1409 UT was poorly resolved. The main fine structure from 1409 to 1411 UT is not identical in relative amplitude in the various HF Doppler channels because noise in the data resulted in the fast fine structure not being clearly resolved. However, the timing of the fine structure was consistent. The fine structure was observed in Leicester also. At 1410.9 UT, $\Delta\Phi$(10-1030A) = 7.3×10^{-4} in Figure 5.4 and 6.7×10^{-4} W m^{-2} in Figure 5.11. The fine structure and the impulsive phase of this flare terminated at 1411.3 UT. The 4.8 MHz radio propagation was an extraordinary wave.

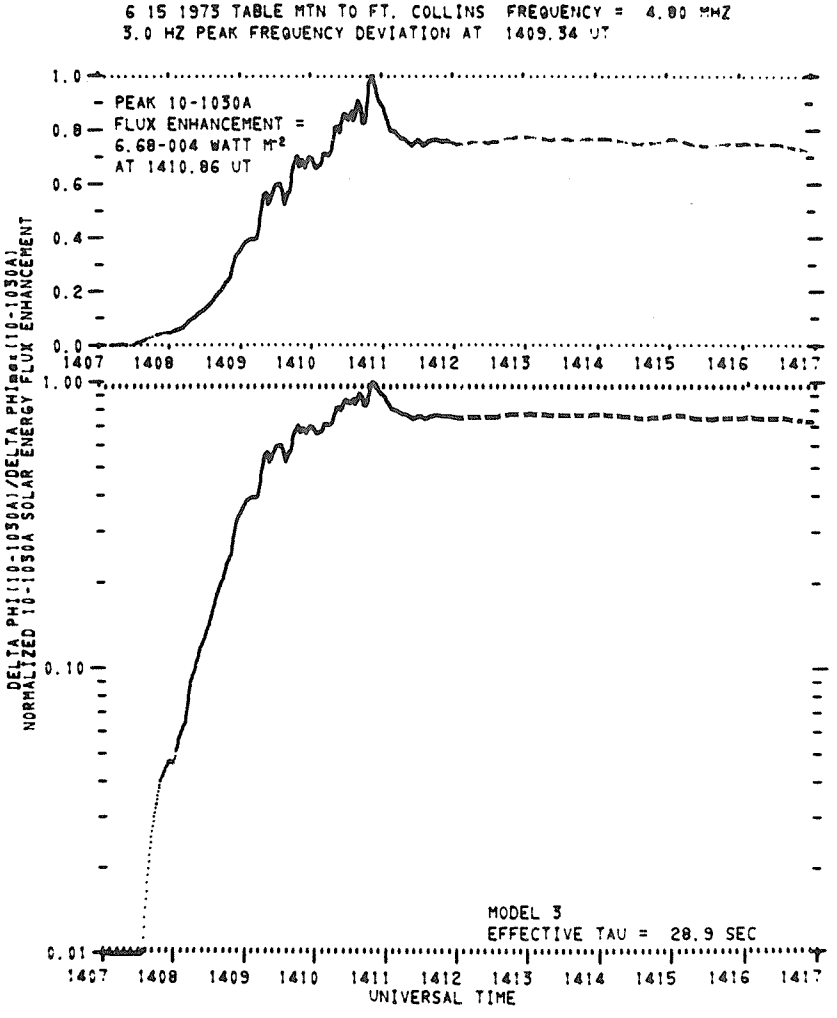

Figure 5.11 Best-estimate 10-1030 A flux enhancement of 1411 UT June 15, 1973, based on 4.8 MHz at Fort Collins, Colorado.

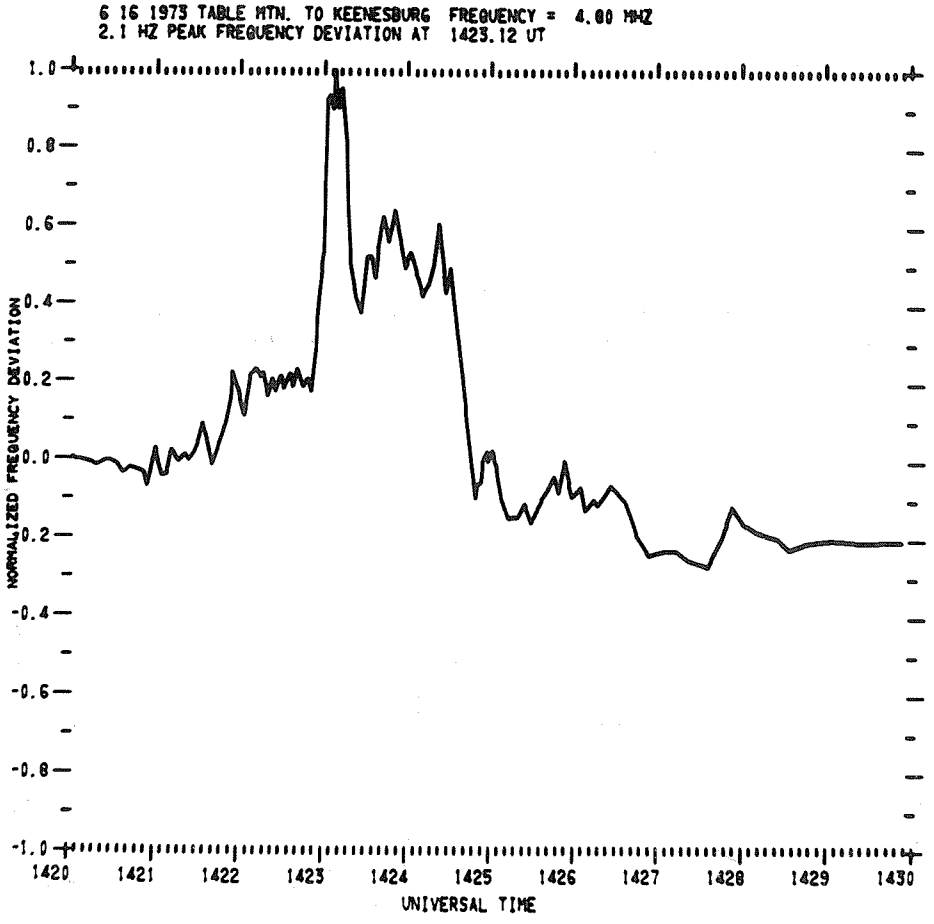

Figure 5.12 SFD of 1423 UT June 16, 1973.

The 2B Hα flare at N13 E11 (McMath Plage Region 12387) started near 1419 UT and reached maximum phase at 1427 UT. The 2-9 GHz radio burst peaked near 1424.5 UT (SGD). The 4.8 MHz radio propagation was an extraordinary wave. The fine structure in Figure 5.2 smaller than 0.05 and lasting about 0.1 minute is probably just noise in the data. This is the only HF Doppler data available having an F-region path, except the F-region path came in on 4.8 MHz at Sunset from 1422 to 1424 UT, which was long enough to corroborate the main part of the SFD.

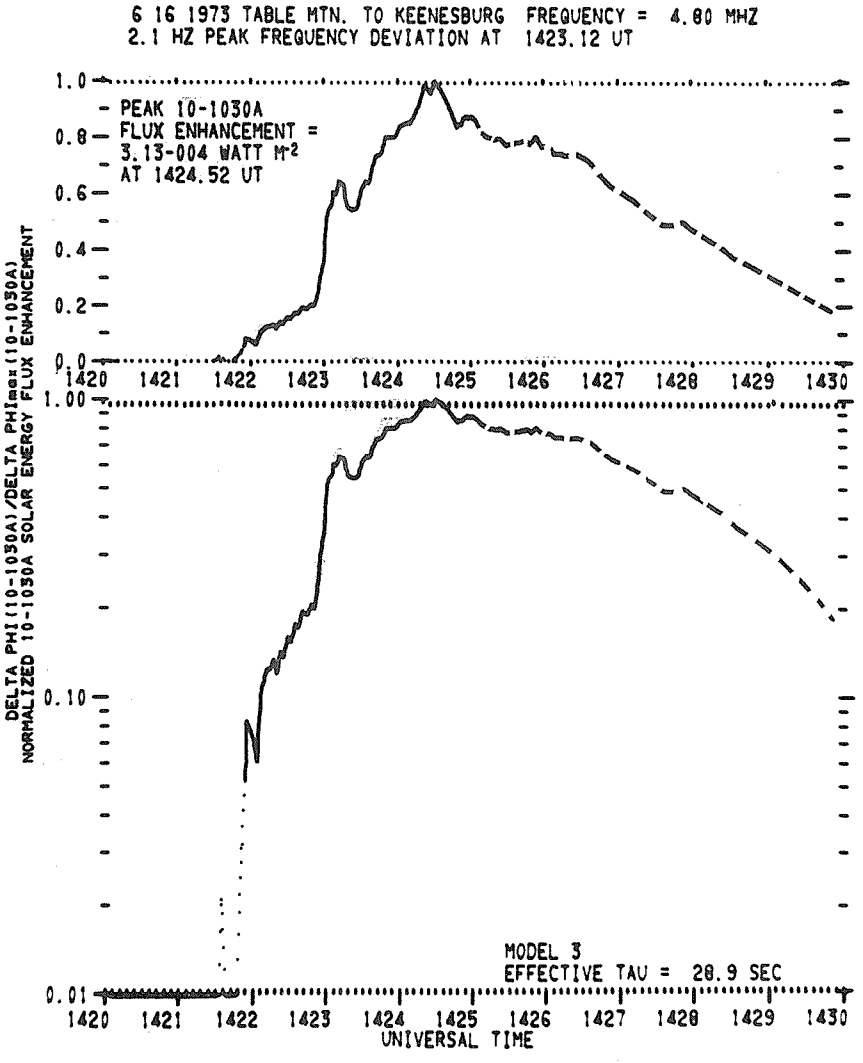

Figure 5.13 Best-estimate 10-1030A flux enhancement of 1424 UT June 16, 1973.

6. OBSERVATIONS DURING THE FIRST UNMANNED MISSION OF ATM-SKYLAB

The last ATM film observations of the first manned mission (SKYLAB II) were taken on June 18, 1973, and the first film observations of the second manned mission (SKYLAB III) were taken on August 7, 1973. The interim period, June 19 through August 6, will be discussed here. The Harvard ATM experiment made observations via telemetry during this unmanned period.

The SFD observing times are shown in Figures 6.1 and 6.2. The Sacramento Peak observations were reduced in sensitivity most of the time by the dominance of HF Doppler propagation paths reflected from the bottom of the E-layer of the ionosphere. The level of solar activity was generally low during this period. Although the daily average Ottawa 10 cm flux did rise above 100 from June 20 through 26, it dipped below 80 to nearly sunspot minimum values in mid-July and early August. The observed SFDs are listed in Table 6.1 and the peak 10-1030A flux values for some of the larger SFDs are listed in Table 6.2. All of these EUV bursts are of small intensity, i.e., $\Delta\Phi_{max}$(10-1030A) < 5×10^{-4} Watts m^{-2}.

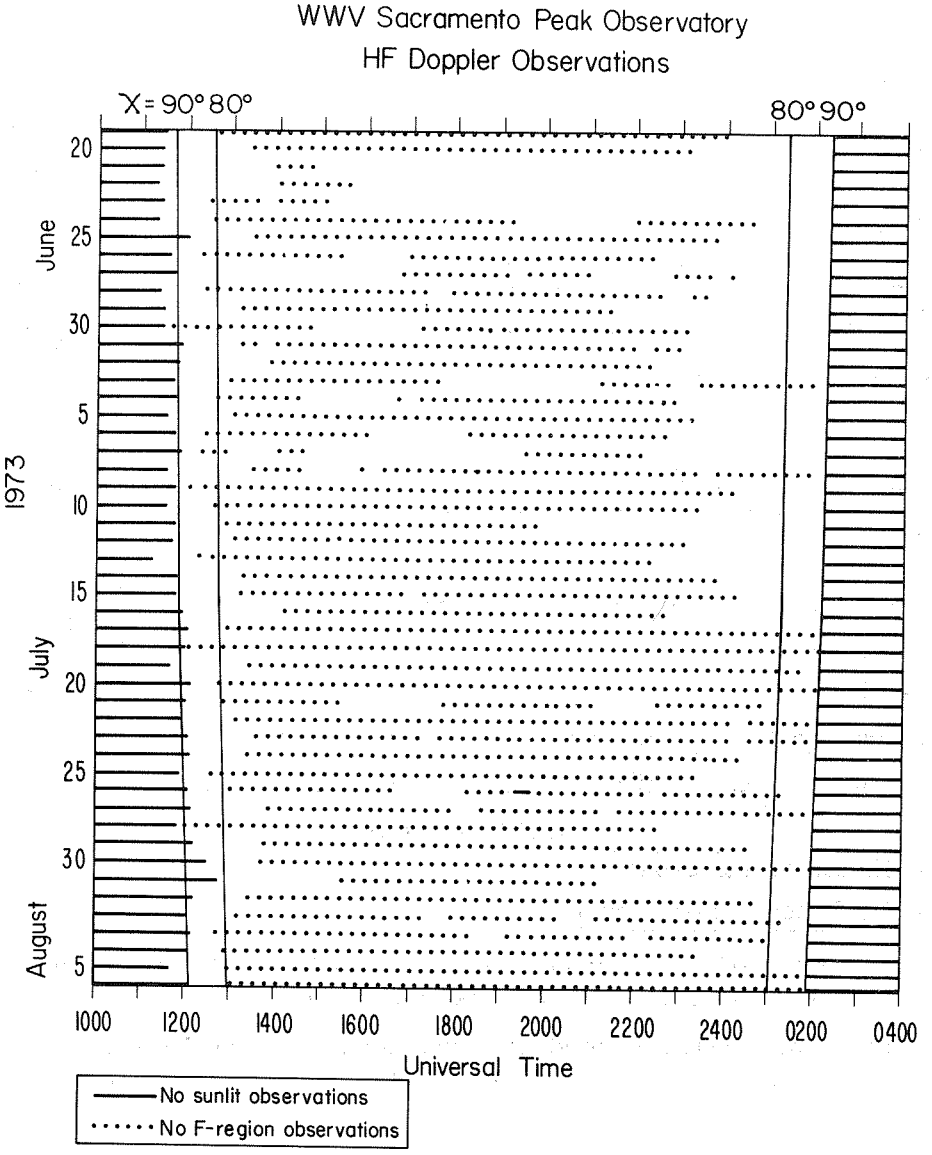

Figure 6.1 SFD observing time at Sacramento Peak Observatory during the first unmanned observations with ATM.

Clear areas indicate good observations, dotted indicate reduced sensitivity, solid line indicates no observations.

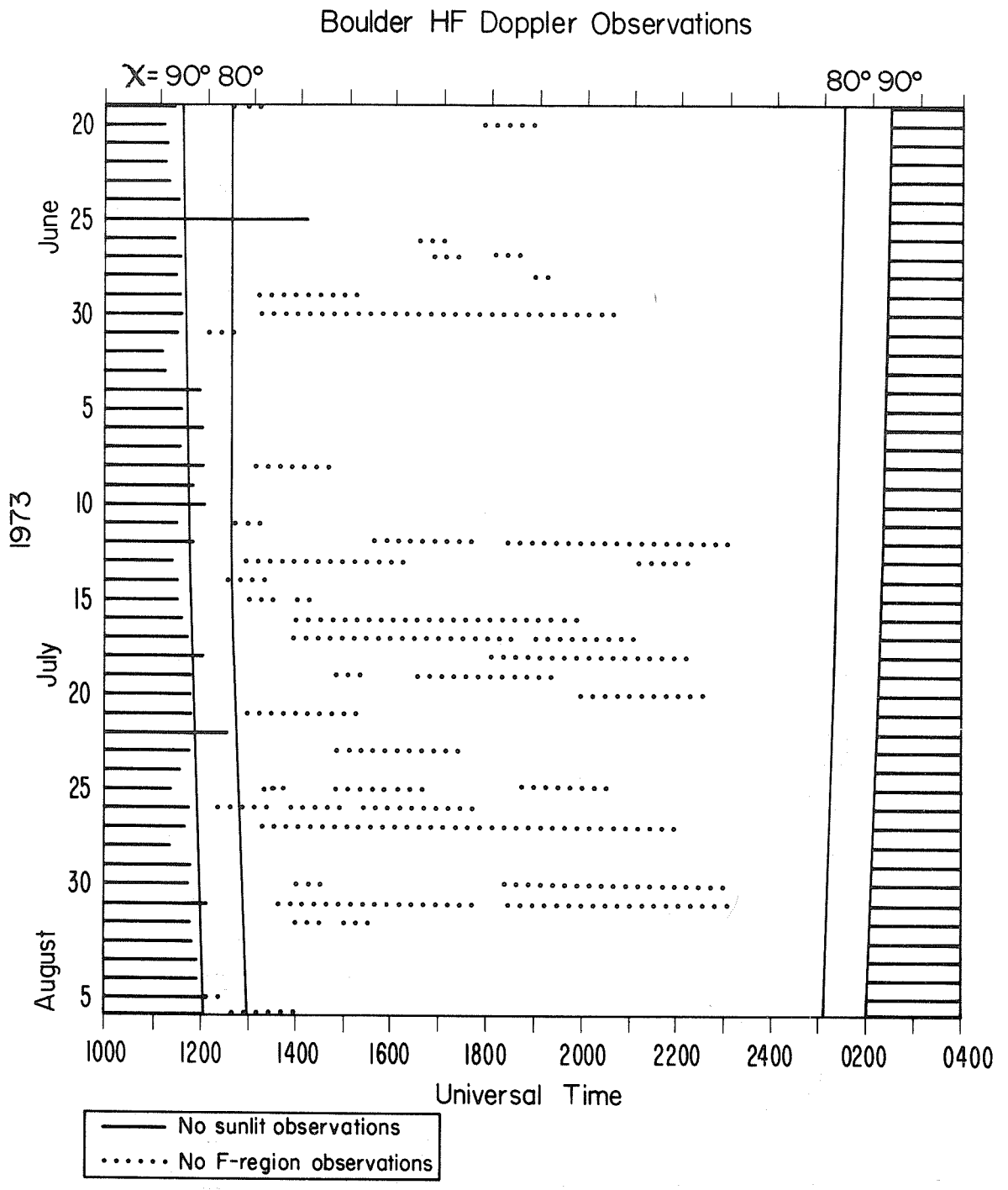

Figure 6.2 SFD observing time near Boulder, Colorado during the first unmanned observations with ATM.

Clear areas indicate good observations, dotted indicate reduced sensitivity, solid line indicates no observations.

Table 6.1 SFDs During the First Unmanned Mission of ATM-SKYLAB

SFD OBSERVATIONS

DATE			UNIVERSAL TIME				PEAK FREQUENCY DEVIATION		TRANSMITTER			
MONTH	DAY	YEAR	START	MAXIMUM	ZERO CROSSING	END	HZ	HF DOPPLER STATION	CALL LETTERS	FREQUENCY MHZ		COMMENTS
6	25	1973	1748.	1749.	1749.4	1752. U	0.1	FT. COLLINS TO SAC PEAK	WWV	15.000	9	15
6	28	1973	1840. U	1841.8	1843.5	1850. U	0.2	FT. COLLINS TO SAC PEAK	WWV	10.000	10	
				1842.9			0.1					
6	28	1973	1839. U	1841.9	1844.0	1849. U	0.8	FORT COLLINS, COLORADO		4.8	10	
				1842.4			1.1					
				1843.4			1.2					
6	28	1973	1840.	1842.4	1843.9	1848. U	0.9	SUNSET, COLORADO		6.0	10	18
				1842.9			0.8					
6	28	1973	1840.	1843.	1846. U	1848. U	0.6	KAUAI TO U. OF HAWAII	WWVH	5.000	10	
6	28	1973	1857.7	1859.8	1909.8	1922. U	0.4	FT. COLLINS TO SAC PEAK	WWV	10.000		
				1901.8			0.4					
6	28	1973	1857.5	1858.6		1913. U	0.4	FORT COLLINS, COLORADO		4.8	13	
6	29	1973	1512.4	1515.9	1516.2	1524. U	4.0	SUNSET, COLORADO		4.8	18	
6	29	1973	1512.2	1516.0	1518.0	1527.	1.0	FT. COLLINS TO SAC PEAK	WWV	5.000		
6	29	1973	1944.3	1947.5	1952.0	2025. U	0.6	FT. COLLINS TO SAC PEAK	WWV	15.000	20	
				1948.8			0.7					
				1949.8			0.3					
6	30	1973	1514.7	1515.8	1517.6	1523. U	1.5	SUNSET, COLORADO		4.8	10	18
				1516.5			1.3					
				1517.4			1.9					
6	30	1973	1514.1	1515.8	1517.7	1522. U	1.2	FORT COLLINS, COLORADO		4.8	10	18
				1517.4			1.9					
6	30	1973	2157.0	2200.2	2201.3	2207.	0.1	FT. COLLINS TO SAC PEAK	WWV	15.000	9	15
7	5	1973	0553.	0554.		0555.	0.2	KAUAI TO U. OF HAWAII	WWVH	10.000		
7	5	1973	0553.	0554.		0555.	0.4	KAUAI TO U. OF HAWAII	WWVH	5.000		

Table 6.1 - (continued)

DATE			UNIVERSAL TIME				PEAK FREQUENCY DEVIATION		TRANSMITTER CALL LETTERS	FREQUENCY	
MONTH	DAY	YEAR	START	MAXIMUM	ZERO CROSSING	END	HZ	HF DOPPLER STATION		MHZ	COMMENTS
7	8	1973	2004. U	2007. U	2008.4	2015.	0.1	FT. COLLINS TO SAC PEAK	WWV	10.000	10 15
7	9	1973	1625.	1628.	1630.5	1640.	0.1	FT. COLLINS TO SAC PEAK	WWV	5.000	3 9 15
7	10	1973	0217.	0218.		0224.	0.3	KAUAI TO U. OF HAWAII	WWVH	5.000	
				0220.			0.4				
				0222.			0.1				
7	10	1973	0324.	0325.	0333. U	0327.	0.7	KAUAI TO U. OF HAWAII	WWVH	5.000	
				0326.			0.5				
7	10	1973	0324.	0325.		0327.	0.3	KAUAI TO U. OF HAWAII	WWVH	10.000	
				0326.			0.2				
7	12	1973	0545.	0546.		0549.	0.1	KAUAI TO U. OF HAWAII	WWVH	10.000	
7	26	1973	0000.	0001.9	0002.	0003.	0.1	FT. COLLINS TO SAC PEAK	WWV	10.000	10 15
7	29	1973	1319.	1320.	1338. U	1345. U	0.6	U. OF LEICESTER, ENGLAND		4.793	8 21
				1321.			0.7				
				1323.			0.6				
				1327.			0.1				
				1337.			0.2				
8	6	1973	0549.	0550.		0554.	0.2	KAUAI TO U. OF HAWAII	WWVH	10.000	
				0551.			0.1				
				0552.			0.1				
				0553.			0.1				
8	6	1973	0556.	0557.		0559.	0.2	KAUAI TO U. OF HAWAII	WWVH	10.000	
8	6	1973	1405.	1412.	1417.	1500. U	0.1	FT. COLLINS TO SAC PEAK	WWV	10.000	3 9 10 15
8	6	1973	1716.7U	1722.5	1724.5	1734.	0.8	FT. COLLINS TO SAC PEAK	WWV	5.000	10
8	6	1973	1719.1U	1722.6	1724.5	1736. U	1.3	FT. COLLINS TO SAC PEAK	WWV	15.000	10 19 20
8	6	1973	1720. U	1722.5	1724.0	1733. U	2.8	FORT COLLINS, COLORADO		6.0	10 18

U uncertain

See Table 4.1 for the numbered comments.

TABLE 6.2

The Impulsive 10-1030A Flux Enhancements Deduced
from SFDs During the First Unmanned Mission of ATM SKYLAB

Date 1973	Number of Channels of SFD Data Analyzed To $\Delta\Phi$(10-1030A)	Start Time UT	Peak Time UT	$\Delta\Phi$ (10-1030A)* Peak	Peak Time UT	$\Delta\Phi$ (10-1030A)* Peak	Peak Time UT	$\Delta\Phi$ (10-1030A)* Peak
June 28	3	1840	1843.4	$\underline{2.2\times10^{-4}}$				
June 28	1	1858	1910†	$\underline{7.2\times10^{-4}}$				
June 29	2	1512.4	1516.0	$\underline{3.8\times10^{-4}}$				
June 29	1	1944.4	1948.8	1.8×10^{-4}	1951†	$\underline{2.0\times10^{-4}}$		
June 30	2	1514.5	1517.4	$\underline{1.5\times10^{-4}}$				
August 6	3	1719	1722.5	9.2×10^{-5}	1723.6	$\underline{1.0\times10^{-4}}$	1724.2	9.4×10^{-5}

Underlined peak flux values are the maximum values for the event.

* $\Delta\Phi$ (10-1030A) flux units are Watts m^{-2}.

† Gradual peak

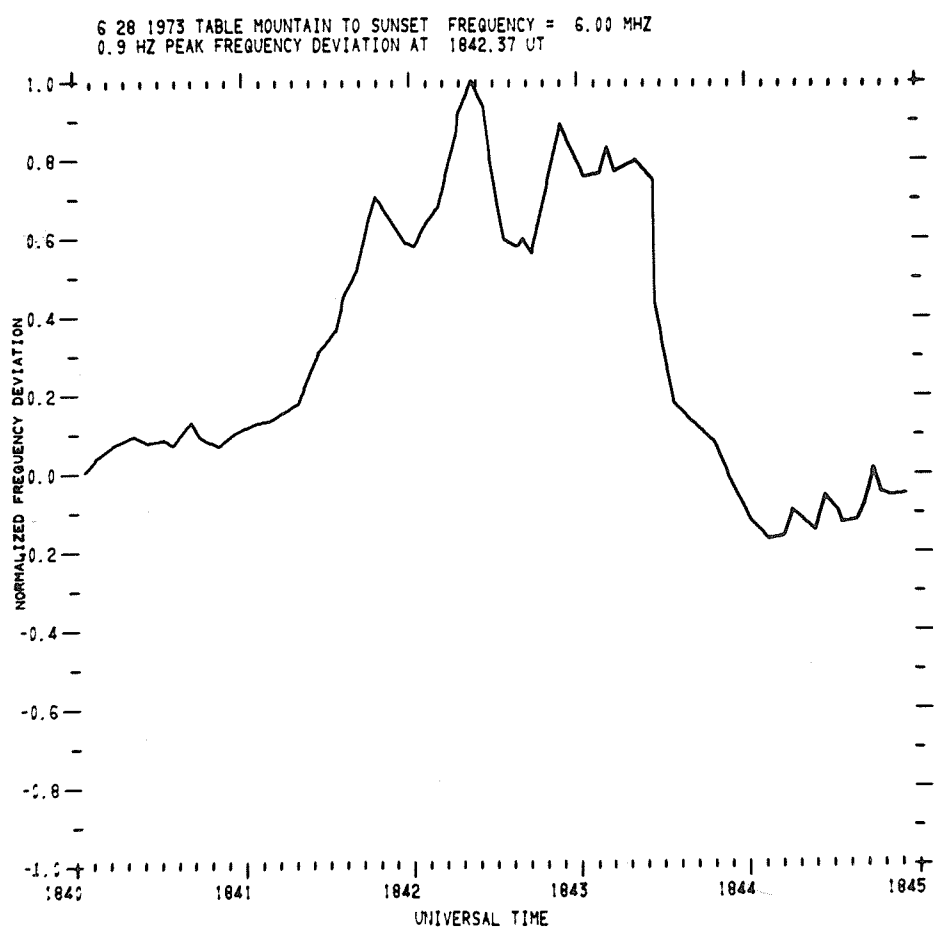

Figure 6.3 SFD of 1842 UT June 28, 1973.

The only H_α flare reported in SGD for this event was a 1B limb flare (N12 E90 McMath Plage Region 12417), which started at 1841 UT and peaked near 1848 UT. The EUV bursts for limb flares tend to be smaller during their impulsive phase than disk flares. The intensity of the slow 10-1030A radiation tends to be larger relative to the impulsive emissions (Donnelly, 1970). No microwave burst was reported in SGD during this EUV burst. The SFD data were of poor quality for this event because of noise from ionospheric variations not related to the solar flare. The 6 MHz radio propagation was an extraordinary wave.

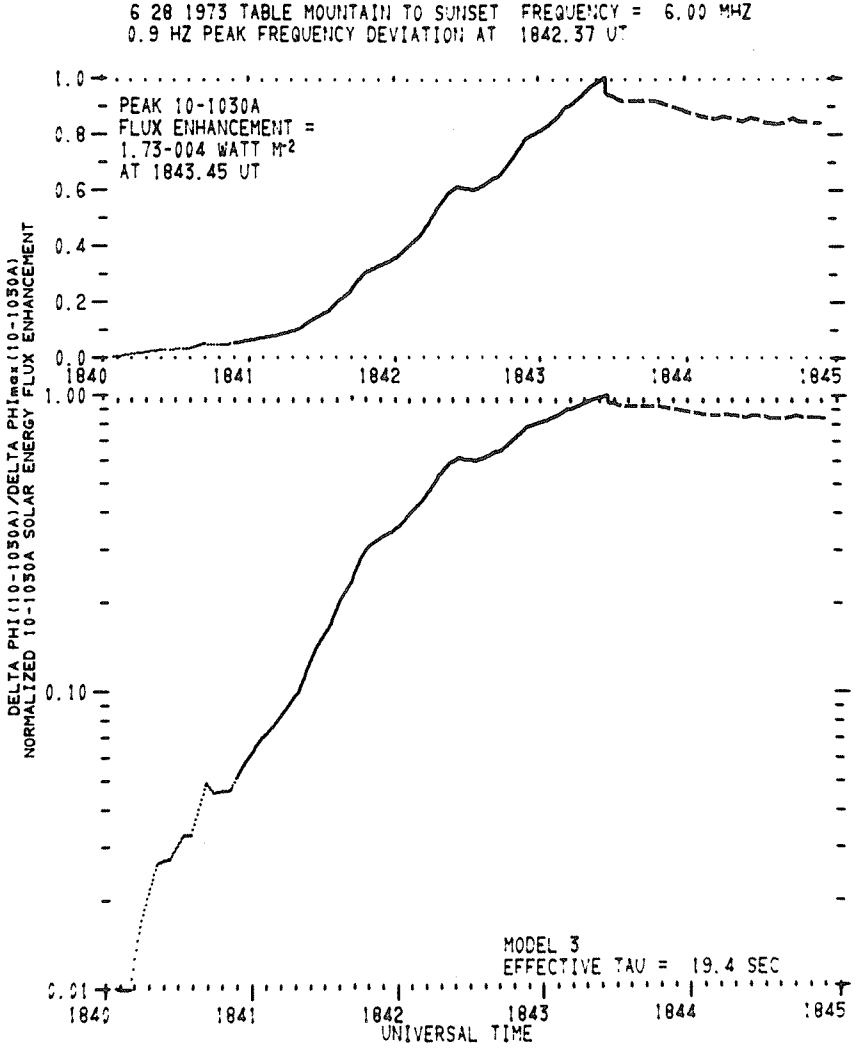

Figure 6.4 Best-estimate 10-1030A flux enhancement of 1843 UT June 28, 1973.

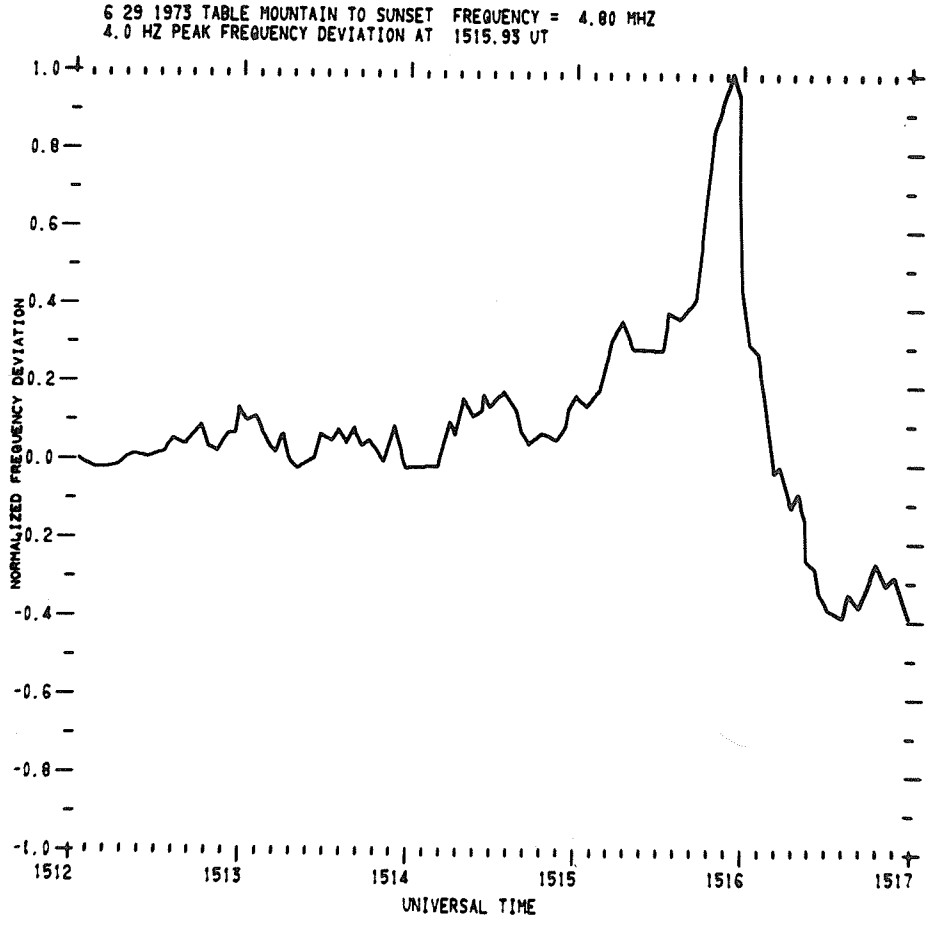

Figure 6.5 SFD of 1516 UT June 29, 1973.

The associated bright subflare at S08 E74 (McMath Plage Region 12414) started near 1513 UT and peaked at about 1517 UT. The 2-9 GHz microwave burst peaked near 1516.4 UT (SGD). The 4.8 MHz radio propagation was an extraordinary wave and $\tau(h)$ increased rapidly with increasing altitude near the height of reflection.

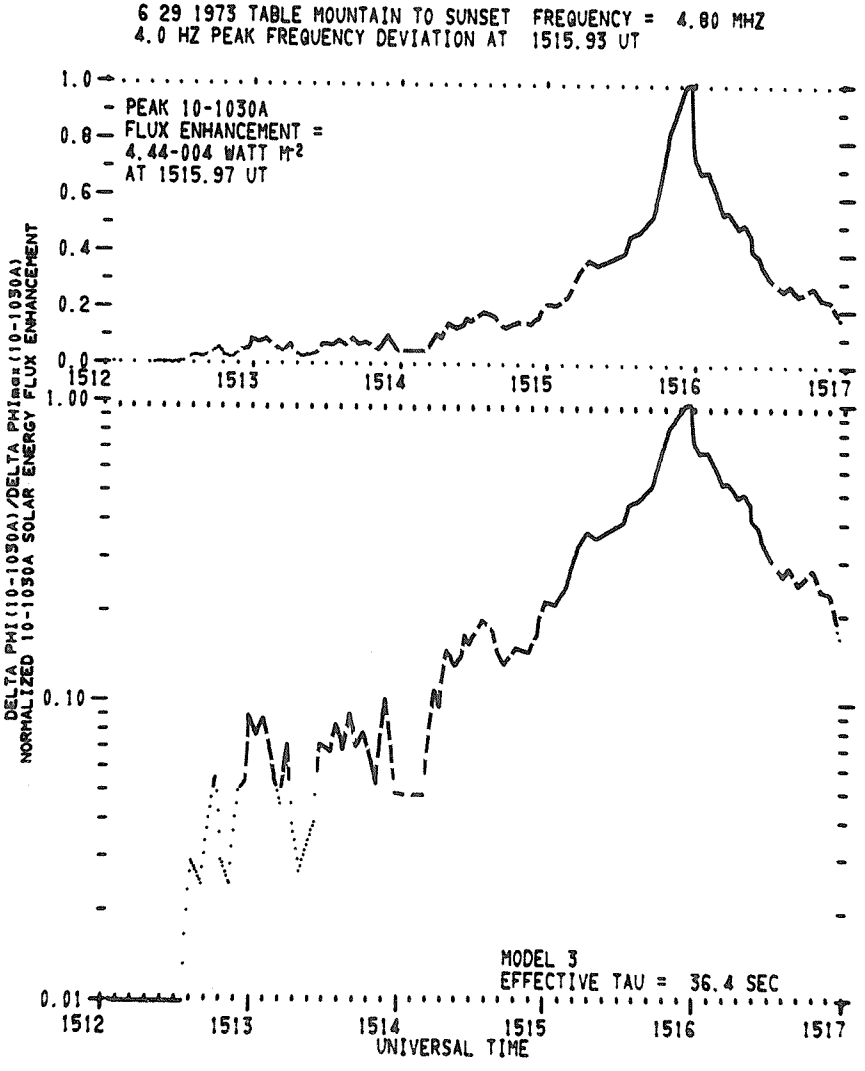

Figure 6.6 Best-estimate 10-1030A flux enhancement of 1516 UT June 29, 1973.

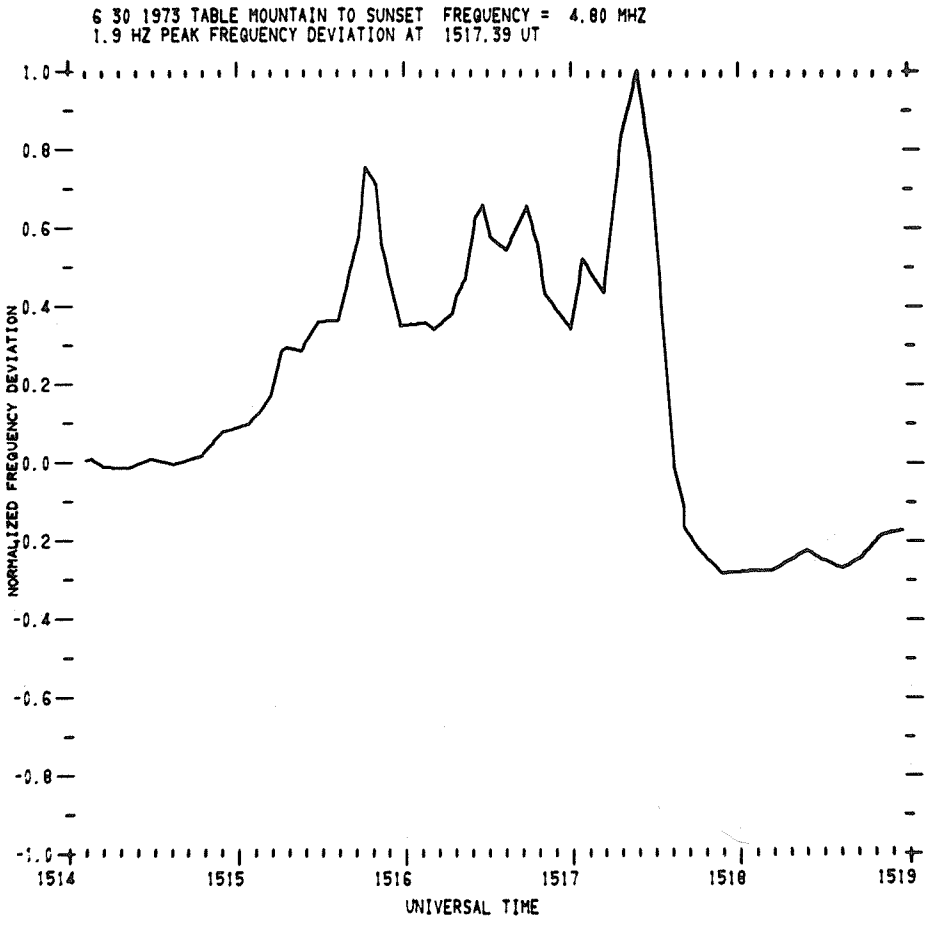

Figure 6.7 SFD of 1517 UT June 30, 1973.

The 1N H_α flare was located at N13 E70 (McMath Plage Region 12417), started at about 1515 UT and peaked at 1518 UT. The 2-15 GHz radio burst peaked near 1517.5 UT (SGD). The SFD data were of poor quality and 4.8 MHz was reflected as an extraordinary wave.

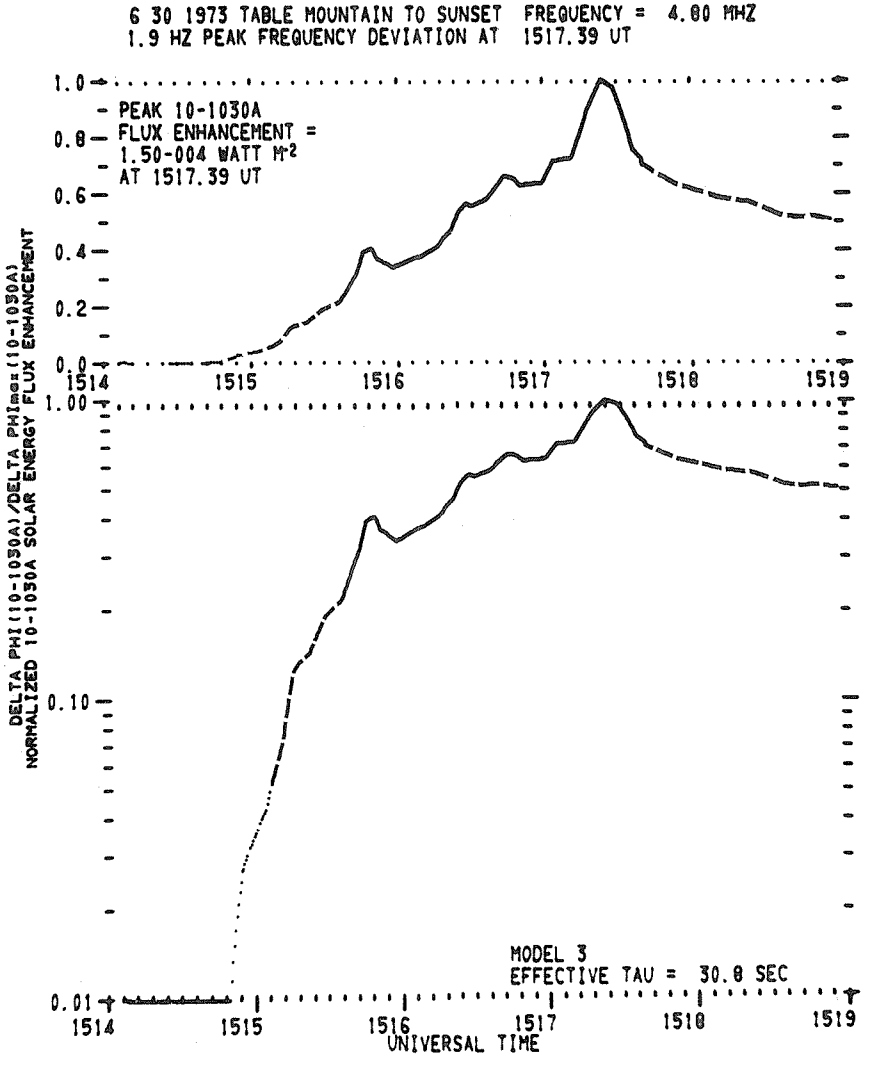

Figure 6.8 Best-estimate 10-1030A flux enhancement of 1517 UT June 30, 1973.

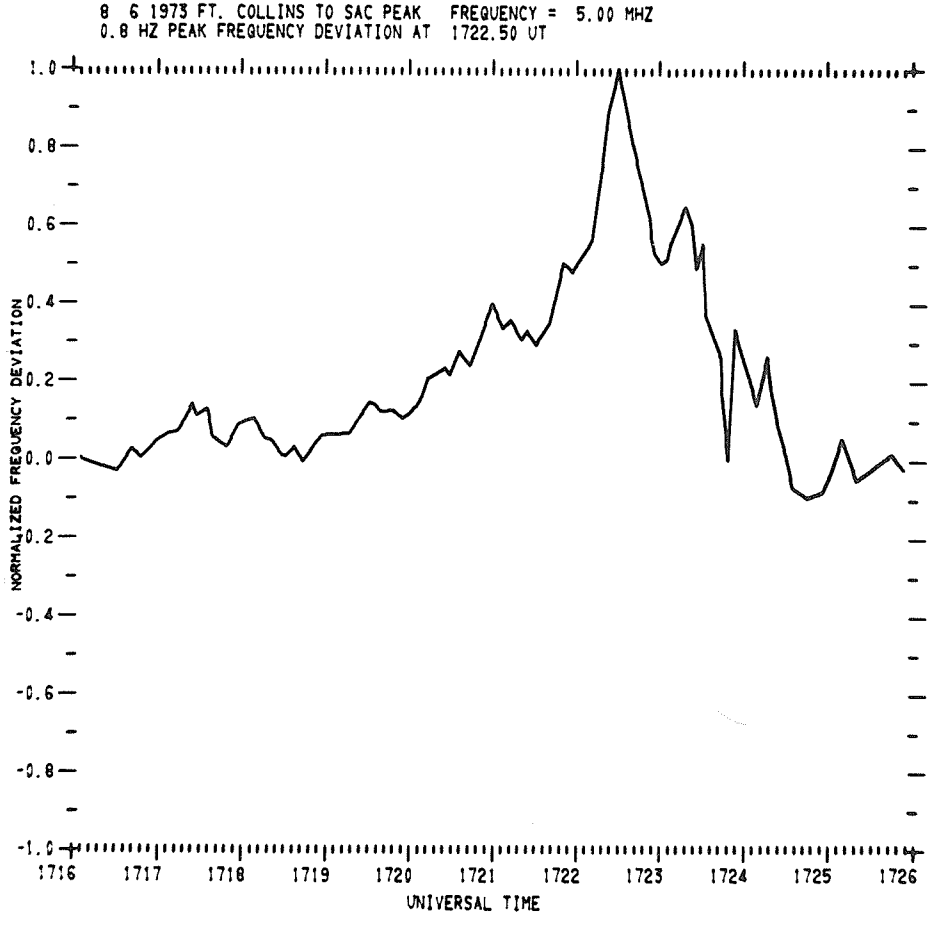

Figure 6.9 SFD of 1723 UT August 6, 1973.

The H_α subflare of normal brightness started before 1713 UT and peaked at about 1724 UT. The flare was located in McMath Plage Region 12474 at N06 W10 . The microwave burst was quite small, only 2.2 radio flux units at the peak at about 1722 UT on 2.8 GHz (SGD). The SFD data were of poor quality.

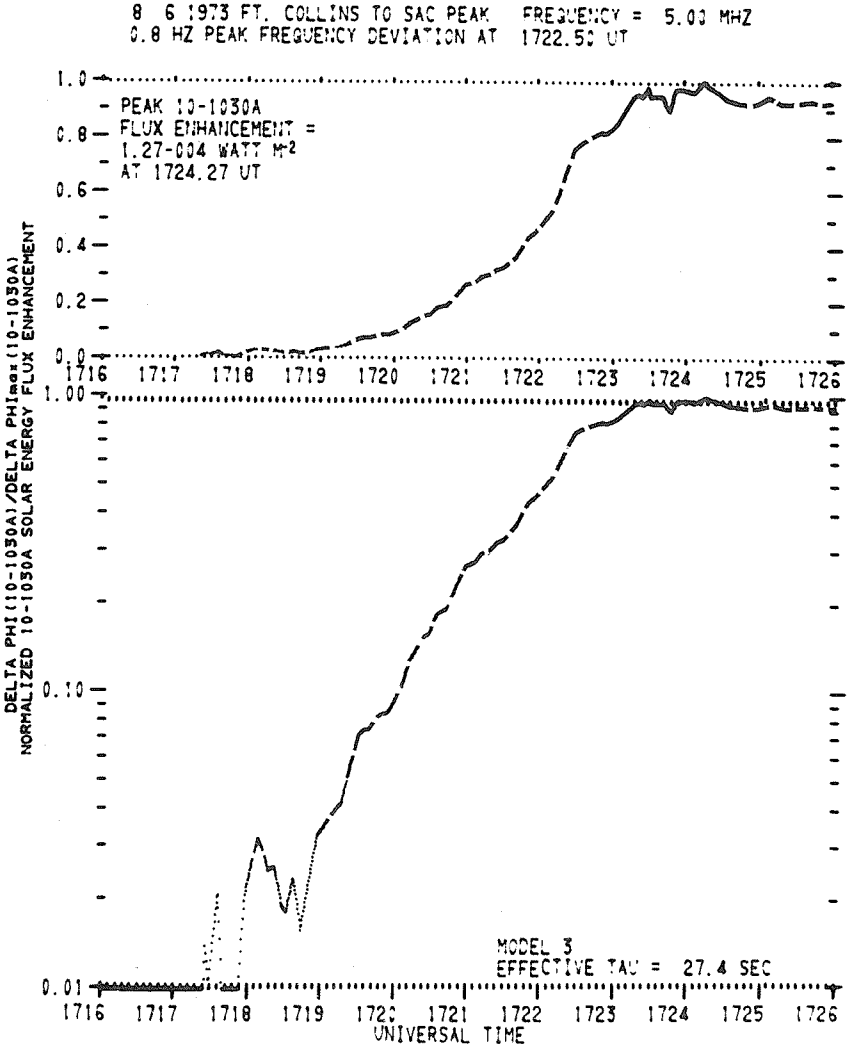

Figure 6.10 Best-estimate 10-1030A flux enhancement of 1724 UT August 6, 1973.

7. OBSERVATIONS DURING THE SECOND MANNED MISSION OF ATM-SKYLAB

The second manned ATM observing period (August 7 to September 21, 1973) was the richest in number of solar flares, although the number of flares was much lower than in the two month period before the ATM mission discussed in Section 4. The level of solar activity rose from low levels, comparable to those of sunspot minimum years, in mid-August, to moderate levels in the first week in September. The Ottawa 10 cm flux reached a daily average of 136.5 on September 3. The observed SFDs are listed in Table 7.1 and the computed flux enhancements are in Table 7.2. All the 10-1030A bursts were small in intensity ($\Delta\Phi$(10-1030A) < 5×10^{-4} Watts m^{-2}), except for the medium sized burst of 0945 UT September 4, 1973. Several events show complex fine structure or are quasi-periodic (September 4 and 5). The periods of SFD observations at Sacramento Peak Observatory and near Boulder are indicated in Figures 7.1 and 7.2 respectively. The daily SFD observing period shortens from summer to fall, but the periods of reduced sensitivity due to the propagation path being reflected from the bottom of the E-layer or from sporadic E are also shorter and less frequent.

Some of the SFDs used to compute $\Delta\Phi$(10-1030A) were noisy or of poor quality, but they were nevertheless analyzed in detail if they were also observed by the ATM experiments. Similar events in Section 4 were not used to compute $\Delta\Phi$(10-1030A). To help clarify what portions of the results may be noise from what must be a real flare enhancement, results from several different channels of SFD data are shown. The results in Table 7.2 are an average over all channels processed, including some not shown in the Figures. The best events from the viewpoint of having interesting impulsive fine structure observed by good SFD data are those on September 4 and 5.

The long lasting 2B flare of 1140 UT September 7, 1973, was probably the largest event of the second manned mission. Figures 7.1 and 7.2 show that this flare occurred too early for SFD observations at Sacramento Peak Observatory or near Boulder. The SFD was observed in England to be a long lasting sequence of small impulsive peaks (see Table 7.1) superposed on a long lasting gradual enhancement. The associated microwave bursts exhibited a large impulsive rise at 1156 UT, with impulsive fine structure peaks lasting until 1207 UT. Any corresponding EUV bursts were not observed in the SFD data because the large soft x-ray enhancement associated with this flare had enhanced the ionospheric absorption (SWF) of the HF Doppler radio waves so much that the data in England were lost just before 1155 UT, at which time the data did not yet indicate the occurrence of any increase.

TABLE 7.1 SFDs During the Second Manned Mission of ATM-SKYLAB

SFD OBSERVATIONS

DATE			UNIVERSAL TIME				PEAK FREQUENCY DEVIATION		TRANSMITTER		
MONTH	DAY	YEAR	START	MAXIMUM	ZERO CROSSING	END	HZ	HF DOPPLER STATION	CALL LETTERS	FREQUENCY MHZ	COMMENTS
8	7	1973	1844.8	1845.3	1848.8	1856. U	0.4	KEENESBURG, COLORADO		4.8	4
				1845.5			0.5				
				1845.9			0.7				
				1846.9			0.7				
				1847.9			0.4				
8	7	1973	1844.8	1845.9	1848.6	1853. U	1.3	FT. COLLINS TO SAC PEAK	WWV	15.000	4 10
				1846.1			0.8				
				1847.0			0.7				
				1847.2			0.6				
				1848.2			0.7				
8	9	1973	1550.3	1550.5	1555.4	1559. U	0.2	KEENESBURG, COLORADO		4.8	5 10
				1552.3			0.6				
				1552.5			0.4				
				1553.5			0.5				
8	9	1973	1550.9	1552.7	1554.1	1601. U	0.2	FT. COLLINS TO SAC PEAK	WWV	10.000	5 10
				1553.5			0.3				
8	9	1973	2139.	2142.3	2147.	2156.	0.1	FT. COLLINS TO SAC PEAK	WWV	5.000	3 9 15
8	10	1973	0012.	0015.2	0017.	0022. U	0.6	KEENESBURG, COLORADO		4.8	3 11 21
8	31	1973	1929.	1931.	1934.	1940. U	0.1	FT. COLLINS TO SAC PEAK	WWV	5.000	3 10 15
8	31	1973	2153. U	2153.8		2205. U	0.3	KAUAI TO U. OF HAWAII	WWVH	5.000	
				2155.8			0.3				
				2156.1			0.4				
9	1	1973	1429. U	1432.5	1434. U	1437. U	0.2	FT. COLLINS TO SAC PEAK	WWV	15.000	10
9	2	1973	0232. U	0232.8	0241.5	0247. U	0.1	KAUAI TO U. OF HAWAII	WWVH	5.000	6 10
				0236.7			0.2				
				0238.4			0.1				
				0240.3			0.3				
9	2	1973	1618. U	1621. U	1628. U	1632. U	0.1	FT. COLLINS TO SAC PEAK	WWV	5.000	10
				1625.5			0.1				
9	2	1973	1807.2	1808.0	1811.8U	1820. U	0.8	FT. COLLINS TO SAC PEAK	WWV	15.000	10 19 20
				1808.8			0.9				
				1809.1			0.6				
				1811.4			0.3				

Table 7.1 - (continued)

DATE			UNIVERSAL TIME				PEAK FREQUENCY DEVIATION		TRANSMITTER		
MONTH	DAY	YEAR	START	MAXIMUM	ZERO CROSSING	END	HZ	HF DOPPLER STATION	CALL LETTERS	FREQUENCY MHZ	COMMENTS
9	2	1973	1805.6	1808.8	1812.5U	1819. U	0.2	KAUAI TO U. OF HAWAII	WWVH	5.000 10	
				1809.4			0.2				
				1810.9			0.1				
9	2	1973	1901. U	1904. U	U	1930. U	0.3	FT. COLLINS TO SAC PEAK	WWV	10.000 10 12	
9	2	1973	2152.2	2153.0	2153.8	2205. U	1.7	FT. COLLINS TO SAC PEAK	WWV	15.000 10 19 20	
				2153.3			1.6				
				2153.6			1.5				
9	2	1973	2152.5	2153.1		2156. U	0.6	KAUAI TO U. OF HAWAII	WWVH	5.000	
				2153.3			0.6				
				2153.7			0.4				
9	3	1973	1559.3U	5595.1	1601.6	603. U	0.1	FT. COLLINS TO SAC PEAK	WWV	10.000 10	
				1600.7			0.2				
9	3	1973	1604.1	1604.6	U	1609. U	0.4	SUNSET, COLORADO		4.8 10	
				1605.2			0.5				
9	3	1973	1613.1	1613.9	1616.2	1625. U	0.6	SUNSET, COLORADO		4.8	
				1615.4			0.5				
9	3	1973	1612.3	1613.8	1616.1	1625. U	0.4	FT. COLLINS TO SAC PEAK	WWV	10.000	
				1615.6			0.5				
9	3	1973	1613.0	1613.8	1616.0	1621. U	0.4	KEENESBURG, COLORADO		4.8	
				1615.7			0.5				
9	3	1973	1613.0	1613.8	1616.0	1625. U	0.7	FT. COLLINS TO SAC PEAK	WWV	15.000 19 20	
				1515.4			0.7				
9	3	1973	1922.7	1923.1	1923.4	1925. U	0.3	FT. COLLINS TO SAC PEAK	WWV	15.000 10 20	
9	3	1973	1925.9	1926.1	U	1928. U	0.4	FT. COLLINS TO SAC PEAK	WWV	15.000 11 20	
9	3	1973	1928.8	1929.5	1930.2	1934. U	0.6	FT. COLLINS TO SAC PEAK	WWV	15.000 20	
				1929.9			0.7				
9	3	1973	2017.2U	2018.2	2018.6	2021. U	0.8	FT. COLLINS TO SAC PEAK	WWV	15.000 11 20	
9	3	1973	2122. U	2123.3	U	2145. U	0.8	FT. COLLINS TO SAC PEAK	WWV	15.000 6 10 20	
				2128.9			0.4				
				2129.5			0.5				
				2133.5			0.4				
				2139.0			0.5				
9	4	1973	0052. U	0053.	U	0110. U	0.3	KAUAI TO U. OF HAWAII	WWVH	5.000 10	
				0054.			0.2				
				0055.			0.1				

Table 7.1 - (continued)

DATE			UNIVERSAL TIME				PEAK FREQUENCY DEVIATION		TRANSMITTER CALL LETTERS	FREQUENCY		
MONTH	DAY	YEAR	START	MAXIMUM	ZERO CROSSING	END	HZ	HF DOPPLER STATION		MHZ		COMMENTS
9	4	1973	0945.	0947.2	0948.7	0954.	1.3	U. OF LEICESTER, ENGLAND		4.793	7	
				0947.6			1.2					
				0948.0			0.7					
				0948.5			0.9					
9	4	1973	1456.5	1502.6	1503.0	1519. U	1.4	FT. COLLINS TO SAC PEAK	WWV	5.000		
9	4	1973	1633.3	1635.6	1637.3	1644. U	0.1	FT. COLLINS TO SAC PEAK	WWV	5.000	3	9 15
9	5	1973	1827.3	1828.2	1832.7	1843.	0.9	KEENESBURG, COLORADO		4.8	6	
				1828.6			0.9					
				1828.8			0.8					
				1829.0			1.0					
				1829.2			1.2					
				1829.8			1.3					
				1830.2			1.6					
				1830.8			0.5					
				1831.5			0.4					
				1832.5			0.5					
9	5	1973	1826.2	1828.1	1832.8	1844.	2.1	FT. COLLINS TO SAC PEAK	WWV	15.000	6	19 20
				1828.6			2.1					
				1829.3			2.7					
				1829.8			2.7					
				1830.2			3.8					
				1830.9			1.3					
				1831.4			2.0					
				1832.4			2.0					
9	7	1973	1140.	1140.0	U	1230. +	0.4	U. OF LEICESTER, ENGLAND		4.793	8	13 21
				1143.4			0.4					
				1146.5			0.4					
				1151.2			0.5					
				1153.4			0.5					
9	10	1973	0252. U	0253.1	0302.6U	0304. U	0.3	KAUAI TO U. OF HAWAII	WWVH	5.000	6	10
				0254.2			0.4					
				0255.5			0.7					
				0257.0			0.8					
				0258.8			0.4					
				0300.9			0.3					
9	11	1973	2109. U	2111.4	U	U	0.3	FT. COLLINS TO SAC PEAK	WWV	10.000	10	

U uncertain

See Table 4.1 for the numbered comments.

TABLE 7.2

The Impulsive 10-1030A Flux Enhancements Deduced from SFDs During the Second Manned Mission of ATM SKYLAB

Date 1973	Number of Channels of SFD Data Analyzed To $\Delta\Phi$(10-1030A)	Start Time UT	Peak Time UT	$\Delta\Phi$ (10-1030A)* Peak	Peak Time UT	$\Delta\Phi$ (10-1030A)* Peak	Peak Time UT	$\Delta\Phi$ (10-1030A)* Peak
August 7	2	1844.8	1845.9	6.9×10^{-5}	1847.0	1.0×10^{-4}	1848.4	$\underline{1.4\times10^{-4}}$
August 9	2	1551.	1552.4	5.9×10^{-5}	1554.†	$\underline{1.0\times10^{-4}}$		
September 2	2	1807U	1808.8	7.0×10^{-5}	1812.	$\underline{1.0\times10^{-4}}$		
September 2	2	2152.3	2153.0	5.5×10^{-5}	2153.3	7.7×10^{-5}	2153.7	$\underline{8.8\times10^{-5}}$
September 3	1	1559.4	1601.0	$\underline{3.8\times10^{-5}}$				
September 3	1	1604.1	1605.2	1.0×10^{-6}	1606.0	1.5×10^{-4}		
September 3	4	1613	1613.9	8.9×10^{-5}	1615.8	$\underline{2.5\times10^{-4}}$		
September 4	1	0052.4	0055.1	8.2×10^{-5}				
September 4	1	0944.8	0948.5	$\underline{8.2\times10^{-4}}$				
September 4	1	1456.8	1502.9	$\underline{4.1\times10^{-4}}$				
September 5	3	1827	1828.2	6.0×10^{-5}	1830.2	2.2×10^{-4}	1832.5	$\underline{2.7\times10^{-4}}$

Underlined peak fluxes are the maximum values for the event.

* $\Delta\Phi$(10-1030A) flux units are Watts m^{-2}.

U Uncertain

† Gradual Peak

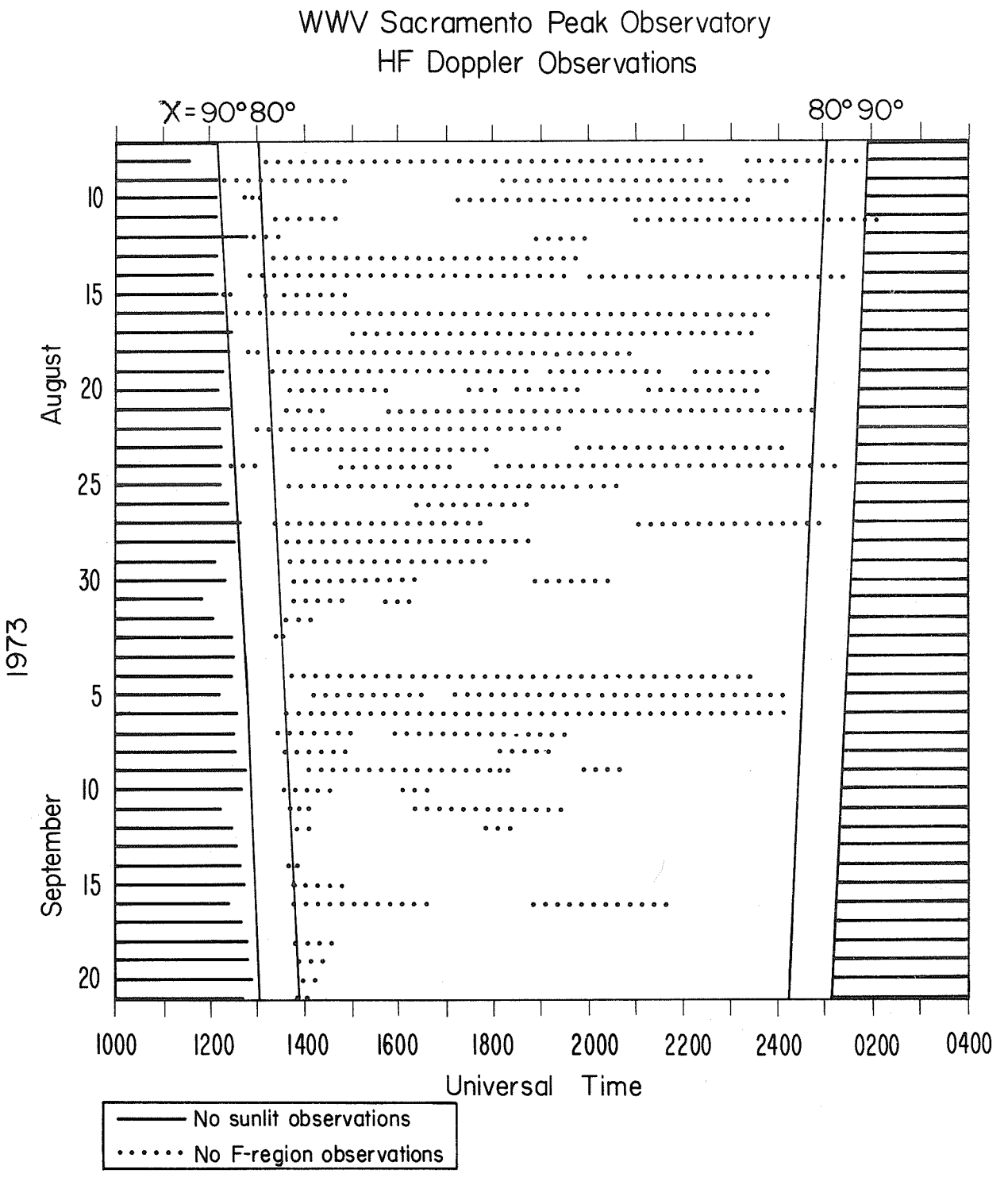

Figure 7.1 SFD observing time at Sacramento Peak Observatory during the second manned observations with ATM.

Clear areas indicate good observations, dotted indicate reduced sensitivity, solid line indicates no observations.

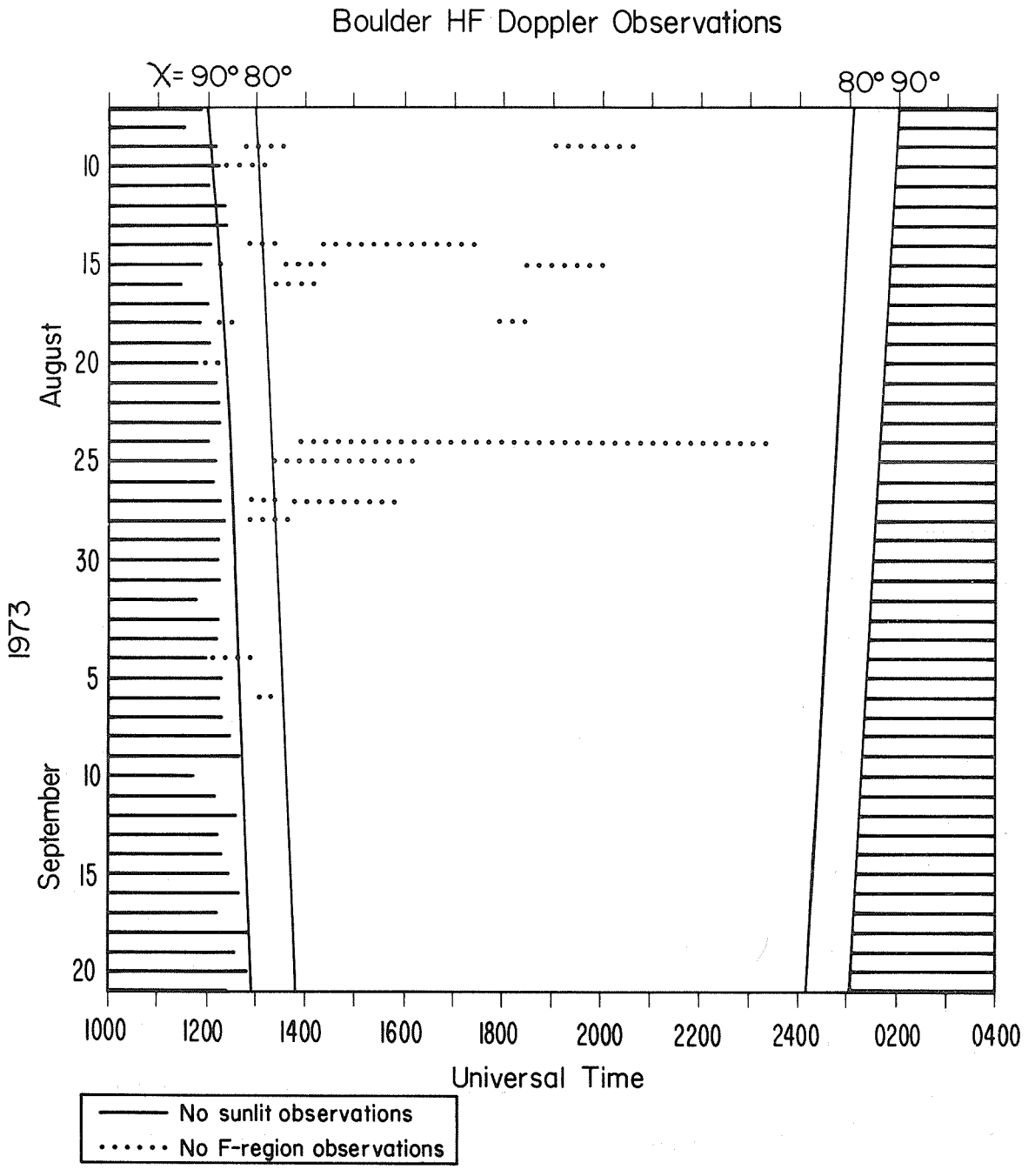

Figure 7.2 SFD observing time near Boulder, Colorado during the second manned observations with ATM.

Clear areas indicate good observations, dotted indicate reduced sensitivity, solid line indicates no observations.

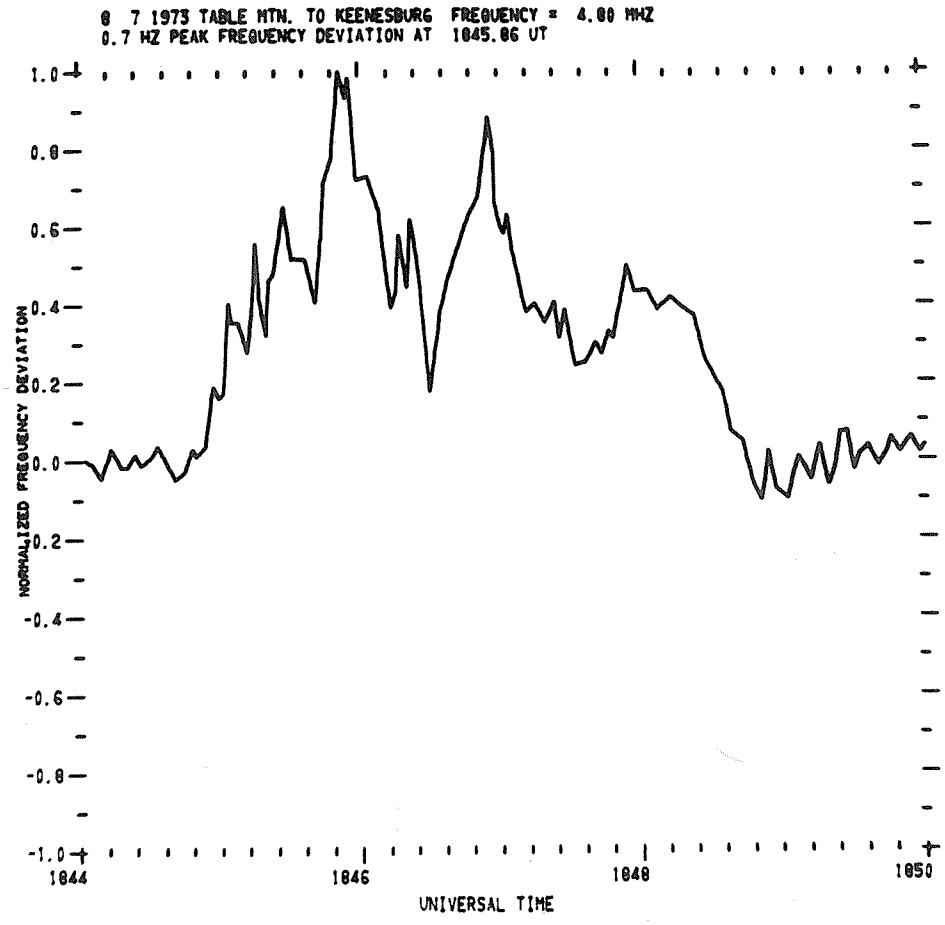

Figure 7.3 SFD of 1846 UT August 7, 1973 on 4.8 MHz at Keenesburg, Colorado.

This SFD accompanied the H_α subflare of normal intensity at N06 W24 in McMath Plage Region No. 12474. The H_α flare started at 1837 UT and peaked at 1847 UT. The 2 to 11 GHz microwave burst peaked from 1845.3 to 1846.5 UT (SGD). The HF Doppler data were noisy for this SFD and much of the fine structure shown in Figure 7.3 cannot be attributed to fine structure in the 10-1030A flare radiation. See Figure 7.5. This small EUV flare was observed by ATM SKYLAB.

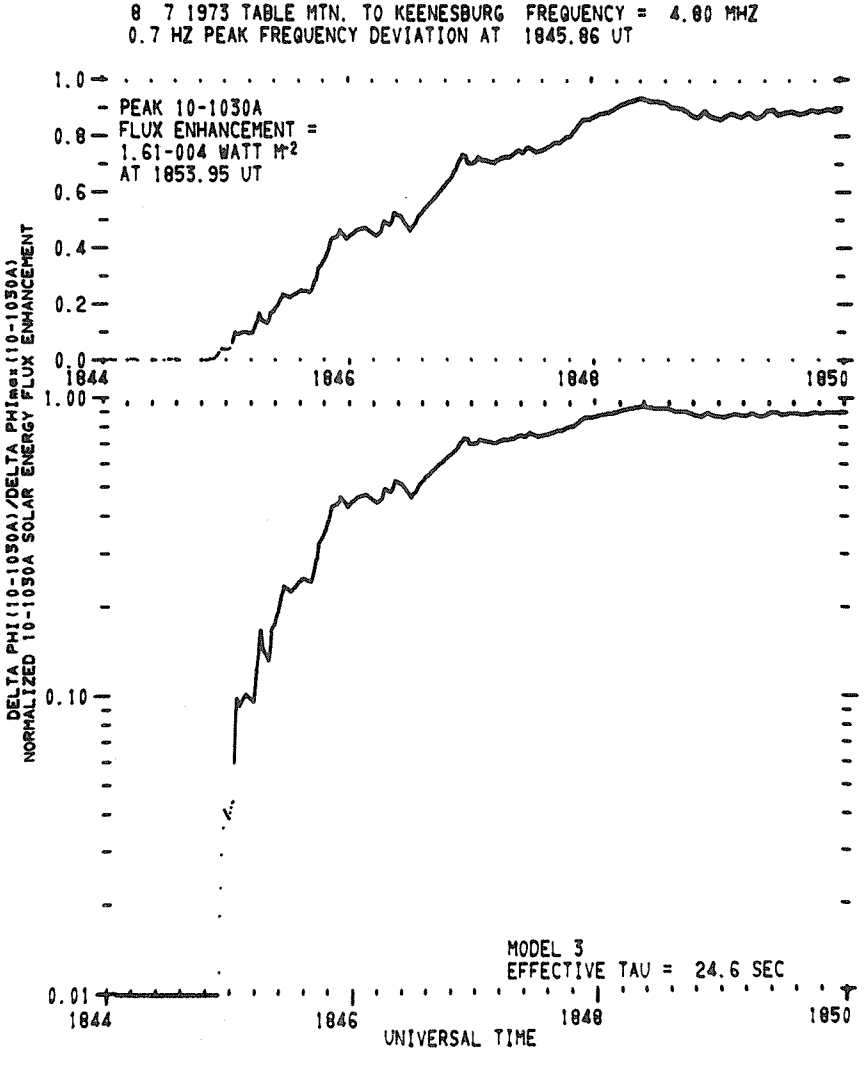

Figure 7.4 Best-estimate 10-1030A flux enhancement of 1848 UT August 7, 1973, based on 4.8 MHz at Keenesburg, Colorado.

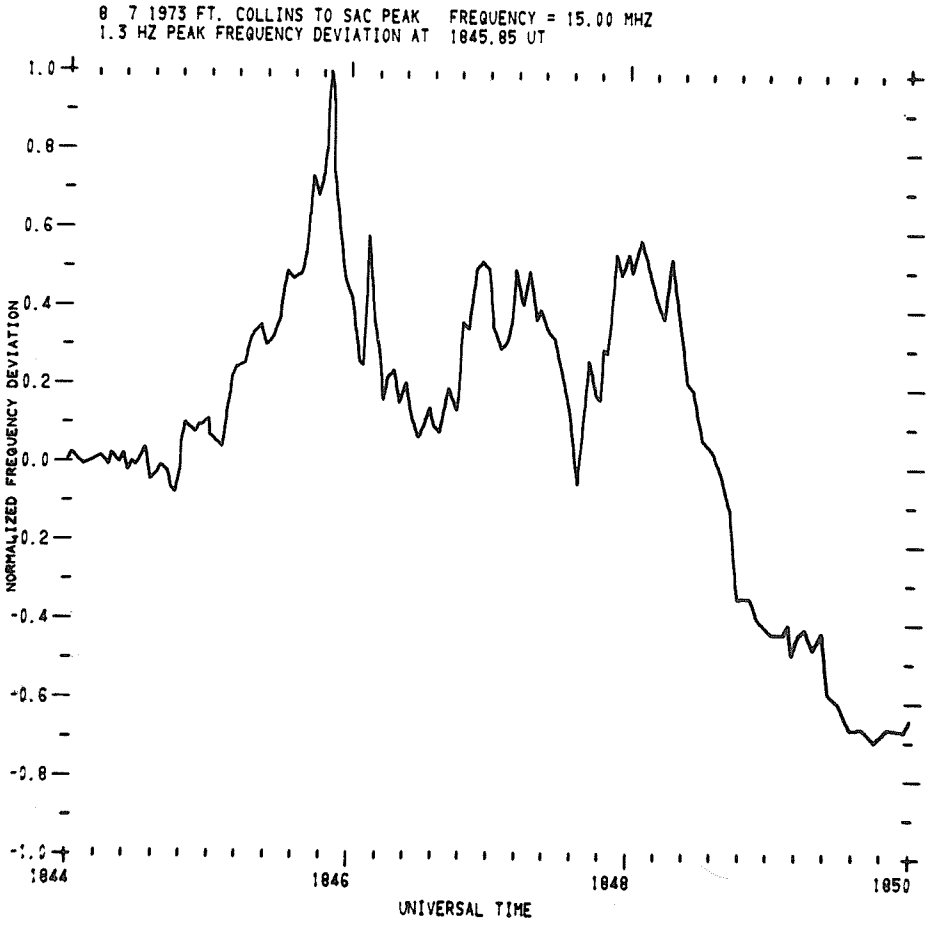

Figure 7.5 SFD of 1846 UT August 7, 1973 on 15 MHz at Sacramento Peak Observatory.

This is another channel of noisy SFD data for the same flare as in Figure 7.3. Fine structure common to Figures 7.3 and 7.5 probably corresponds to real fine structure in the 10-1030A flare radiation. Most of the dissimilar fine structure is noise due to ionospheric variations unrelated to the solar flare. Note the similarities in Figures 7.4 and 7.6 before 1849 UT. The impulsive fine structure in the 10-1030A radiation was quite weak relative to the rise from 1845 UT to $\Delta\Phi_{max}$ at 1848.3 UT.

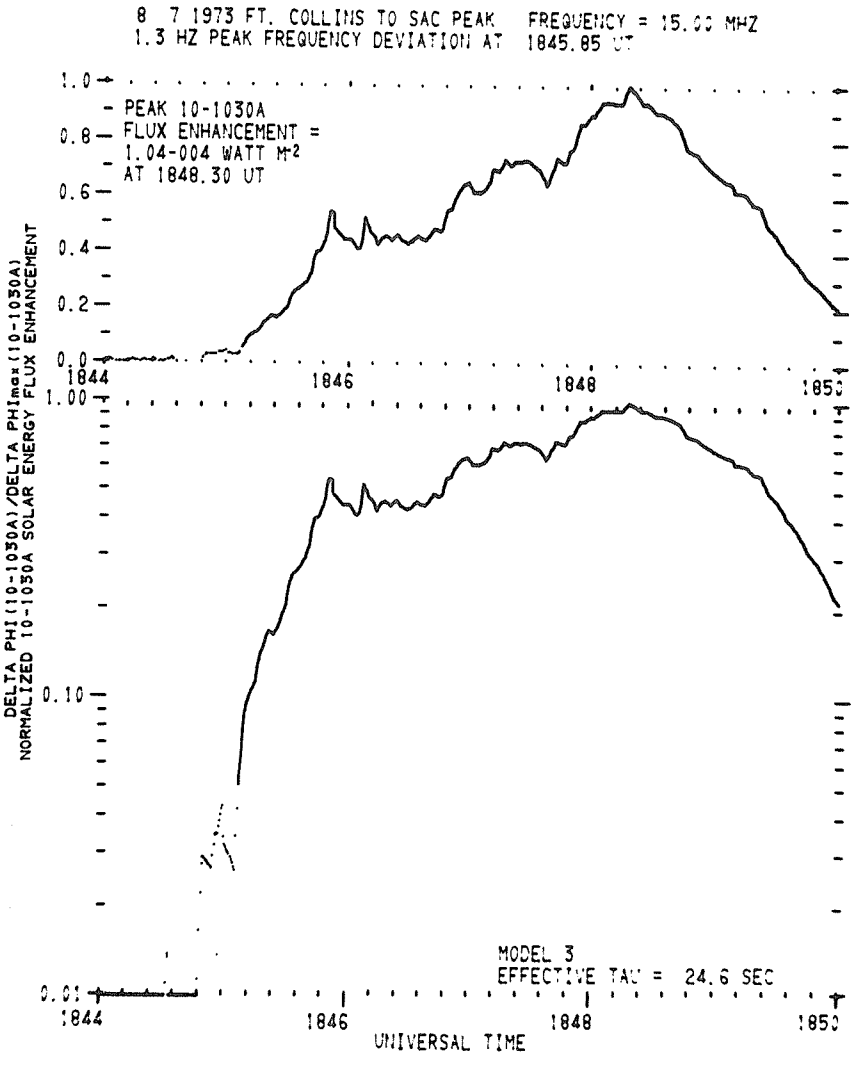

Figure 7.6 Best-estimate 10-1030A flux enhancement 1848 UT August 7, 1973, based on 15 MHz at Sacramento Peak Observatory.

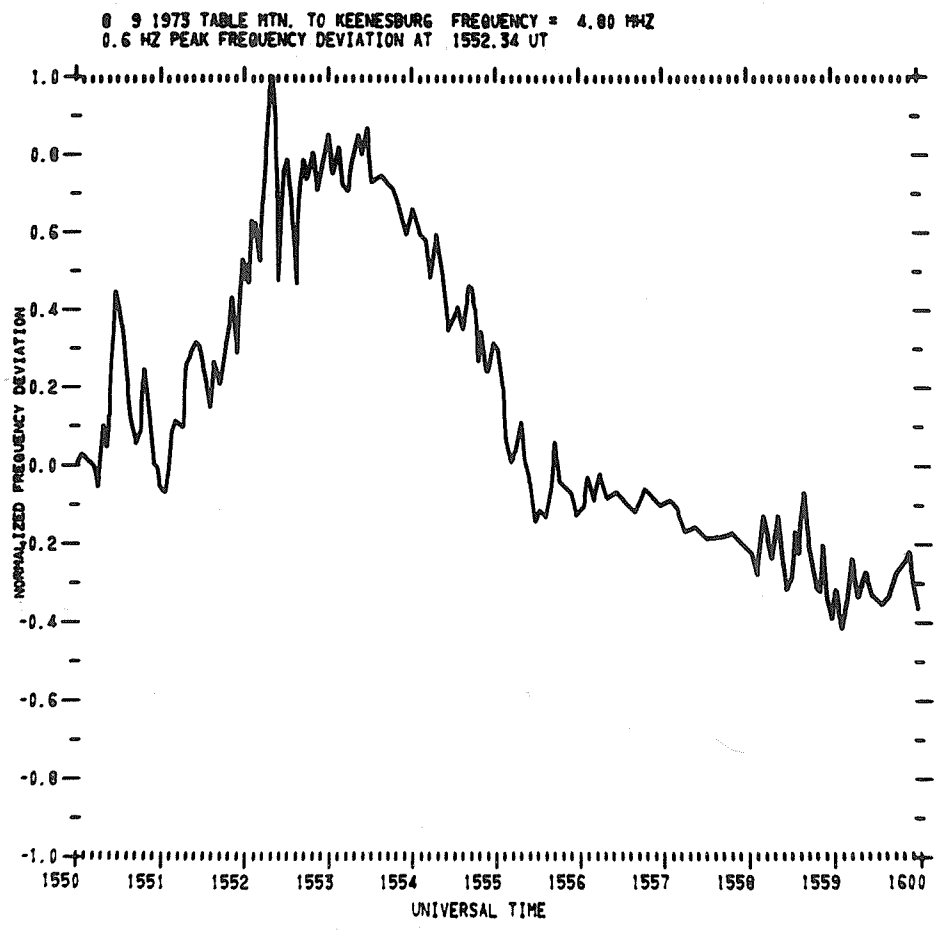

Figure 7.7 SFD of 1552 UT August 9, 1973.

The associated $H\alpha$ subflare (SN) started at 1551 UT, peaked in the period 1553 to 1555 UT and ended at about 1600 UT. The $H\alpha$ flare was located in McMath Plage Region No. 12474 at N08 W49 . The 2-15 GHz radio burst peaked near 1552.3 UT (SGD). The HF Doppler data were again noisy. The impulsive peak at 1552.3 was evident in other channels of HF Doppler data, but its intensity relative to $\Delta\Phi_{max}$ is not known accurately. This small 10-1030A flare was mainly a gradual rise and fall event. It was observed by ATM SKYLAB.

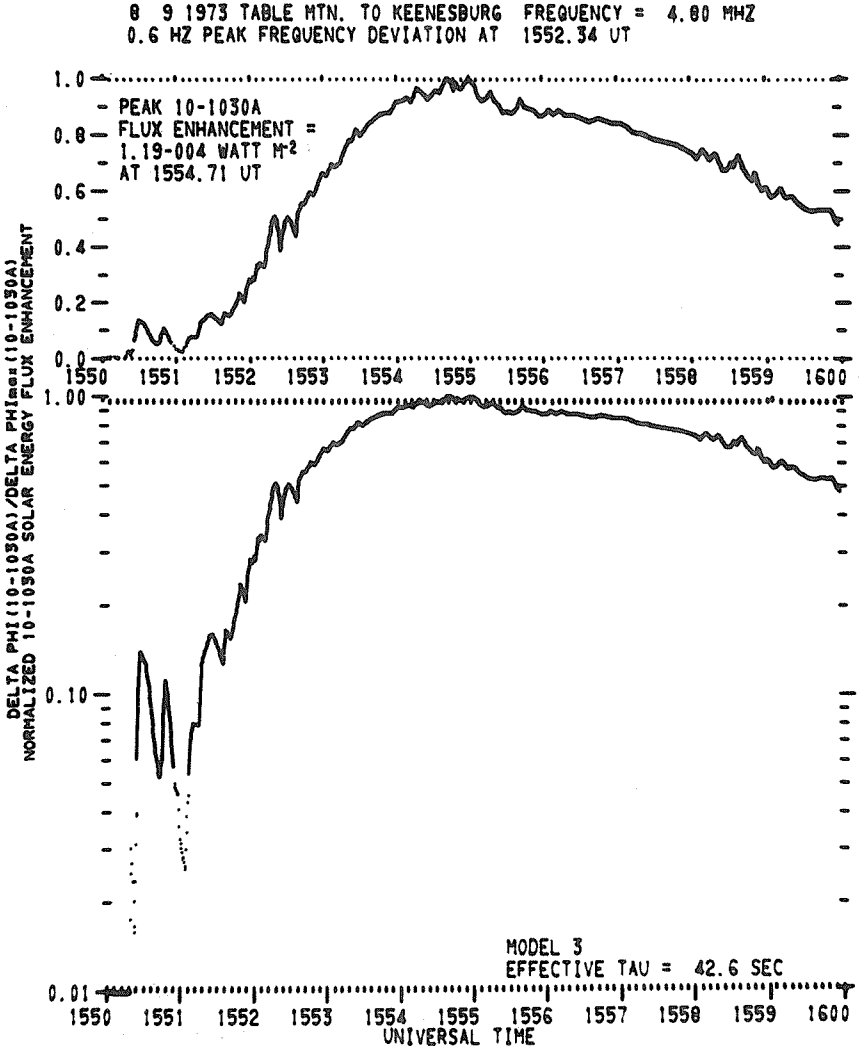

Figure 7.8 Best-estimate 10-1030A flux enhancement of 1555 UT August 9, 1973.

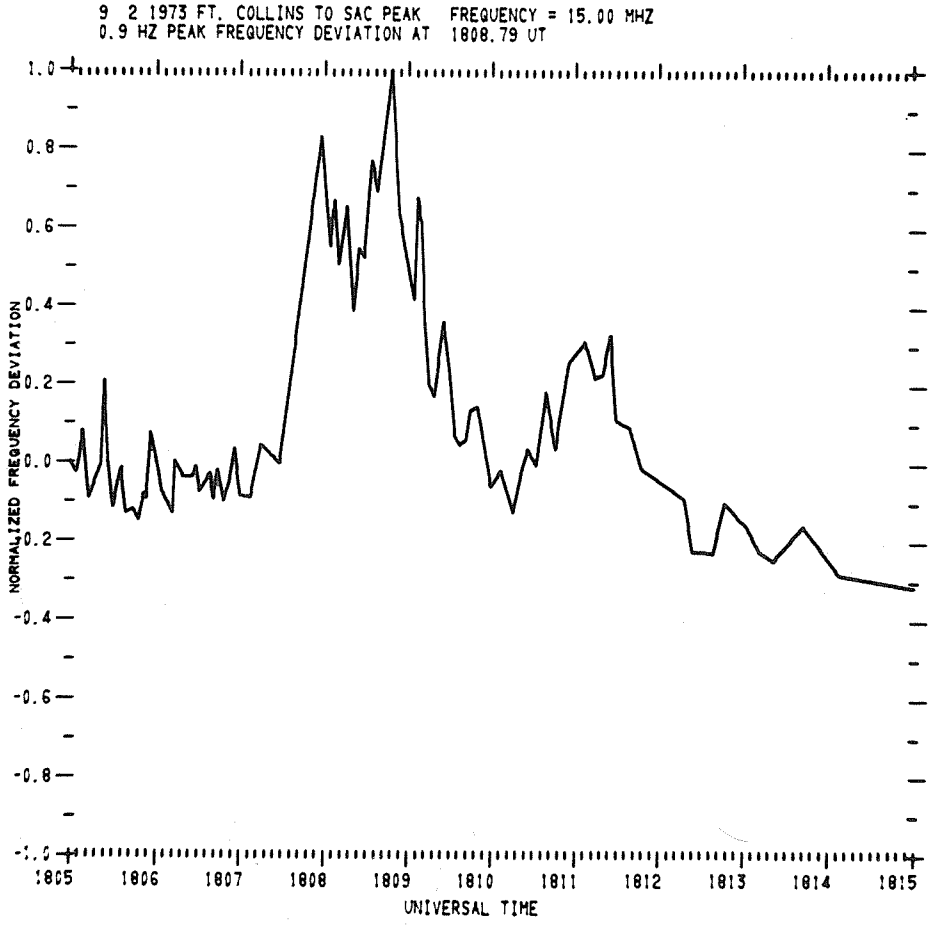

Figure 7.9 SFD of 1809 UT September 2, 1973 on 15 MHz at Sacramento Peak Observatory.

This small SFD accompanied a faint H_α subflare at S16 E50 (McMath Plage Region 12512), which started at 1809 UT and peaked at 1811 UT. The radio burst was observed at fixed frequencies from 2.7 to 8.8 GHz to peak at 1808 UT (SGD). The propagation path for this channel of data was not determined. It may have been WWVH Hawaii to Sacramento Peak Observatory. The $\Delta\Phi$ estimate was based on the 10 MHz WWV path to Sacramento Peak using the 15 MHz time dependence for $\Delta f(t)/\Delta f_{max}$ by renormalizing to Δf_{max} for 10 MHz. See Figure 7.11.

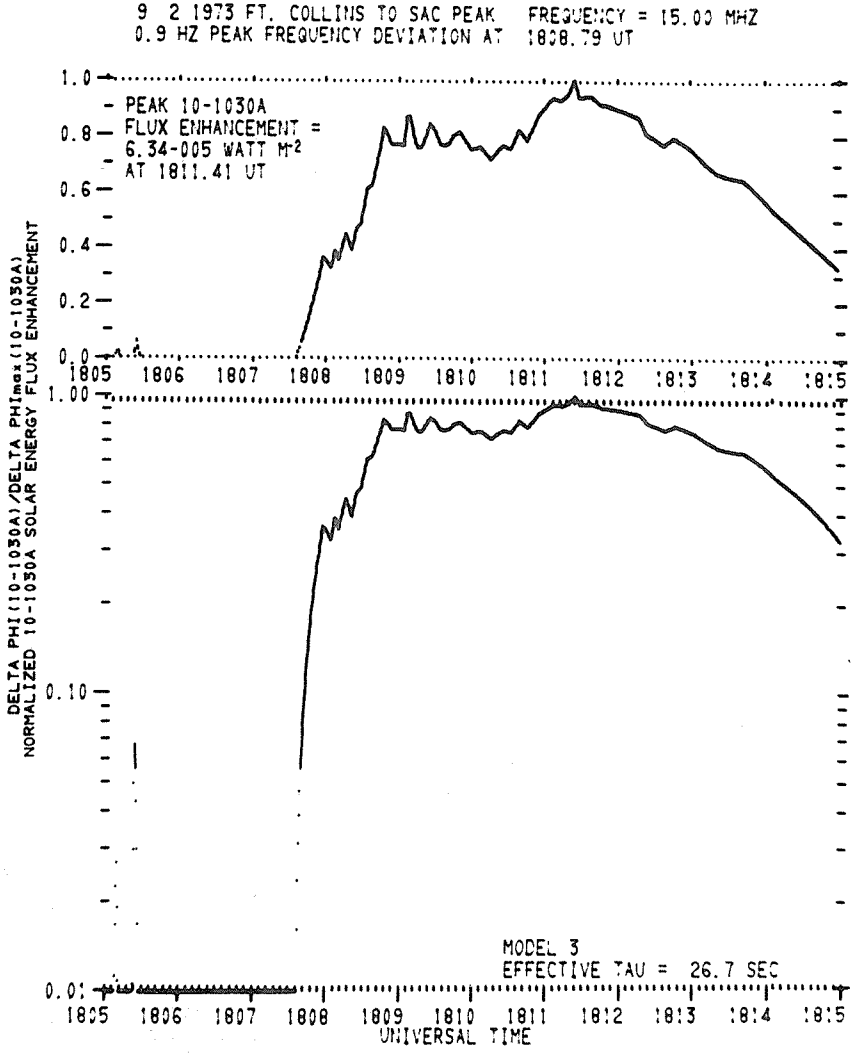

Figure 7.10 Best-estimate 10-1030A flux enhancement of 1811 UT September 2, 1973.

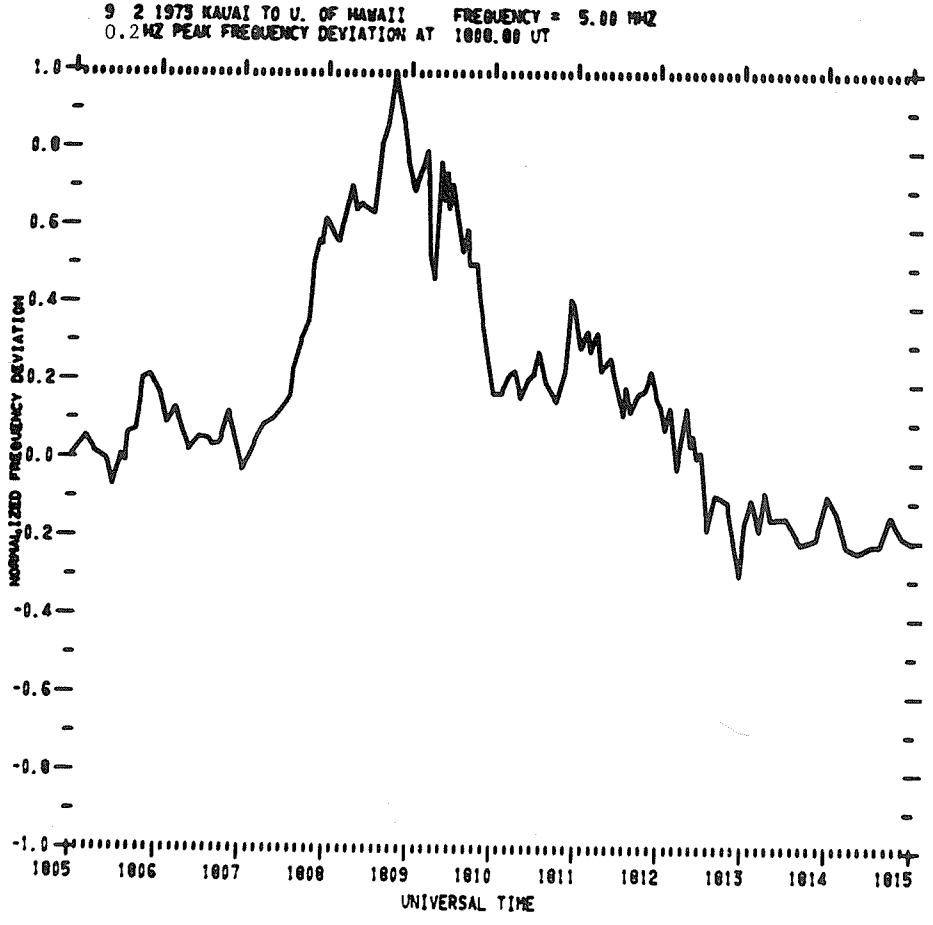

Figure 7.11 SFD of 1809 UT September 2, 1973
on 5 MHz at the University of Hawaii.

A second channel of data is shown for the same event as in Figure 7.9. All available channels of HF Doppler data were noisy for this event. The combined data show the 10-1030A flux rose to a minor peak near 1809 UT with the main maximum near 1812 UT. It is a very small EUV flare with only weak impulsive fine structure.

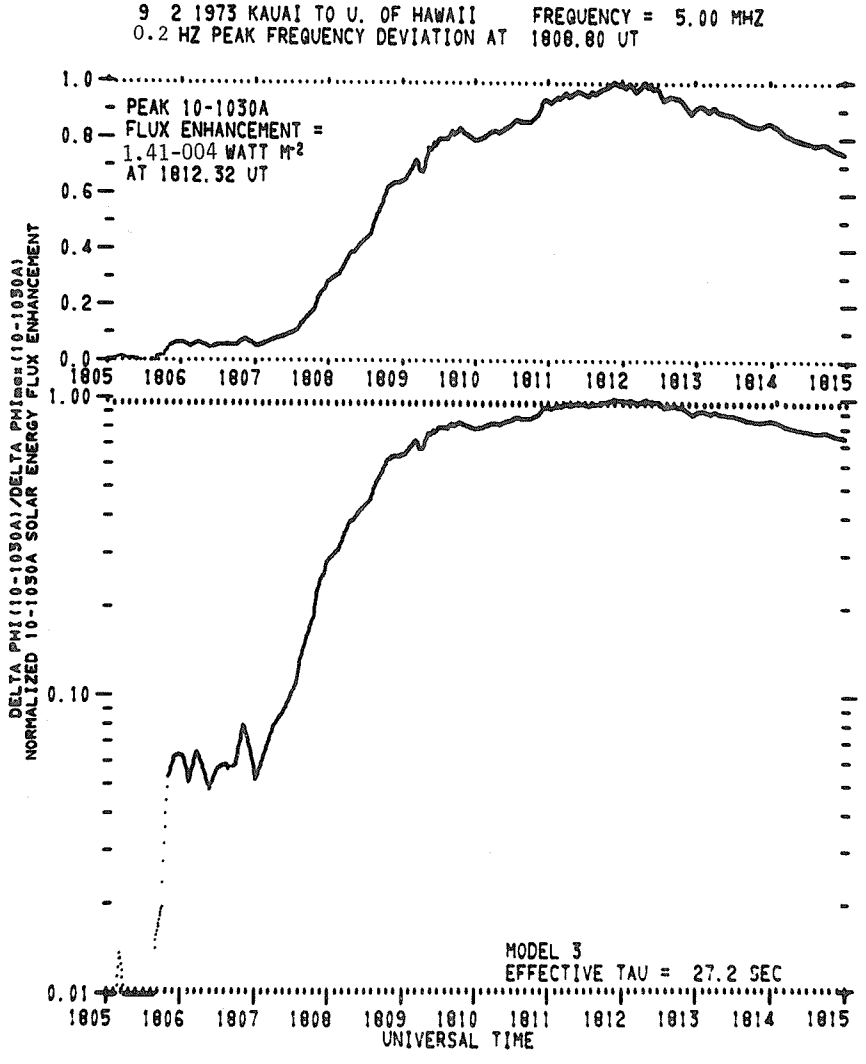

Figure 7.12 Best-estimate 10-1030A flux enhancement
of 1812 UT September 2, 1973, based on 5 MHz at the University of Hawaii.

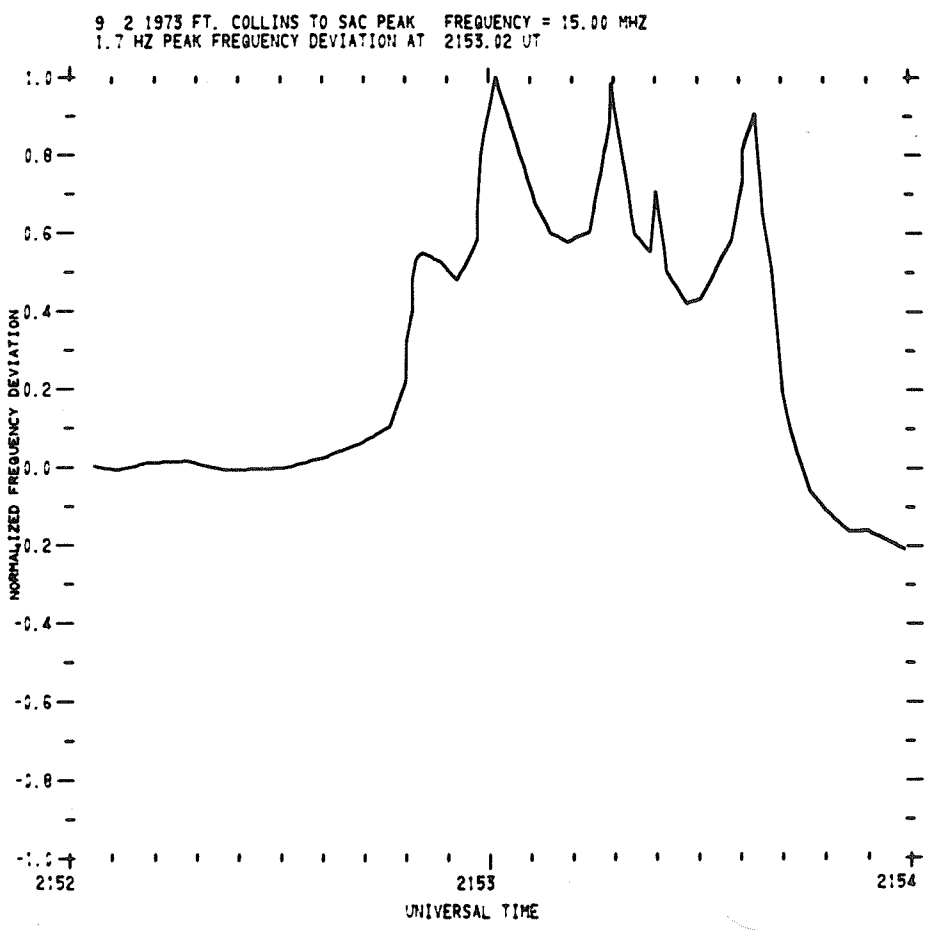

Figure 7.13 SFD of 2153 UT September 2, 1973 on 15 MHz at Sacramento Peak Observatory.

No H_α flare was reported in SGD for this event. "No Flare Patrol" was listed before 2130 UT and after 2205 UT, so perhaps the optical observations at the time of this flare were poor. No impulsive microwave burst was reported. A soft x-ray flare started at 2153 and peaked near 2154 UT below 8A (SGD). The HF Doppler data were noisy, so results for a second channel are shown in Figure 7.15. The propagation path for 15 MHz was not determined. It may have been WWVH Hawaii to Sacramento Peak. The $\Delta\phi$ solution was made using the 10 MHz WWV path to Sacramento Peak and renormalizing the data to Δf_{max} for 10 MHz.

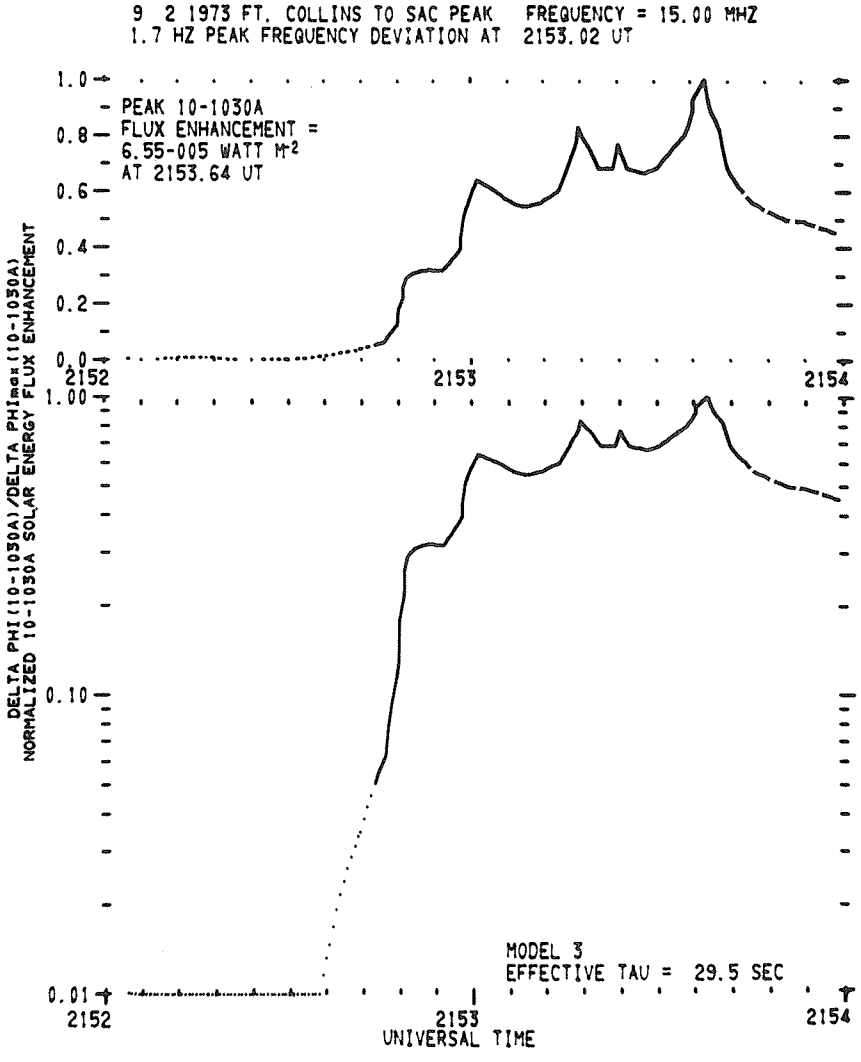

Figure 7.14 Best-estimate 10-1030A flux enhancement of 2154 UT September 2, 1973, based on 15 MHz at Sacramento Peak Observatory.

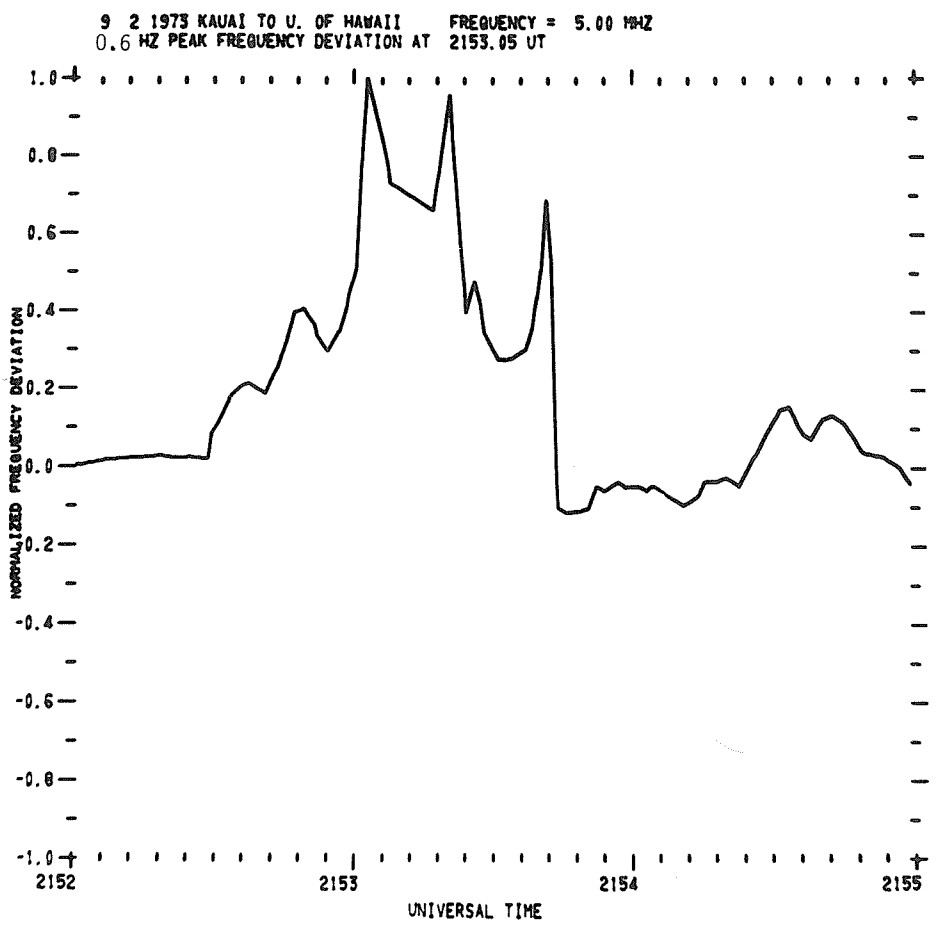

Figure 7.15 SFD of 2153 UT September 2, 1973, on 5 MHz at the University of Hawaii.

This second channel of HF Doppler data for the same event as in Figure 7.13 suggests the five fine structure peaks from 2152.8 to 2153.7 UT correspond to real fine structure in the 10-1030A flux. The fine structure in Figure 7.15 before 2152.8 UT and after 2153.8 UT may be noise in the HF Doppler data. This small EUV burst was observed by ATM SKYLAB.

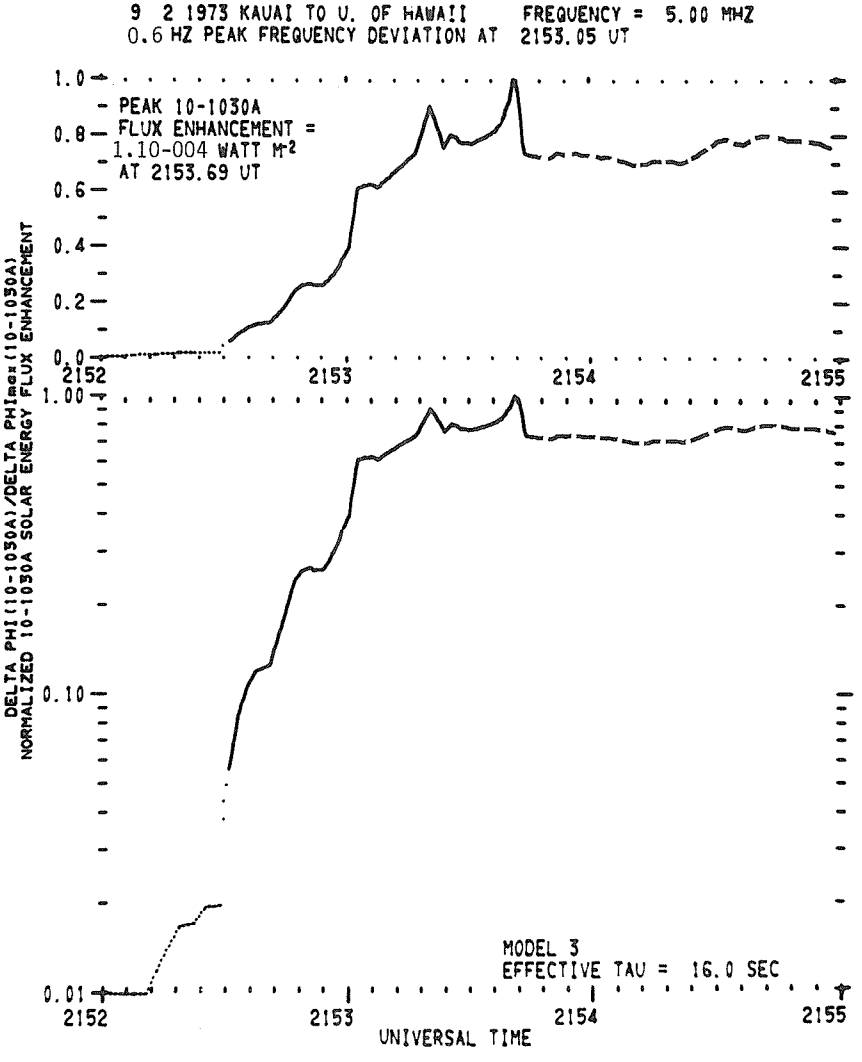

Figure 7.16 Best-estimate 10-1030A flux enhancement of 2154 UT September 2, 1973, based on 5 MHz at the University of Hawaii.

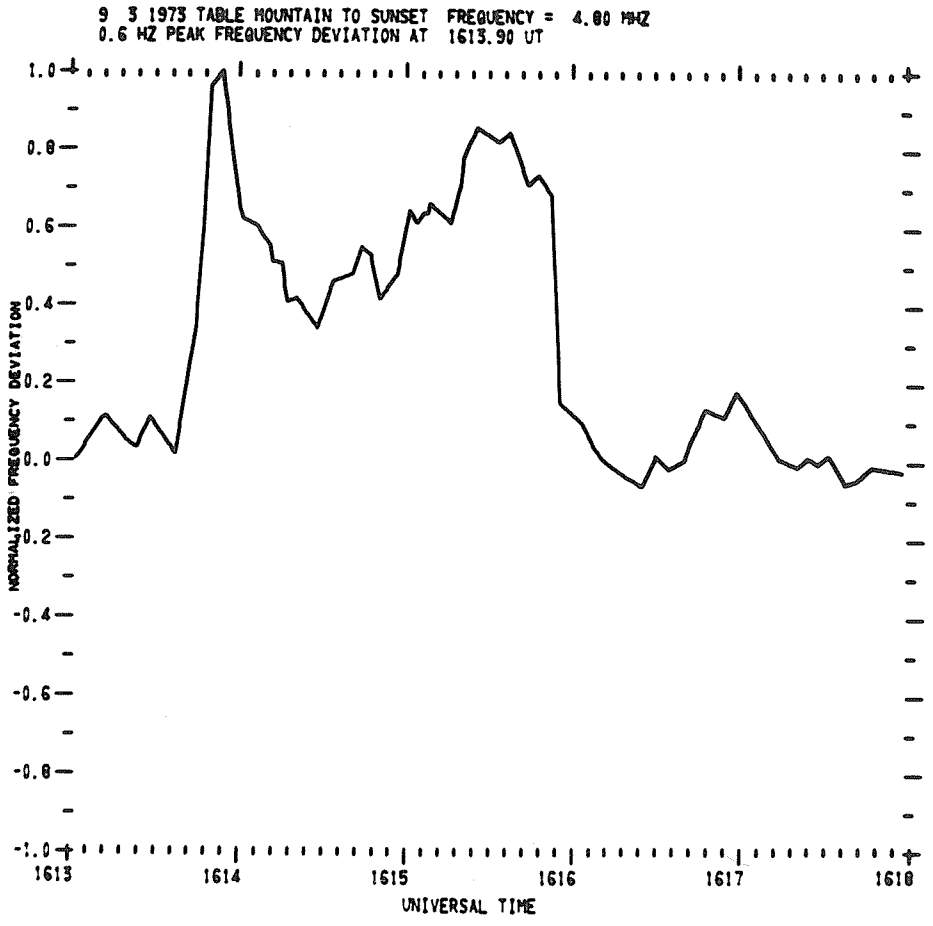

Figure 7.17 SFD of 1614 UT September 3, 1973 on 4.8 MHz at Sunset, Colorado.

This SFD followed two small events, one at 1601 UT and another at 1605 UT. See Tables 7.1 and 7.2. Because the HF Doppler data were noisy, SFD data from two other channels are shown in Figures 7.19 and 7.21. The associated H_α subflare (SN) was located at N23 W04 (McMath Plage 12508). The H_α flare started at about 1614 UT and peaked near 1616 to 1618 UT. The 2-10 GHz radio burst peaked at about 1615.7 UT. (SGD)

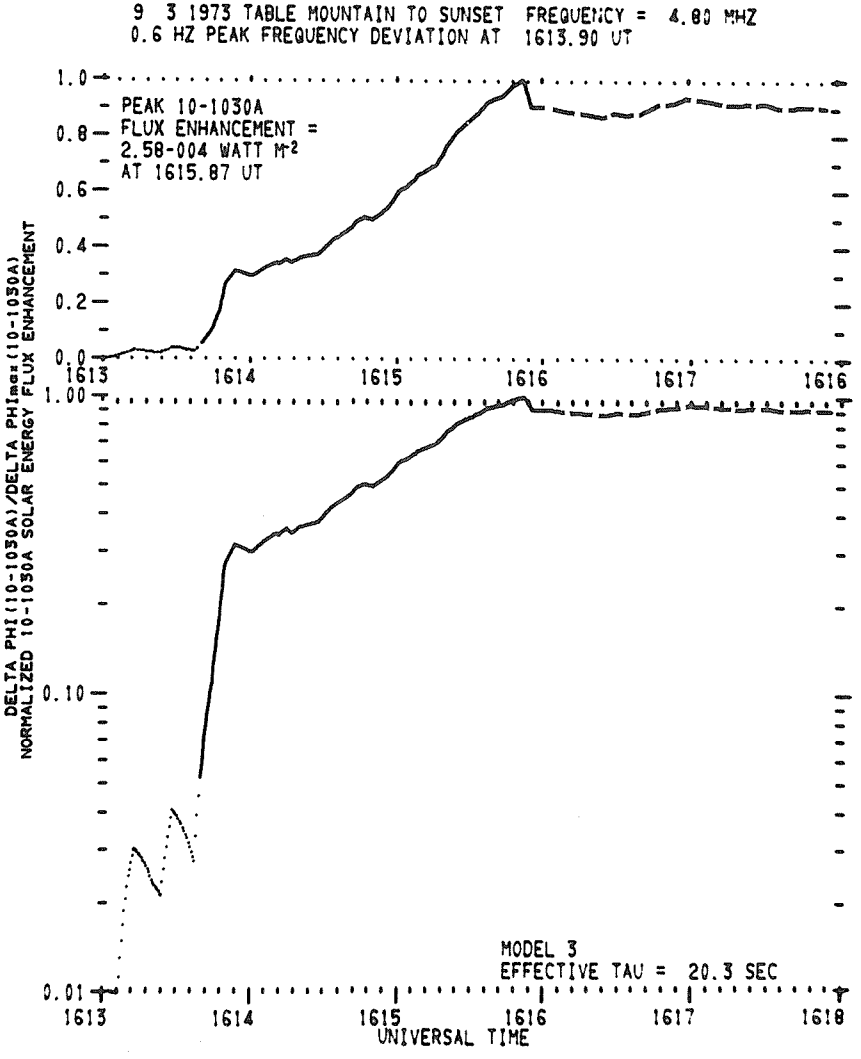

Figure 7.18 Best-estimate 10-1030A flux enhancement of 1616 UT September 3, 1973, based on 4.8 MHz at Sunset, Colorado.

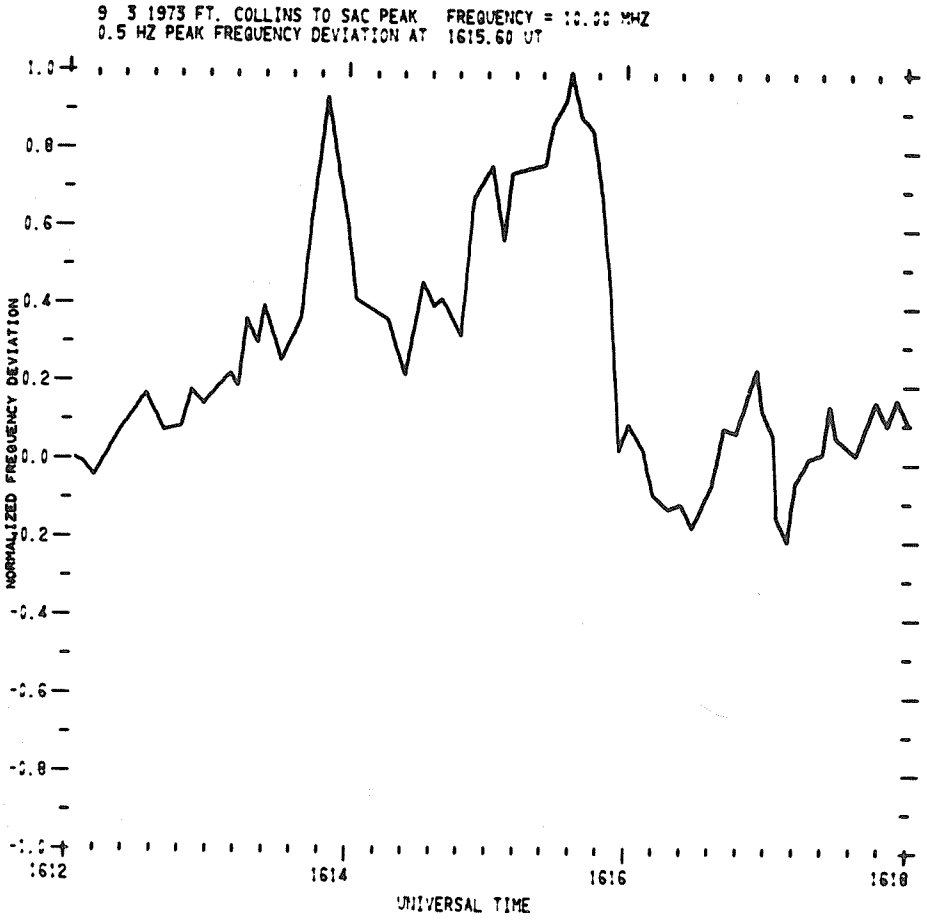

Figure 7.19 SFD of 1616 UT September 3, 1973 on 10 MHz at Sacramento Peak Observatory.

A second channel of HF Doppler data for the same SFD as in Figures 7.17 and 7.21. Some of the fine structure in $\Delta f(t)$ differs from one channel to another probably because of noise in the HF Doppler data. On the other hand, Figures 7.18, 7.20 and 7.22 are quite similar.

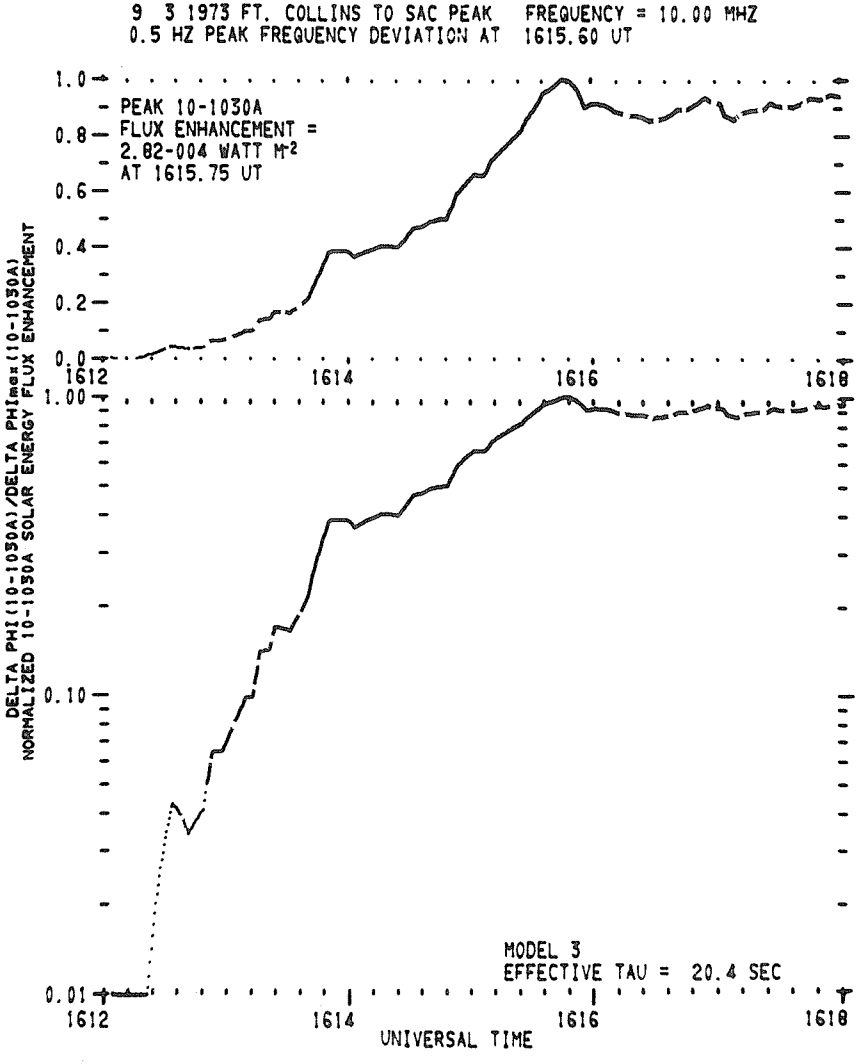

Figure 7.20 Best-estimate 10-1030A flux enhancement of 1616 UT September 3, 1973, based on 10 MHz at Sacramento Peak Observatory.

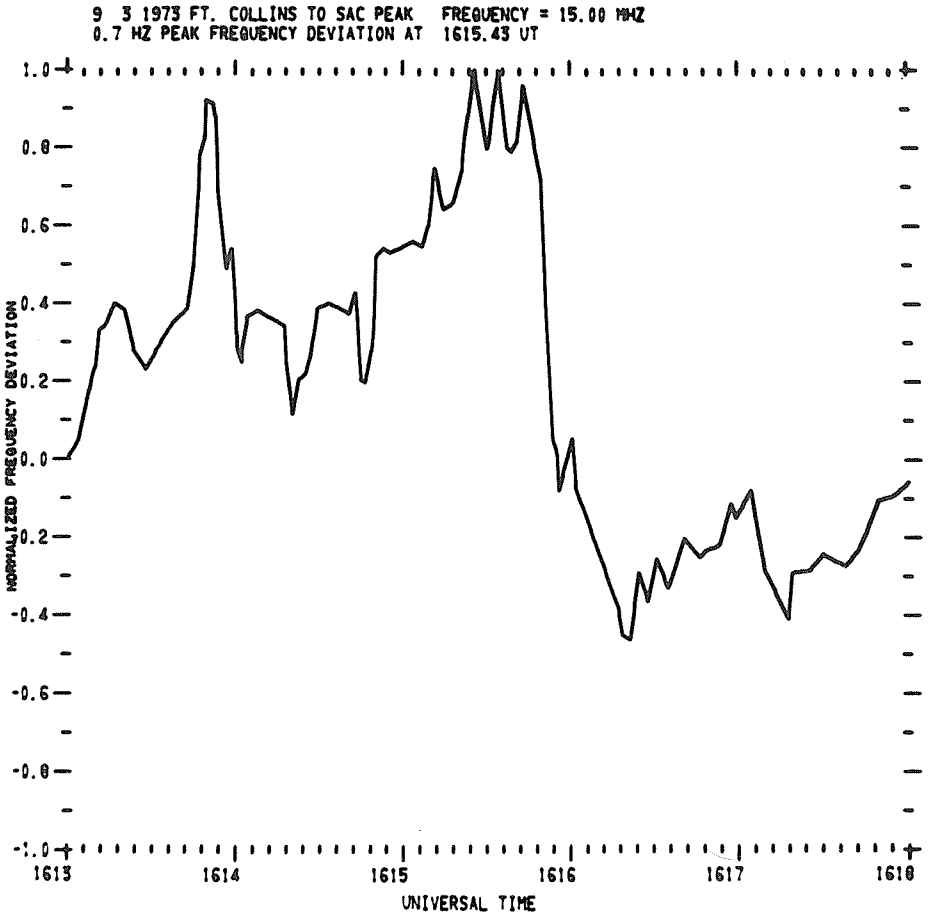

Figure 7.21 SFD of 1615 UT September 3, 1973, based on 15 MHz at Sacramento Peak Observatory.

The propagation path for 15 MHz was not determined. It may have been WWVH Hawaii to Sacramento Peak Observatory. The $\Delta\Phi$ solution in Figure 7.22 is based on the 4.8 MHz vertical path at Boulder with the $\Delta f(t)/\Delta f_{max}$ of Figure 7.21 renormalized to Δf_{max} for 4.8 MHz.

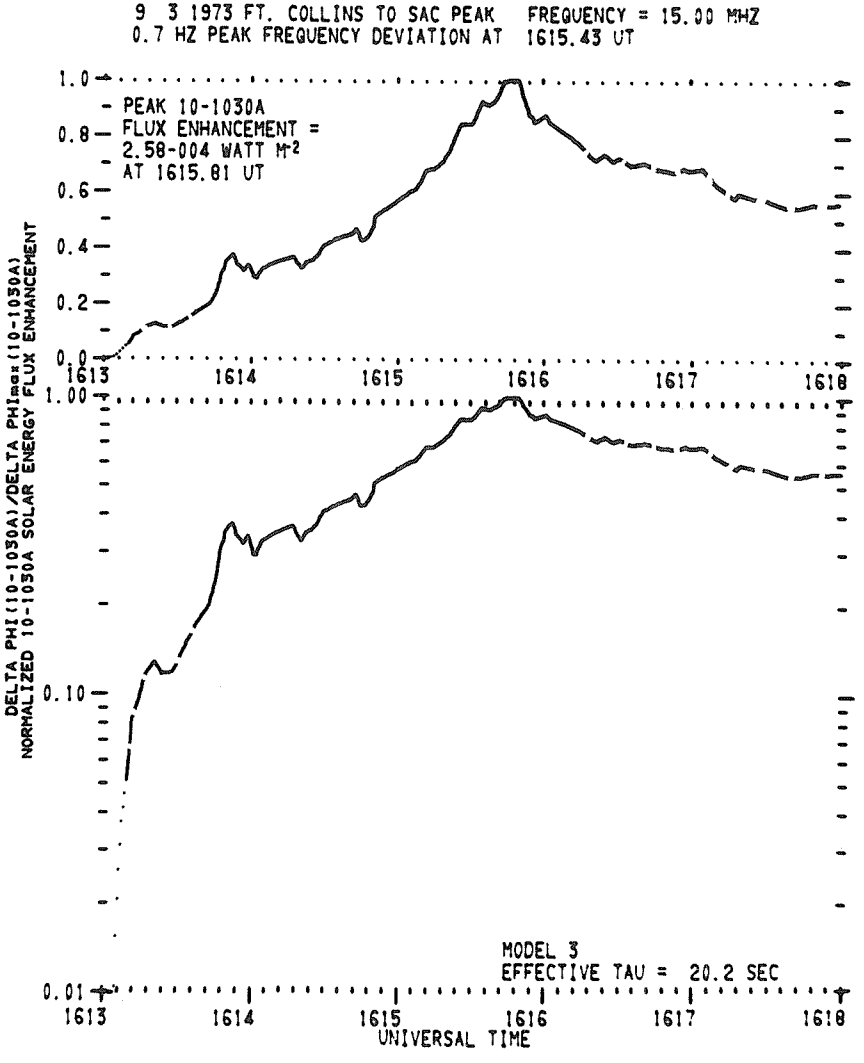

Figure 7.22 Best-estimate 10-1030A flux enhancement of 1616 UT September 3, 1973, based on 15 MHz at Sacramento Peak Observatory.

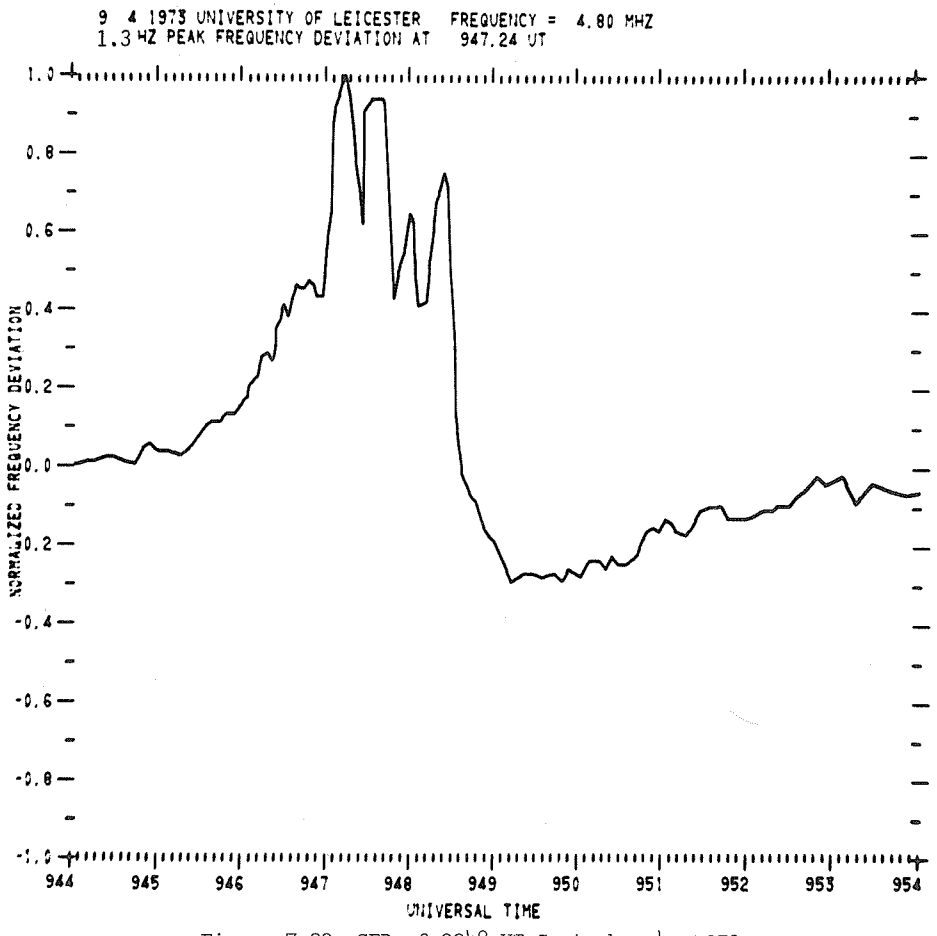

Figure 7.23 SFD of 0948 UT September 4, 1973.

This nice SFD was observed in England on three channels. This flare was partially observed by the ATM Harvard experiment near the edge of their raster scan. The associated bright H_α subflare was located at N14 E19 (McMath Plage Region No. 12510), started at about 0946 UT, and peaked near 0949 UT. The 2-11 GHz radio burst peaked near 0948 UT (SGD). The four peaks in Δf from 0947 to 0948 UT are real, i.e., they are caused by fine structure peaks in the 10-1030A flare radiation.

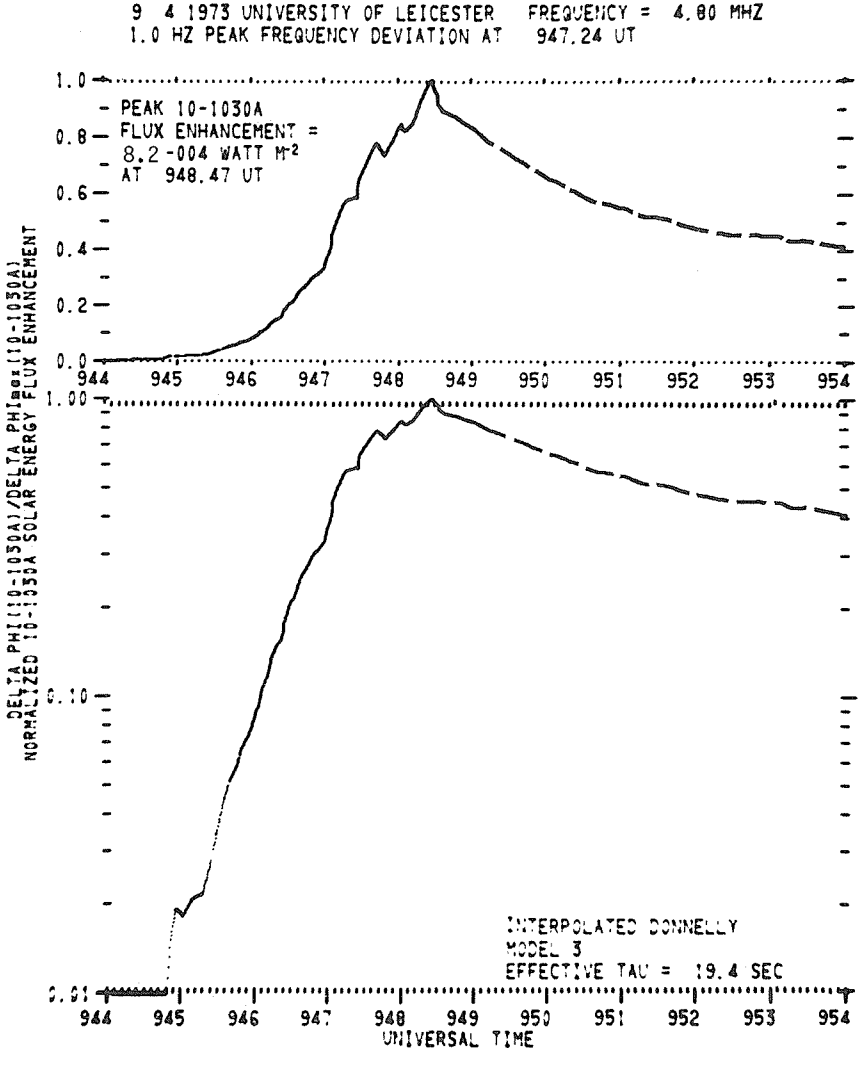

Figure 7.24 Best-estimate 10-1030A flux enhancement of 0948 UT September 4, 1973.

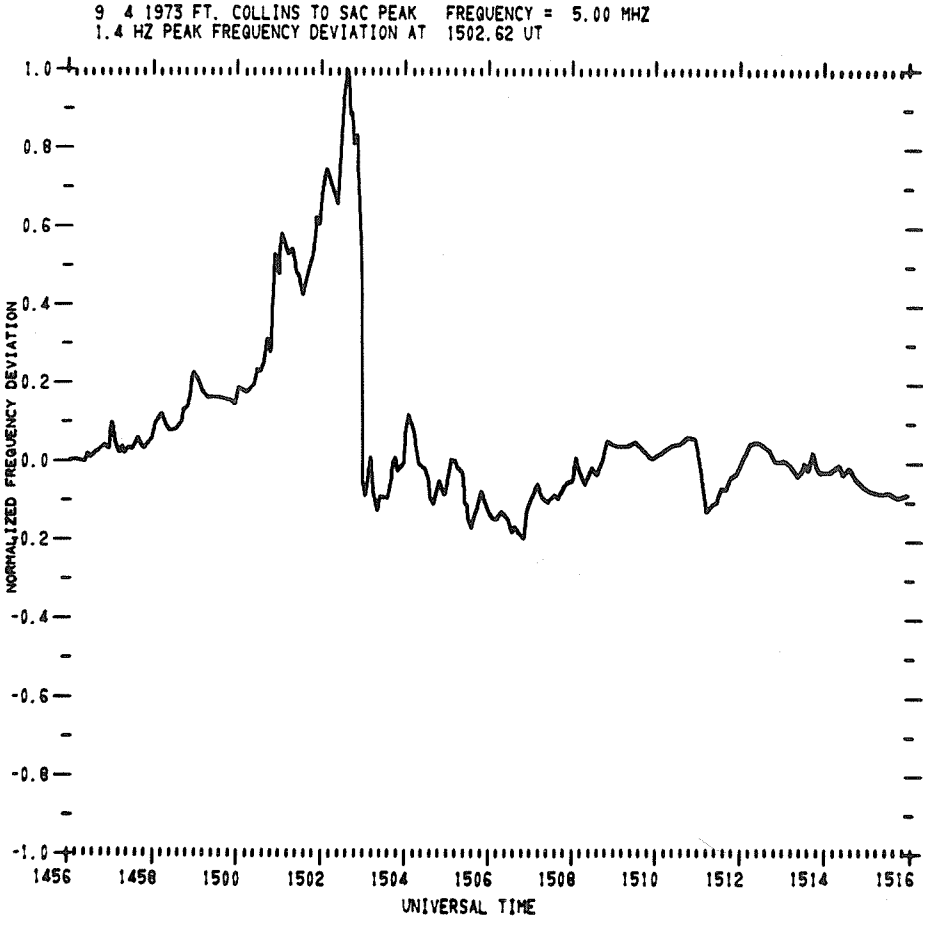

Figure 7.25 SFD of 1503 UT September 4, 1973.

This nice SFD was apparently not observed by ATM. It accompanied a bright H_α subflare at N12 E18 (McMath Plage 12510), which started near 1459 UT and peaked somewhere in the range 1503 to 1507 UT. The peak time of the microwave burst varied from one fixed observing frequency to another in the 2-15 GHz range from 1501 to 1506.3 UT with the higher frequencies generally peaking later than the lower frequencies (SGD).

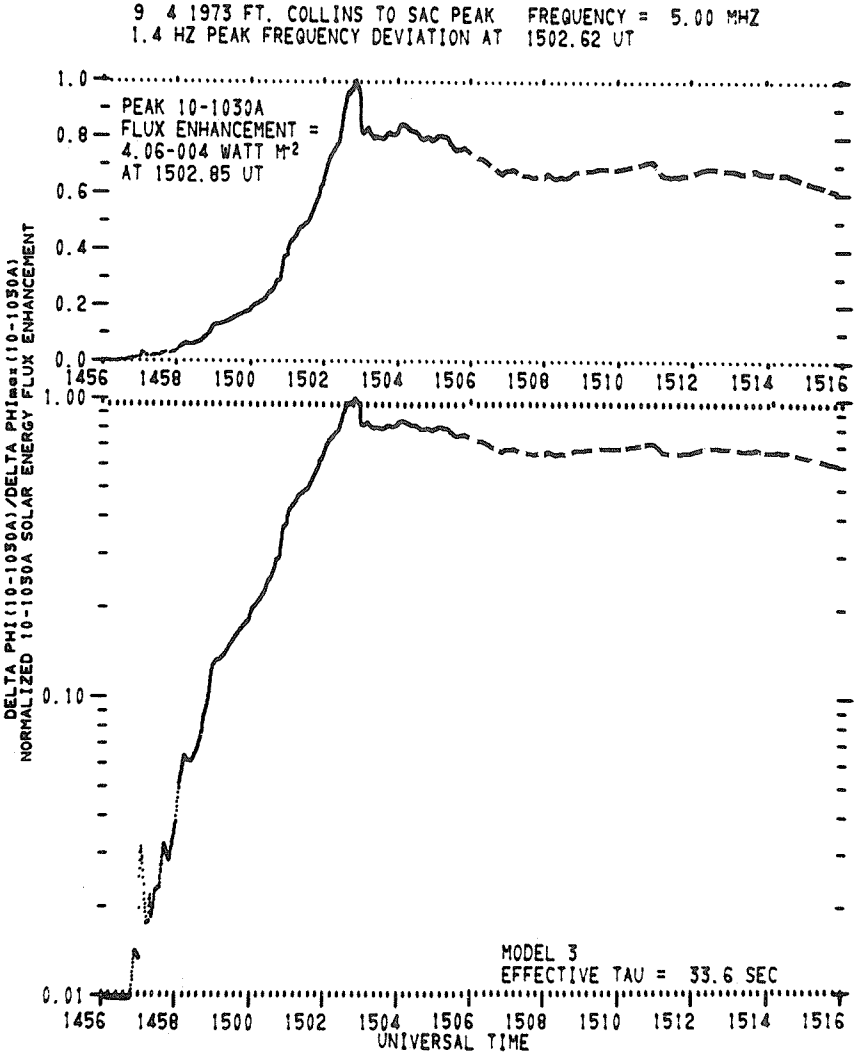

Figure 7.26 Best-estimate 10-1030A flux enhancement of 1503 UT September 4, 1973.

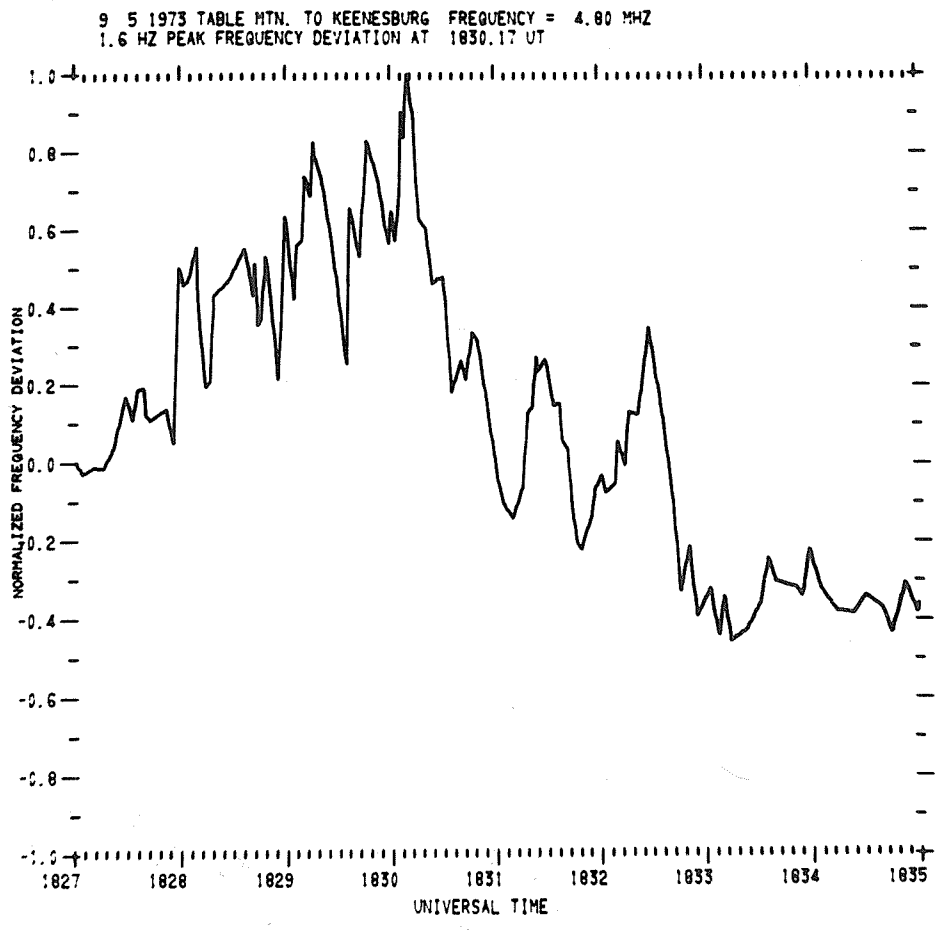

Figure 7.27 SFD of 1830 UT September 5, 1973, on 4.8 MHz at Keenesburg, Colorado.

This small complex EUV burst was observed by ATM. The HF Doppler observations were noisy. Several channels of SFD data are also shown in Figures 7.29-7.31. Those fine structure features not corroborated in any other channel should be considered to be noise. The H_α subflare was of normal intensity and was located at N11 E04 (McMath Plage 12510). The flare was observed between periods of "No Flare Patrol", starting before 1828 and peaking after 1834 UT. The radio burst peaked from 1830 to 1831.5 UT at frequencies in the 2-15 GHz range (SGD).

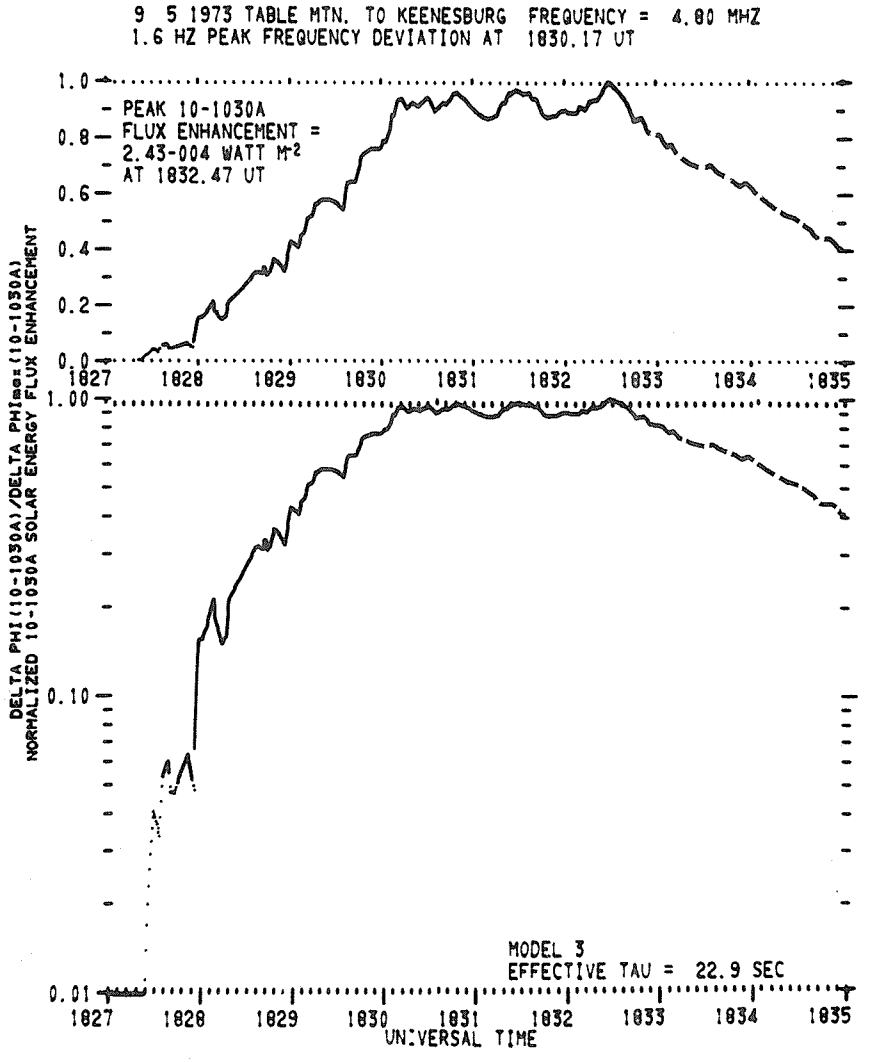

Figure 7.28 Best-estimate 10-1030A flux enhancement of 1832 UT September 5, 1973, based on 4.8 MHz at Keenesburg, Colorado.

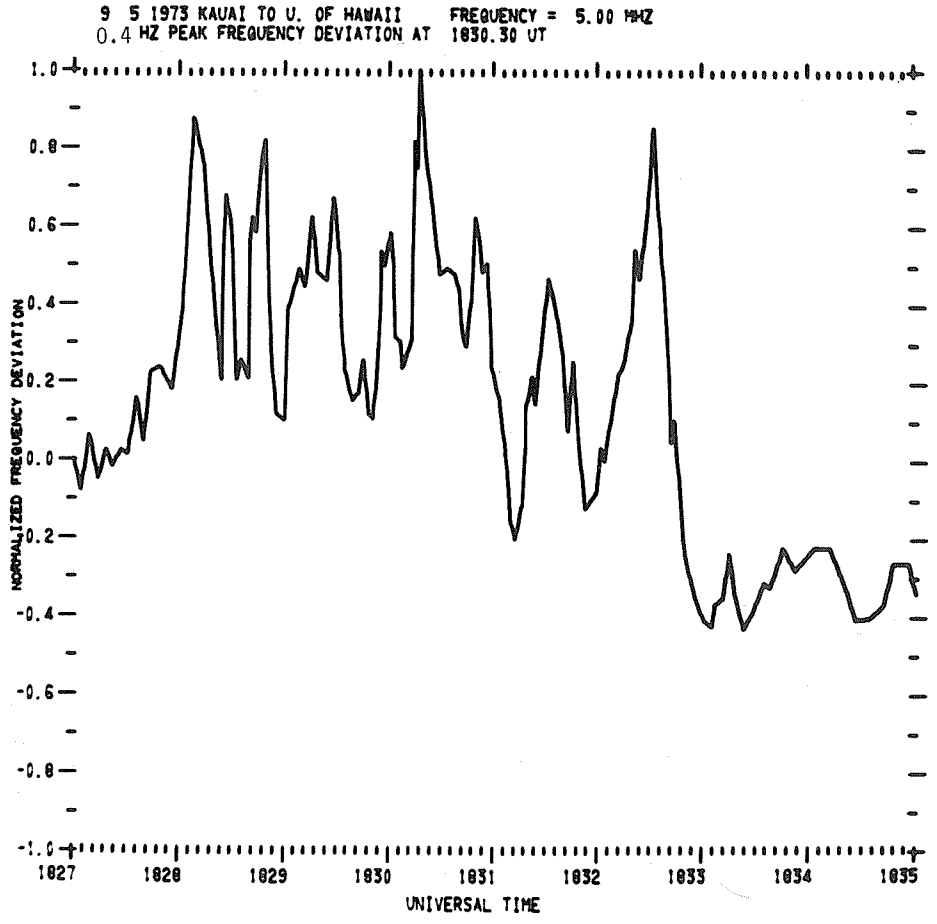

Figure 7.29 SFD of 1830 UT September 5, 1973, on 5 MHz at the University of Hawaii.

Note that some of the fine structure above differs from that in Figure 7.27, or in Figure 7.31. On the other hand, note the similarity between Figures 7.30 and 7.32. The fact that $\Delta\Phi(t)/\Delta\Phi_{max}$ near 1830 UT is higher in Figure 7.28 than in Figures 7.30 and 7.32 may result from a swell in $\Delta f(t)$ in the Keenesburg data due to local ionospheric variations unrelated to the solar flare effects. The earlier local time and the corresponding high solar zenith angle resulted in Δf_{max} being smaller in Hawaii than near Boulder. The smaller Δf_{max} is the more difficult it is to resolve the fine structure. Some would call the fine structure "quasi periodic", but the varying spacing between fine structure peaks results in very weak peaks in a Fourier spectral analysis of the burst.

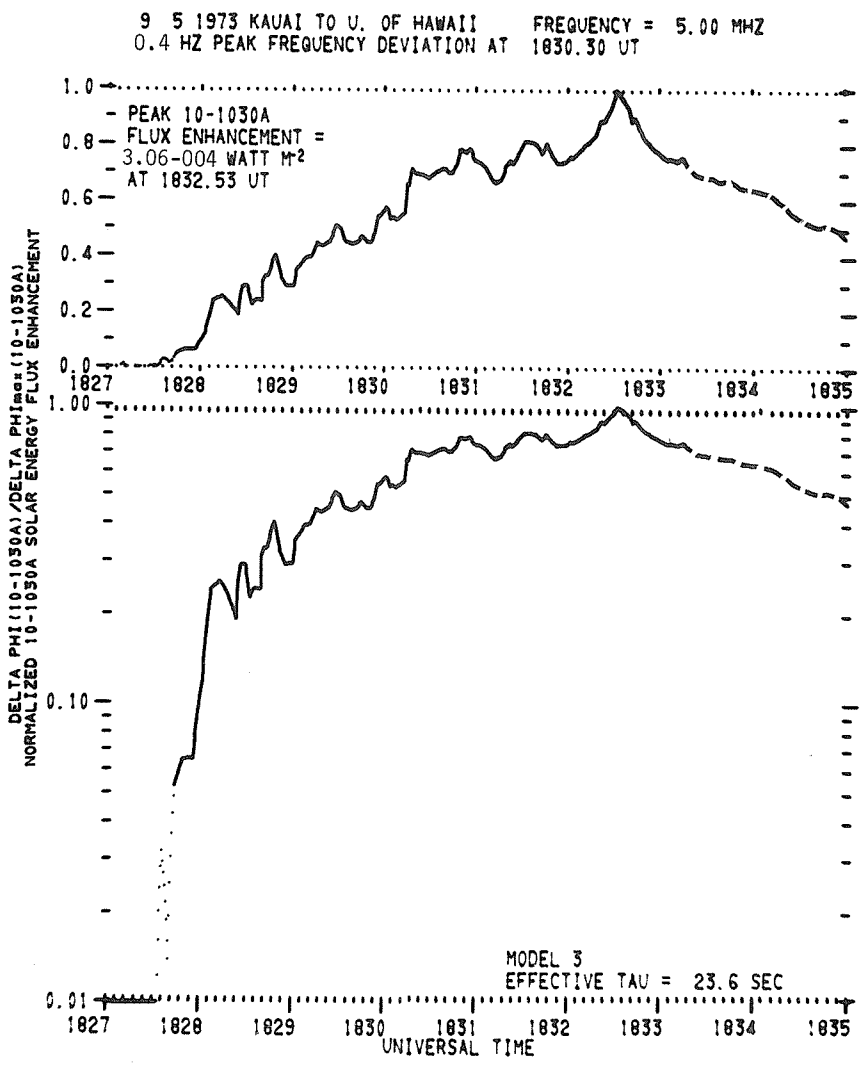

Figure 7.30 Best-estimate 10-1030A flux enhancement of 1833 UT September 5, 1973, based on 5 MHz at the University of Hawaii.

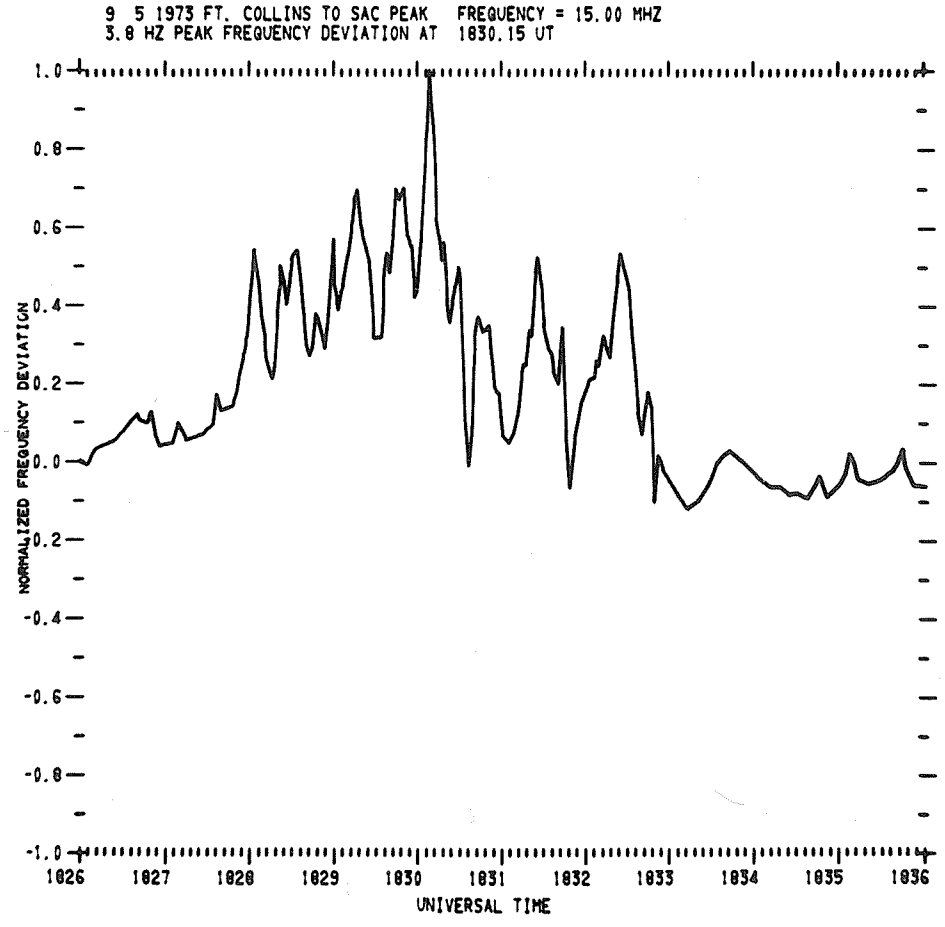

Figure 7.31 SFD of 1830 UT September 5, 1973, on 15 MHz at Sacramento Peak Observatory.

This channel of HF Doppler data shows best the fine structure (larger Δf_{max}). On the other hand, the propagation path was not determined. It may have been WWVH Hawaii to Sacramento Peak Observatory. The $\Delta\Phi$ solutions were made using the 4.8 MHz path and renormalizing $\Delta f(t)/\Delta f_{max}$ in Figure 7.31 to Δf_{max} for 4.8 MHz near Boulder. Note that the $\Delta\Phi$ results in Figure 7.37 based on the Mitra and Banerjee [1971] models of $\alpha_{eff}(h)$ and $\beta(h)$ agree closely with the results in Figure 7.32. Although $\Delta\Phi_{max}$ in Figures 7.32-7.37 varies inversely proportional to τ_{eff}, the size of individual impulsive rises or falls with times shorter than τ_{eff} are relatively independent of τ_{eff}.

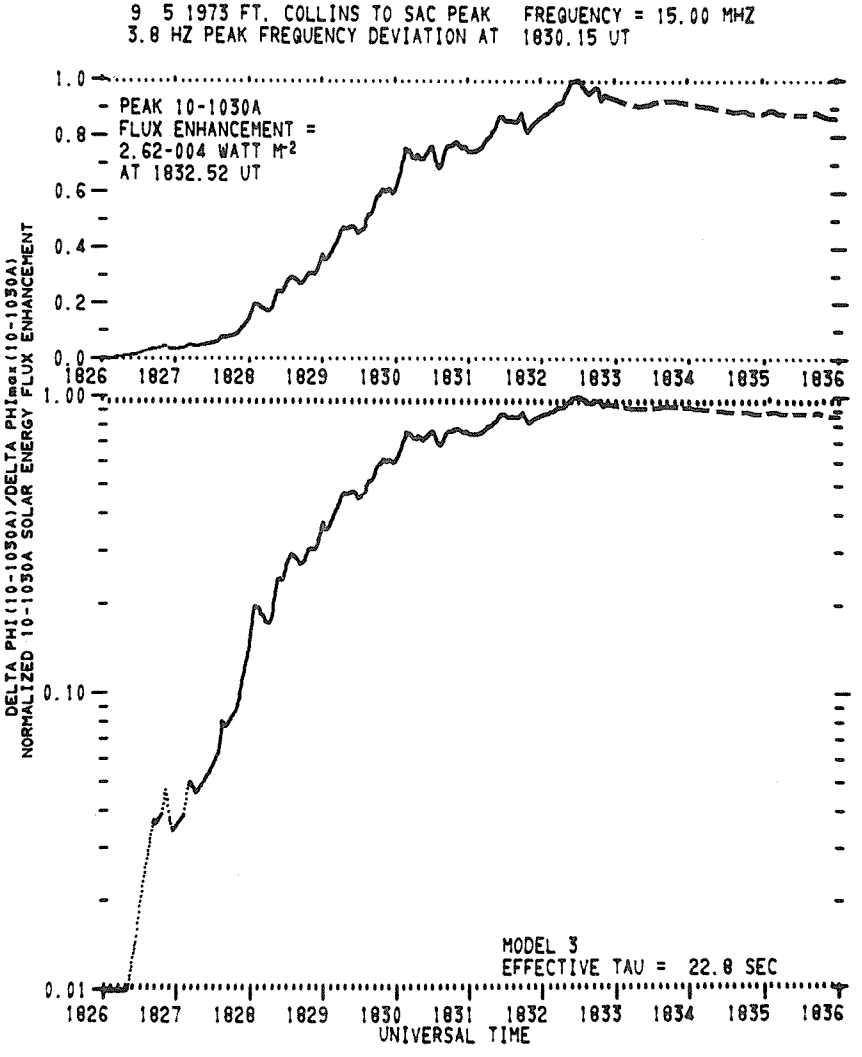

Figure 7.32 Best-estimate 10-1030A flux enhancement of 1833 UT September 5, 1973, based on 15 MHz at Sacramento Peak Observatory.

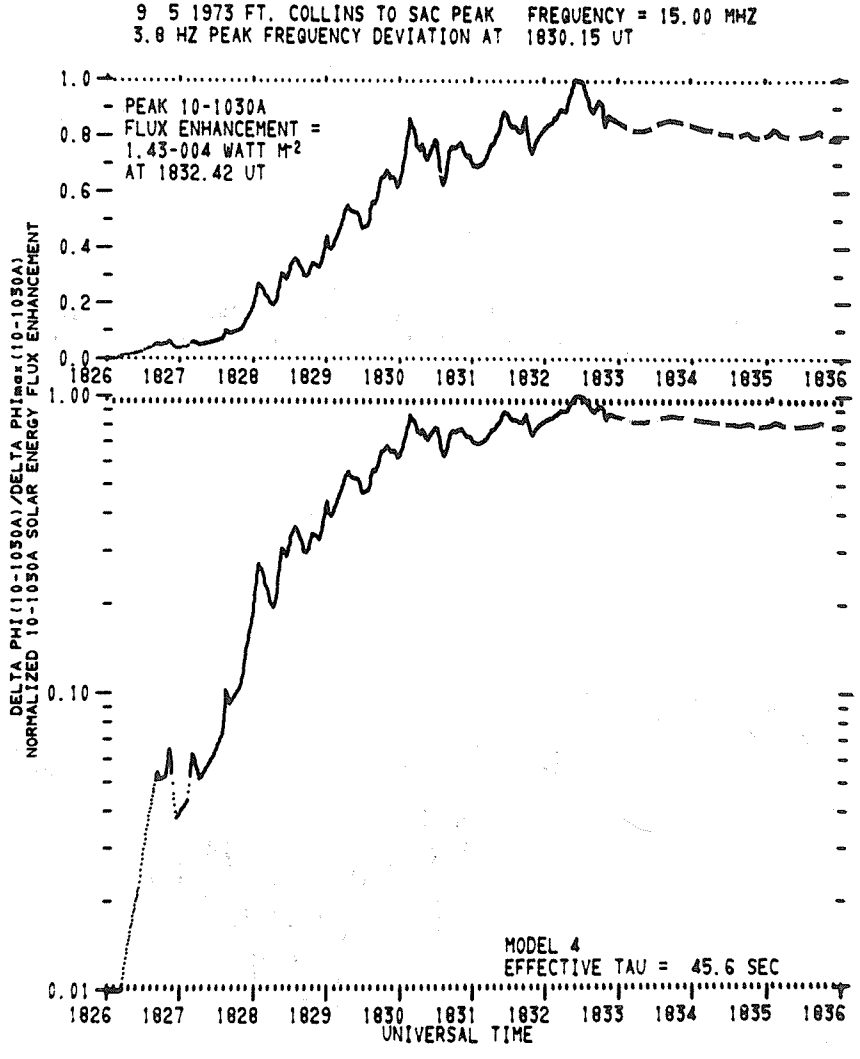

Figure 7.33 The 10-1030A flux enhancement of 1833 UT September 5, 1973, based on very low ionospheric electron loss rates.

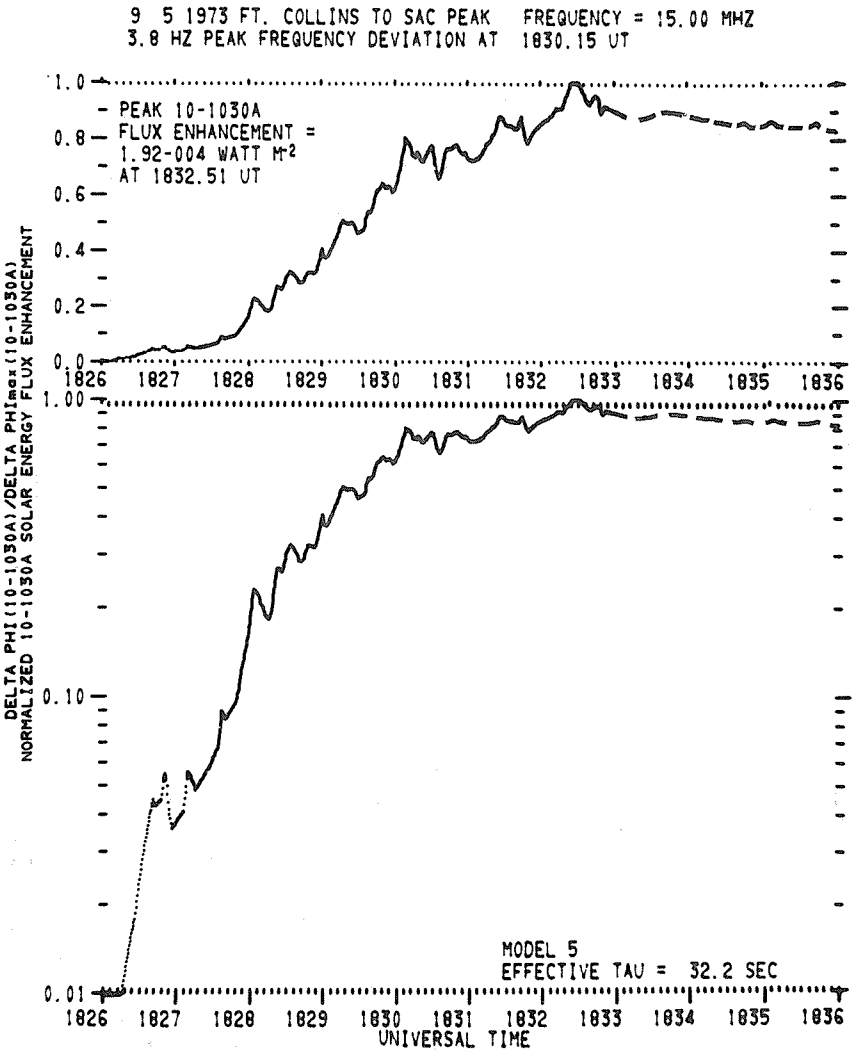

Figure 7.34 The 10-1030A flux enhancement of 1833 UT September 5, 1973, based on low ionospheric electron loss rates.

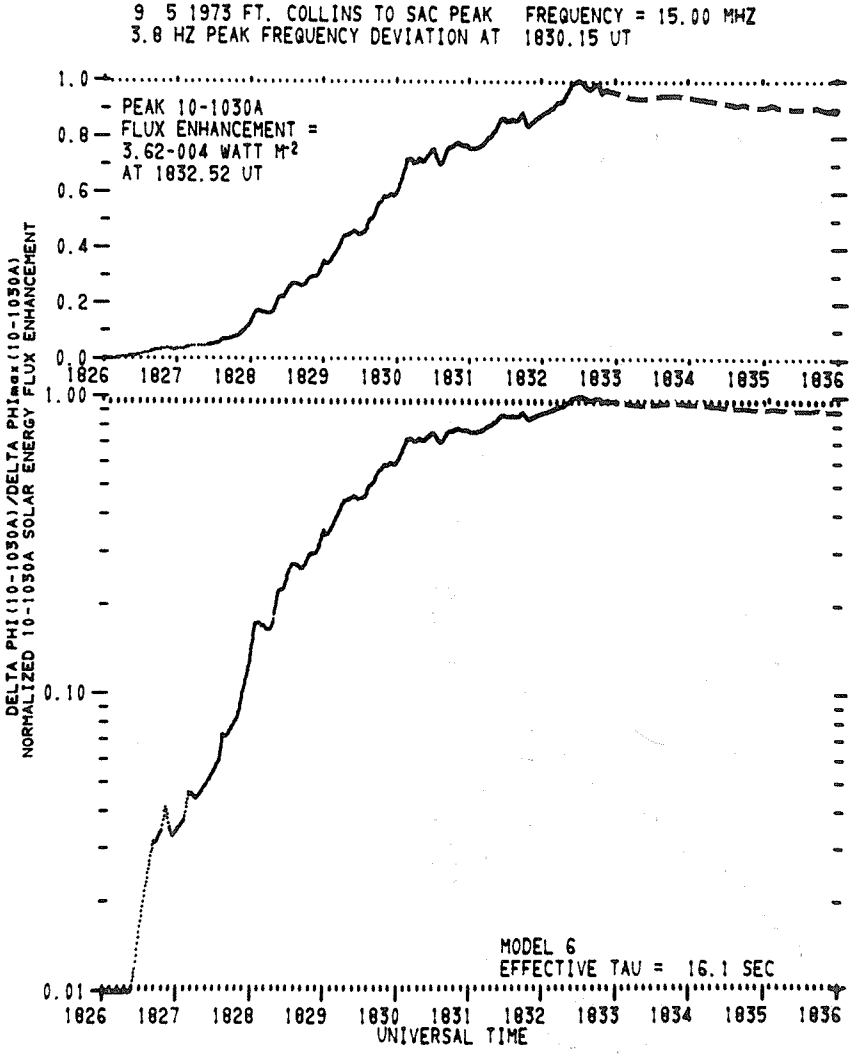

Figure 7.35 The 10-1030A flux enhancement of 1833 UT September 5, 1973, based on high ionospheric electron loss rates.

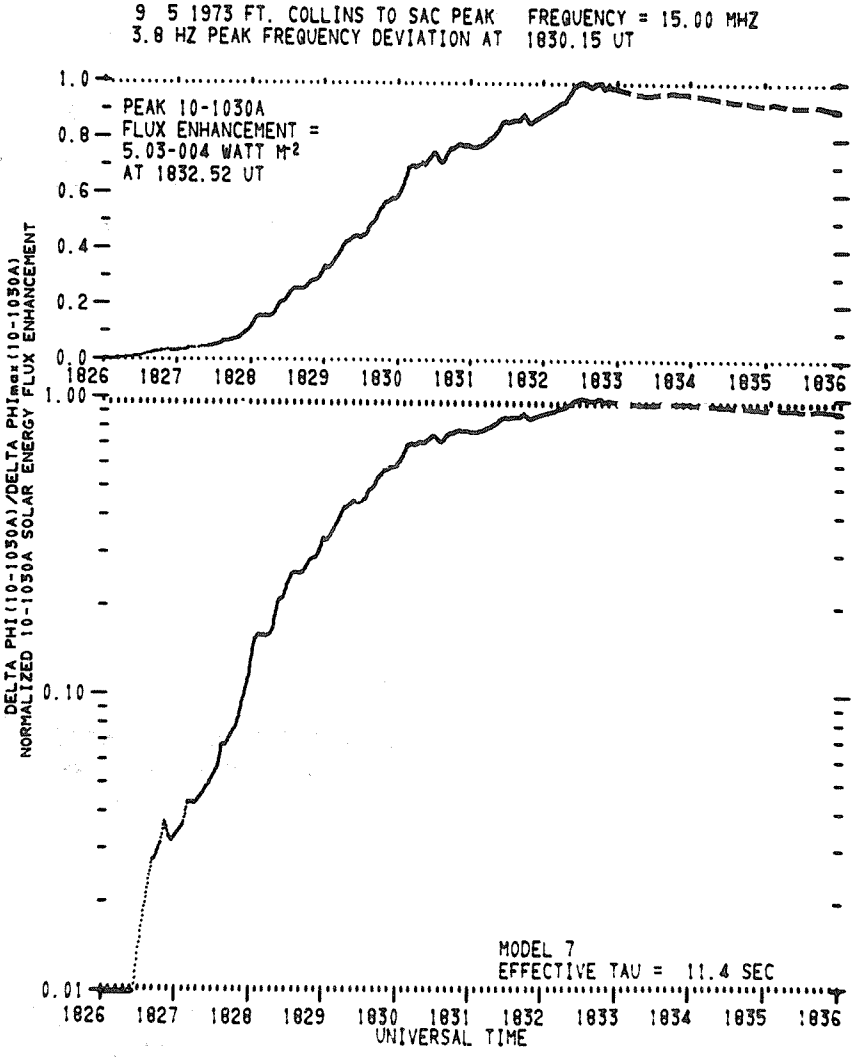

Figure 7.36 The 10-1030A flux enhancement of 1833 UT September 5, 1973, based on very high ionospheric electron loss rates.

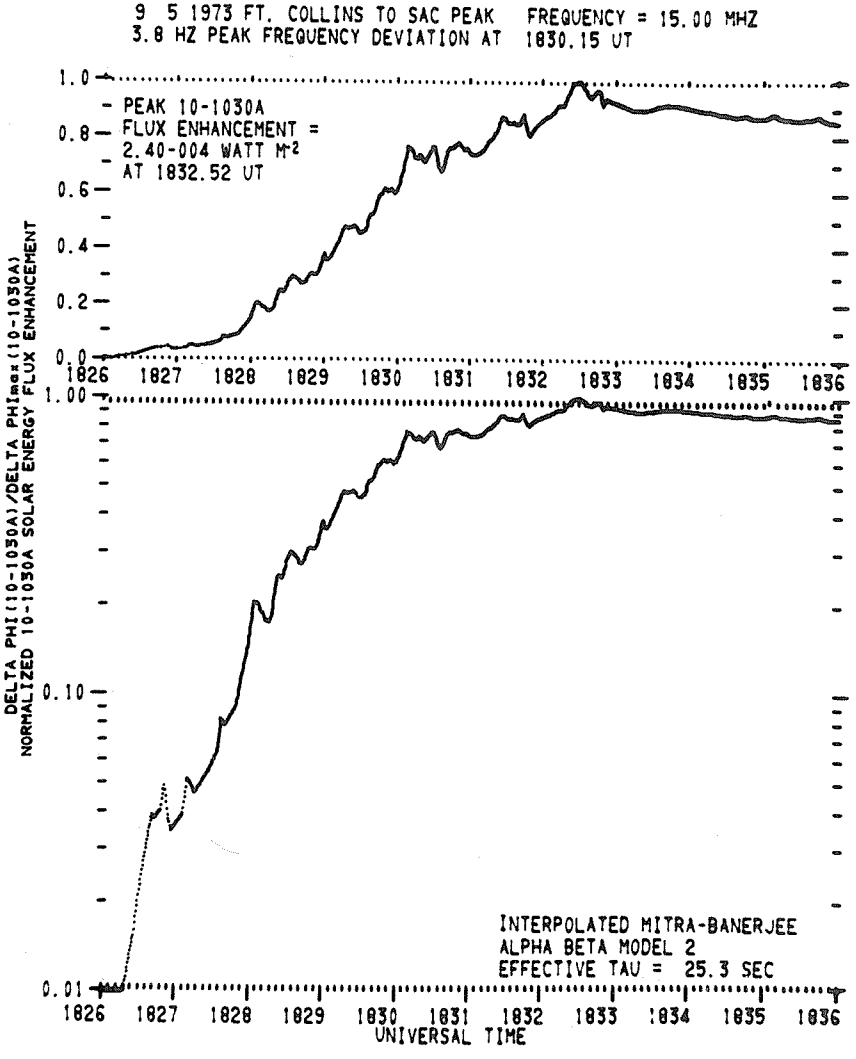

Figure 7.37 The 10-1030A flux enhancement of 1833 UT September 5, 1973, based on Mitra-Banerjee models of the ionospheric electron loss rates.

8. OBSERVATIONS DURING THE SECOND UNMANNED MISSION OF AT ATM-SKYLAB

The last ATM film observations of the second manned mission (SKYLAB III) were taken on September 21, 1973, and the first film observations of the third manned mission were taken after 1900 UT on November 26, 1973. Because the SFDs observed in Boulder on November 26 occurred before 1900 UT, we have designated September 22 through November 26 as the second unmanned period of ATM observations. Some ATM observations were made during this period, e.g., by Harvard's experiment; however, it is very unlikely that ATM observations were made during the impulsive phase of solar flares.

The SFD observing times at Sacramento Peak Observatory and at Boulder are shown in Figures 8.1 and 8.2, respectively. The Boulder data were lost on October 8. The level of solar activity was quite low. The daily average 10 cm flux dipped below 80 to nearly sunspot minimum values from October 9 through 20, and from November 4 through 20. Relatively few solar flares occurred during the second unmanned mission. The few SFDs observed are listed in Table 8.1. All of these SFDs were small or of poor quality; therefore $\Delta\Phi$(10-1030A, t) was not computed for any of the events. In general the SFD observations in Hawaii were better than at Sacramento Peak and Boulder for this period. It is very fortunate indeed that no manned ATM mission occurred during this period so barren of solar activity of terrestrial significance.

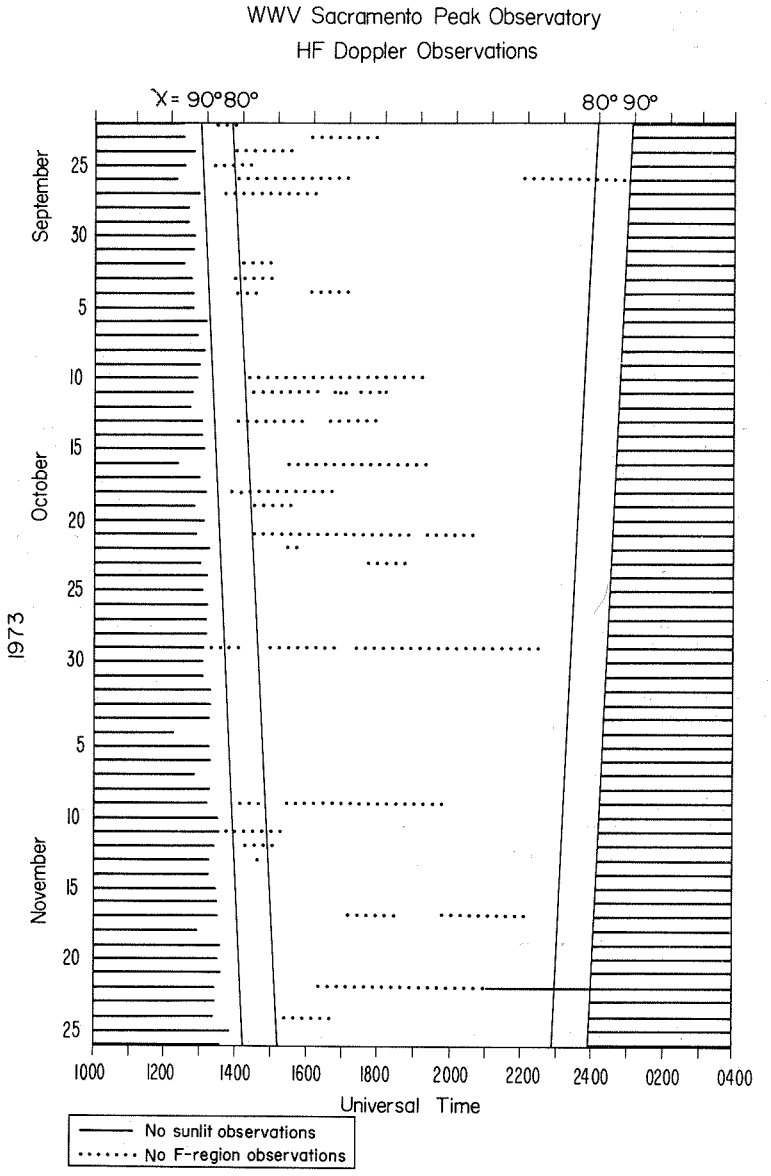

Figure 8.1 SFD observing time at Sacramento Peak Observatory during the second unmanned observations with ATM.

Clear areas indicate good observations, dotted indicate reduced sensitivity, solid line indicates no observations.

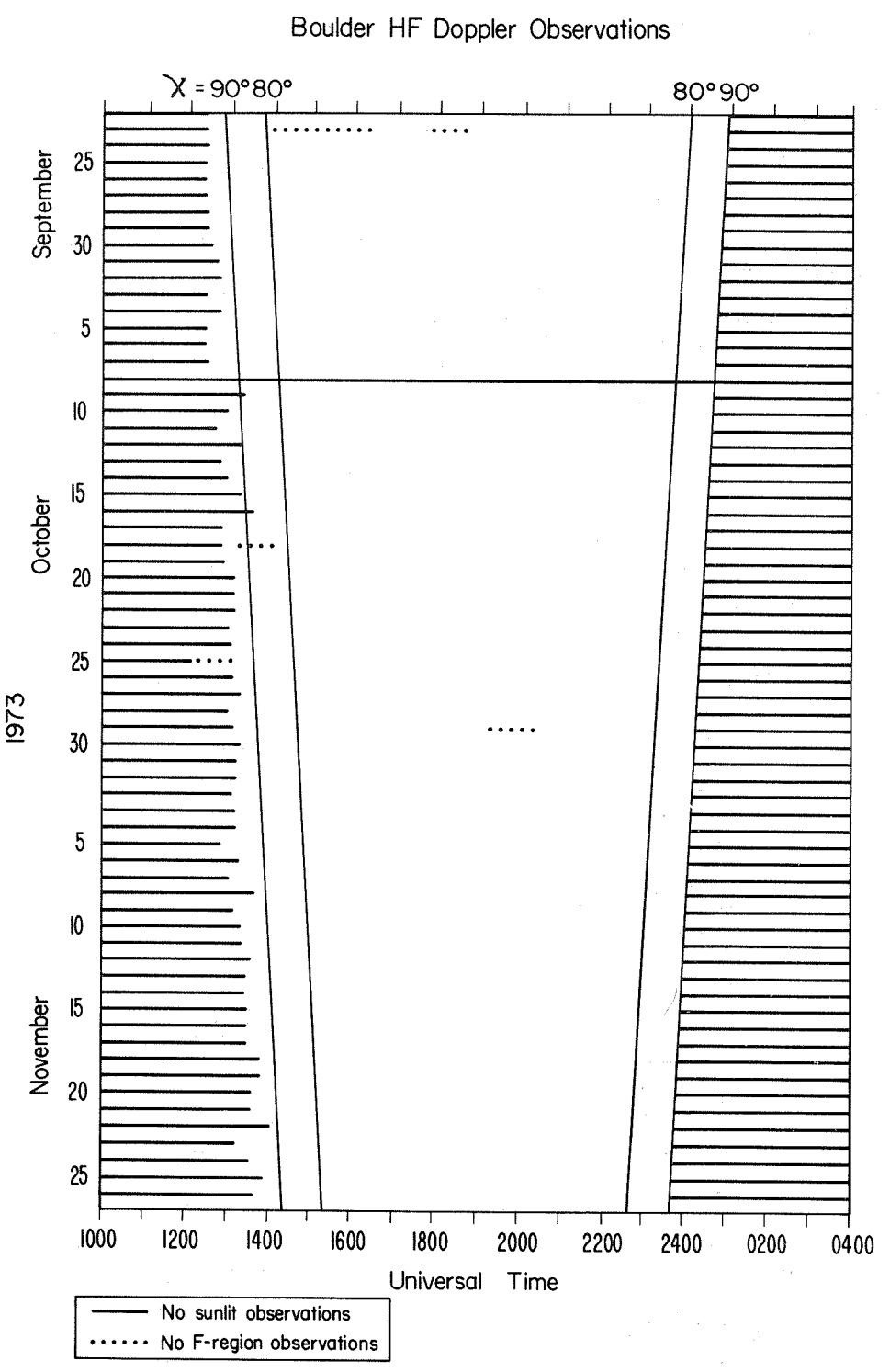

Figure 8.2 SFD observing time at Boulder, Colorado during the second unmanned observations with ATM.

Clear areas indicate good observations, dotted indicate reduced sensitivity, solid line indicates no observations.

TABLE 8.1 SFDs During the Second Unmanned Mission of ATM-SKYLAB

DATE			UNIVERSAL TIME				PEAK FREQUENCY DEVIATION		TRANSMITTER		
MONTH	DAY	YEAR	START	MAXIMUM	ZERO CROSSING	END	HZ	HF DOPPLER STATION	CALL LETTERS	FREQUENCY MHZ	COMMENTS
10	1	1973	1800. U	1806. U	1808.	1822. U	0.2	FT. COLLINS TO SAC PEAK	WWV	10.000	11 22
10	3	1973	0145.	0146.	0147.	0149.	0.3	KAUAI TO U. OF HAWAII	WWVH	5.000	10 21
10	3	1973	0145.	0146.	0147.	0149.	0.2	KAUAI TO U. OF HAWAII	WWVH	10.000	10
10	4	1973	2021. U	2022.3	2022.7	2026. U	0.8	FT. COLLINS TO SAC PEAK	WWV	15.000	11 20
10	4	1973	2026.6	2027.7	2029.5	2045. U	1.6	FT. COLLINS TO SAC PEAK	WWV	15.000	10 20
10	10	1973	1843.	1843.5	1843.7	1846. U	0.4	SUNSET, COLORADO		4.8	10 21 22
10	10	1973	1842.	1843.	U	1844.	0.2	KAUAI TO U. OF HAWAII	WWVH	5.000	11
10	10	1973	1848.	1849.	U	1850.	0.2	KAUAI TO U. OF HAWAII	WWVH	10.000	11
10	12	1973	2221.	2224.	U	2227. U	0.5	KAUAI TO U. OF HAWAII	WWVH	10.000	10 21
10	12	1973	2218.	2224.0	U	2252. U	0.4	FT. COLLINS TO SAC PEAK	WWV	15.000	10 20
10	26	1973	2238.8	2239.7	2240.1	2242.6	0.4	KAUAI TO U. OF HAWAII	WWVH	5.000	1
11	3	1973	0012.	0013.8	0018.0U	0035. U	0.8	KAUAI TO U. OF HAWAII	WWVH	5.000	13
				0014.5			0.8				
				0015.5			0.2				
11	3	1973	0012.	0014.6	U	0020. U	0.2	KAUAI TO U. OF HAWAII	WWVH	10.000	
11	3	1973	0012.4	0013.9	U	0025. U	1.1	FT. COLLINS TO SAC PEAK	WWV	15.000	10 20
				0014.8			1.3				
				0015.7			0.7				
11	23	1973	2350.	2351.	U	2356. U	0.2	KAUAI TO U. OF HAWAII	WWVH	5.000	11
				2354.			0.1				
				2355.			0.1				
11	24	1973	2002.	2004.	U	2020. U	0.6	KAUAI TO U. OF HAWAII	WWVH	5.000	
				2006.			0.5				
				2007.			0.2				
				2010.			0.2				
				2014.			0.2				
11	24	1973	2003.	2003.9	U	2024. U	0.5	FT. COLLINS TO SAC PEAK	WWV	10.000	8 10
				2005.9			0.2				
				2009.4			0.1				
				2014.8			0.2				
11	25	1973	2345.	2346.5	2348.5	2350. U	0.3	KAUAI TO U. OF HAWAII	WWVH	5.000	
				2348.			0.2				

TABLE 8.1 (Cont'd.)

DATE			UNIVERSAL TIME			PEAK FREQUENCY DEVIATION		TRANSMITTER CALL LETTERS	FREQUENCY	
MONTH	DAY	YEAR	START	MAXIMUM	ZERO CROSSING	END	HZ	HF DOPPLER STATION		MHZ	COMMENTS
11	26	1973	0023.	0025.	0031.	0035.	0.5	KAUAI TO U. OF HAWAII	WWVH	5.000	
				0028.			0.4				
				0030.			0.2				
11	26	1973	0106.	0107.	0111	0117. U	0.2	KAUAI TO U. OF HAWAII	WWVH	5.000	
				0110.			0.3				
11	26	1973	1424. U	1428.2	1430.3	1440. U	0.2	FT. COLLINS TO SAC PEAK	WWV	5.000	11
11	26	1973	1518.	1521.2	1528.0	1545. U	0.5	FT. COLLINS TO SAC PEAK	WWV	10.000	8 10
				1525.0			0.4				

U uncertain

COMMENT NUMBERS

1. Large SFD, $\Delta f_{max} \geq 4.5$ Hz.
2. Simple spike.
3. Gradual rise and fall, no impulsive structure.
4. Combination of impulsive spikes and gradual fall and rise.
5. Impulsive structure is weak relative to the gradual rise and fall.
6. Much fine-time structure.
7. Marked quasi-periodic fine time structure.
8. SFD very long lasting, $\Delta f > 0$ for >5 minutes.
9. SFD too small for quantitative analysis.
10. Poor SFD data.
11. SFD data too poor for quantitative analysis.
12. SWF
13. Large SWF, SFD trace lost.
14. Time code is inaccurate.
15. Propagation path reflected off the bottom of the E layer, causing the SFD observation to be insensitive to the impulsive EUV burst.
16. Peak frequency deviation not measurable.
17. Δf data inverted.
18. Extraordinary wave.
19. No solution for propagation path.
20. Possibly WWVH rather than WWV.
21. Vertical-incidence data affected by local ionospheric time variations.
22. Data complicated by tape recorder noise.

9. OBSERVATIONS DURING THE THIRD MANNED MISSION OF ATM-SKYLAB

The third and last manned ATM observations (SKYLAB IV) spanned the time from about 1900 UT November 26, 1973, to February 3, 1974, for the photographic recordings. The level of solar activity was low. The daily average 10 cm radio flux was below 100 radio flux units during this entire mission and dipped below 80 to nearly sunspot minimum values during the periods December 4 to 16, 1973; December 29, 1973, to January 9, 1974; and January 24 to the end of the mission. Relatively few flares occurred that were large enough to cause detectable terrestrial effects. The short daily observing period at northern latitudes further reduced the number of SFDs detected at Sacramento Peak and Boulder. See Figures 9.1 and 9.2. The detected SFDs are listed in Table 9.1 and the computed 10-1030A flux enhancement in Table 9.2. Many of the SFDs detected during this period were observed at the University of Hawaii, where the daily observing period was significantly longer than at the other observatories and the mid-day solar zenith angle significantly smaller.

The Boulder and Sacramento Peak data were poor in quality for most of these flares. Consequently, the EUV flux enhancement was computed only for the flare of 2334 UT December 23, 1973, shown in Figures 9.3 and 9.4, which was well observed in Hawaii.

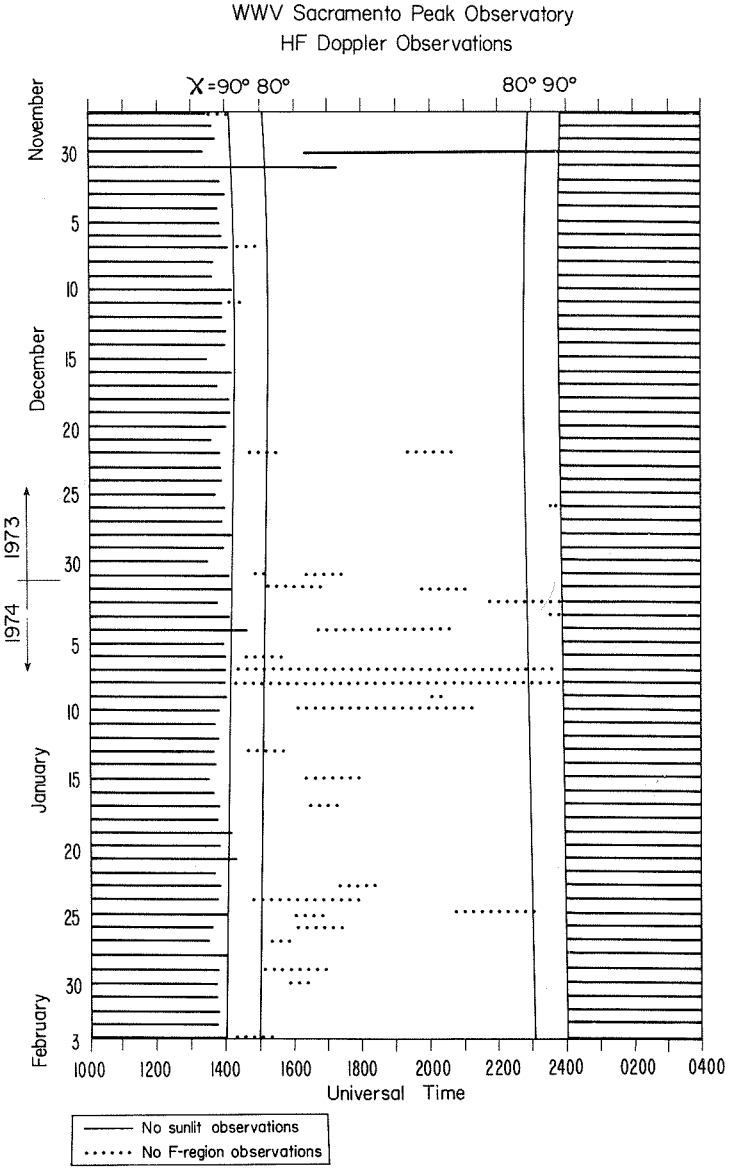

Figure 9.1 SFD observing time at Sacramento Peak Observatory during the third manned observations with ATM.

Clear areas indicate good observations, dotted indicate reduced sensitivity, solid line indicates no observations.

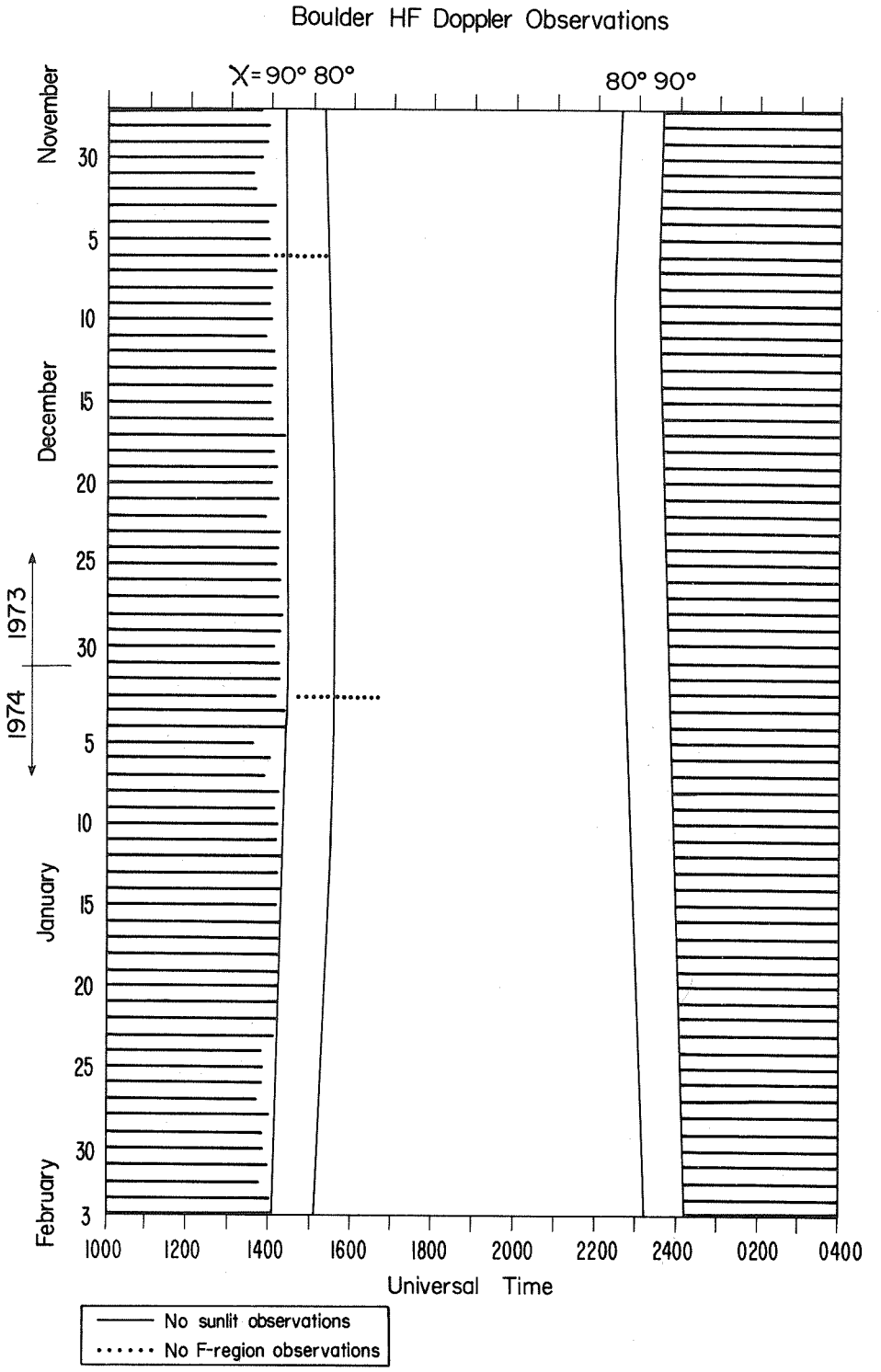

Figure 9.2 SFD observing time near Boulder, Colorado during the third manned observations with ATM.

Clear areas indicate good observations, dotted indicate reduced sensitivity, solid line indicates no observations.

TABLE 9.1 SFDs During the Third Manned Mission of ATM-SKYLAB

SFD OBSERVATIONS

DATE			UNIVERSAL TIME				PEAK FREQUENCY DEVIATION		TRANSMITTER		
MONTH	DAY	YEAR	START	MAXIMUM	ZERO CROSSING	END	HZ	HF DOPPLER STATION	CALL LETTERS	FREQUENCY MHZ	COMMENTS
11	26	1973	2327.	2329.	2331.5	2336. U	0.5	KAUAI TO U. OF HAWAII	WWVH	5.000	
				2331.			0.4				
11	27	1973	0122.	0124.	0125.	0131. U	0.3	KAUAI TO U. OF HAWAII	WWVH	5.000	
11	30	1973	1947.	1948.5	1949.3	2000. U	0.6	KAUAI TO U. OF HAWAII	WWVH	5.000	
12	2	1973	1459.	1500.0	1505. U	1506. U	0.4	FT. COLLINS TO SAC PEAK	WWV	10.000	10
12	2	1973	1512.	1516.4	1519. U	1530. U	0.4	FT. COLLINS TO SAC PEAK	WWV	10.000	10
12	2	1973	1532. U	1540. U	1544. U	1550. U	0.3	FT. COLLINS TO SAC PEAK	WWV	10.000	11
12	2	1973	1554. U	1558.3U	1602. U	1605. U	0.2	FT. COLLINS TO SAC PEAK	WWV	10.000	9 11
12	2	1973	1827. U	1829.4	1830.0	1837.	0.3	FT. COLLINS TO SAC PEAK	WWV	10.000	10
12	2	1973	1828.	1829.	1830. U	1831. U	0.4	KAUAI TO U. OF HAWAII	WWVH	5.000	
12	2	1973	2006.	2010.3	2018. U	2020. U	0.4	FT. COLLINS TO SAC PEAK	WWV	10.000	10
12	2	1973	2005.	2007.	2010.5U	2015. U	0.4	KAUAI TO U. OF HAWAII	WWVH	5.000	
				2009.			0.2				
12	5	1973	0011.	0012.5	2013.	0014.	0.4	KAUAI TO U. OF HAWAII	WWVH	5.000	
12	10	1973	2232.	2333.	U	2335.	0.3	KAUAI TO U. OF HAWAII	WWVH	10.000	
12	16	1973	2143. U	2145.7	2149. U	2200. U	0.2	FT. COLLINS TO SAC PEAK	WWV	10.000	10
12	17	1973	0028.	0030.	0034. U	0038. U	0.9	KAUAI TO U. OF HAWAII	WWVH	5.000	
12	17	1973	1627.	1627.3	1628.0	1630. U	0.2	FT. COLLINS TO SAC PEAK	WWV	10.000	2
12	20	1973	1802.3	1803.5	U	1805. U	0.1	FT. COLLINS TO SAC PEAK	WWV	10.000	11
12	20	1973	1945.4	1947.2	1950.0	1958.	0.4	FT. COLLINS TO SAC PEAK	WWV	10.000	10
12	22	1973	0022.	0023.	0024	0026. U	0.6	KAUAI TO U. OF HAWAII	WWVH	5.000	
12	23	1973	2332.	2333.6	2334.9	2341. U	0.9	FT. COLLINS TO SAC PEAK	WWVH	15.000	
				2333.9			1.2				
12	23	1973	2332.	2333.9	2334.0	2338. U	0.9	KAUAI TO U. OF HAWAII	WWVH	5.000	
12	23	1973	2332.	2333.9	U	U	0.5	KAUAI TO U. OF HAWAII	WWVH	10.000	10 21
1	4	1974	1757.	1758.	1800. U	1808. U	0.2	KAUAI TO U. OF HAWAII	WWVH	5.000	10 21
1	12	1974	2052.	2053.	2054. U	U	0.6	KAUAI TO U. OF HAWAII	WWVH	5.000	
1	21	1974	2041. U	2045.0	U	2055. U	1.0	FT. COLLINS TO SAC PEAK	WWV	15.000	10 20
				2045.3			0.8				
				2046.7			0.2				
				2047.7			0.7				

Table 9.1 (Cont'd)

DATE			UNIVERSAL TIME				PEAK FREQUENCY DEVIATION		TRANSMITTER		
MONTH	DAY	YEAR	START	MAXIMUM	ZERO CROSSING	END	HZ	HF DOPPLER STATION	CALL LETTERS	FREQUENCY MHZ	COMMENTS
1	22	1974	1739.	1741.3	1744.3	1754. U	0.8	FT. COLLINS TO SAC PEAK	WWV	15.000	10 20
				1743.7			0.8				
1	22	1974	1916. U	1918.3	1920.	1930. U	0.2	FT. COLLINS TO SAC PEAK	WWV	10.000	10
1	22	1974	2116.	2117.	U	2120. U	0.4	KAUAI TO U. OF HAWAII	WWVH	5.000	
1	26	1974	2326.	2327.	U	2328. U	0.4	KAUAI TO U. OF HAWAII	WWVH	10.000	
1	31	1974	2133.6	2134.4	2138. U	2141. U	0.6	FT. COLLINS TO SAC PEAK	WWV	15.000	10 20
				2136.8			0.2				
1	31	1974	2133.	2134.	2136. U	U	0.2	KAUAI TO U. OF HAWAII	WWVH	5.000	

U uncertain

COMMENT NUMBERS

1. Large SFD, $\Delta f_{max} \geq 4.5$ Hz.
2. Simple spike.
3. Gradual rise and fall, no impulsive structure.
4. Combination of impulsive spikes and gradual fall and rise.
5. Impulsive structure is weak relative to the gradual rise and fall.
6. Much fine-time structure.
7. Marked quasi-periodic fine time structure.
8. SFD very long lasting, $\Delta f > 0$ for >5 minutes.
9. SFD too small for quantitative analysis.
10. Poor SFD data.
11. SFD data too poor for quantitative analysis.
12. SWF
13. Large SWF, SFD trace lost.
14. Time code is inaccurate.
15. Propagation path reflected off the bottom of the E layer, causing the SFD observation to be insensitive to the impulsive EUV burst.
16. Peak frequency deviation not measurable.
17. Δf data inverted.
18. Extraordinary wave.
19. No solution for propagation path.
20. Possibly WWVH rather than WWV.
21. Vertical-incidence data affected by local ionospheric time variations.
22. Data complicated by tape recorder noise.

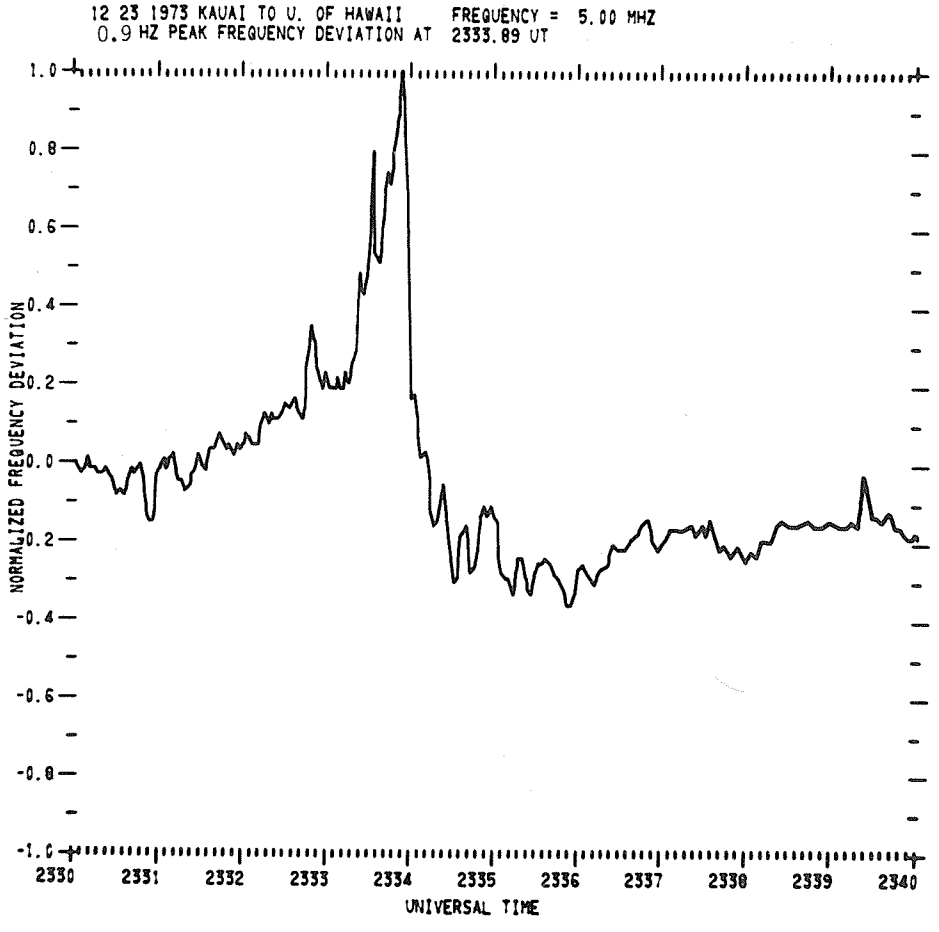

Figure 9.3 SFD of 2334 UT December 23, 1973, on 5.0 MHz at the University of Hawaii.

This small EUV burst accompanied a subflare of normal intensity located at S15 W43 , which started earlier than 2332 UT and reached its maximum phase at about 2334 UT. Manila reported a small microwave burst in the 1-5 GHz range peaking at 2333.5 UT (SGD).

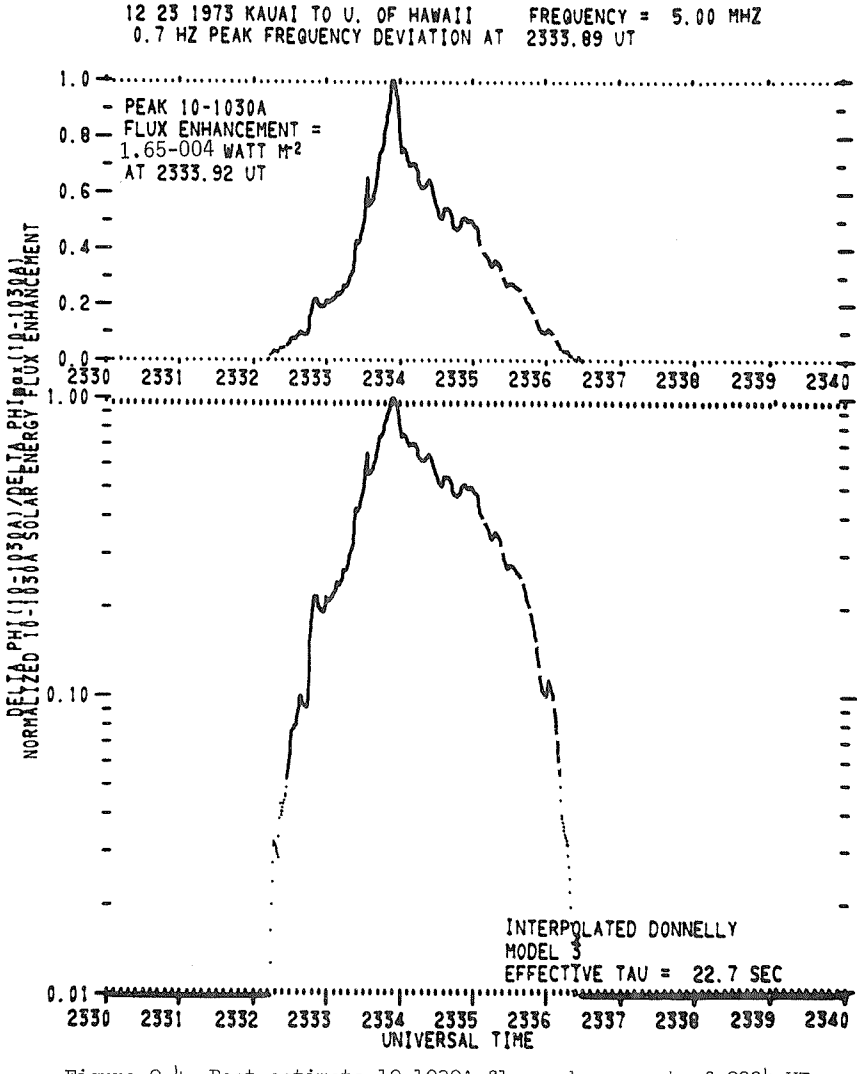

Figure 9.4 Best-estimate 10-1030A flux enhancement of 2334 UT December 23, 1973, based on 5.0 MHz at the University of Hawaii.

TABLE 9.2

THE IMPULSIVE 10-1030A FLUX ENHANCEMENT DEDUCED FROM SFDs DURING THE THIRD MANNED MISSION OF ATM SKYLAB

Date 1973	Number of Channels of SFD Data Analyzed To $\Delta\Phi$(10-1030A)	Start Time UT	Peak Time UT	$\Delta\Phi$*(10-1030A)
December 23	2	2332.2	2333.9	1.57×10^{-4}

* $\Delta\Phi$(10-1030A) flux units are Watts m^{-2}.

10. DISCUSSION

The SFDs and estimates of 10-1030A flux enhancements reported here provide information on the impulsive EUV flare emissions before and during the ATM-SKYLAB observations. Hopefully these results will be useful for studying the impulsive flare emissions and the relation of these impulsive emissions to the slower soft x-ray emissions. These results should also be useful as background information to scientists studying the ATM observations of the evolution of active regions and the flare productivity of these regions.

The level of solar activity was relatively low during the ATM-SKYLAB missions. The 10 cm flux was below 100 most of the time and dipped below 80 to near sunspot minimum values frequently during the last manned mission. Consequently, the frequency of occurrence of events was lower than during most of this sunspot cycle. Fortunately, a good solar rotation of flare activity was well observed with ATM experiments in early September during the second manned mission.

All the EUV bursts observed via SFDs during the ATM observations were more than an order of magnitude smaller than the largest events observed from September, 1960 to July, 1970. However, several nice medium-sized EUV bursts were observed via SFDs. Some of the events had extensive fine time structure or were quasi-periodic (e.g., 1411 UT June 15, 1973; 2153 UT September 2, 1973; and 1830 UT September 5, 1973). Considering the high spatial resolution and extensive spectral coverage of the ATM observations, significant advances in our knowledge of solar flares should be obtainable.

Further information on the SFD and 10-1030A results for particular events may be obtained by writing to *Dr. R. F. Donnelly, Space Environment Laboratory, NOAA Environmental Research Laboratories, Boulder, Colorado, 80302, USA.* The absolute accuracy of the 10-1030A flux enhancement varies from event to event and during events, but is generally about a factor of four. The absolute and relative timing accuracy also varies from one event to another and from one data set to another. When the ATM data are analyzed to where the flares observed during the third manned mission are known, it may be possible to obtain further information on the corresponding SFD observations in England, U.K., Alabama and Hawaii, USA.

11. ACKNOWLEDGEMENTS

We gratefully acknowledge financial support as follows: The HF Doppler measurements at Boulder were made as part of ARPA Order No. 1361. The HF Doppler measurements of the University of Hawaii Radio Science Laboratory were sponsored by the Atmospheric Sciences Section, National Science Foundation Grant #GA-23964. Analysis of SFDs during the ATM-SKYLAB missions were supported by NASA Marshall Space Flight Center Order No. H-2532B. We wish to recognize the help of Frank Cowley of the NOAA Space Environment Laboratory (SEL), who wrote the computer programs used to analyze the SFD and compute $\Delta\Phi$(10-1030A). We are also thankful for aid in processing SFD and ionogram data to Lois Wescott of the NOAA Environmental Data Service, Boulder, Colorado; Richard Salaz of the University of Colorado, and Brian Kutara of the University of Hawaii. John Taylor of the NOAA SEL Instrumentation Group helped prepare the HF Doppler receiving and recording equipment used at Sacramento Peak Observatory during the ATM mission. Furthermore, we appreciate the acrobatics of J. Edward Coleman installing the receiving antennas in the tall pine trees at Sacramento Peak Observatory.

REFERENCES

AGY, V., D. M. BAKER, and R. M. JONES — 1965 — Studies of solar flare effects and other ionospheric disturbances with a high frequency Doppler technique, NBS Tech. Note No. 306 (U. S. Government Printing Office, Washington, D. C.).

BAKER, D. M. N. CHANG, K. DAVIES, R. F. DONNELLY and J. E. JONES — 1968 — A review of some ionospheric studies based on a high-frequency Doppler technique, ESSA Tech. Rept. ERL 78-SDL 1 (U. S. Government Printing Office, Washington, D. C.).

DONNELLY, R. F. — 1970 — Extreme ultraviolet flashes of solar flares observed via sudden frequency deviations, ESSA Tech. Rept. ERL 169-SDL 14, (U. S. Government Printing Office, Washington, D. C.).

MITRA, A. P., and P. BANERJEE — 1971 — Models for the effective recombination coefficients in the ionosphere, *Space Res. XI*, ed. K. Ya. Kondratyev, M. J. Rycroft and C. Sagan (Akademie-Verlag, Berlin), 1019-1025.

REEVES, E. M., R. W. NOYES and G. L. WITHBROE — 1972 — Observing programs in solar physics during the 1973 ATM SKYLAB program, *Solar Phys.*, *27*, 251-270.

SMITH, N. — 1939 — The relation of radio sky wave transmission to ionosphere measurements, *Proc. IRE*, *27*, 322.

WRIGHT, J. W. — 1967 — Ionospheric electron-density profiles with continuous gradients and underlying ionization corrections. III Practical procedures and some instructive examples, *Radio Sci.*, *2* (New Series), 1159-1168.

UAG Series of Reports

Prepared by World Data Center A for Solar-Terrestrial Physics, NOAA, Boulder, Colorado, U.S.A.

These reports are for sale through the National Climatic Center, Federal Building, Asheville, NC 28801, Attn: Publications. Subscription price: $9.00 a year; $2.50 additional for foreign mailing; single copy price varies. These reports are issued on an irregular basis with 6 to 12 reports being issued each year. Therefore, in some years the single copy rate will be less than the subscription price, and in some years the single copy rate will be more than the subscription price. Make check or money order payable to: Department of Commerce, NOAA.

Some issues are now out of print and are available only on microfiche as indicated. Requests for microfiche should be sent to World Data Center A for Solar-Terrestrial Physics, NOAA, Boulder, Co 80302, with check or money order made payable to Department of Commerce, NOAA.

UAG-1 "IQSY Night Airglow Data", by L. L. Smith, F. E. Roach and J. M. McKennan of Aeronomy Laboratory, ESSA Research Laboratories, July 1968, 305 pages, price $1.75.

UAG-2 "A Reevaluation of Solar Flares, 1964-1966", by Helen W. Dodson and E. Ruth Hedeman of McMath-Hulbert Observatory, The University of Michigan, August 1968, 28 pages, microfiche only, price 45 cents.

UAG-3 "Observations of Jupiter's Sporadic Radio Emission in the Range 7.6-41 MHz, 6 July 1966 through 8 September 1968", by James W. Warwick and George A. Dulk, Department of Astro-Geophysics, University of Colorado, October 1968, 35 pages, microfiche only, price 45 cents.

UAG-4 "Abbreviated Calendar Record 1966-1967", by J. Virginia Lincoln, Hope I. Leighton and Dorothy K. Kropp of Aeronomy and Space Data Center, Space Disturbances Laboratory, ESSA Research Laboratories, January 1969, 170 pages, price $1.25.

UAG-5 "Data on Solar Event of May 23, 1967 and its Geophysical Effects", compiled by J. Virginia Lincoln, World Data Center A, Upper Atmosphere Geophysics, ESSA, February 1969, 120 pages, microfiche only, price 90 cents.

UAG-6 "International Geophysical Calendars 1957-1969", by A. H. Shapley and J. Virginia Lincoln, ESSA Research Laboratories, March 1969, 25 pages, microfiche only, price 45 cents.

UAG-7 "Observations of the Solar Electron Corona: February 1964-January 1968", by Richard T. Hansen, High Altitude Observatory, Boulder, Colorado and Kamuela, Hawaii, October 1969, 12 pages, price 15 cents.

UAG-8 "Data on Solar-Geophysical Activity October 24-November 6, 1968", Parts 1 and 2, compiled by J. Virginia Lincoln, World Data Center A, Upper Atmosphere Geophysics, ESSA, March 1970, 312 pages, price (includes Parts 1 and 2) $1.75.

UAG-9 "Data on Cosmic Ray Event of November 18, 1968 and Associated Phenomena", compiled by J. Virginia Lincoln, World Data Center A, Upper Atmosphere Geophysics, ESSA, April 1970, 109 pages, price 55 cents.

UAG-10 "Atlas of Ionograms", edited by A. H. Shapley, ESSA Research Laboratories, May 1970, 243 pages, price $1.50.

UAG-11 "Catalogue of Data on Solar-Terrestrial Physics", June 1970. (now obsolete).

UAG-12 "Solar-Geophysical Activity Associated with the Major Geomagnetic Storm of March 8, 1970", Parts 1, 2 and 3, compiled by J. Virginia Lincoln and Dale B. Bucknam, World Data Center A, Upper Atmosphere Geophysics, NOAA, April 1971, 466 pages, price (includes Parts 1-3) $3.00.

UAG-13 "Data on the Solar Proton Event of November 2, 1969 through the Geomagnetic Storm of November 8-10, 1969", compiled by Dale B. Bucknam and J. Virginia Lincoln, World Data Center A, Upper Atmosphere Geophysics, NOAA, May 1971, 76 pages, microfiche only, price 90 cents.

UAG-14 "An Experimental, Comprehensive Flare Index and Its Derivation for 'Major' Flares, 1955-1969", compiled by Helen W. Dodson and E. Ruth Hedeman, McMath-Hulbert Observatory, The University of Michigan, July 1971, 25 pages, price 30 cents.

UAG-15 "Catalogue of Data on Solar-Terrestrial Physics", July 1971. (now obsolete).

UAG-16 "Temporal Development of the Geographical Distribution of Auroral Absorption for 30 Substorm Events in each of IQSY (1964-65) and IASY (1969)", by F. T. Berkey, V. M. Driatskiy, K. Henriksen, D. H. Jelly, T. I. Shchuka, A. Theander and J. Yliniemi, September 1971, 131 pages, price 70 cents.

UAG-17 "Ionospheric Drift Velocity Measurements at Jicamarca, Peru (July 1967-March 1970)", by Ben B. Balsley, Aeronomy Laboratory, National Oceanic and Atmospheric Administration, Boulder, Colorado, and Ronald F. Woodman, Jicamarca Radar Observatory, Instituto Geofisico del Perú, Lima, Peru, October 1971, 45 pages, microfiche only, price 45 cents.

UAG-18 "A Study of Polar Cap and Auroral Zone Magnetic Variations", by K. Kawasaki and S. -I. Akasofu, Geophysical Institute, University of Alaska, June 1972, 21 pages, price 20 cents.

UAG-19 "Reevaluation of Solar Flares 1967", by Helen W. Dodson and E. Ruth Hedeman, McMath-Hulbert Observatory, The University of Michigan, and Marta Rovira de Miceli, San Miguel Observatory, Argentina, June 1972, 15 pages, price 15 cents.

UAG-20 "Catalogue of Data on Solar-Terrestrial Physics", October 1972. (now obsolete).

UAG-21 "Preliminary Compilation of Data for Retrospective World Interval July 26 - August 14, 1972", compiled by J. Virginia Lincoln and Hope I. Leighton, World Data Center A for Solar-Terrestrial Physics, November 1972, 128 pages, price 70 cents.

UAG-22 "Auroral Electrojet Magnetic Activity indices (AE) for 1970", by Joe Haskell Allen, National Geophysical and Solar-Terrestrial Data Center, Environmental Data Service, November 1972, 146 pages, price 75 cents.

UAG-23 "U.R.S.I. Handbook of Ionogram Interpretation and Reduction", Second Edition, November 1972, edited by W. R. Piggott, Radio and Space Research Station, Slough, U.K., and K. Rawer, Arbeitsgruppe für Physikalische Weltraumforschung, Freiburg, G.F.R., November 1972, 324 pages, price $1.75.

UAG-24 "Data on Solar-Geophysical Activity Associated with the Major Ground Level Cosmic Ray Events of 24 January and 1 September 1971", Parts 1 and 2, compiled by Helen E. Coffey and J. Virginia Lincoln, World Data Center A for Solar-Terrestrial Physics, December 1972, 462 pages, price (includes Parts 1 and 2) $2.00.

UAG-25 "Observations of Jupiter's Sporadic Radio Emission in the Range 7.6-41 MHz, 9 September 1968 through 9 December 1971", by James W. Warwick, George A. Dulk and David G. Swann, Department of Astro-Geophysics, University of Colorado, February 1973, 35 pages, price 35 cents.

UAG-26 "Data Compilation for the Magnetospherically Quiet Periods February 19-23 and November 29 - December 3, 1970", compiled by Helen E. Coffey and J. Virginia Lincoln, World Data Center A for Solar-Terrestrial Physics, May 1973, 129 pages, price 70 cents.

UAG-27 "High Speed Streams in the Solar Wind", by D. S. Intriligator, University of Southern California, Department of Physics, Los Angeles, California, 90007, June 1973, 16 pages, price 15 cents.

UAG-28 "Collected Data Reports on August 1972 Solar-Terrestrial Events", Parts 1, 2 and 3, edited by Helen E. Coffey, World Data Center A for Solar-Terrestrial Physics, July 1973, 932 pages, price (includes Parts 1-3) $4.50.

UAG-29 "Auroral Electrojet Magnetic Activity Indices AE (11) for 1968", by Joe Haskell Allen, Carl C. Abston and Leslie D. Morris, National Geophysical and Solar-Terrestrial Data Center, Environmental Data Service, October 1973, 148 pages, price 75 cents.

UAG-30 "Catalog of Data on Solar-Terrestrial Physics", prepared by Environmental Data Service, NOAA, Boulder, Colorado, October 1973, 317 pages, price $1.75.

UAG-31 "Auroral Electrojet Magnetic Activity Indices AE (11) for 1969", by Joe Haskell Allen, Carl C. Abston and Leslie D. Morris, National Geophysical and Solar-Terrestrial Data Center, Environmental Data Service, February 1974, 142 pages, price 75 cents.

UAG-32 "Synoptic Radio Maps of the Sun at 3.3 mm for the Years 1967-1969", by Earle B. Mayfield and Kennon P. White III, San Fernando Observatory, Space Physics Laboratory and Fred I. Shimabukuro, Electronics Research Laboratory, Laboratory Operations, The Aerospace Corporation, El Segundo, California, 90245, April 1974, 26 pages, price 35 cents.

UAG-33 "Auroral Electrojet Magnetic Activity Indices AE(10) for 1967", by Joe Haskell Allen, Carl C. Abston and Leslie D. Morris, National Geophysical and Solar-Terrestrial Data Center, Environmental Data Service, May 1974, 142 pages, price 75 cents.

UAG-34 "Absorption Data for the IGY/IGC and IQSY", compiled and edited by A. H. Shapley, National Geophysical and Solar-Terrestrial Data Center, NOAA, Boulder, Colorado, U.S.A., W. R. Piggott, Science Research Council, Slough, U.K., and K. Rawer, Arbeitsgruppe für Physikalische Weltraumforschung, Freiburg, G.F.R., June 1974, 381 pages, price $2.00.

UAG-35 "Catalogue of Digital Geomagnetic Variation Data at World Data Center A for Solar-Terrestrial Physics", prepared by Environmental Data Service, NOAA, Boulder, Colorado, July 1974, 20 pages, price 20 cents.

USCOM-NOAA-ASHEVILLE-10-30-74-450